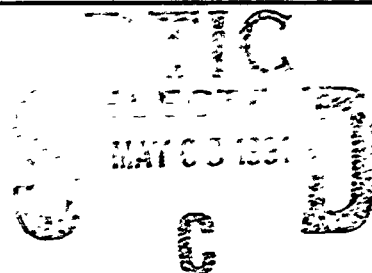


AD-A235 166



2

CONTRACTOR REPORT BRL-CR-661

BRL

DEVELOPMENT OF A PEBBLE-BED
LIQUID-NITROGEN EVAPORATOR AND
SUPERHEATER FOR THE SCALED
LARGE BLAST/THERMAL SIMULATOR FACILITY

I. B. OSOFSKY
G. P. MASON
M. J. TANAKA
SPARTA, INC.

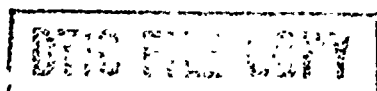
APRIL 1991

APPROVED FOR PUBLIC RELEASE; DISTRIBUTION IS UNLIMITED.

U.S. ARMY LABORATORY COMMAND

BALLISTIC RESEARCH LABORATORY
ABERDEEN PROVING GROUND, MARYLAND

91 5 07 071



NOTICES

Destroy this report when it is no longer needed. DO NOT return it to the originator.

Additional copies of this report may be obtained from the National Technical Information Service, U.S. Department of Commerce, 5285 Port Royal Road, Springfield, VA 22161.

The findings of this report are not to be construed as an official Department of the Army position, unless so designated by other authorized documents.

The use of trade names or manufacturers' names in this report does not constitute indorsement of any commercial product.

UNCLASSIFIED

REPORT DOCUMENT PAGE			Form Approved OMB No. 0704-0188	
<small>Public reporting burden for this collection of information is estimated to average 1 hour per response, including the time for reviewing instructions, searching existing data sources, gathering and maintaining the data needed, and completing and reviewing the collection of information. Send comments regarding this burden estimate or any other aspect of this collection of information, including suggestions for reducing this burden, to Washington Headquarters Service, Directorate for Information Operations and Reports, 1215 Jefferson Davis Highway, Suite 1204, Arlington, VA 22202-4302, and to the Office of Management and Budget, Paperwork Reduction Project (0704-0188), Washington, DC 20503.</small>				
1. AGENCY USE ONLY (Leave blank)		2. REPORT DATE April 1991		3. REPORT TYPE AND DATES COVERED Final Sep 87 - Dec 88
4. TITLE AND SUBTITLE Development of a Pebble-Bed Liquid-Nitrogen Evaporator and Superheater for the Scaled Large Blast/Thermal Simulator Facility			5. FUNDING NUMBERS PR: 1L162120AH25	
6. AUTHOR(S) I.B. Osafsky, G.P. Mason and M.J. Tanaka				
7. PERFORMING ORGANIZATION NAME(S) AND ADDRESS(ES) SPARTa, Inc. 3440 Carson Street, Suite 200 Torrance, California 90503			8. PERFORMING ORGANIZATION REPORT NUMBER LA-88-TR-033	
9. SPONSORING/MONITORING AGENCY NAME(S) AND ADDRESS(ES) U.S. Army Ballistic Research Laboratory ATTN: SLCBR-DD-T Aberdeen Proving Ground, MD 21005-5066			10. SPONSORING/MONITORING AGENCY REPORT NUMBER BRL-CR-661	
11. SUPPLEMENTARY NOTES This work was performed under Contract No. DAAA15-86-C-0115 and sponsored by U.S. Army Harry Diamond Laboratories, ATTN: SLCHD-NW-P, 2800 Powder Mill Road, Adelphi, MD				
12a. DISTRIBUTION/AVAILABILITY STATEMENT Approved for public release; distribution is unlimited.			12b. DISTRIBUTION CODE	
13. ABSTRACT (Maximum 200 words) In the context of feasibility studies for the U.S. Large Blast/Thermal Simulator (LB/TS) facility, a 1/48-scale model pebble-bed LN ₂ heat exchanger was designed and built that would produce hot nitrogen gas at a predetermined temperature from a cryogenic LN ₂ source at pressures up to 1700 psig and at a flow rate sufficient to fill the LB/TS driver tubes rapidly enough to minimize heat losses through the uninsulated driver walls and to maintain the required nitrogen gas temperatures. The pebble-bed LN ₂ evaporator and superheater was successfully tested and delivered to the U.S. Army Ballistic Research Laboratory (BRL). The results of the tests will be used to provide design data for a larger pebble-bed LN ₂ evaporator and superheater to be used in a 1/6-scale LB/TS test-bed facility under development at BRL, and eventually for the full-scale LB/TS facility.				
14. SUBJECT TERMS Liquid Nitrogen Heat Exchangers Gas Dynamics Blast Shock Tubes Evaporators Superheaters Simulators High Pressure High Temperature Hot Gases			15. NUMBER OF PAGES 251	
			16. PRICE CODE	
17. SECURITY CLASSIFICATION OF THIS PAGE UNCLASSIFIED	18. SECURITY CLASSIFICATION OF THIS PAGE UNCLASSIFIED	19. SECURITY CLASSIFICATION OF ABSTRACT UNCLASSIFIED	20. LIMITATION OF ABSTRACT UL	

NSN 7540-01-280-5500

Standard Form 298 (Rev. 2-89)
Prescribed by ANSI Std. Z39-18 298-102

UNCLASSIFIED

INTENTIONALLY LEFT BLANK.

TABLE OF CONTENTS

1.	INTRODUCTION	1
2.	BACKGROUND	1
3.	OBJECTIVE	5
4.	DESIGN REQUIREMENTS	5
4.1	LB/TS Driver Design Conditions	5
4.2	Pebble-bed Heater Design Conditions	6
4.2.1	Heatup Time Design Condition	6
4.2.2	Full Scale Driver Heating Requirements	11
4.2.3	1/6th Scale Driver Heating Requirements	12
4.2.4	1/48th Scale Prototype Pebble-Bed LN ₂ Evaporator/Superheater Thermal Design Requirements	14
4.3	Mechanical Design Requirements	16
5.	PEBBLE-BED THERMODYNAMIC MODELING AND PRELIMINARY DESIGN	17
5.1	Pebble-bed Thermal Storage Mass Selection	17
5.2	Pebble-bed Thermodynamic Modeling	19
5.2.1	LN ₂ Heat Transfer and Flow Modeling	24
5.3	Full Scale Sizing	25
5.4	1/6th Scale Sizing	28
5.5	1/48th Scale Sizing & Preliminary Design	28
5.5.1	1/48th Scale Superheat Pebble-Bed Heater	29
5.5.2	1/48th Scale Pebble-Bed Combined Evaporator and Superheater	30
6.	1/48TH SCALE DETAILED MECHANICAL DESIGN	34
6.1	Pebble-bed Heater System Components	36
6.1.1	Heater Pressure Containment Shells	36
6.1.2	Cryogenic LN ₂ Components	39
6.1.3	Pebble-bed Design	39
6.1.4	Insulation Design	39
6.1.5	Thermal Mixer Design	42
6.1.6	Exhaust Back Pressure Generator	43
6.1.7	Electrical Thermal Charging System	43
6.2	Hydrotests and Strain Measurement	46
	47
6.3	Engineering Design Drawings	47
6.4	Parts List	48
7.	INSTRUMENTATION AND CONTROL SYSTEM DESIGN	48
7.1	Measurement of Pressure and Temperature	48
7.1.1	Temperature Measurement Grid	48
7.1.2	Pressure Drop Measurement	48
7.1.3	Flow Measurement	48
7.2	Data Recording System	50
7.3	Mixer Outlet Temperature Controls	50

8.	NITROGEN GAS SHUTDOWN TESTS	51
8.1	Test Apparatus	51
8.2	Test Data and Observations	51
8.3	Equipment Handling and Operation	51
9.	LN ₂ FLOW TESTS	52
9.1	Test Apparatus	52
9.2	Test Data and Observations	52
9.3	Equipment Handling and Operation	52
10.	LN ₂ TEST RESULTS DATA REDUCTION AND ANALYSIS	52
10.1	Significant Test Results	52
10.2	Heat Transfer Analyses and Correlation	52
11.	SAFETY AND OPERATION PROCEDURES	56
11.1	Safety Considerations for Assembly and Operation	56
11.1.1	Safety Precautions	56
11.1.2	Safety Procedures	56
11.1.2.1	High Pressure Piping	56
11.1.2.2	Electrical Systems	58
11.2	Pebble-Bed Evaporator/Superheater Operation	58
12.	CONCLUSIONS	59
13.	RECOMMENDATIONS	59
	APPENDIX A - TEST REPORT AND GRAPHICAL TEST DATA	61
	APPENDIX B - GRAPHICAL ANALYSIS RESULTS	203
	APPENDIX C - ENGINEERING DRAWINGS	217
	REFERENCES	239

LIST OF FIGURES

FIGURE 2-1	LARGE BLAST THERMAL SIMULATOR FACILITY CONCEPT	2
FIGURE 4-1	COMPARISON OF SINDA CODE HEAT TRANSFER RESULTS WITH ENGINEERING ANALYSIS	10
FIGURE 4-2	DRIVER GAS TEMPERATURE HISTORY FOR 1.0 AND 2.0 METER INSIDE DIAMETER LB/Ts DRIVERS	10
FIGURE 5-1a	THERMAL MASS STORAGE MEDIA PERFORMANCE h = 25 W/(m ² · °C)	20
FIGURE 5-1b	THERMAL MASS STORAGE MEDIA PERFORMANCE h = 50 W/(m ² · °C)	20
FIGURE 5-2	GEOMETRIC THERMAL MODEL OF A GENERIC PACKED BED SINGLE PASS REGENERATIVE HEATER	21
FIGURE 5-3	ENERGY TRANSFERRED TO GAS BY PEBBLE BED HEATER FOR FLOWRATE = .045 KG/SEC (0.1 LBM/SEC) . .	31
FIGURE 5-4	ENERGY TRANSFERRED TO GAS BY PEBBLE BED HEATER FOR FLOWRATE = .0225 KG/SEC (0.05 LBM/SEC) .	32
FIGURE 5-5	ENERGY TRANSFERRED TO GAS BY PEBBLE BED HEATER FOR FLOWRATE = .030 KG/SEC (0.066 LBM/SEC) .	33
FIGURE 6-1	MECHANICAL DESIGN FOR HEATER PRESSURE SHELL .	37
FIGURE 6-2	MECHANICAL DESIGN FOR MIXER PRESSURE SHELL .	38
FIGURE 6-3	MECHANICAL DESIGN OF PEBBLE-BED LINER AND BAFFLE ASSEMBLIES	40
FIGURE 6-4	TURBULENT MIXER DESIGN SCHEMATIC	44
FIGURE 6-5	ELECTRICAL CHARGING SYSTEM SCHEMATIC	45
FIGURE 7-1	1/48TH SCALE PEBBLE-BED EVAPORATOR/SUPERHEATER TEMPERATURE AND PRESSURE SENSOR LOCATIONS . .	49
FIGURE 10-1	TEST RESULTS AND DATA REDUCTION FOR LN ₂ TEST @ 4 GPM & 1000 PSIG	53
FIGURE 10-2	TEST RESULTS AND DATA REDUCTION FOR LN ₂ TEST @ 6 GPM & 1000 PSIG	54
FIGURE 10-3	TEST RESULTS AND DATA REDUCTION FOR LN ₂ TEST @ 8 GPM & 1000 PSIG	55



Accession For	
NTIS GRA&I	<input checked="" type="checkbox"/>
DTIC TAB	<input type="checkbox"/>
Unannounced	<input type="checkbox"/>
Justification	
By	
Distribution/	
Availability Codes	
Dist	Avail and/or Special
A-1	

INTENTIONALLY LEFT BLANK.

LIST OF TABLES

TABLE 4-1	FULL SCALE LB/TS DESIGN REQUIREMENTS (REF 2) . . .	6
TABLE 4-2	UPDATED FULL SCALE LB/TS DESIGN REQUIREMENTS (REF 3)	6
TABLE 4-3	BRL HIGH PRESSURE LIQUID NITROGEN PUMPING SYSTEM	7
TABLE 4-4	FULL SCALE LB/TS GAS REQUIREMENTS (REF 3)	11
TABLE 4-5	FULL SCALE LB/TS DRIVER GAS HEATING REQUIREMENTS	12
TABLE 4-6	1/6TH SCALE LB/TS NOMINAL DRIVER DIMENSIONS . . .	12
TABLE 4-7	1/6TH SCALE LB/TS DRIVER GAS EVAPORATION AND SUPERHEAT REQUIREMENTS	14
TABLE 4-8	1/6TH SCALE SUPERHEAT PEBBLE BED HEATER REQUIRE- MENTS	15
TABLE 4-9	1/48TH SCALE SUPERHEAT PEBBLE-BED HEATER DESIGN REQUIREMENTS	16
TABLE 5-1	THERMAL STORAGE MATERIALS EVALUATION CHART . . .	18
TABLE 5-2	LB/TS DRIVER GAS EVAPORATION HEATING REQUIREMENTS	26
TABLE 5-2	LB/TS FULL SCALE GEOMETRY SUMMARY	27
TABLE 7-1	LN ₂ PUMP FLOWRATE CALCULATIONS	50

INTENTIONALLY LEFT BLANK.

ACKNOWLEDGEMENTS

This program was conducted by SPARTA, Incorporated, 3440 Carson Street, Suite 300, Torrance, CA 90503 under the Contract DAAA15-86-C-0115 with the U.S. Army Armament, Munitions, and Chemical Command Ballistic Research Laboratory, Aberdeen Proving Ground, Maryland. The contract technical monitor was Richard Pearson at BRL.

The SPARTA principle investigator for the program was Dr. Irving B. Osofsky. He was assisted by Gregory P. Mason and Michael J. Tanaka.

Dynamics Technology, Incorporated was SPARTA's subcontractor for heat transfer analysis, instrumentation, controls and testing. The DTI program manager was Duane T. Hove.

INTENTIONALLY LEFT BLANK.

1. INTRODUCTION

The following report documents the work performed for the U.S. Army Armament, Munitions and Chemical Command (AMCCOM) Ballistic Research Laboratory (BRL) located at the Aberdeen Proving Ground, Maryland under contract DAAA15-86-C-0115 & Modification P00001 during the period 29 September 1986 through 31 May 1988. The contract was a research and development program entitled "Development of a Pebble-bed Liquid Nitrogen Evaporator and Superheater for the Scaled Large Blast/Thermal Simulator (LB/TS) Facility" and its objective was to develop, design, fabricate and test a scale model of a pebble-bed type heat exchanger intended for rapidly evaporating cryogenic liquid nitrogen and controllably heating the high pressure gas for use in the proposed LB/TS test facility.

2. BACKGROUND

The rapid growth of Soviet tactical and theater nuclear capability has increased the need to improve the nuclear survivability of U.S. tactical nuclear and conventional forces. The concern over nuclear survivability is reflected in DoD instructions and Army procurement regulations requiring specific nuclear hardness levels on military systems. There are within the Army alone over 150 systems with nuclear survivability requirements. At present the U.S. lacks the simulation capability to test full scale systems to the full range of nuclear blast and thermal effects required. To answer this problem and reduce the cost of blast simulation, the Defense Audit Service recommended that the Defense Nuclear Agency (DNA) develop a Large Blast/Thermal Simulator (LB/TS). The U.S. Army Ballistics Research Laboratory has taken a leading role in research and development of LB/TS designs for DNA and the US Army Harry Diamond Laboratory. The development of a Pebble-bed LN₂ Evaporator/Superheater is part of a continuing program to develop a practical LB/TS design.

The high pressure driver portion of the proposed LB/TS would use an array of steel driver tubes to drive a blast wave in a large expansion tunnel. An artist's conception of a LB/TS facility is shown in Figure 2-1. Earlier work performed by BRL and their contractors has shown that to simulate the higher shock overpressure and weapon yields of interest, it will be necessary to use high pressure gas heated to elevated temperatures as high as 700°F (644°K) in the driver tube array. At the start of this program, the maximum LB/TS driver gas conditions were a temperature of 650°K (710°F) and a pressure of 12 MPa (1740 psig). Since that time, additional calculations and experiments have indicated that pressures as high as 15 Mpa (2200 psig) may be required to provide the required simulation. The design pressure for the pebble-bed heater developed under this program was established at 1740 psig with an allowance for increasing the pressure up 2000 psig.

LARGE BLAST / THERMAL SIMULATION FACILITY

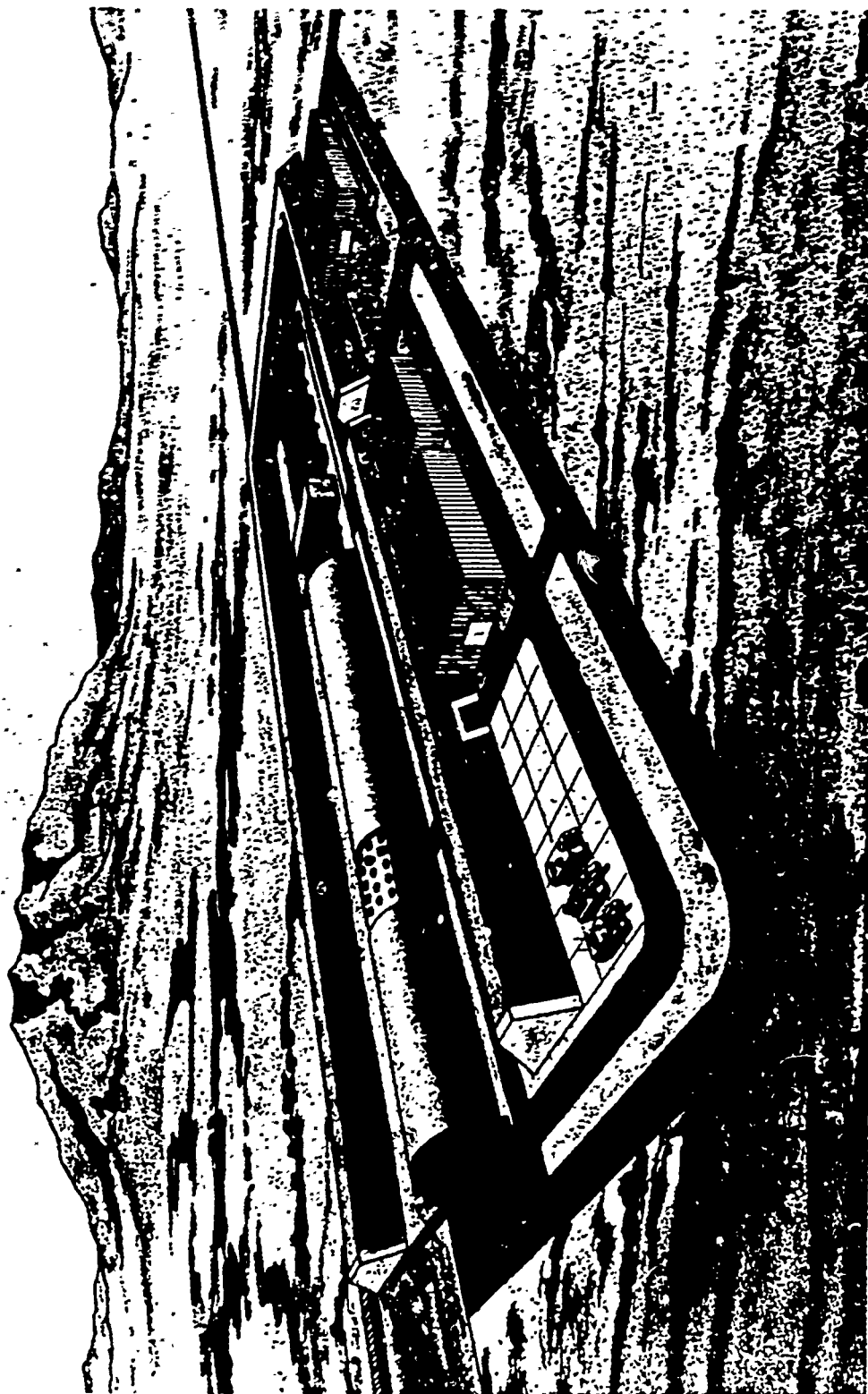


FIGURE 2-1 LARGE BLAST THERMAL SIMULATOR FACILITY
CONCEPT (REFERENCE 1)

In earlier LB/TS design studies, several concepts were developed for providing high pressure, hot driver gas. These studies concluded that two types of gas pressurization systems are practical for the LB/TS; oil free reciprocating piston type air compressors with dehumidifiers and cryogenic LN₂ pumps with vaporizers. Both of these systems provide ambient temperature gas at high pressure. Air compressor systems for the LB/TS would be very large and costly systems and would take in the order of 10-16 hours to pump up the LB/TS drivers. Also, the pressurized air produced by the compressors will have a sizeable residual moisture content, even with the best of air dryers. This moisture condenses in the expansion test section and produces moisture clouds that obscure optical recording instruments. In contrast, SPARTA has shown that relatively small LN₂ pumping systems can be sized to provide the required maximum driver pressure and temperature conditions in less than an hour (even in 5-10 minutes if necessary) and the nitrogen gas produced by a LN₂ pumping/vaporizing system is pure and completely dry. Therefore no moisture condensation will take place in the test section.

Heating of the driver gas can be accomplished by either of two schemes; heating during driver pressurization (single pass heatup) and heating ambient temperature gas after pressurization (bypass recirculation heatup).

Two major problems have been encountered with the design of heated gas drivers which use slow fill time air compression systems and bypass recirculation heating.

The first problem was the large heat loss from the driver gas to the steel driver tube walls. Conventional high temperature insulation materials will not survive the conditions of high temperature, high pressure and rapid decompression with negative pressures experienced in the LB/TS driver tubes. The development of a special insulation system which could withstand these adverse conditions is under study by BRL.

The second problem encountered was the lack of available high pressure, high temperature, large flowrate gas bypass blower recirculation systems that can recirculate initially cold pressurized driver gas from the driver through a conventional heat exchanger and back to the driver to slowly raise the temperature and pressure of the gas to the required design condition.

During the design of the bypass recirculation system, it was found that circulation blowers which can produce the mass flow rates necessary at the high pressure and temperatures needed are not commercially available. Furthermore, very large horsepower motors and gearboxes would be required to power the blowers. This meant that the blowers, drive systems and heaters would have to be specially developed. This development of the cir-

ulation/heating system and the complexity of the valving and piping required to operate a bypass heating system would make the bypass system extremely costly.

The concept of using LN_2 as the source for LB/TS hot compressed gas utilizes the mechanical advantage of compressing a relatively incompressible dense liquid with a relatively small positive displacement reciprocating piston type liquid pumping system compared to the large gas (air) compressors which would otherwise be required (see reference ²). Evaporation of the LN_2 and heating of the driver gas could be performed in a single pass with an in line pebble-bed heater (i.e. through which the pressurized LN_2 passes while pressurizing the drivers) rather than trying to use a bypass system.

An additional advantage of the LN_2 pressurizing and heating concept is that a LB/TS driver (pressure vessel) could be rapidly filled in under 10 minutes using a high capacity off the shelf positive displacement cryopump in combination with a high flow/-high heating rate pebble-bed evaporator and superheater. Rapid filling of the driver would greatly decrease the complexity of the driver system by eliminating the need for thermally insulating the interior walls of the driver to prevent large heat losses associated with a bypass systems's slow heating time (typically in the order of 1-2 hours). Because hazardous conditions exist in the test section when the LB/TS drivers are pressurized with ambient or hot gas, rapid filling and heating would allow LB/TS experimenters to correct any instrumentation or experiment problems in the test section up to 10 minutes prior to test without venting the drivers.

The original scope of the program was to develop and characterize the heat transfer performance of a pebble-bed superheater for heating room temperature nitrogen gas up to the required LB/TS maximum design condition (approx. 700°F at maximum working pressures approaching 1700 psig). During the course of the program, a critical requirement was established for characterizing cryogenic liquid nitrogen (LN_2) heat transfer rather than nitrogen gas in a packed pebble-bed. This requirement arose out of previous studies which demonstrated the feasibility of using liquid nitrogen as the source for hot nitrogen gas in a LB/TS compressed gas driver system but SPARTA lacked the proper heat transfer design data to design a LN_2 pebble-bed heat exchanger.

As a result of the LN_2 requirement, the scope of the program was modified to development of a pebble-bed evaporator/superheater for evaporating cryogenic liquid nitrogen (LN_2) and superheating the resulting gas to the LB/TS design temperature condition. The program evolved into the development of a 1/48th scale LN_2 Pebble-Bed Evaporator and Superheater to obtain heat transfer performance data which can be used to design a LN_2 pebble-bed evaporator/superheater for the BRL 1/6th scale LB/TS testbed (8 foot shocktube

modification) and eventually for the full scale LB/TS.

3. OBJECTIVE

The revised objective of the program was to develop a pebble-bed heat exchanger that would produce hot nitrogen gas at a predetermined temperature from a cryogenic LN₂ source at pressures up to 1700 psig at a flowrate sufficient to fill the LB/TS driver tubes rapidly enough to minimize gas heat losses to an uninsulated driver wall and maintain the required nitrogen temperatures. For this program, a scale model LN₂ pebble-bed evaporator/superheater was successfully designed, developed, tested and delivered to BRL. The results of the tests will be used to provide design data for a larger LN₂ pebble-bed evaporator/superheater for a LB/TS testbed shock facility under development at BRL and eventually for the full scale LB/TS facility.

4. DESIGN REQUIREMENTS

4.1 LB/TS Driver Design Conditions

The LB/TS driver conditions were calculated by BRL using a quasi one dimensional shock tube simulation computer program, BRL-Q1D. The program calculates the shock properties for a given shocktube driver and driven section geometry. Two sets of data were provided to SPARTA by BRL. The first set of design requirements data was delivered in October 1986 and the second set in January 1987. The updated data (Jan 1987) documented more recent parametric calculations performed by BRL. Because the more recent data arrived when the pebble-bed preliminary design had not been completed, SPARTA was able to incorporate the new design requirements into the final design.

The following full scale LB/TS design requirements data was received from BRL on 29 October 1986 (Reference ³).

There are six series of driver gas temperature, pressure, and volume conditions which are to be considered for the full scale LB/TS for a 600 kT simulated yield. The maximum case is the critical case that is used to design the pebble-bed heater pressure system. For this set of data, Case 1 is the maximum design condition. Table 4-1 lists the initial (OCT 1986) design data.

TABLE 4-1 FULL SCALE LB/TS DESIGN REQUIREMENTS (REF 2)

CASE	SHOCK OVERPRESSURE (psig/kPa)	DRIVER PRESSURE (psig/kPa)	DRIVER TEMPERATURE (°R/°K)	DRIVER VOLUME (kft ³ /m ³)
1	35/241	1727/11910	1137/632	29.3/830
2	30/207	1507/10388	1037/579	48.4/1370
3	25/172	1249/8609	947/526	58.5/1657
4	20/138	1017/7010	857/476	84.3/2386
5	15/103	785/5410	763/424	85.5/2421
6	10/69	309/2128	671/373	104.7/2965

The following Table 4-2 shows the updated design data provided to SPARTA by BRL in January 1987 (Reference ⁴). Once again a 600 kT simulation was used for the calculations. In this set of data, seven design points were provided and the maximum case (i.e. maximum gas mass, pressure, and temperature) is Case 1.

TABLE 4-2 UPDATED FULL SCALE LB/TS DESIGN REQUIREMENTS (REF 3)

CASE	SHOCK OVERPRESSURE (psig/kPa)	DRIVER PRESSURE (psia/kPa)	DRIVER TEMPERATURE (°R/°K)	DRIVER VOLUME (kft ³ /m ³)
1	35/241	1690/11653	1154/640	43.3/1227
2	30/207	1465/10102	1042/579	43.3/1227
3	20/138	1014/6991	845/469	43.3/1227
4	15/103	794/5472	731/406	43.3/1227
5	10/69	573/3951	637/344	43.3/1227
6	5/69	279/1925	570/317	54.1/1534
7	2/14	99/684	534/296	81.1/2300

4.2 Pebble-bed Heater Design Conditions

4.2.1 Heatup Time Design Condition

The thermal design conditions of the pebble-bed heater are derived from the LB/TS driver operation parameters as outlined above in Tables 4-1 and 4-2. The LN₂ pumping system capacity determines the pump up time for the driver. For a single pass pebble-bed heater, the pump capacity also determines what the heatup time would be. Initially, a LN₂ pumping system located at BRL was considered for use in pumping up the 1/6th scale test bed driver. The specifications of this pump system are given in Table 4-3.

TABLE 4-3 BRL HIGH PRESSURE LIQUID NITROGEN PUMPING SYSTEM

Manufacturer:	ACD Inc. (formerly AIRCO Cryogenics Co.) 1900 Main St. Irvine, CA 92714 1-714-261-7533
LN ₂ Pump:	Type DP, P/N 43015-2, S/N 84153711 Maximum pressure - 3600 psig (24.8 MPa) Flow rating - .88 gpm @ 3600 psig 3.33 lpm @ 24.8 MPa
Pump Drive:	5 hp (3.73 kW), P/N 35969-4
Evaporator:	KRYOFIN, Ambient Air Vaporizer P/N 39200-1, S/N 882063 Rating - 5000 SCFH @ 70°F (141.5 Skl/h @ 21°C) Maximum pressure - 3600 psig (24.8 MPa) Proof pressure - 5400 psig (37.2 MPa)

This pumping system would be adequate for filling the 1/6th scale LB/TS if pump/heat up times were in the order of 1-2 hours. In this case, the driver tube would most certainly have to be heated or internally insulated to prevent heat loss from the gas and a resulting temperature drop. With modifications such as changing pulleys/belts and increasing the motor size, this pumping system capacity may be increased to 2 GPM. A detailed examination of this modification has not been performed.

Without the limitation of a LN₂ pumping system, the critical heatup time would be dominated by the heat losses from the hot gas to the driver wall (insulated or uninsulated). A calculation was made to predict the heat loss to the wall of a cold, uninsulated driver.

In order to reduce excessive heat loss to the wall/atmosphere and a subsequent temperature drop, the driver filling time should be short (in the order of 5 to 10 minutes) and the driver firing time delay (hold time) should be minimized. For safety and operational reasons, it is envisioned that the driver will only be pressurized and fired after all test articles, experiments and instrumentation in the test section have been checked out and verified. It is also assumed that all holds (if any) would occur while the drivers are not pressurized.

Heat transfer to the driver walls is a maximum when the differential temperature between the gas and wall is the greatest. The mechanism for heat transfer is free convection in a closed horizontal cylinder. The ratio of enthalpy of the driver gas to the steel driver, R , is computed as follows:

$$R = \frac{m_s \cdot Cp_s}{m_g \cdot Cp_g} \quad (\text{EQ 4-1})$$

where,

m_s , mass per unit length of the steel driver, kg/m

Cp_s , specific heat of the steel driver material, J/kg/°K

m_g , mass per unit length of the high pressure hot gas, kg/m

Cp_g , specific heat of the hot gas, J/kg/°K

The mass per unit length of the carbon steel driver (for $d = 1.0$ m & $t = .057$ m) is approximately 1396 kg/m and for the gas ($T_{g_0} = 700^\circ\text{K}$ & $P_g = 12$ MPa gives a density, $\delta_g = 58$ kg/m³) is approximately 45.5 kg/m. For $Cp_s = 450$ J/kg/°K and $Cp_g = 1097$ J/kg/°K, the ratio of enthalpy, R , is approximately 13.

This result shows that the heat capacity of the steel driver is one order of magnitude greater than the gas. This implies that the driver wall does not appreciably rise in temperature over short periods of time and is assumed to be at ambient temperature, T_0 , throughout the pressurization of the driver.

The heat loss can be calculated using a the classical exponential temperature decay formula:

$$q/L = h \cdot \pi \cdot D \cdot (T_g - T_0) = \frac{d}{dt} \left[\delta_g \cdot \pi \cdot D^2 / 4 \cdot Cp_g \cdot (T_g - T_0) \right] \quad (\text{EQ 4-2})$$

Integrating & Solving for $T_g - T_0$:

$$\frac{T_g - T_0}{T_{g_0} - T_0} = e^{(-t/\tau)} \quad (\text{EQ 4-3})$$

where;

T_g , temperature of the gas at time t , °K

T_{g_0} , initial temperature of the gas, °K

T_0 , initial and constant temperature of the steel driver, °K

t , time, sec

τ , time constant defined by the following, sec

$$\tau = \frac{\delta_g \cdot D \cdot Cp_g}{4 \cdot h} \quad (\text{EQ 4-4})$$

δ_g , gas density, kg/m³

h , the convective heat transfer coefficient, W/m²/°K.

The convective film coefficient is calculated from the following relation correlation ⁵:

$$Nu_D = \frac{h \cdot D}{k_g} = 0.40 \cdot (Gr_D \cdot Pr)^{0.20} \quad (EQ 4-5)$$

where,

Nu_D , Nusselt number
 Gr_D , Grashof number

$$\text{given by; } Gr_D = \frac{g \cdot \beta \cdot (T_o - T_{g_o}) \cdot D^3}{(\mu / \delta_g)^2} \approx 2 \cdot 10^{13} \quad (EQ 4-6)$$

g , gravitational constant
 β , volume coefficient of expansion $\approx 1/T_{g_o}$
 μ , dynamic viscosity of gas @ T_g , kg/m/s
 Pr , Prandtl number $\approx .7$
 k_g , thermal conductivity of gas ≈ 0.04 W/m/°K
 D , driver internal diameter = 1.0 m

therefore: $h \approx 7.0$ W/m²/°K

The time constant is calculated as:

$$\tau \approx 2270 \text{ sec (38 minutes)}$$

This implies that the gas temperature will be reduced by e^{-1} ($\approx 37\%$) in 38 minutes.

For a wall temperature of 290°K, in 5 minutes the gas temperature will drop from 700°K to approximately 649°K (8% reduction). In 10 minutes the gas temperature drops to approximately 605°K (14% reduction).

To validate these analyses, a heat transfer model was developed and run using the SINDA program. Figure 4-1 shows the comparison of the SINDA calculations with the above theoretical exponential relation. The comparison shows that the above relation is acceptable for a 1st order analysis. Figure 4-2 shows the driver gas temperature drop for two cases ($D=1.0$ m and 2.0 m). The exponential relation above implies that the driver gas will lose its heat more slowly with a larger diameter driver (i.e. increases time constant) and more quickly with a larger heat transfer coefficient. The correlation used for the heat transfer coefficient is valid for Grashof numbers up to 10^8 . In this case the Grashof number was calculated to be 5 orders of magnitude greater. Thus the heat transfer coefficient correlation used in this analysis is uncertain.

The above calculations indicate that the full scale driver will retain heat much longer than the scaled driver. However, the

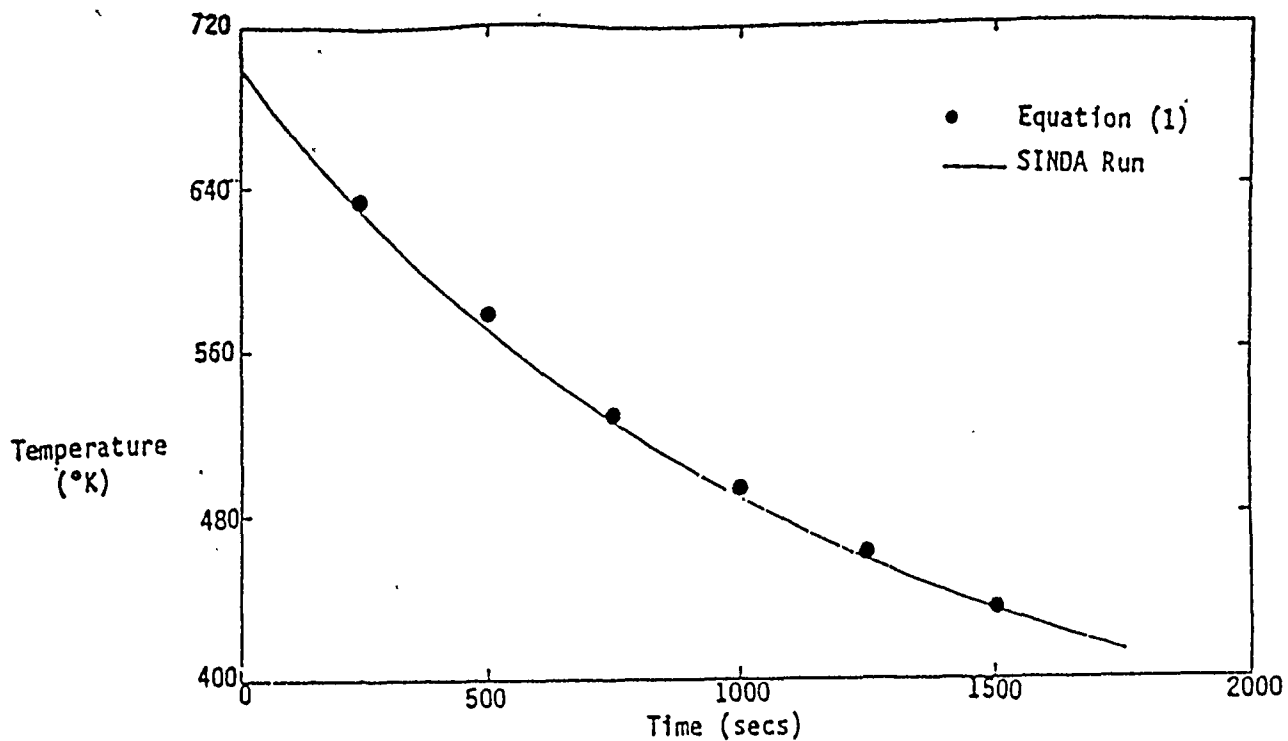
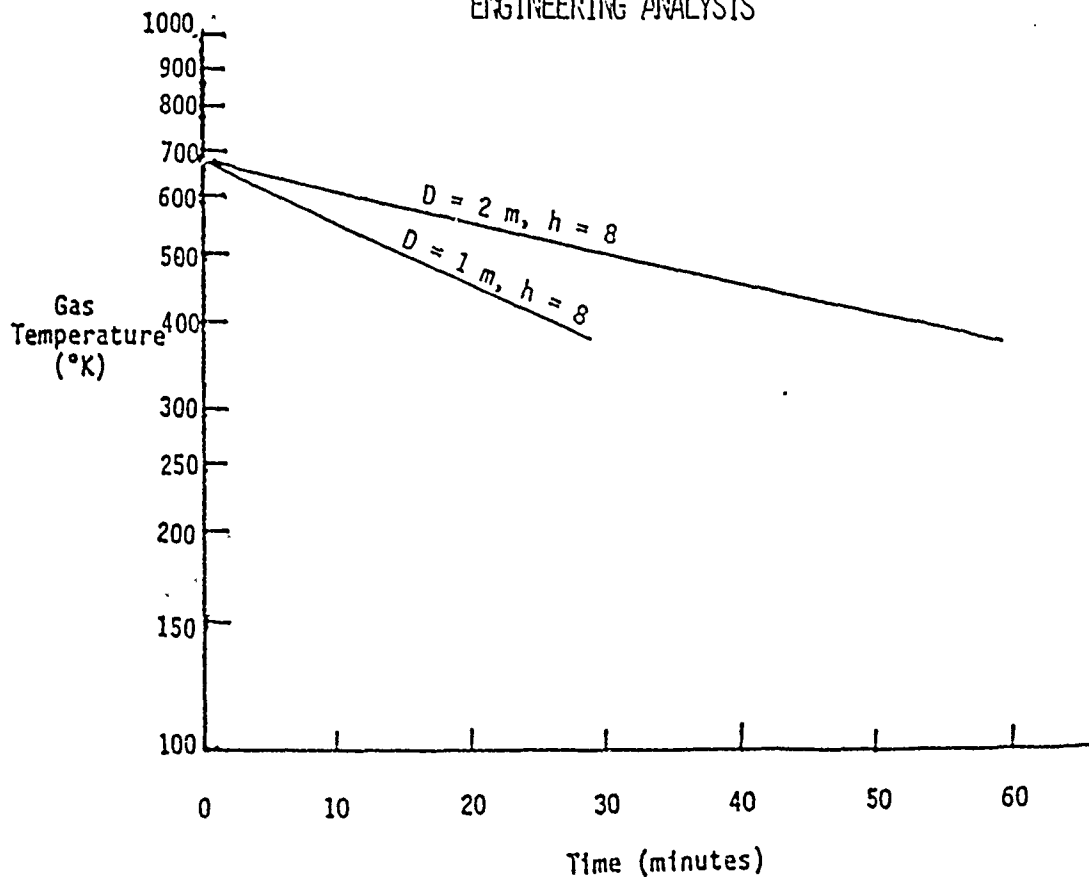


FIGURE 4-1 COMPARISON OF SINDA CODE RESULTS WITH
ENGINEERING ANALYSIS



REF: Dynamics Technology Inc., Memo Report, DTH-8705A-01-DTH/SIJ

FIGURE 4-2 GAS TEMPERATURE HISTORY AT VARIOUS CONDITIONS

uncertainty of the heat transfer correlation indicates that heat transfer tests should be performed in the scaled driver before the full scale design is completed or internal insulation is used.

Assuming that the above analysis is valid, the heating time for the 1.0 m diameter driver can be as little as 5 minutes if a large enough flow capacity LN₂ cryogenic pump is used (such high capacity cryogenic LN₂ pumps are "off the shelf" items). For a larger 2.0 m diameter driver, the time constant increases, thus implying that a full scale driver could be heated in 5 minutes or less, provided that sufficient LN₂ pumping capacity is available.

4.2.2 Full Scale Driver Heating Requirements

The full scale driver heating requirements are derived from the data presented in Table 4-2. Table 4-4 gives the required driver nitrogen mass, liquid heat of vaporization and gas enthalpy requirements for the seven full scale pebble-bed heating system conditions. The calculations are based on a constant specific heat over the range of temperatures of interest.

TABLE 4-4 FULL SCALE LB/TS GAS REQUIREMENTS (REF 3)

CASE	T _d , DRIV TEMP (°R/°K)	m _g , DRIVER GAS MASS (klbm/Mg)	LN ₂ HEAT OF VAPOR (MBtu/GJ)	N ₂ HEAT c _p (T _d -T _b) (MBtu/GJ)	TOTAL HEAT (MBtu/GJ)
1	1154/640	166.0/75.5	14.2/15.0	41.7/44.0	55.9/59.0
2	1042/579	159.1/72.3	13.6/14.4	35.6/37.5	49.2/51.9
3	845/469	135.9/61.8	11.6/12.3	23.7/25.0	35.3/37.3
4	731/406	122.9/55.8	10.5/11.1	18.0/19.0	28.5/30.1
5	637/344	104.7/47.6	8.9/9.5	12.9/13.6	21.8/23.1
6	570/317	55.4/25.2	4.7/5.0	5.9/6.2	10.6/11.2
7	534/296	39.5/17.9	3.4/3.6	3.9/4.1	7.3/7.7

based on the following constants:

Gas Constant, R = 296 J/kg/°K (55.15 ft-lbf/lbm/°R)

Boiling Temperature, T_b = 78°K (140°R)

LN₂ Heat of Vaporization, h_{fg} = 199 kJ/kg (85.6 Btu/lbm)

Specific Heat, c_p = 1038 J/kg/°K (.248 Btu/lbm/°R)

The design conditions for the pebble-bed heater are used to size the heating system. The heater is sized according to the maximum "Total Heat" case given in Table 4-4. The heat into the gas is calculated by starting with the energy state of LN₂ as zero and calculating the enthalpy required to first vaporize the liquid into gas and then raising the gas temperature from the boiling point up to the required temperature. The specific heat of vaporization, h_{fg}, is the amount of heat required to vaporize a liquid into gas while remaining at a constant boiling tempera-

ture. The following relation calculates the required heat, H , for vaporizing the gas mass, m_g , from the boiling point, T_b , to the final temperature, T_d .

$$H = m_g \cdot (c_p \cdot (T_d - T_b) + h_{fg}) \quad (\text{EQ 4-7})$$

The following Table 4-5 summarizes the heating requirements for the maximum operating condition of the full scale LB/TS.

TABLE 4-5 FULL SCALE LB/TS DRIVER GAS HEATING REQUIREMENTS

CASE	CONDITION	DESIGN REQUIREMENT
1	Maximum gas temperature:	640°K (1154°R)
1	Maximum gas pressure:	11.6 MPa (1690 psig)
1	Maximum heat into gas:	59 GJ (55.9 MBtu)
1	Maximum gas volume:	1227 m ³ (105 kft ³)
	Heating time:	5 minutes

4.2.3 1/6th Scale Driver Heating Requirements

BRL is presently developing a scale model of the LB/TS to produce a working testbed for the various component technologies presently under study. The testbed will utilize an existing 8 foot diameter shock tube driven test section which is approximately 1/6th the size of the equivalent diameter of the full scale LB/TS test section which is substantially a 163 m² cross section hemisphere. One of the components included in the testbed design is the pebble-bed LN₂ evaporator/superheater system with a cryogenic LN₂ supply and pumping system. A pebble-bed LN₂ evaporator/superheater will be sized to heat and pressurize the 1/6th scale LB/TS testbed. This 1/6th scale pebble-bed LN₂ evaporator/superheater will then be scaled down by a 1/8th factor resulting in a 1/48th scale LB/TS pebble-bed LN₂ evaporator/superheater prototype development.

For the 1/6th scale LB/TS gas pressurization and heating system, the design requirements for pressure, temperature and pressurization/heating time are the same as the full scale LB/TS. Only the driver volume, gas mass and total heat input vary directly with the decreased driver volume. The BRL 1/6th scale model LB/TS driver design has the approximate dimensions which are given in Table 4-6.

TABLE 4-6 1/6TH SCALE LB/TS NOMINAL DRIVER DIMENSIONS

Driver Internal Diameter:	3 ft (.91 m)
Driver Nominal Length:	35 ft (10 m)
Driver Calculated Volume:	247 ft ³ (7.0 m ³)

By comparison of driver volumes, the scale of the BRL 8 ft. shock tube testbed is approximately 1/5th of the full scale LB/TS.

To size the pebble-bed heater, the required gas volume must include the pebble-bed evaporator/superheater volume and the miscellaneous piping volume. This volume has been estimated to be approximately 5% of the driver volume. Other allowances are made for heat losses in the heater system and driver and for potential holding times which may require additional heated gas to keep the driver gas temperature at required levels.

Driver gas heat losses are accounted for by increasing the driver gas temperature input requirement. A value of 50°K (90°R) was chosen because the results of the heat loss to the driver wall calculation performed above indicated that the temperature of the gas will drop from 700°K to 649°K in 5 minutes.

If the temperature in the driver is initially too hot for the required simulation after pump up, the driver walls will cool the gas to the required temperature in a matter of minutes. Compensating for the pressure drops due to the decreased gas temperature can be performed by continually pumping more gas into the driver while simultaneously venting gas out. Once required driver conditions are met, the driver diaphragm/valve will be initiated. Adequate temperature and pressure monitoring in the driver will ensure that the proper conditions are satisfactory before initiating the diaphragm/valve. Detailed analyses on the influence of small pressure and temperature perturbations in the driver on the produced shock properties must be performed in order to properly design the pressure and temperature controls.

After allowing for the miscellaneous piping and makeup gas, the total heated gas volume becomes 7.35 m³ (259 ft₃). The gas mass at the maximum pressure of 11.6 MPa and gas temperature of 640°K + 50°K = 690°K (1242°R) is 417.5 kg (918.4 lbm). The heat input to the gas is 83.1 MJ (78.8 kBtu) for vaporization and 265.2 MJ (251.4 kBtu) for superheat (boiling temperature to 690°K) for a total heat input of 348.3 MJ (330.2 kBTU). The requirements for the 1/6th scale LN₂ pebble-bed evaporator/superheater are summarized in Table 4-7.

TABLE 4-7 1/6TH SCALE LB/TS DRIVER GAS EVAPORATION AND SUPERHEAT REQUIREMENTS

CASE	CONDITION	DESIGN REQUIREMENT
1	Required gas temperature:	640°K (1154°R)
1	Gas temperature overheat:	50°K (90°R)
1	Maximum gas pressure:	11.6 MPa (1690 psig)
1	Mass of heated gas:	417.5 kg (948 lbm)
1	Maximum heat into gas:	348.3 MJ (330.2 MBtu)
1	Driver gas volume:	7.00 m ³ (247 kft ³)
1	Misc gas volume:	0.35 m ³ (12 kft ³)
	Heating time:	5 minutes (300 secs)
	Flowrates:	
	Mass:	1.4 kg/s (3.06 lbm/s)
	Standard volumetric *:	71.8 kl/min (2534 SCFM)
	LN ₂ volumetric:	103 l/min (27.2 GPM)

* Standard Temperature and Pressure: 293.1°K & 101.35 kPa (530°R & 14.7 psia)

4.2.4 1/48th Scale Prototype Pebble-Bed LN₂ Evaporator/Superheater Thermal Design Requirements

The thermal design requirements for the 1/48th scale LN₂ pebble-bed evaporator/superheater are derived from the 1/6th scale requirements. The 1/48th scale design is intended to produce 1/8th of the required driver gas heating for the 1/6th scale BRL driver, thus the pebble-bed heater design became a 1/48th scale system. However, because the modification of the engineering development effort eliminated the superheat only pebble-bed heater development and adopted a combined LN₂ evaporation and superheat pebble-bed capability, the scale of the LN₂ pebble-bed heater in terms of its capacity to produce a fraction of the required driver gas was uncertain. The term 1/48th scale was carried over for the LN₂ system design and may or may not be an accurate representation of the actual scaled capacity of the unit.

Table 4-8 gives the thermal design requirements for the original superheat only pebble-bed heater system. This system intended to use 8 heated pebble-bed units; 4 pebble-bed heaters in parallel that evaporated LN₂ to ambient conditions connected in series with 4 pebble-bed heaters in parallel that superheated the ambient compressed nitrogen gas to the required driver gas temperature.

TABLE 4-8 1/6TH SCALE SUPERHEAT PEBBLE BED HEATER REQUIREMENTS

CONDITION	DESIGN REQUIREMENT
Driver gas temperature:	640 °K (1152 °R)
Driver gas pressure:	11.6 MPa (1690 psia)
Driver gas volume:	7.0 m ³ (247 ft ³)
Driver gas mass:	430 kg (946 lbm)
Heat into gas (no loss)*:	156 MJ (148 kBTU)
Assumed heat loss (10%):	15 MJ
Heating time:	40 minutes
Hold time:	30 minutes

* Based on superheat from 290°K (522°R)

A heating time of 40 minutes was used in the original sizing analysis because the system was sized for a cryogenic pumping and evaporating system was available at BRL that was capable of pumping and evaporating approximately 0.1 lbm/sec of LN₂ (see Table 4-3). This pump was to be used for the proof of principle experiments on a single pebble-bed superheater and to obtain performance data. The modification, however, adopted the use of a high flowrate pump which was rated at flowrates up to 8 GPM LN₂ capacity.

Using the 0.1 lbm/sec (0.88 GPM) flowrate, 40 minutes of LN₂ pumping would produce about 1/4th of the required gas for the 1/6th scale driver, hence a larger pump with four times the capacity would be required to pressurize and heat the 1/6th scale BRL driver in 40 minutes. The original pebble-bed superheater was therefore sized and designed for use with the available BRL LN₂ pumping and evaporating system.

The heat loss for the scaled driver and heating system is estimated to be approximately 10 percent of the total required heat added to the gas. As originally designed, 4 pebble-bed superheaters are required to heat the pressurized room temperature nitrogen gas to working temperature for the single 1/6th scale driver and therefore each scaled pebble-bed superheater must provide 1/4th of the total heat added to the gas over the 40 minute heating time.

An additional requirement for the pebble-bed heater is to account for the temperature drop of the driver gas due to heat loss to the driver walls during the 40 minute pressurization and heating cycle. Insulation was assumed to cover the driver interior so that heat losses are minimal during the 40 minute heatup cycle. Because of this requirement, the heater will provide nitrogen gas at 50°K (90°R) greater (as was stated above in Section 4.2.1) than the required driver gas temperature. This will increase the total heat requirement by 22.3 MJ (21.1 kBTU) and the individual pebble bed heat requirements by 5.6 MJ (5.3 kBTU).

The total heat required from the superheating system is therefore 193.3 MJ (183.2 kBtu). Therefore, each individual pebble-bed heater must provide 1/4th of the total heat requirement or 48.3 MJ (45.8 kBtu) of energy. For the heating time of 40 minutes (2400 seconds) the average power output of the heater (i.e. the heat transfer rate from the bed to the gas) is approximately 20.1 kW (68.7 kBtu/h). Table 4-9 summarizes the heating requirements for the 1/48th scale pebble-bed superheater.

TABLE 4-9 1/48TH SCALE SUPERHEAT PEBBLE-BED HEATER DESIGN REQUIREMENTS

CONDITION	DESIGN REQUIREMENT
Driver gas temperature:	640 °K (1152 °R)
Driver gas pressure:	11.6 MPa (1690 psia)
Driver gas mass:	107.5 kg (236.6 lbm)
Heat into gas (no loss):	39 MJ (37 kBtu)
Heat losses (10%):	3.9 MJ (3.7 kBtu)
Overheat ($\Delta T=50^{\circ}\text{K}$):	5.6 MJ (5.3 kBtu)
Total heat:	48.5 MJ (46 kBtu)
Heating time:	40 minutes
Hold time:	30 minutes

4.3 Mechanical Design Requirements

The mechanical design requirements for the pebble-bed evaporator superheater primarily facilitate the safe operation of a high pressure and elevated temperature vessel. The requirements are taken primarily from the 1983 American Society for Mechanical Engineers (ASME) Boiler and Pressure Vessel Code. Other design requirements are developed from standard safe engineering practice.

The structural requirements for the pressure components of the pebble-bed heater were developed according to guidelines in the ASME Boiler and Pressure Vessel Code. The following three conditions constitute the primary design parameters for pressure vessels:

- (a) Design Working Temperature
- (b) Design Working Pressure
- (c) External Loadings

According to the ASME code the design temperature is the maximum mean metal temperature expected during the most severe operation of the vessel. The metal surface temperature must never exceed the material's rated maximum temperature as given in the ASME code for the class of materials being used.

The design pressure is the maximum pressure differential achieved across the inner and outer walls of the vessel. External loading

requirements include the following factors:

- (a) Weight of the vessel
- (b) Hydrostatic head of the fluid or mass in the vessel.
- (c) External support structural loads.
- (d) Thermal expansion/stress induced loads.
- (e) Dynamic loading from environment or pressure surges

The important aspects of the ASME code requirement are that the appropriate structural materials be selected for the service environment, the vessel be designed according to the rules outlined in the code, the vessel be fabricated by qualified ASME Code rated manufacturers and lastly that the vessel be hydrostatically pressure tested to a minimum of 1.5 times the working pressure. Elevated temperature vessels require higher pressure tests if tests cannot be performed at the working temperature.

All aspects of the ASME requirements were followed for the pebble-bed heater design and ASME certification documents were issued for all pressure components in the design.

5. PEBBLE-BED THERMODYNAMIC MODELING AND PRELIMINARY DESIGN

5.1 Pebble-bed Thermal Storage Mass Selection

The desirable characteristics for a thermal storage material include the following:

- (1) High specific heat
- (2) High thermal diffusivity
- (3) High density
- (4) Reversible heating and cooling
- (5) Chemical and geometric stability
- (6) High operation temperature
- (7) Low cost
- (8) Sufficient strength to support compression load from packing of material
- (9) Resistance to thermal shock

Table 5-1 shows a material evaluation chart which ranks density, heat capacity, thermal resistance, temperature limit, cost and compressive strength for three material classes of interest.

TABLE 5-1 THERMAL STORAGE MATERIALS EVALUATION CHART

MAT CLASS		DENS	C _p	K	T _{max}	COST	COMP STR
WEIGHT	TOTAL RANK	5%	25%	25%	25%	10%	10%
FE	1.00	1.00	1.00	1.00	1.00	1.00	1.00
STEEL	0.98	1.00	1.00	1.33	1.00	0.50	0.50
Al ₂ O ₃	1.60	1.93	0.49	2.85	2.00	1.00	0.75

Each criterion is ranked relative to the iron class material (FE) which has the value 1.00 for all 6 criterion. Weighting factors are used to show the relative importance of each criterion in the total thermal storage system design. Heat capacity, thermal resistance (inverse of thermal conductivity) and temperature limit are weighted the highest at 25% followed by cost and strength at 10% and density at 5%. Total ranking values which are less than 1.0 show a decreased performance in the thermal storage application and greater increased performance over iron materials.

Only the ceramic, Al₂O₃, material class that was studied has an increased performance rank over iron. Because the iron class and ceramic class both are relatively inexpensive, readily available and possess ideal physical properties as a thermal storage material, these two classes of materials will be considered for use in the high temperature pebble-bed heater.

The type of material specifications within these two classes to be considered are castable corrosion resistant iron alloys (i.e. Ni-Resist) and ceramic metal oxides (i.e. alumina, etc.). Nominal thermophysical properties of typical Ni-Resist alloys and 90% dense alumina ceramics are as follows:

	Ni-Resist	Alumina
Density (kg/m ³):	6960	3600
Specific Heat (J/(kg·°C)):	450	920
Conductivity (W/(m·°C) @ 400°C:	20	7
Maximum use temperature (°C):	870	1500

For an identical volume of each of the materials, the ratio of the specific heat times density for Ni-Resist and alumina is approximately 1.0. This implies that as far as heat storage per unit volume is concerned, either material is suitable for use as the thermal storage media. In terms of the material's ability to give up or absorb heat rapidly (i.e. thermal conductivity), Ni-Resist has about 1/3 the thermal resistance than that of alumina at 400°C (also at higher and lower temperatures). The material temperature use limitation for Ni-Resist is about 1/2 that of alumina. This shows that alumina can hold more heat if the

capability to heat alumina to its maximum use temperature of 1500 °C (2730°F) is available.

Calculations were performed to evaluate the time dependent convective heat transfer response of Ni-Resist and alumina to a sudden flow of air. For two convective heat transfer conditions, Figure 5-1a & b show the relative heat loss versus time of a .025 meter diameter (1 inch) sphere for Ni-Resist and alumina. Calculations were made for two different heat transfer coefficients, h , which illustrate the influence of gas velocity. Referring to the figure, Ni-Resist gives up 10 to 20 percent more heat during the time interval running from approximately 5 minutes up to 20 minutes from the start of sphere cooling. At longer times, the heat given up is about the same for both materials. This shows that for small time periods, Ni-Resist is a much better heat transfer mass than alumina and for longer periods they have about the same performance. Cost and availability of each of the materials are approximately the same for small quantities (≈ 1000 lbs).

Ni-Resist offers the best performance in terms of thermal conductance for short heating times as long as the maximum bed temperature is held below 870°C. The electrical heating system which is considered for use in charging the pebble-bed has a maximum use temperature of approximately 1500°F (816°C). Additionally, the use of LN_2 has introduced a thermal stress problem with the hot material being subjected to cryogenic fluid. The response of ceramics to high thermal stresses is unpredictable because ceramics are brittle materials and fracture easily. Because Ni-Resist is a ductile material with a high strength capability, it was selected as a pebble material rather than ceramics (90% dense alumina) to achieve a higher reliability with pebbles which are known not to fracture from high thermal stress environments.

5.2 Pebble-bed Thermodynamic Modeling

A thermodynamic model of the pebble-bed heater was developed to parametrically calculate the time dependent bed temperatures for the various pebble-bed design conditions. A reference on the modeling of regenerative pebble-bed type heat exchangers was used to help develop the thermodynamic model of the pebble-bed heater. This document is reference ⁶. Many of the equations were taken directly from this text and are duplicated here.

Figure 5-2 shows the thermal and geometric model of a generic packed bed single pass regenerative heater. In the figure, X corresponds to the distance from the upstream edge of the bed to some axial point downstream. The bed is assumed to be cylindrical

FIGURE 5-1A
THERMAL MASS STORAGE MEDIA PERFORMANCE
 $h = 25 \text{ W/(m}^2 \cdot ^\circ\text{C)}$

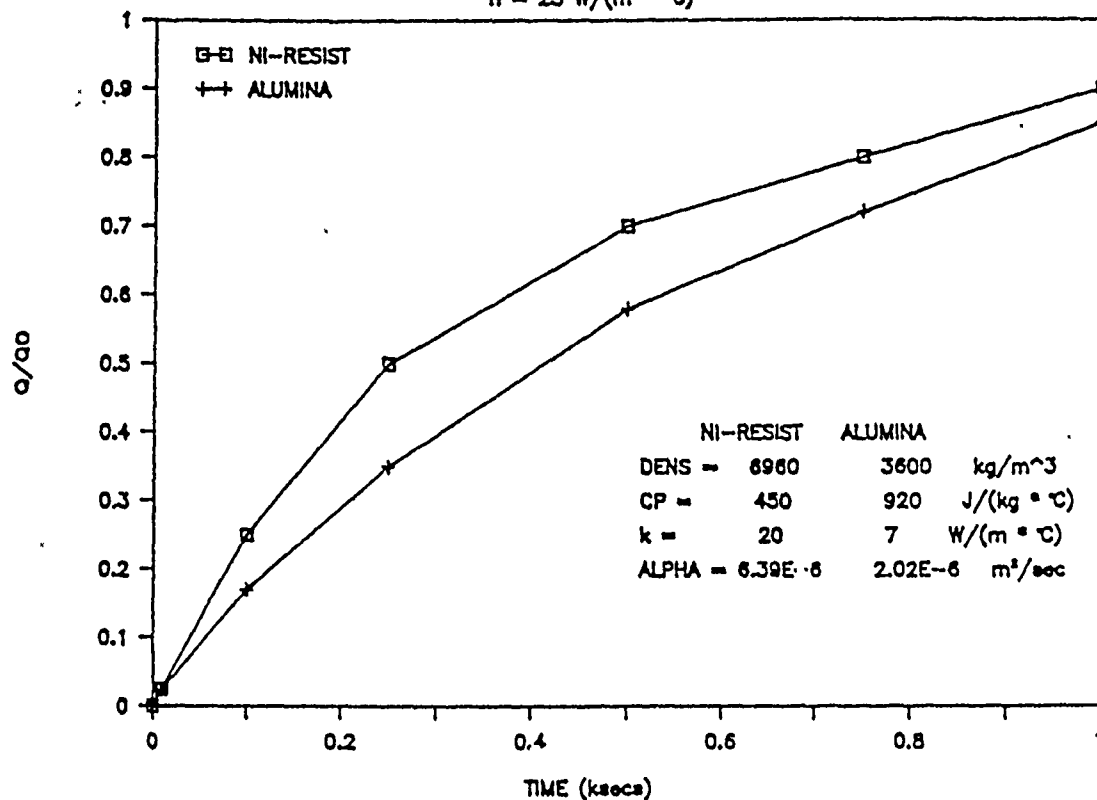
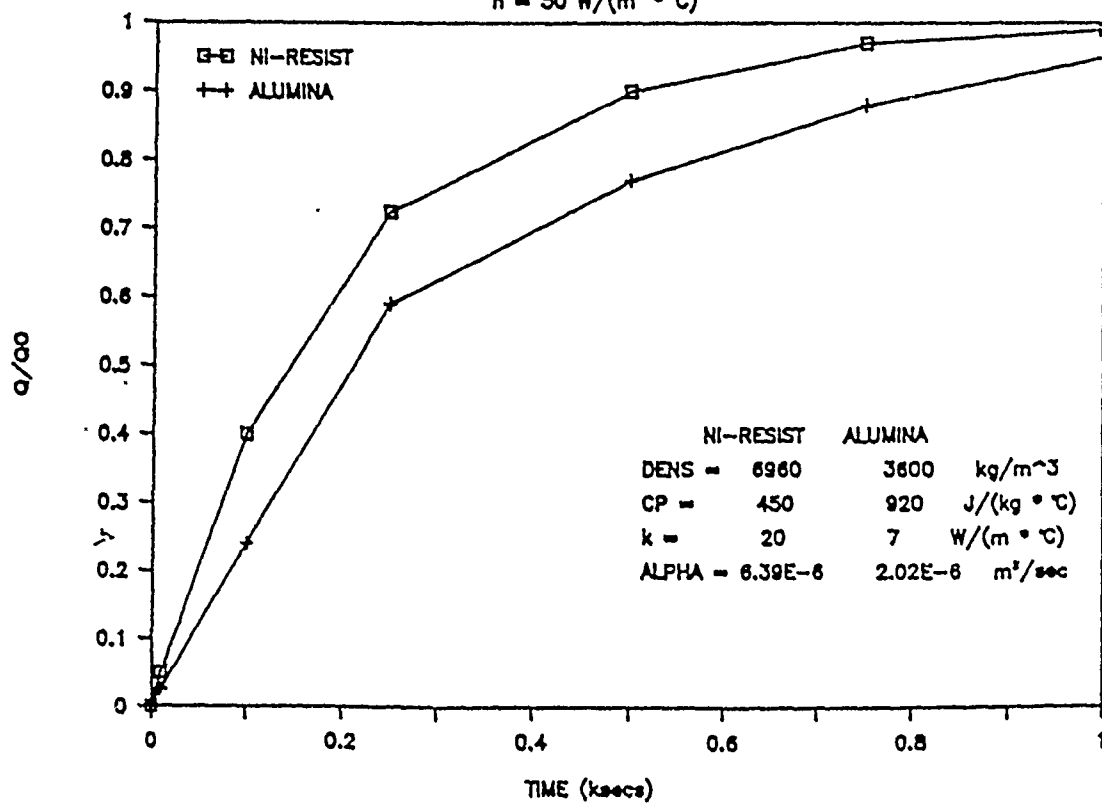


FIGURE 5-1B
THERMAL MASS STORAGE MEDIA PERFORMANCE
 $h = 50 \text{ W/(m}^2 \cdot ^\circ\text{C)}$



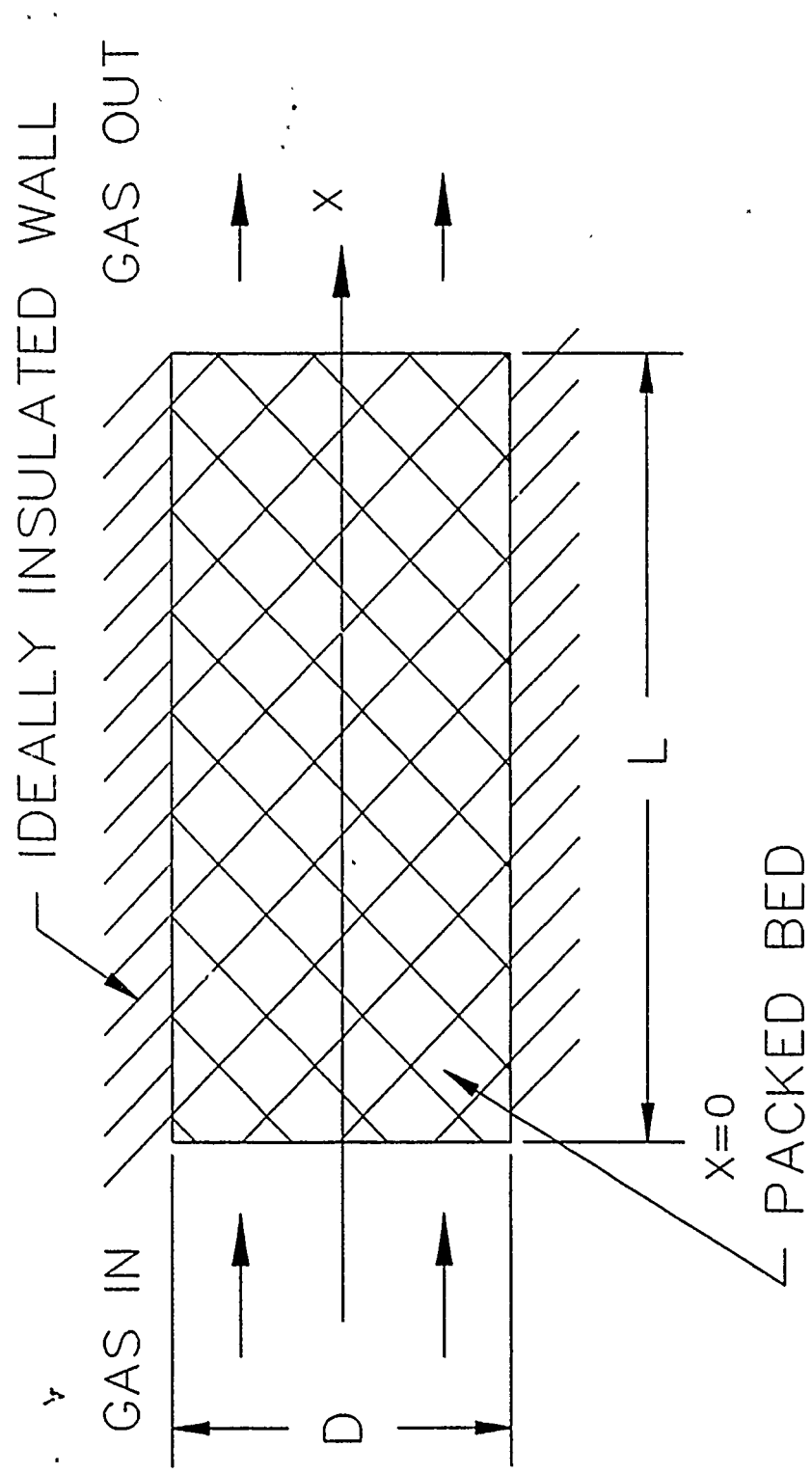


FIGURE 5-2 SCHEMATIC OF PEBBLE-BED HEATER THERMODYNAMIC MODEL

in cross section and D is the diameter of the pebble-bed of length L. The mathematical model consists of two energy balance equations, one for the fluid medium and another for the packed bed medium. The model only takes into account the exchange of heat by means of convection to or from the fluid and neglects heat loss to the walls of the bed. In our design, this is a reasonable assumption because the interior pebble-bed wall is thin and is insulated from the pressure vessel wall.

For the fluid, the amount of heat convected from the bed to the constant mass flow fluid is equal to the rise of internal energy of the fluid. For the bed, the amount of heat convected away from the bed is equal to the change in internal energy of the bed material with respect to time. A simplified one dimensional mathematical model of the single pass packed bed regenerative heater consists of the following two energy balance equations:

for the fluid/gas:

$$h \cdot A \cdot (t_m - t_f) = \dot{m} \cdot L \cdot c_f \cdot \frac{dt_f}{dx} \quad (\text{EQ 5-1})$$

for the bed:

$$h \cdot A \cdot (t_f - t_m) = S_{fr} \cdot (1 - \epsilon) \cdot L \cdot p_m \cdot c_{pm} \cdot \frac{dt_m}{d\tau} \quad (\text{EQ 5-2})$$

where:

- x, distance along the bed, m (ft)
- τ , time from the start of blowdown, sec
- h, convective heat transfer coefficient, W/m²/°K (Btu/(sec·ft·°R) - obtained from available heat transfer correlations for packed beds.
- A, convective heat transfer surface area, m² (ft²) (surface area of all the particles in the bed)
- t_m, temperature of the bed at distance x and time τ , °K (°R)
- t_f, temperature of the fluid at distance x and time τ , °K (°R)
- m, mass flowrate of the fluid, kg/sec (lbm/sec)
- L, length of the bed, m (ft)
- c_f, specific heat of the fluid, J/kg/°K (Btu/lbm/°F)
- S_{fr}, frontal area of the pebble-bed, m² (ft²)
- ϵ , volumetric efficiency of the bed, dimensionless (volume of the particles/volume of the container vessel)
- p_m, density of the bed material, kg/m³ (ft³)
- c_{pm}, specific heat of the bed material, J/kg/°K (Btu/lbm/°F)

The assumptions of this model follow:

1. The particles have infinite thermal conductivity.
2. One dimensional fluid flow.

3. No heat loss to the container walls; i.e. perfectly insulated.
4. Thermal and physical properties do not vary with temperature.
5. Uniform convective heat transfer coefficient.
6. The fluid is in plug flow and the fluid velocity does not vary along the bed length.
7. The bed is initially at a uniform temperature.
8. Radiation effects are neglected.

The above equations neglect two significant effects in packed bed heat transfer. These are intraparticle conduction, the conduction of heat from the center of the particle to the surface and axial dispersion, extensive mixing of the fluid in small eddys within the bed which enhances heat transfer.

If intraparticle conduction and axial dispersion effects are not accounted for, the heat transfer calculated from the above relations would be conservative. Axial dispersion greatly increases the heat transfer from extensive mixing and intraparticle conduction decreases heat transfer from a resulting decreased surface temperature of the pebbles. Including these effects in our model would introduce a second order term, making the solution much more complex. A modification of the standard correlation heat transfer coefficient was used and can implicitly account for these effects provided some bed conditions are met.

To account for intraparticle conduction and axial dispersion effects on the pebble-bed heat transfer, an effective heat transfer coefficient is calculated and is used instead of the standard correlation heat transfer coefficient. The following equation is used to calculate the effective heat transfer coefficient:

$$\frac{1}{h_e} = \frac{1}{h} \cdot \left[1 + \frac{Bi}{5} \right] \cdot \beta^2 + \frac{1}{Pe} \quad (EQ 5-3)$$

where,

h_e , effective heat transfer coefficient, $W/m^2/^{\circ}K$
($Btu/(sec \cdot ft \cdot ^{\circ}R)$)

h , standard correlation heat transfer coefficient, $W/m^2/^{\circ}K$
($Btu/(sec \cdot ft \cdot ^{\circ}R)$)

Bi , Biot Number, dimensionless

calculated by: $Bi = \frac{h \cdot r_o}{k_m} \quad (EQ 5-4)$

V_H , Heat capacity ratio

calculated by:
$$V_H = \frac{pm \cdot cm \cdot (1 - \epsilon)}{pf \cdot cf \cdot \epsilon} \quad (\text{EQ 5-5})$$

β , Thermal capacity ratio, dimensionless

calculated by:
$$\beta = \frac{V_H}{V_H + 1} \quad (\text{EQ 5-6})$$

Pe, Peclet Number, dimensionless

calculated by:
$$Pe = \frac{(p_f \cdot c_f \cdot v_a)^2 \cdot S_{fr} \cdot L \cdot \epsilon}{k_f \cdot A} \quad (\text{EQ 5-7})$$

The three parameters, Bi, β , and Pe, determine if the simplified model presented above could satisfactorily predict the performance of the pebble-bed heat exchanger. If the thermal conductivity (k_m) of the bed particle is very large compared to the heat transfer from the bed particle ($h \cdot r_o$), the resulting Biot number is small and approaches zero as a limit. Thus the bed material would have a uniform temperature making intra-particle conduction not a limiting factor for heat transfer. The Biot number is ultimately a measurement of the material's ability to give up heat to a convective environment.

5.2.1 LN₂ Heat Transfer and Flow Modeling

Analyses were made to predict the performance of the pebble bed heater using LN₂ as the heat transfer fluid. Since multiple phase flow always exists during evaporation and superheat of a cryogenic fluid, finite difference modeling of the heat transfer within the bed becomes extremely difficult.

Two phase heat transfer involves several simultaneous flow and heat transfer predictions in order to calculate the heat flow from the pebbles to the liquid/gas. Several flow regimes are usually present and each flow regime has a different heat transfer correlation function. The solution to a 2 phase heat transfer problem involves first predicting the type of flow regime that is present along the bed path, applying the heat transfer correlation to that flow regime and then predicting the influence of the heat transfer on the flow type. There are a minimum of seven different possible flow regimes possible for vertical pipe flow. These are (Reference ⁷):

1. Liquid - single phase
2. Bubble or Emulsion - 2 phase
3. Slug - 2 phase
4. Semiannular - 2 phase
5. Annular - 2 phase

6. Annular Dispersed - 2 phase
7. Gas - single phase

Prediction of flow regimes for simple pipe flow with water or other noncritical liquids are readily available. Flow prediction in a LN₂ pebble-bed with turbulent mixing and uncertain radial dispersion effects is not practical under the present scope of this effort. This type of detailed flow analysis, therefore, was abandoned for an energy balance method combined with the model already developed.

By conducting pebble-bed experiments with LN₂ heat transfer flow, a heat transfer coefficient could be generated for several different flow rates. This coefficient can then in turn be used to predict the pebble-bed sizes for other bed geometries.

5.3 Full Scale Sizing

The full scale LB/TS pebble-bed heating system is sized according to the requirements set forth in Section 4.2.1. Table 4-4 gave the seven required shock overpressure simulation conditions and the pebble-bed driver gas heating requirements. The full scale LB/TS will be sized in two stages, parts each treated separately. The first part will perform the evaporation stage and the second part will perform the superheat stage.

Evaporator Sizing

An estimate was made as to the amount of pebble bed material required for the evaporator stage of the LN₂ driver gas supply system. A simple lumped heat capacity calculation was made to determine evaporator sizes using the following equation:

$$m_b = \frac{h_g \cdot m_g \cdot (1 + \epsilon_{th})}{Cp_b \cdot (Tb_i - Tb_f)} \quad (EQ 5-8)$$

where:

m_b , mass of bed material required, kg (lbm)
 h_g , total specific enthalpy required by gas, J/kg (Btu/lbm).
 m_g , total mass of gas to evaporate, kg (lbm).
 ϵ_{th} , thermal efficiency of system including heat losses, %.
 Cp_b , specific heat of the bed material, J/kg/°K (Btu/lbm/°R).
 $Tb_{i(f)}$, initial (final) temperature of the bed, °K (°R)

The specific enthalpy from cryogenic liquid to room temperature gas is a function of two components; the heat of vaporization and the sensible heat to 290°K (520°R). The following lists the properties of liquid Nitrogen.⁸

Cryogenic Nitrogen Properties @ 101.35 kPa (14.7 psia)

Boiling Point:	77.4°K (139.3°R)
Density of Liquid:	808.29 kg/m ³ (50.46 lbm/ft ³)
Latent Heat of Vaporization:	199 kJ/kg (85.6 Btu/lbm)
Sensible Heat (to 290°K):	229 kJ/kg (98.5 Btu/lbm)
Total Heat to 290°K:	428 kJ/kg (184.1 Btu/lbm)

At higher pressures, the total heat (vaporization and sensible) required decreases since the pressurization process adds energy to the liquid pressurized liquid. Normally, this amount is small compared to the vaporization heat and is ignored in the simplified analysis.

The following Table 5-2 gives the full scale LB/TS evaporation heat requirement for each of the seven (7) cases.

TABLE 5-2 LB/TS DRIVER GAS EVAPORATION HEATING REQUIREMENTS

CASE NO	GAS MASS OR LIQUID VOLUME				HEAT INPUT	
	kg	liter	klbm	gal	MJ	kBtu
1	74996	92612	164.9	24464	32098	30425
2	71811	88679	157.9	23425	30735	29133
3	61285	75681	134.8	19991	26230	24863
4	55446	68470	121.9	18086	23731	22494
5	45904	56687	100.9	14974	19647	18623
6	31270	38615	68.8	10200	13384	12686
7	17790	21969	39.1	5803	7614	7217

The maximum operation condition, Case 1, is used to size the pebble-bed evaporator. For a thermal efficiency (i.e. pebble-bed and driver heat loss) of 10%, a bed initial temperature of 1035°K (1863°R), a bed final temperature of 50°K above final gas temperature of 290°K, and a bed heat capacity (steel assumed) of .45 kJ/kg/°K (.10 Btu/lbm/°R); the total pebble bed mass is calculated to be approximately 112,895 kg (248,370 lbm).

LB/TS Evaporator Bed Mass Requirement: 112,895 kg (248,370 lbm)

LB/TS Geometry Configuration

The present configuration of the full scale LB/TS consists of 9 separate compressed gas driver vessels in parallel. Although in practice the individual driver lengths vary to minimize driver rarefaction wave interference; it is presumed for this analysis that each driver holds the same amount of gas. Finally, there will be one pebble-bed superheater per driver to simplify operation and minimize heater size.

The following Table 5-3 summarizes the geometry of the full scale LB/TS which has evolved through the years of study by BRL, DNA,

HDL and their contractors. The effective diameter is equivalent diameter of the driver if only 1 driver is used. This effective diameter is only used in calculating shock flowfields using various shocktube models.

TABLE 5-2 LB/TS FULL SCALE GEOMETRY SUMMARY

Driver Parameter	Units	Value
Volume	m ³ (ft ³)	1227 (43,330)
Effective Diameter	m (ft)	5.49 (18.0)
No. of Drivers	- -	9
Inner Diameter (each)	m (ft)	1.83 (6.0)
Average Length	m (ft)	52 (171)

Full Scale LB/TS Superheater and Evaporator

For simplicity of design, the full scale pebble bed heaters are assumed to be fabricated from the same pressure vessel shell as the drivers. The evaporator and superheater will be combined in series with each of the evaporation and superheat sections which are designed separately. For both the evaporator and superheater, the inner diameter of the bed is a function of the driver inner diameter (1.83 m), the insulation thickness required for the hot pebble bed, and the liner which contains the bed material and prevents crushing of the insulation. Assuming an insulation thickness of .04 m (1.5 inch) and a bed containment liner thickness of .013 m (.5 inch), the bed inner diameter is approximately 1.72 m (5.65 ft).

Due to the complex nature of the 2 phase flow within the cryogenic evaporator, the computer program PEBBED cannot not be used with confidence to calculate the pebble bed performance for liquid nitrogen vaporization. Therefore, using the simplified heat capacity formulation for the evaporator bed, the bed length is calculated from the bed mass required, the spherical particle bed packing void fraction, and the bed cross sectional area in the following equation:

$$L_{bed} = \frac{m_{bed}}{p_{bed} \cdot A_{bed} \cdot (1 - \epsilon)} \quad (EQ 5-9)$$

L_{bed} , length of pebble bed, m

m_{bed} , mass of bed material required (from eq. 1), kg

ϵ , void fraction of the bed $\approx .35$

p_{bed} , density of the bed material, kg/m³
 $= 7897 \text{ kg/m}^3 \text{ } (.284 \text{ lb/in}^3)$

A_{bed} , crossectional area of bed, m²
 $= 1.72 \cdot \pi / 4 = 2.32 \text{ m}^2$

For the bed mass of 112,895 kg, the total evaporator bed length for all 9 drivers combined is calculated as 9.48 meters (31.10 feet). For each of the 9 evaporators, the required length is 1.05 meters (3.44 feet). This is the minimum length required by the pebble bed and only takes into account the heat losses within the heater and driver. If a high flowrate is desired, as is the case with filling an uninsulated driver, the heat drawn from the bed may not be sufficient due to the limiting value of the thermal conductivity of the balls. Therefore, either smaller diameter balls, hollow balls or a longer bed is required to account for the inability of the present 0.75 inch diameter balls to transfer the required heat in the allowed heating time.

Superheater Sizing

The superheater for the LB/TS is sized using the computer program PEBBED. As a starting point in the analysis, the lumped heat capacity equation is used to predict initial sizes. For the same bed geometry as the evaporator (see above), the length of the superheater can be calculated using equations 1 and 2. The total mass of material required using case 1 as the design point is calculated from equation 5-8.

For the superheater, the initial bed temperature is assumed to be 1035°K and the bed final temperature is assumed to be 50°K above the required fluid outlet temperature of 644°K. Using a thermal heat loss of 10% of the total heat required and a heat energy of 27561 MJ, the bed mass of the superheater required is calculated to be approximately 152,769 kg (336,093 lbm).

LB/TS Superheater Bed Mass Requirement: 152,769 kg (336,093 lbm)

The bed length is calculated from equation 2. The length minimum length required is 12.86 m (42.1 ft). For each of the 9 drivers the average length is 1.43 m (4.69 ft).

5.4 1/6th Scale Sizing

1/6th scale pebble-bed sizing will be made under a follow-on program to provide a pebble-bed evaporator/superheater to BRL for the 2.44 meter shocktube LB/TS tesbed.

5.5 1/48th Scale Sizing & Preliminary Design

The 1/48th scale superheater sizing was performed for a superheater design first. The combined evaporator/superheater design used the old superheater size configuration because the design was complete, parts had been ordered and fabrication had commenced. Only modifications to the design to account for LN₂ use were made.

5.5.1 1/48th Scale Superheat Pebble-Bed Heater

Using the requirements from Table 3-9, pebble bed performance calculations were made using nitrogen gas and a Ni-Resist pebble-bed to determine the minimum size requirement for the superheat pebble-bed.

The bed constant parameters are as follows:

Inner diameter:	0.305 m (1.0 ft)
Particle diameter:	0.01905 m (.75 inch)
Porosity:	0.35
Initial temperature:	760°C (1400°F)

The Ni-Resist properties used in the analysis are as follows:

Density:	6960 kg/m ³ (.251 lb/in ³)
Specific heat:	450 J/kg/°K (.105 Btu/lbm/°R)
Thermal conductivity:	20 W/m/°K (12 Btu/h/ft/°F) (@ 425°C, 800°F)

The nitrogen gas properties used in the analysis are as follows:

Initial pressure:	101.3 kPa (1 atm)
Inlet temperature:	15°C (60°F)
Final pressure:	11.6 Mpa (1690 psia)
Outlet temperature:*	417°C (782°F)

* Includes additional 50°C (90°F) to account for temperature drop.

The specific heat and thermal conductivity of nitrogen is dependent on temperature and is calculated within the computer program. Density is temperature and pressure dependent and is calculated from the ideal gas law: $PV = mRT$.

The parameters which were varied in the calculations were pebble bed length and gas flow rate. The bed length was varied from 1.0 meter (3.28 ft) to 2.00 meters (6.56 ft) in increments of .25 meter (.82 ft). The instantaneous bed temperature profile was calculated for two nitrogen flow rates to simulate the effect of bypassing the cool inlet gas to a mixer downstream of the heater to cool the superheated gas exiting from the pebble bed. The flow rates used were the maximum capacity of the BRL LN₂ pumping system, 0.045 kg/sec (0.1 lbm/sec), and one half the pumping capacity, 0.0225 kg/sec (0.05 lbm/sec).

Figure 5-3 and 5-4 show the energy transferred to the gas for each bed length as a function of time for the two flow rates of interest (0.045 and 0.0225 kg/sec). Considering the lower flow rate condition as the design point, a 50 MJ energy requirement (actual heat needed is 48.3 MJ) could be met with a 2.0 meter long bed in about 48 minutes. This exceeds the heating time

requirement (40 minutes) by 8 minutes.

For the higher flow condition, the same bed length could supply the 50 MJ heat in about 25 minutes. This is roughly 1/2 the lower flow rate heating time requirement. For a 1 meter long bed, the 50 MJ heat time is approximately 57 minutes for the lower flow and 32 minutes for the higher flow condition. This also shows a 2 to 1 relationship between the higher and lower flow conditions.

Because the flow rate through the bed will vary during the gas heating cycle due to bleed off to the mixing chamber, an average flow condition would have to be used to size the heater bed. Assuming an inversely linear relationship between flow rate and heating time for constant heat output as was shown by the two flow rate calculations (i.e. a doubled flow rate will decrease the heating time by 1/2), an optimal average flow rate through the bed for a 40 minute heating requirement works out to 2/3 the maximum flow rate of 0.045 kg/sec or 0.030 kg/sec (0.066 lbm/sec).

An additional calculation was made using a flow rate of 0.030 kg/sec and the results are shown in Figure 5-5. The length of the bed can now be taken directly off of the figure and is approximately 1.25 meters (4.1 feet) for the 50 MJ and 40 minute heatup time requirements.

It is apparent from Figure 5-5 that a significant amount of energy still remains stored in the pebble bed after the 40 minute heatup time and energy requirements are met. This is an important added benefit of the pebble bed heater. It can store heat required to supply additional hot gas during test hold periods. As an example, the maximum amount of heat which is stored in the pebble bed heater is approximately 138.5 MJ assuming the bed is cooled from the initial temperature of 760°C to the gas inlet temperature of 15°C. If the bed is cooled to the required gas outlet temperature of 417°C, the maximum heat stored is approximately 72.5 MJ. If a heat transfer rate of 20 kW is assumed, then the additional heat stored in the bed (referenced to the gas outlet temperature) after heatup is approximately 25 MJ which corresponds to a holding time of approximately 20 minutes. This is a very conservative estimate because the bed does not cool down uniformly. The inlet part of the bed will actually be cooled to a much lower temperature than the required gas outlet temperature.

5.5.2 1/48th Scale Pebble-Bed Combined Evaporator and Superheater

The theoretical calculations for the 1/48th scale pebble-bed evaporator/superheater design were calculated by "PEBBED" using an initial gas temperature of 78°K and a constant flowrate of 4, 6 and 8 GPM LN₂. The calculations made are given in Appendix B.

FIGURE 5-3

ENERGY TRANSFERRED TO GAS BY PEBBLE BED HEATER

FLOWRATE = 0.045 KG/SEC (0.1 LBM/SEC)

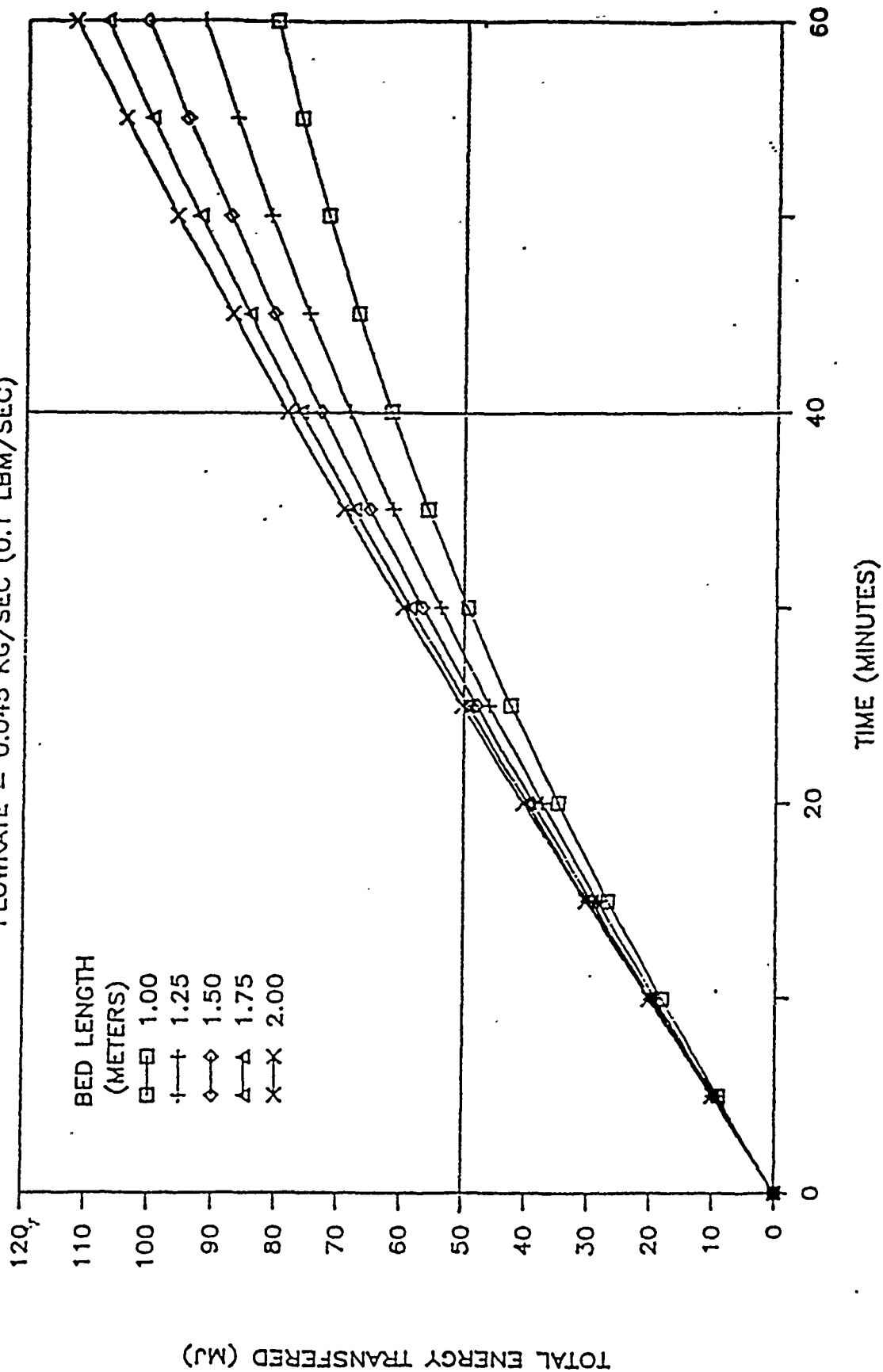


FIGURE 5-4

ENERGY TRANSFERRED TO GAS BY PEBBLE BED HEATER

FLOWRATE = 0.0225 KG/SEC (0.05 LBM/SEC)

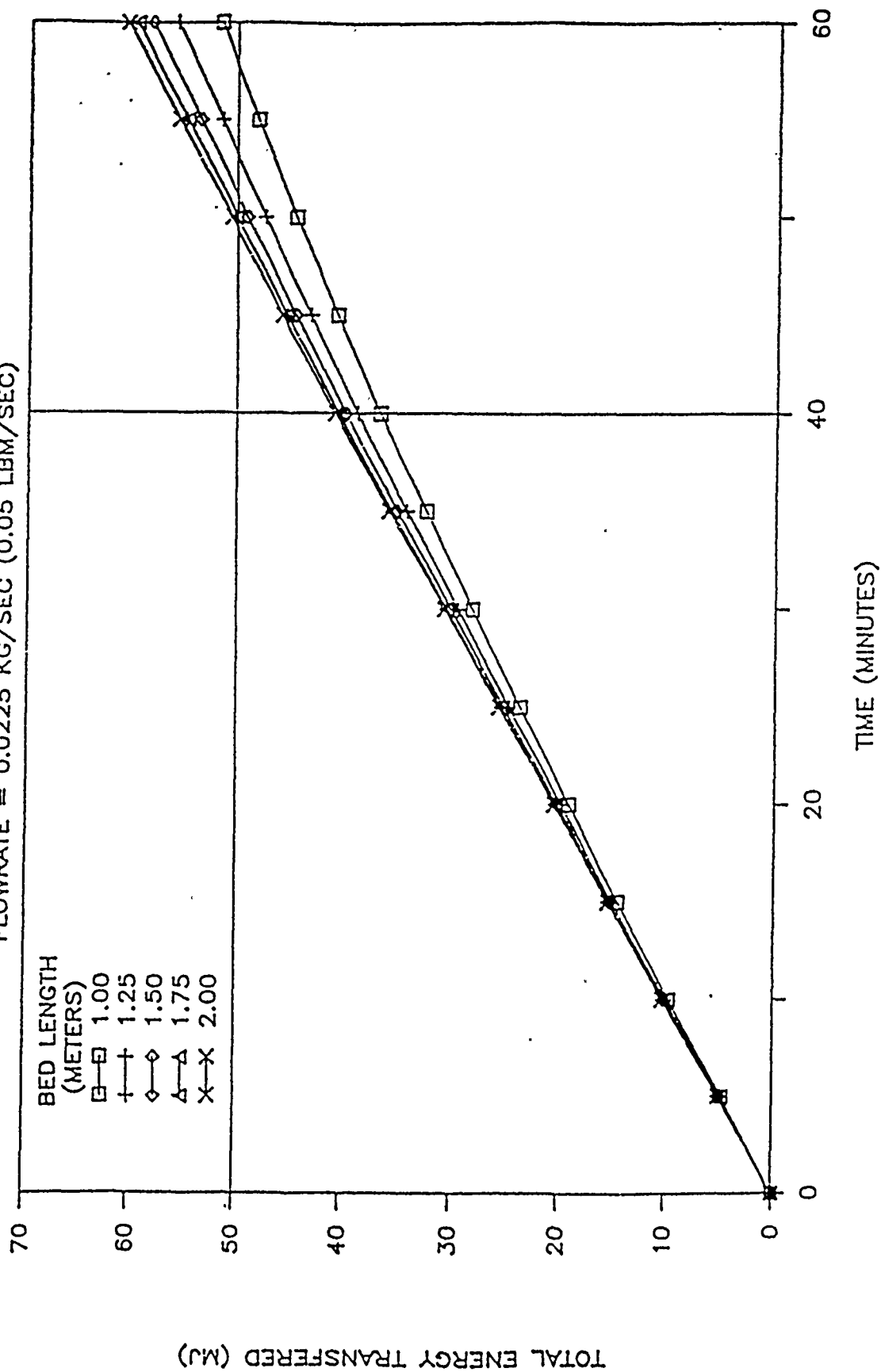
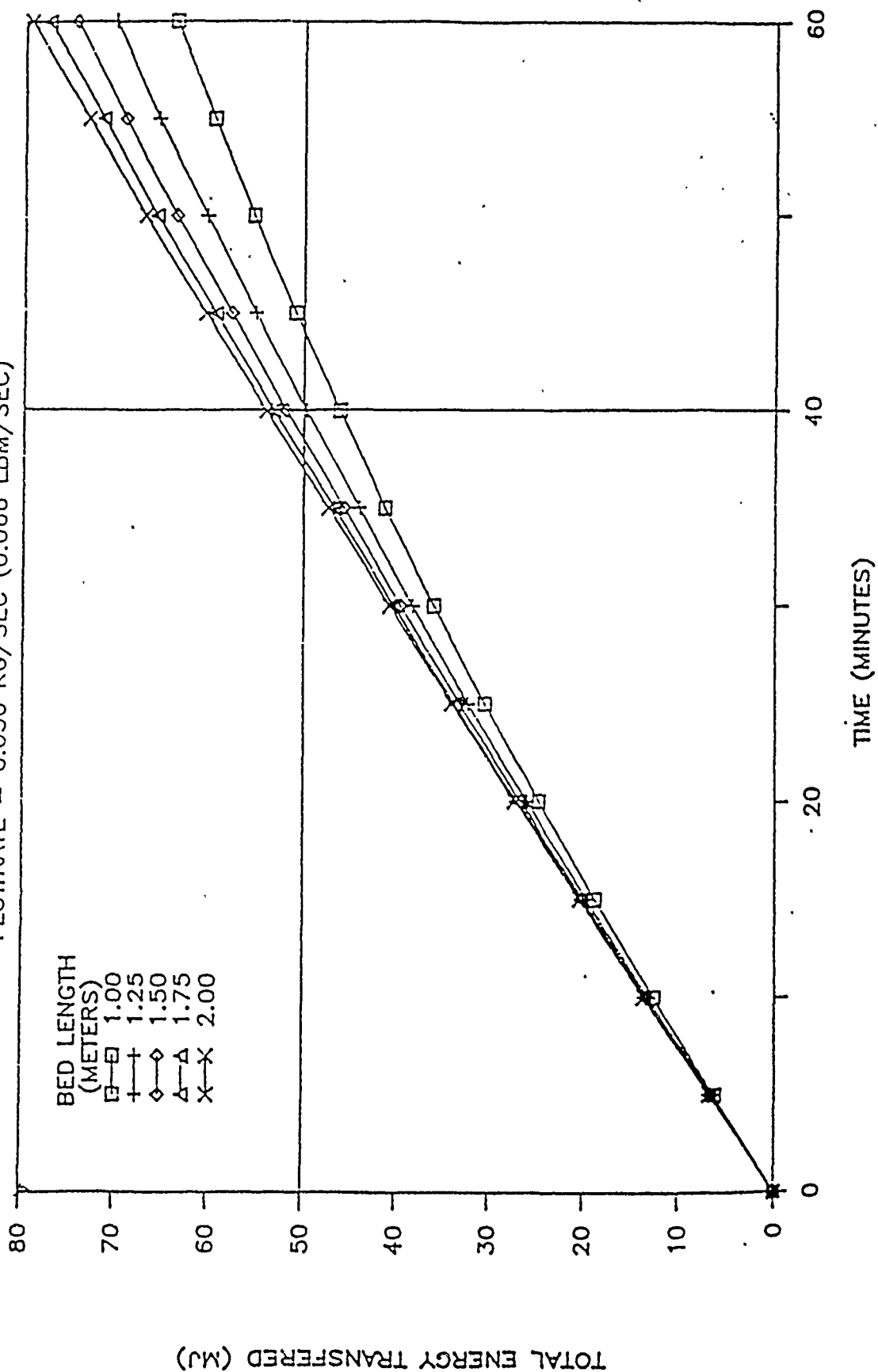


FIGURE 5-5

ENERGY TRANSFERRED TO GAS BY PEBBLE BED HEATER

FLOWRATE = 0.030 KG/SEC (0.066 LBM/SEC)



6. 1/48TH SCALE DETAILED MECHANICAL DESIGN

ASME Pressure Vessel Code

The pebble-bed heater mechanical design is according to the rules and practices of the American Society of Mechanical Engineers (ASME) Boiler and Pressure Vessel Code. Section VIII, Division 1 of the ASME code provides basic requirements for the design methodology and fabrication of pressure vessels which operate at pressures up to 3000 psig and at temperatures to the maximum ASME specified temperature rating for the material for all nonnuclear rated pressure containment vessels. Section VIII, Division 2 provides alternate rules for pressure vessel design and allows for higher pressure vessels (>3000 psig) that require a more thorough and precise design methodology. Division 2 rules and practices are meant for use on specially constructed pressure vessels for high pressure. Division 1 provides adequate safety allowances and fabrication control for the pressures and temperatures of the pebble-bed heater design. Thus because the pebble bed heater containment and piping will be fabricated from available off-the-shelf pressure components which are rated according to ASME accepted ANSI ratings, Division 2 will not be applied to the pebble bed heater design. The following outlines the design methodology applicable to the heater design under Division 1 of the ASME code.

Subsection A: General Requirements

Part UG: General Requirements for All Methods of
Construction and All Materials

Scope:	UG-1
Materials:	UG-4 through UG-15
Design:	UG-16 through UG-35
Openings and Reinforcements:	UG-36 through UG-46
Braced and Stayed Surfaces:	UG-47 through UG-50
Ligaments:	UG-53 through UG-55
Fabrication:	UG-75 through UG-85
Inspection and Tests:	UG-90 through UG-103
Marking and Reports:	UG-115 through UG-120
Pressure Relief Devices:	UG-125 through UG-136

Subsection B: Requirements Pertaining to Methods of Fabrication of Pressure Vessels

Part UW: Requirements for Pressure Vessels
Fabricated by Welding

Part UF: Requirements for Pressure Vessels Fabricated by
Forging

Subsection C: Requirements Pertaining to Classes of Materials

Part UCS: Requirements for Pressure Vessels Constructed of

Carbon and Low-Alloy Steels
 Part UHA: Requirements for Pressure Vessels Constructed of
 High-Alloy Steel
 Part UHT: Requirements for Pressure Vessels Constructed of
 Ferritic Steels with Properties Enhanced by Heat
 Treatment

ASME Design Equations

The first equation calculates the thickness of a pressure shell based on the maximum circumferential (hoop) stress:

$$t = \frac{P \cdot R}{S \cdot E - 0.6 \cdot P} \quad \text{or} \quad P = \frac{S \cdot E \cdot t}{R + 0.6 \cdot t} \quad (\text{EQ 6-1})$$

The second equation calculates the thickness of the shell based on the maximum longitudinal stress:

$$t = \frac{P \cdot R}{2 \cdot S \cdot E + 0.4 \cdot P} \quad \text{or} \quad P = \frac{2 \cdot S \cdot E \cdot t}{R - 0.4 \cdot t} \quad (\text{EQ 6-2})$$

where,

- P, design working pressure, psig
- R, internal radius of the shell, in
- S, maximum allowable tensile stress at the design working temperature, psi
- E, joint efficiency

The design working pressure should account for all possible pressure forces including hydrostatic head and impulses. The allowable tensile stress is calculated from a number of design safety factors and material design criteria and is tabulated in the ASME code for each material covered under the code. The design working temperature is the maximum mean metal temperature through the thickness that the material will exhibit under service. The joint efficiency is a factor that takes into account the type of welded joint used in the design. For a butt welded joint where both the OD and ID are welded (i.e. double-welding) and the weld is not spot radiograph examined for flaws, the joint efficiency per the ASME code is 0.7 (Section UW-12; Table UW-12).

Considering a pressure vessel made to the specification of SA-106 carbon steel for seamless pipe and tube. The design working temperature of that material is 500°F and the allowable stress at that temperature is 15 ksi from -20 to 65 °F. From equations 6-1 & 6-2, the minimum wall thickness of a 18 NPS Schedule 160 pipe (ID = 14.438") vessel at a design pressure 2000 psig and temperature of 500°F; and for a joint efficiency of 0.7 is 1.55 and 0.66 inches, respectively. ASME requires the greater thickness from

the two equations.

ASME Material Specifications and Selection

The ASME material specifications were examined to determine what materials are required and applicable for the various components of the pebble bed heater design. The examination of Code materials indicate the use of the following materials in the respective application.

Pebble Bed Pressure Vessel and Misc Piping:

SA-105	Forgings, Carbon Steel, for Piping Components
SA-106	Seamless Carbon Steel Pipe for High Temperature Service
SA-182	Forged or Rolled Alloy-Steel Pipe, Flanges, Forged Fittings, and Valves and Parts for High Temperature Service
SA-312	Seamless and Welded Austenitic Stainless Steel Pipe for High Temperature and General Corrosive Service
SA-403	Wrought Austenitic Stainless Steel Fittings

6.1 Pebble-bed Heater System Components

There are 6 main components of the pebble bed heater assembly. These are:

- (1) Heater Bed Pressure Shell & Heads, Carbon Steel.
- (2) Thermal Mixer Pressure Shell, Stainless Steel.
- (3) Pebble-Bed Liner, Stainless Steel.
- (4) Pebble-Bed Baffle Assembly, Stainless Steel.
- (5) Bypass Gas Adapter Flange, Stainless Steel.
- (6) Outlet Gas Adapter Flange, Alloy Steel.

The mechanical design for the heater bed pressure shell in Figure 6-1. The thermal mixer pressure shell design is shown in Figure 6-2.

6.1.1 Heater Pressure Containment Shells

The heater pressure shell is composed of standard pressure parts rated according to ASME pressure vessel code standards. ANSI (American National Standards Institute) pressure/temperature standards are excepted within ASME as qualified for code use. The heater pressure shell assembly is a welded assembly composed of three main components plus two bolted flange heads. Bolting materials are also listed below. The certification documents for the heater and mixer pressure shells are on file with SPARTA and are available upon request.

FIGURE 6-1

MECHANICAL DESIGN FOR HEATER PRESSURE SHELL

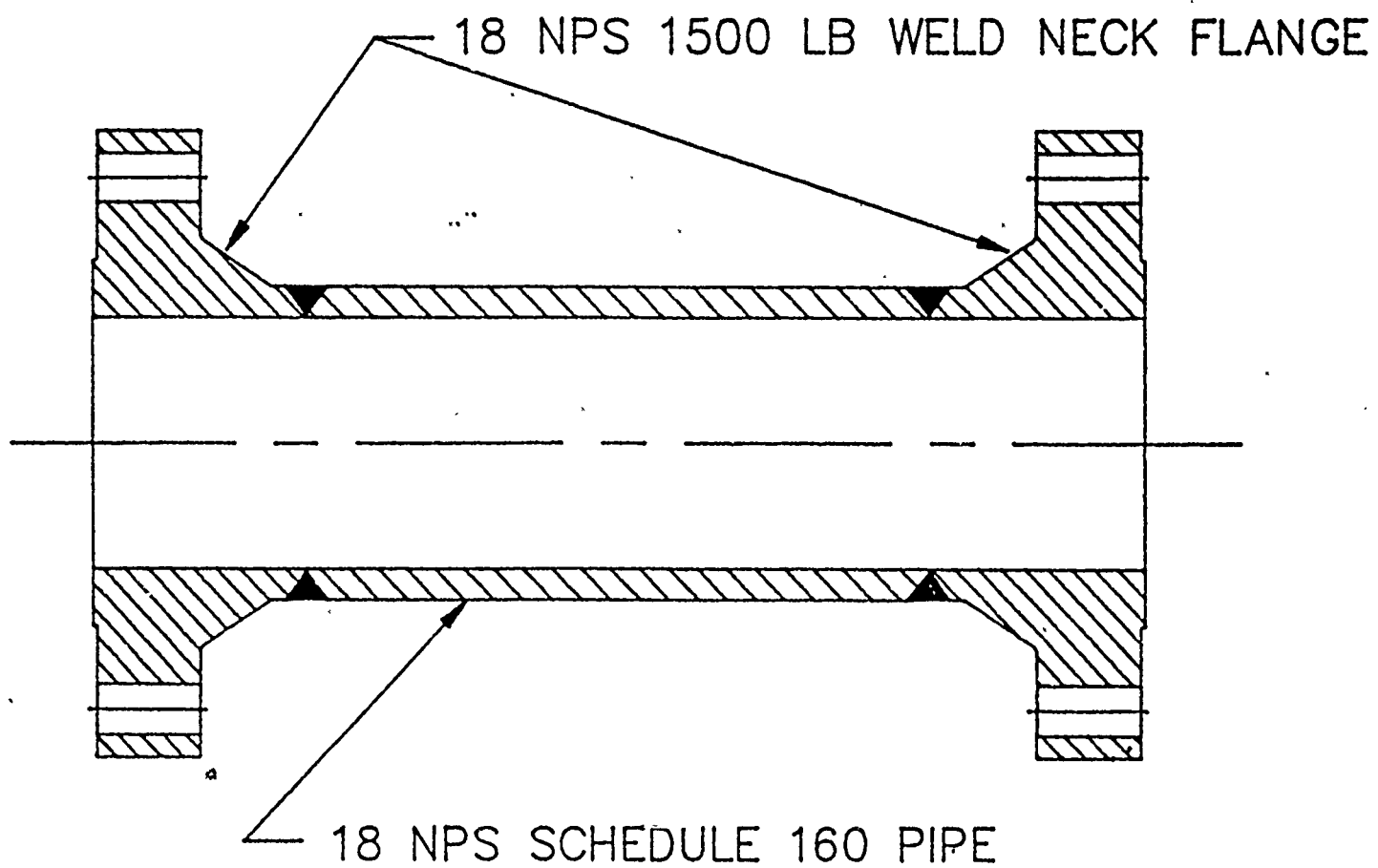
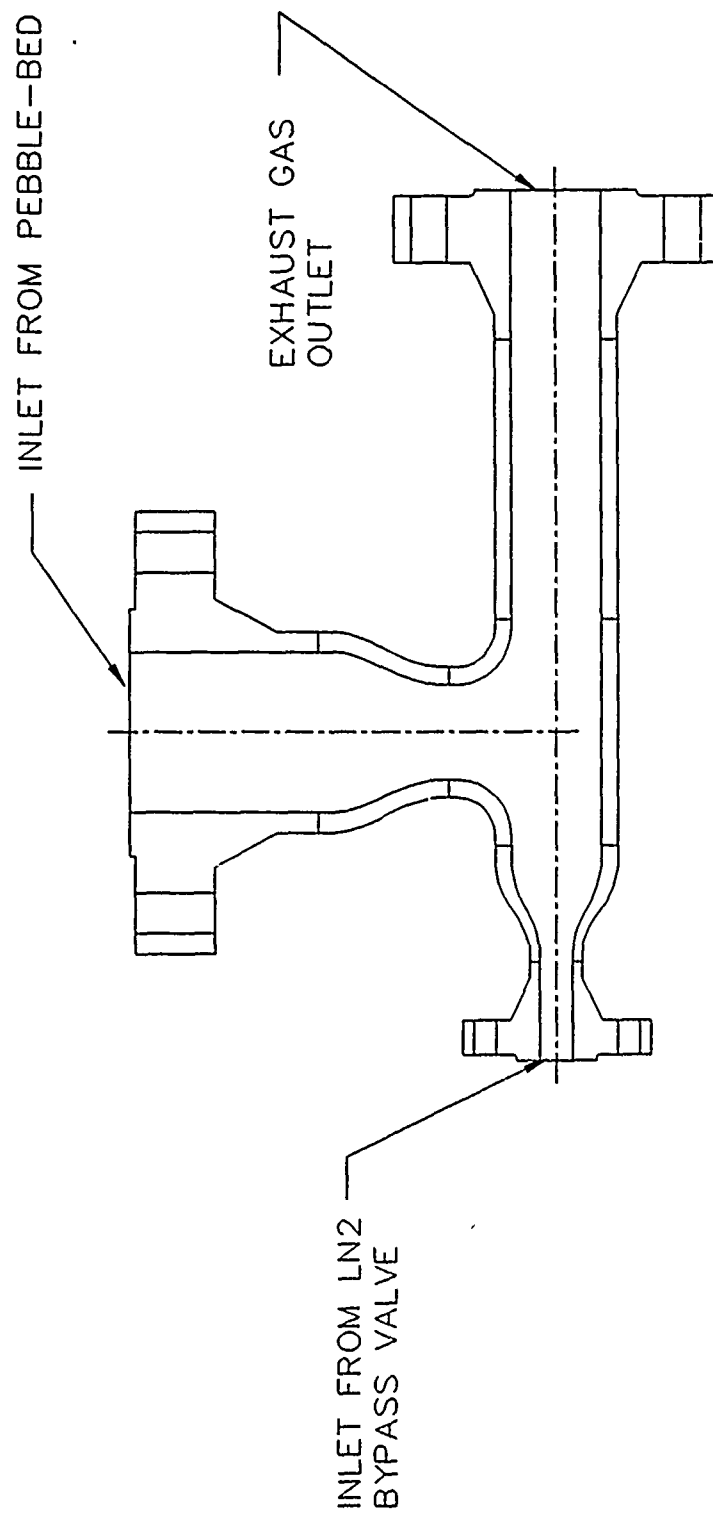


FIGURE 6-2 MECHANICAL DESIGN OF MIXER PRESSURE SHELL



The following list is a summary description of each part and the associated specifications and ratings.

1 each
18" NPS, Schedule 160 Seamless Steel Pipe
18" OD x 1.781" wall (14.438" ID) x 40" long
ASME material specification: SA-106 Grade C Carbon steel pipe
Yield Stress: 40 ksi
ASME pressure rating (-20 to 650 °F, E=0.7): 2256 psig

2 each (Inlet and Outlet Flange)
18" NPS, ANSI Class 1500 Weld Neck Flange
Bore diameter: 14.438"
ASME material specification: SA-105 Carbon steel forged fittings
ANSI pressure-temperature rating: 2995 psig @ 500 °F

2 each (Inlet and Outlet Heads)
18" NPS, ANSI Class 1500 Blind Flange
ASME material specification: SA-105 Carbon steel forged fittings
ANSI pressure-temperature rating: 2995 psig @ 500 °F

32 each Studs with 64 Washers and Nuts (16 studs per Flange)
2 3/4 - 8 x 20 long: ASME SA-354 Grade BD Stud
2 3/4 - 8 Heavy Hex Nut: ASME SA-194 Grade 2H
2 3/4 Hardened Washer: ASTM F436

6.1.2 Cryogenic LN₂ Components

The components used for cryogenic fluid transport at high pressure are required to be made from stainless steel to prevent embrittlement common with carbon steel material that is or may be subjected to cryogenic temperatures. All components which are subject to be exposed to LN₂ are constructed of type 304 or type 316 stainless steel. Both of these grades are approved by ASME for use at cryogenic temperatures.

6.1.3 Pebble-bed Design

Heater Bed Liner

The heater bed liner is shown in Figure 6-3 without the pebbles installed. The electric heaters are inserted axially into the circular array of tubes shown in the figure. There are a total of 4 equally spaced baffle plates which aid in the dispersion of the gas as it flows through the heater and prevents channeling of the flow through lower flow resistant regions.

6.1.4 Insulation Design

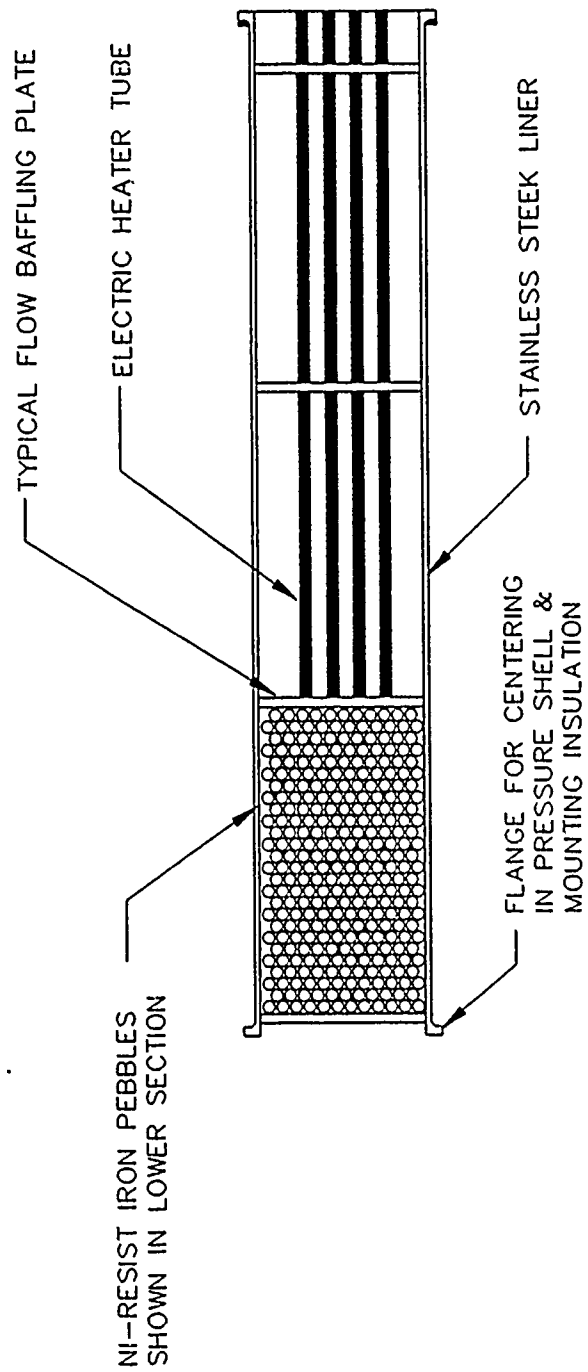


FIGURE 6-3 MECHANICAL DESIGN OF PEBBLE-BED LINER
AND BAFFLE ASSEMBLIES

The heat loss through the insulation of the pebble bed heater was predicted for the steady state condition. The following heat transfer equation for one dimensional steady state conduction inconcentric cylinders was used:

$$Q = \frac{2 \cdot \pi \cdot L \cdot (T_1 - T_2)}{\ln(R_2/R_1)/k_i + \ln(R_4/R_3)/k_s} \quad (\text{EQ 6-3})$$

where,

Q, heat flow rate, W (Btu/h)

L, cylinder length, 1.83 m (72 in)

T₁, temperature on inner wall of insulation, 815 °C (1500 °F)

T₂, temperature on outer wall of steel pipe, 15 °C (60 °F)

R₁, inner wall insulation radius, 0.162 m (6.375 in)

R₂, outer/inner wall insulation/steel radius, 0.183 m (7.219 in)

R₃, radius of outer wall of steel pipe, 0.229 m (9 in)

k_i, insulation thermal conductivity, .1 W/m/°C (0.058 Btu/h/ft/°F)

k_s, thermal conductivity of steel, 35 W/m/°C (20.2 Btu/h/ft/°F)

The assumptions used are that no heat is convected to the insulation inner wall nor the steel inner wall and that a constant temperature difference of T₁-T₂ is maintained (i.e. steady state).

The calculated steady state heat loss through the insulation and steel is approximately 7.5 kW (25.6 kBtu/h). The total heating rate requirement for the Ni-Resist pebbles and steel liner assembly is calculated from the following equation:

$$Q = \frac{m \cdot C_p \cdot (T_f - T_i)}{t} \quad (\text{EQ 6-4})$$

where,

Q, heat flow rate, W (Btu/h)

m, mass of material to be heated, kg (lbm)

C_p, specific heat of material, J/kg/°C (Btu/lbm/°F)

T_f, final temperature of material, °C (°F)

T_i, initial temperature of material °C (°F)

t, heating time, seconds (hours)

For approximately 1250 lbs of Ni-Resist iron and stainless steel heated from 15°C (60°F) to 815°C (1500°F) and a specific heat of 0.45 kJ/kg/°C (0.1 Btu/lbm/°F) the heat required is 190 MJ (180 kBtu). For a 4 hour heatup time, the heating rate required is 13.2 kW (45 kBtu/h).

The total heat rate required from the electric heating system is therefore approximately 21 kW (71.6 kBtu/h). The heater elements

are rated at 2.5 kW each, thus a total of 9 elements are required to achieve the pebble bed maximum operating temperature of 1500 °F. Electrical power requirements for the heater system are approximately 102 Amps @ 220 Volts for single phase and for a three phase power supply 60 Amps @ 220 Volts per pair of electrical legs. In the single phase circuit, all heaters are connected in parallel to the two available power legs and in the three phase circuit, each pair of legs (3 pairs total) has three heater elements connected in parallel.

6.1.5 Thermal Mixer Design

Mixer Pressure Shell

The mixer pressure shell is a welded assembly which is composed of seven (7) main parts. The following is a description of each of the parts and their associated specifications and ratings:

1 each: 8 NPS, ANSI Class 1500 Weld Neck Flange
Bore Diameter: 6.875" - XX Heavy Wall
ASME material specification: SA-182 F316 Alloy steel fittings
ANSI pressure-temperature rating: 2030 psig @ 850 °F

1 each: 8 x 4 NPS, Butt Weld Concentric Reducer
Bore Diameter: XX Heavy Wall
Large End: OD=8.625", Wall=.875, ID=6.875"
Small End: OD=4.5", Wall=.674, ID=3.152"
ASME material specification: SA-403 WP-S 316 Austenitic Steel Fittings
ASME pressure rating: Large End - 2427 psig
Small End - 3740 psig

1 each: 4 x 2 NPS, Butt Weld Concentric Reducer
Bore Diameter: XX Heavy Wall
Large End: OD=4.5", Wall=.674, ID=3.152"
Small End: OD=2.375", Wall=.436, ID=1.503"
ASME material specification: SA-403 WP-S 316 Austenitic Steel Fittings
ASME pressure rating: Large End - 3740 psig
Small End - 4730 psig

1 each: 2" NPS ANSI Class 1500 Weld Neck Flange
Bore Diameter: 1.503" - XX Heavy Wall
ASME material specification: SA-182 F316 Alloy steel fittings
ANSI pressure-temperature rating: 2030 psig @ 850 °F

1 each: 4" NPS ANSI Class 1500 Weld Neck Flange
Bore Diameter: 3.152" - XX Heavy Wall
ASME material specification: SA-182 F316 Alloy steel fittings
ANSI pressure-temperature rating: 2030 psig @ 850 °F

1 each: 4" NPS Butt Weld Tee

Bore Diameter: 3.152" - XX Heavy Wall
ASME material specification: SA-403 WP316 Alloy steel fittings

Thermal Mixer Bed

The mixer bed is much like the heater bed in appearance but performs a much different function. Figure 6-4 schematically shows the mixer assembly. The mixer bed consists of the same Ni-Resist balls as in the pebble-bed for ease in design although smaller diameter balls would be better here. The hot gas enters from the heater bed and cold gas or LN_2 is injected through the bypass gas adapter. The dispersion of the flow in the mixer pebble-bed aids in efficiently mixing the hot and cold gases so that a correct gas temperature measurement can be made downstream.

6.1.6 Exhaust Back Pressure Generator

The exhaust back pressure generator is nothing more than a throttle valve that can be manually operated to increase or decrease the back pressure during the pebble-bed operation. The globe type valve which is manufactured by Dresser Industrial Valve Division is a HANCOCK Model 7150 T-Type with a fixed backseat. The valve end connections are the recessed socket weld type. Two standard fittings were welded onto the valve for ease of installation and removal.

The specifications for the valve are as follows:

Material: ASME SA-182-F22 Alloy Steel

Pressure-Temperature Rating:

3600 psig (24.8 MPa) up to 850°F (454°C)

2800 psig (19.3 MPa) @ 950°F (510°C)

1560 psig (10.7 MPa) @ 1050°F (566°C)

6.1.7 Electrical Thermal Charging System

The electrical thermal charging systems is composed of 9 individual 2500 watt electrical resistive heating elements and a control system. The heaters operate of 220/240 volt alternating current and require a minimum of 22.5 kW of power. Figure 6-5 shows a schematic heater elements and the operating controls.

The specifications for the heating elements are as follows:

Manufacturer:	WATLOW Electric Manufacturing Company
Model:	Firerod Cartridge Heater Element
Voltage:	220/240 VAC
Power:	2500 Watts each
Length:	72" overall
Unheated length:	12" from leads end
Misc:	NPT pipe fitting on lead end
	Pressure tested to 2000 psig

FIGURE 6-4 TURBULENT MIXER DESIGN SCHEMATIC

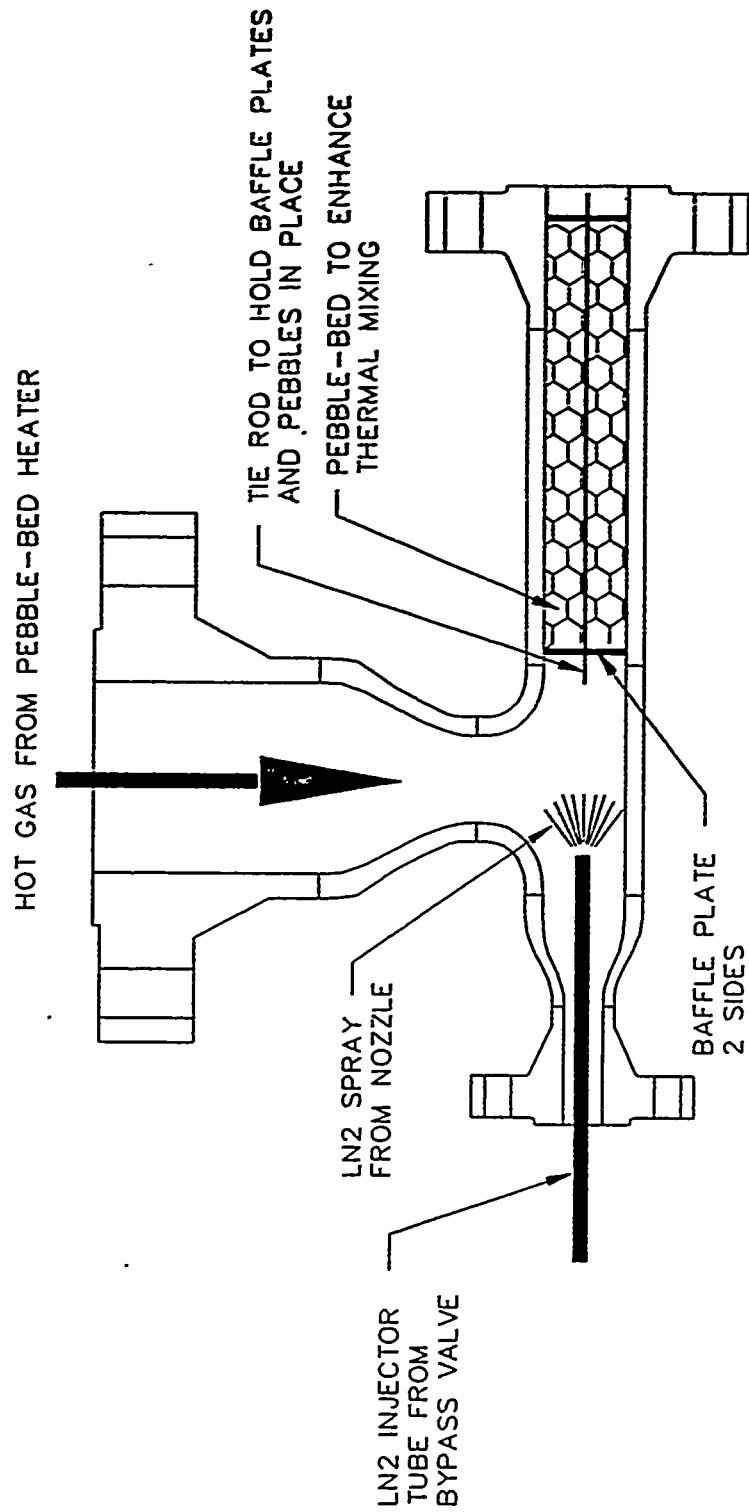
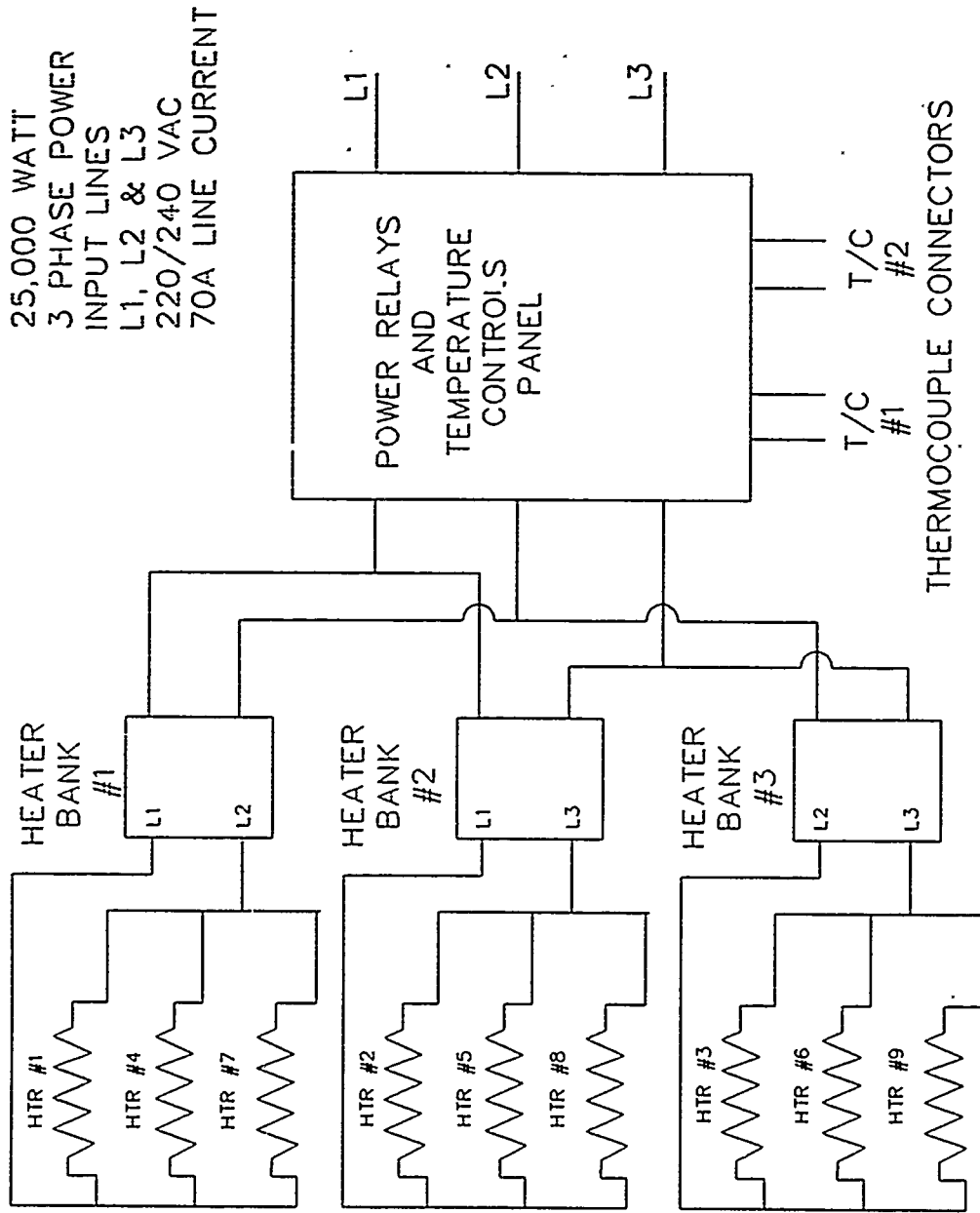


FIGURE 6-5 ELECTRICAL HEATING SYSTEM SCHEMATIC



The electrical controls consist of a 3 ϕ power relay distribution enclosure and 3 circuit breaker enclosures with one 15 amp circuit breaker per element. These enclosures are mounted on a woodskid and are rated for outdoor use. A 3 ϕ 100 amp fused disconnect is supplied to facilitate connection to the external power supply.

The 3 ϕ power relay enclosure consists of the following components:

- 3 each: 2 pole mercury displacement power relays.
Rating: DPST-NO, 60 resistive amps @ 240 VAC.
120 VAC control coil
- 2 each: Temperature controllers, 0-1999°F normally open relays.
120 VAC power
Type K thermocouple inputs.
- 3 each: On/off switches with lamp status display.
120 VAC power, 1 switch per relay.
- 1 each 120 VAC supply power switch.

The relay control panel distributes the 3 ϕ power supply into 3 separate 2 ϕ circuits. The connection is standard DELTA which allows the line voltage to remain constant. Each 2 ϕ circuit is connected to a 2 ϕ power distribution enclosure. The 2 ϕ enclosure has 3 15A circuit breakers along with 3 220/240 VAC female receptacle plugs for connection to the heater elements. Approximately 30 feet of cable is provided from the enclosure to the female plug end. This length proved to be more than adequate for the test installation.

6.2 Hydrotests and Strain Measurement

Hydrostatic proof pressure tests were performed on the pressure components which were manufactured and ASME certified by SPARTA. Two pressure vessels were fabricated and tested. The first hydrotest was performed on the main heater bed pressure shell which was manufactured from carbon steel. Its ASME design working pressure is 2000 psig at the design working temperature of 500°F. The second pressure vessel tested was the mixer shell manufactured from type 316 stainless steel. Its ASME design working pressure is 2000 psig at the design working temperature of 1000°F.

According to the ASME code, Section UG-99 "Standard Hydrostatic Test", the hydrostatic test pressure is determined from the following relation:

$$P_h = P_d \cdot 1.5 \cdot \frac{SA_t}{SA_d} \quad (\text{EQ 6-1})$$

where,

P_h , Hydrostatic test pressure at all points in the vessel, psig
 P_d , Design working pressure of the vessel, psig
 SA_t , Allowable stress of the material at the test temperature, psi
 SA_d , Allowable stress of the material at the design working temperature, psi.

The hydrostatic test pressure for the heater pressure shell is 3000 psig and for the mixer shell is 3750 psig. The difference is because the mixer is designed to operate at a higher temperature than the heater pressure shell.

6.3 Engineering Design Drawings

The following is a list of the engineering design drawings that SPARTA produced under the program for the 1/48th scale pebble-bed evaporator/superheater system.

DWG# PB87IB001 (1 OF 1): PEBBLE BED HEATER THERMAL STORAGE BALLS

PB87HS001 (1 OF 4): PEBBLE BED SUPERHEATER PRESSURE SHELL WELD ASSEMBLY
(2 OF 4): HEATER PRESSURE SHELL UPPER 18" WELD NECK FLANGE DETAILS
(3 OF 4): HEATER PRESSURE SHELL LOWER UPPER 18" WELD NECK FLANGE DETAILS
(4 OF 4): HEATER PRESSURE SHELL 18" CARBON STEEL PIPE DETAILS

PB87EH001 (1 OF 3): PEBBLE BED SUPERHEATER EXHAUST HEADER BASE WELD ASSEMBLY
(2 OF 3): PEBBLE BED SUPERHEATER EXHAUST HEADER DETAILS - 18" BLIND FLANGE
(3 OF 3): PEBBLE BED SUPERHEATER EXHAUST HEADER BASE LEG SUPPORT DETAILS

PB87IH001 (1 OF 1): PEBBLE BED SUPERHEATER INLET HEADER DETAILS - 18" BLIND FLANGE

PB87MS001 (1 OF 2): PEBBLE BED SUPERHEATER THERMAL MIXER SHELL WELD ASSEMBLY
(2 OF 2): PEBBLE BED SUPERHEATER THERMAL MIXER SHELL WELD NECK FLANGE DETAILS

PB87HL001 (1 OF 6): PEBBLE BED SUPERHEATER - HTR LINER/BAFFLE ASSEMBLY
(2 OF 6): PEBBLE BED SUPERHEATER - HEATER LINER PIPE DETAILS
(3 OF 6): PEBBLE BED SUPERHEATER - HEATER LINER BAFFLE PLATE DETAILS
(4 OF 6): PEBBLE BED SUPERHEATER - LINER BAFFLE

WELD ASSEMBLY

(5 OF 6): PEBBLE BED SUPERHEATER - HEATER LINER
PIPE WELD ASSEMBLY

(6 OF 6): PEBBLE BED SUPERHEATER - HEATER LINER
PIPE DETAILS

PB88MB001 (1 OF 1): PEBBLE BED SUPERHEATER - MIXER BAFFLE
PLATE

PB88EX001 (1 OF 2): OUTLET FLANGE WELD ASSEMBLY DETAILS
(2 OF 2): OUTLET VALVE WELD ASSEMBLY

PB88SH001 (1 OF 1): PEBBLE BED SUPERHEATER ASSEMBLY

A complete set of the 21 drawings was reduced to a 8 1/2 x 11 size pages and they are presented in Appendix D.

6.4 Parts List

A complete parts list was generated by SPARTA and is included in the assembly drawing for the pebble bed evaporator/superheater.

7. INSTRUMENTATION AND CONTROL SYSTEM DESIGN

7.1 Measurement of Pressure and Temperature

7.1.1 Temperature Measurement Grid

Figure 7-1 gives the locations of all the thermocouples (T/Cs) installed in the pebble-bed heater. Pebble-bed T/Cs are grouped into 3 areas; namely the upper, middle and lower bed. The angular locations of the T/Cs with respect to heater element #1 are given in Figure 7-2.

7.1.2 Pressure Drop Measurement

Pressure drop measurement was accomplished by electronic pressure transducers installed at the LN₂ inlet and the exhaust exit. Figure 7-1 shows the location of pressure transducers 4 & 5 which were used to measure the pressure drop during LN₂ flow tests.

7.1.3 Flow Measurement

Flow measurements were made using pressure transducers 1-4 and orifice plates mount at positions FM1, 2 & 3 as shown in Figure 7-1. Because high pressure fluctuations were present due to the LN₂ pump pulsations, flow data were not useful. In the future, the piston pump should be equipped with a pulsation damper. The pump output, however, was known and is calculated from the following relation.

$$Q_L = \pi/4 \cdot D_b^2 \cdot S_p \cdot \epsilon_v \cdot R_p / C \quad (\text{EQ 7-1})$$

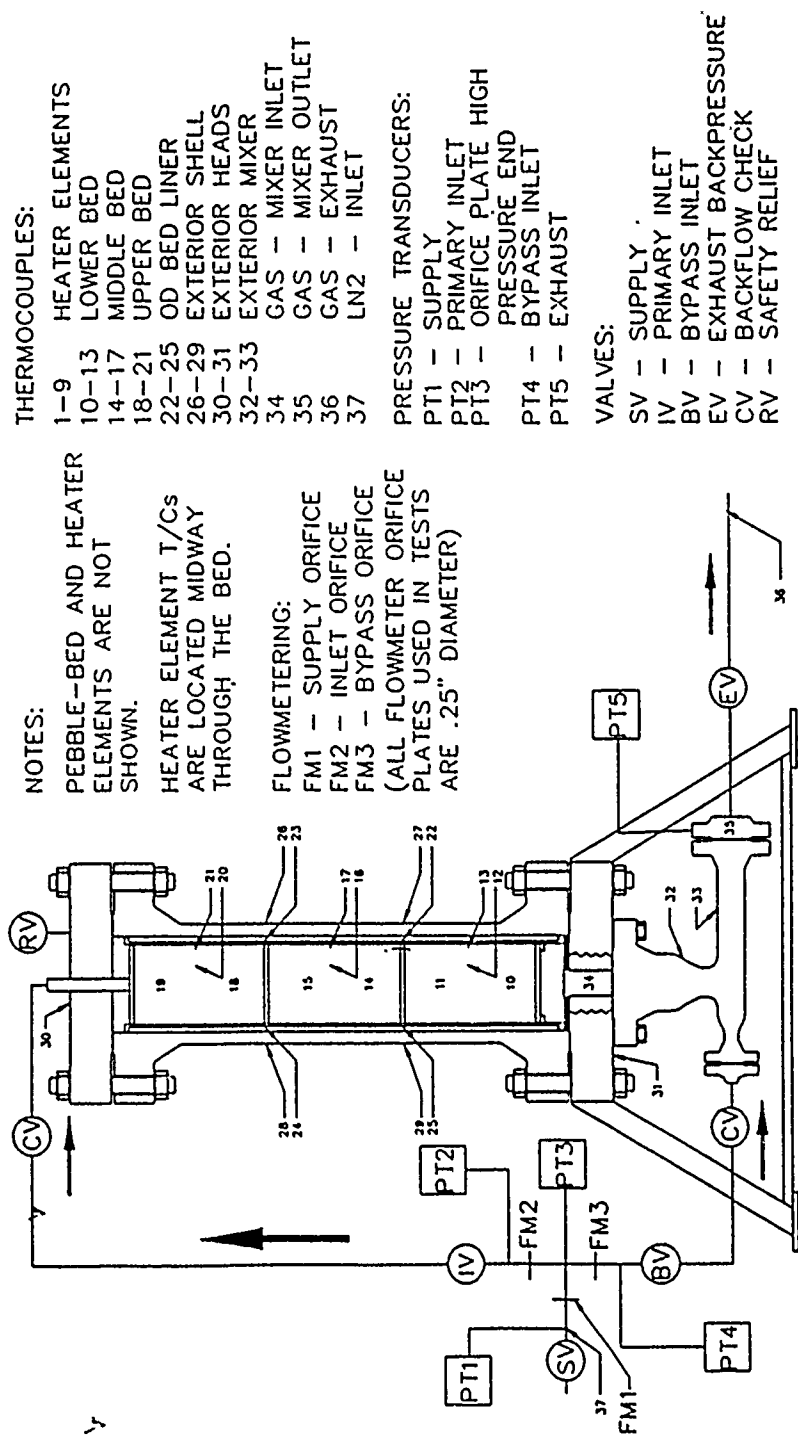


FIGURE 7-1 1/48TH SCALE PEBBLE-BED EVAPORATOR/SUPERHEATER
TEMPERATURE AND PRESSURE SENSOR LOCATIONS

where,

Q_L , Flowrate of LN_2 , GPM
 D_b^2 , Piston bore diameter = 1.625 in
 S_p , Piston stroke length = 1.26 in
 ϵ_v , Volumetric efficiency of pump, assumed $\approx .87$
 R_p , Speed of the pump, RPM
 C , Conversion factor = 231 in³/gallon

Pump speed is determined by the electric drive motor speed and the drive pulley sprocket sizes on the pump and motor. The AC induction electric motor has a constant speed of 1770 RPM.

$$R_p = R_m \cdot T_m / T_p \quad (EQ 7-2)$$

where,

R_m , motor speed = 1770 RPM
 T_m , # Teeth on motor sprocket
 T_p , # Teeth on pump sprocket

The following Table 7-1 gives the three flowrates for each of the three pulley sprocket combinations used in the LN_2 tests.

TABLE 7-1 LN_2 PUMP FLOWRATE CALCULATIONS

PUMP SPROCKET # OF TEETH	MOTOR SPROCKET # OF TEETH	PUMP SPEED RPM	Q LN_2 GPM
144	34	418	4.11
144	52	639	6.29
144	68	836	8.23

7.2 Data Recording System

The data recording system is described in APPENDIX A.

7.3 Mixer Outlet Temperature Controls

The temperature of the mixer exhaust gas was controlled manually by monitoring the outlet temperature (T/C # 35, Figure 7-1) and by manually operating a bypass valve which controlled injection of LN_2 into the mixer pressure vessel upstream of the mixer thermal bed. The bypass valve opening was manually changed to regulate the outlet temperature for the duration of the test. Manual control often produced temporary fluctuations in gas exhaust temperature due to the inability of the operator to adequately anticipate and respond to temperature changes within the bed. Automatic control would be preferable because temperature set

points could vary significantly from test to test and accuracy and repeatability of automatic controls is established in industry.

8. NITROGEN GAS SHAKEDOWN TESTS

A battery of tests was performed at the laboratory facilities of Dynamics Technology Inc. using room temperature bottled high pressure nitrogen gas to check out the heater/heater control systems, to familiarize the test personnel with the heat up characteristics of the heater and to finalize the written test plan and incorporate the necessary revisions. Due to the lack of sufficient electrical power at DTI, only banks of seven heater elements were active at any time, otherwise the written test plan was closely followed.

8.1 Test Apparatus

The pebble-bed heater was powered using two phase power (15 amps/phase, 210 volts) distributed first through a breaker box then through the heater controller box. Heater control was provided by Omega type K (chromel/alumel) thermocouples attached to the heater housing tubes within the pebble bed. The controllers powered the heaters according to manually inputted temperature setpoints. Test data were recorded with an HP9920 computer, a Trans Era MDAS-7000 16 channel digitizer and data acquisition software developed by DTI. This data acquisition system (DAS) sampled and recorded temperature signals generated by eleven thermocouples distributed throughout the pebble bed. In addition to the DAS a bank of digital meters monitored other bed temperatures and heater pressures. A six pack of compressed nitrogen gas was plumbed to the inlet for these tests.

8.2 Test Data and Observations

Test data is given in Appendix A. Both graphical representation and raw tabular listings are given.

8.3 Equipment Handling and Operation

Equipment handling and operation for the high pressure nitrogen gas test were straightforward and no problems were encountered. The high pressure nitrogen gas was supplied in 6 pack configurations. The supply pressure was approximately 2400 psig and was regulated to the pebble-bed by regulation of the exhaust backpressure valve.

Air was purged from the pebble-bed by flowing nitrogen gas through the system before commencement of the heat up cycle. During the heat up cycle, the pebble-bed was kept at a nominal pressure of 100 psig to ensure an oxygen free environment and to test for minor leaks in the system due to temperature effects.

9. LN₂ FLOW TESTS

Following the successful completion of the shakedown tests at DTI in Torrance, CA the heater unit was moved by Heavy Transport to the cryogenic facility, Cosmodyne, Inc. which is nearby in Torrance, California.

9.1 Test Apparatus

In addition to the equipment used at DTI, a scaffold was erected to readily access to the upper part of the heater which is 12 feet high. A LN₂ pump was set up adjacent to the heater and the appropriate inlet tubing was constructed and connected. The LN₂ tests were supplied from two sources of liquid nitrogen. The primary source was a fixed 2500 gallon storage tank used by the Cosmodyne facility to supply liquid nitrogen and nitrogen gas to their shops. The secondary source was a tanker truck trailer filled with approximately 3,000 gallons of LN₂.

9.2 Test Data and Observations

The test data are given in Appendix A. Both graphical representations and tabular listing are included.

9.3 Equipment Handling and Operation

The equipment handling and operation of the pebble-bed unit during the LN₂ tests were the same as for the nitrogen gas tests with the exception of the operation of the LN₂ pump system. This was performed by Cosmodyne Corp personnel.

10. LN₂ TEST RESULTS DATA REDUCTION AND ANALYSIS

10.1 Significant Test Results

The significant test results are given in Figure 10-1 for the 4 GPM LN₂ test, in Figure 10-2 for the 6 GPM LN₂ test and Figure 10-3 for the 8 GPM LN₂ test. These three figures are for the 1000 psig backpressure tests. Temperature data for thermocouple numbers 10, 34 & 35 are given in the figures.

10.2 Heat Transfer Analyses and Correlation

A heat transfer correlation calculation is given in the second (lower) graph given in Figures 10-1 through 3 for the respective 3 significant tests; 4, 6 and 8 GPM LN₂ at 1000 psig backpressure. The data reduction graphs show the heat absorbed by the gas and the heating rate versus test time. The analysis used both heat of vaporization for LN₂; specific heat of nitrogen gas; the LN₂ pump constant flowrate; and the overall nitrogen gas temperature change (i.e. thermocouple 35 minus inlet cryogenic temperature

FIGURE 10-1 TEST RESULTS AND DATA REDUCTION FOR LN₂ TEST @ 4 GPM & 1000 PSI

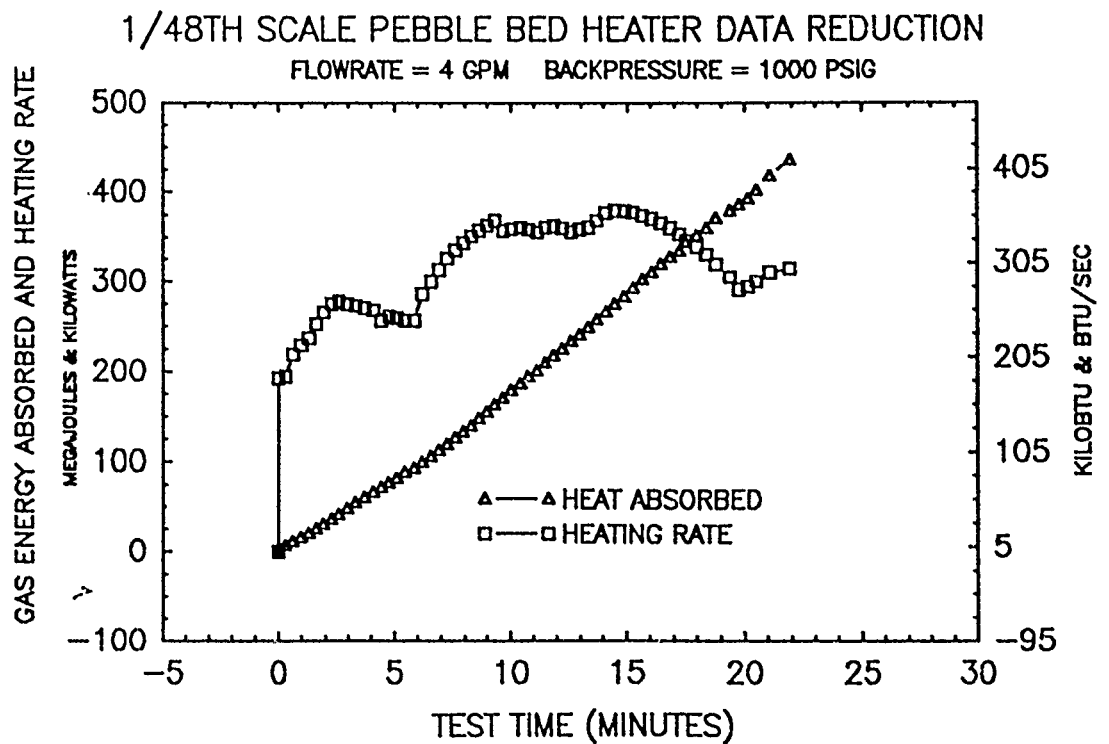
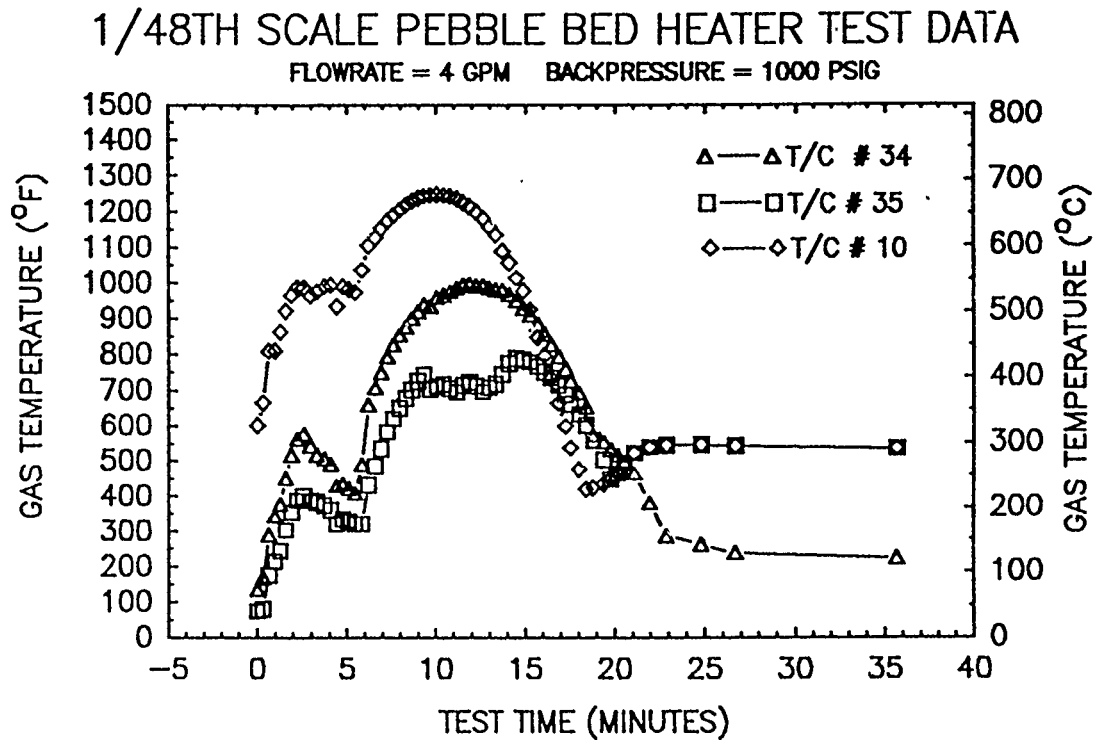
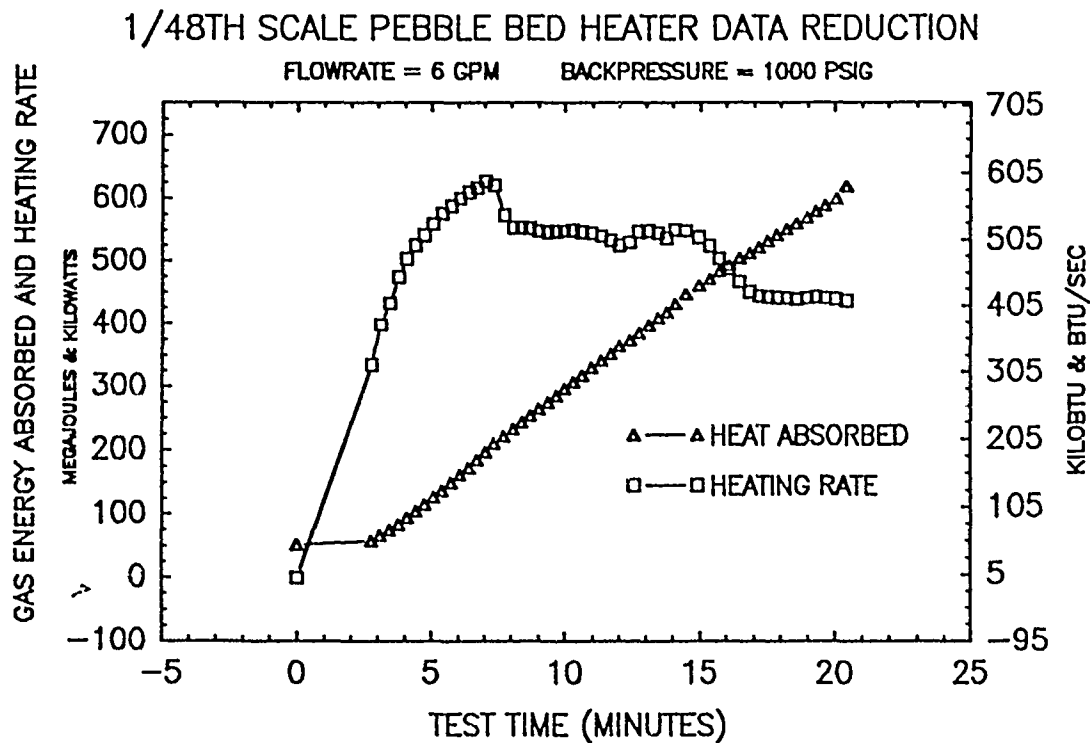
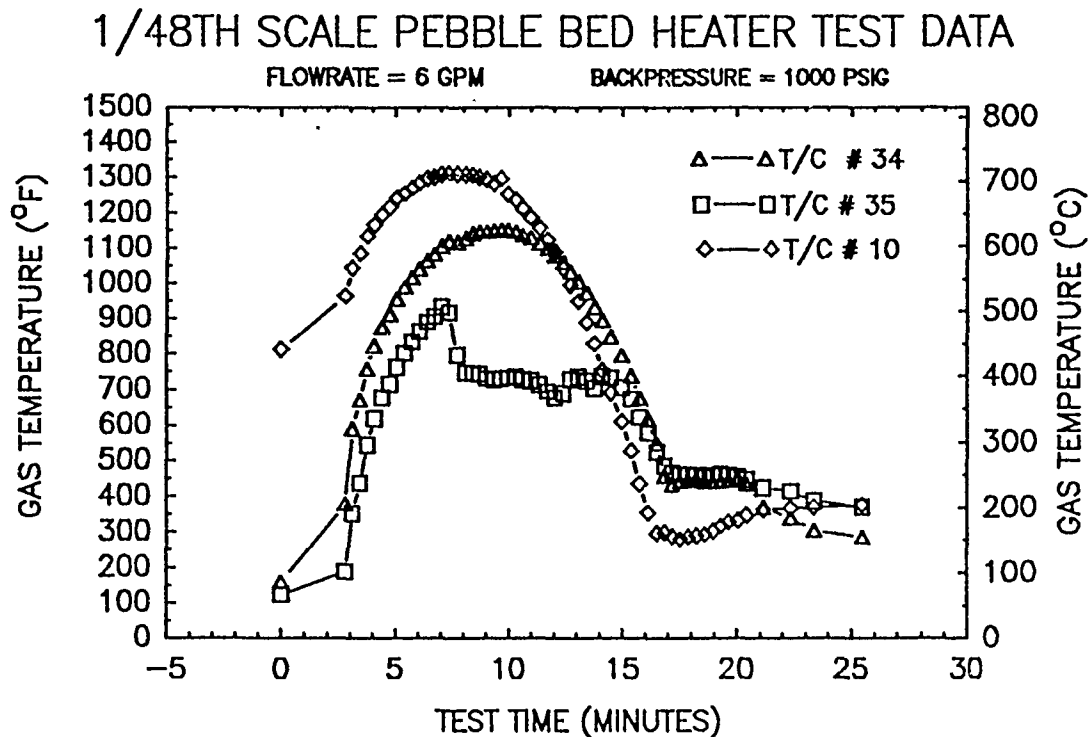
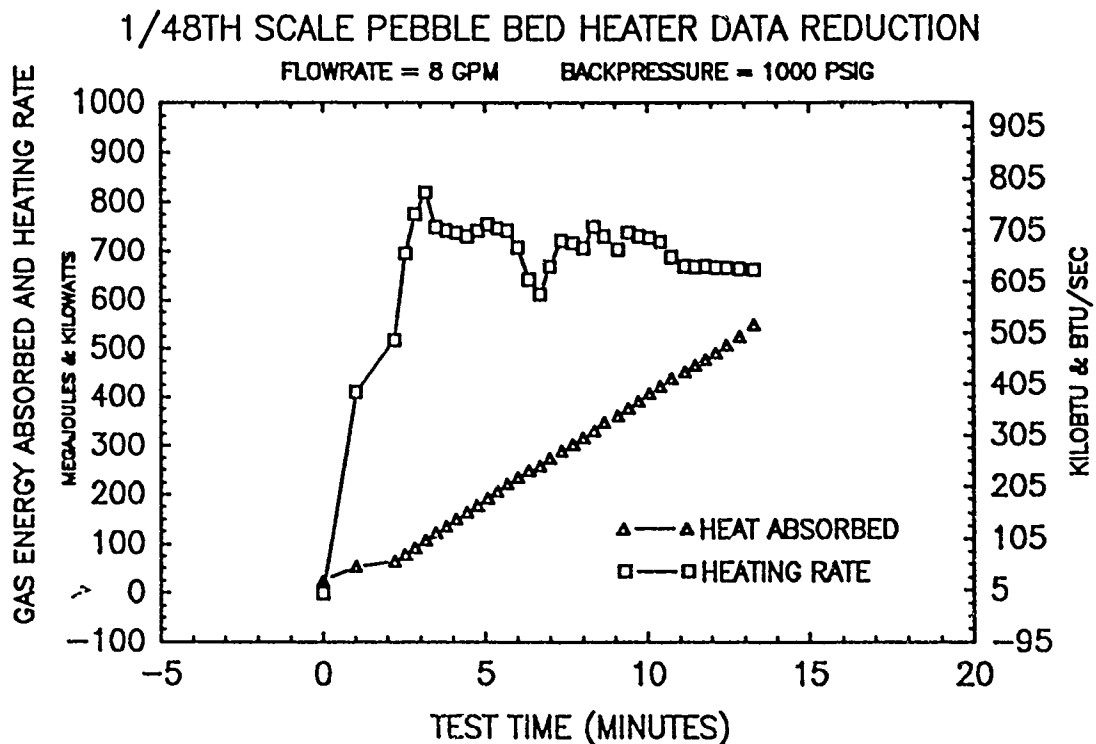
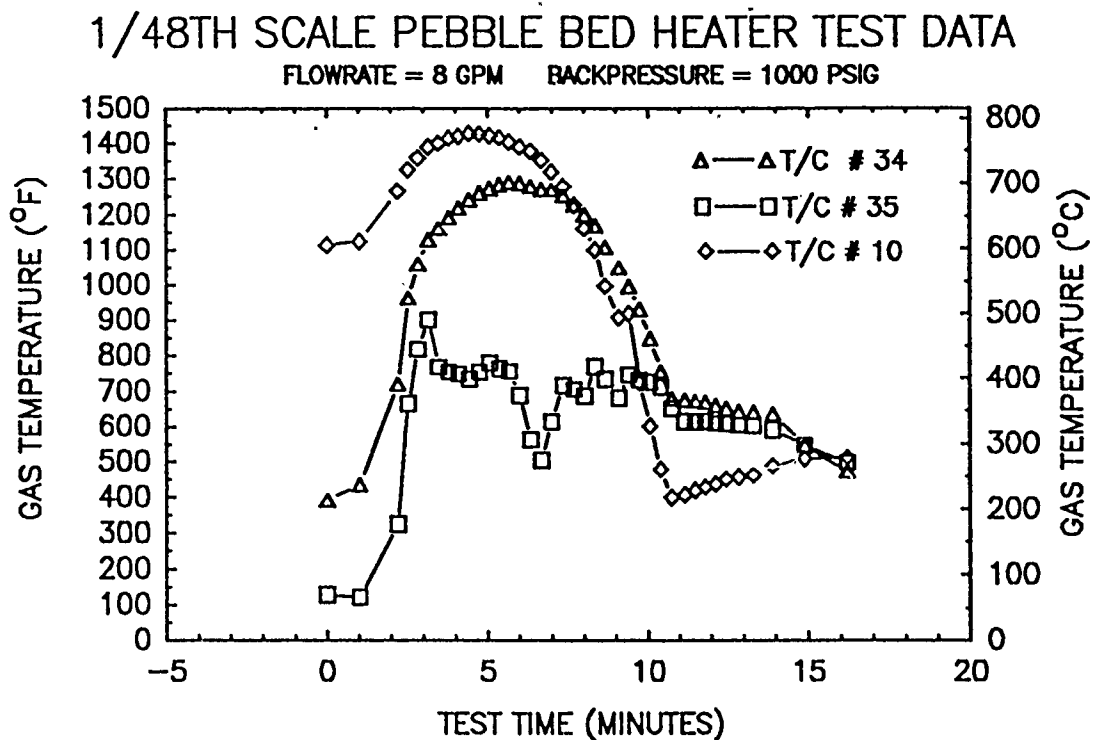


FIGURE 10-2 TEST RESULTS AND DATA REDUCTION FOR LN₂ TEST @ 6 GPM & 1000 PSI





(assumed constant at 78°K) to calculate the total heat absorbed by the gas.

11. SAFETY AND OPERATION PROCEDURES

11.1 Safety Considerations for Assembly and Operation

The following safety procedures are to be practiced whenever the pebble-bed evaporator/superheater unit is operated. All of the precautions and safety procedures were developed from actual engineering tests with the pebble-bed unit or from standard safety procedures commonly utilized in industry.

11.1.1 Safety Precautions

1. The pebble-bed evaporator/superheater unit operates at high pressure and elevated temperature. All personnel within a 20 foot radius of the pebble-bed unit and support equipment must wear protective eyewear at all times during operation.
2. When the pebble-bed heater is operated without connecting the exhaust line opening to a vessel, personnel must wear protective ear coverage while LN₂ flow is in progress.
3. All handling of liquid nitrogen supply lines and high pressure lines while liquid is flowing should be made using protective covering for hands to prevent freeze burns.
4. The pebble-bed electric thermal charging system uses high voltage and draws high currents. All equipment must be grounded to an approved grounding device before activating the electrical controls. The voltage potential of the pebble-bed pressure vessel shall be measured with respect to ground with the heaters energized and **NO WORK ON THE SYSTEM WILL BE ALLOWED UNTIL ANY MEASURED VOLTAGE POTENTIAL IS REDUCED TO ZERO.**
5. The pebble-bed system is constructed of heavy parts. Some components weigh as much as 4000 lbs. The total pebble-bed assembly weighs approximately 7 tons. Lifting points are located on the pebble-bed structure and are called out on the assembly drawing. All lifting should be performed by qualified personnel using equipment rated for a minimum of 10 tons capacity. PERSONNEL SHALL WEAR SAFETY SHOES AND GLOVES WHEN MOVING HEAVY PARTS.

11.1.2 Safety Procedures

11.1.2.1 High Pressure Piping

The pebble-bed heater system has piping which is subjected to high pressures ranging to 2000 psig at temperatures ranging from

cryogenic (-300°F) to 1000°F. The cold inlet piping is fabricated from stainless steel tubing and compression (SWAGELOK) type fittings. All currently used tubes and fittings are interchangeable in like sizes, however, SWAGELOK fittings are NOT interchangeable with other compression fittings. Do not use any other compression fitting type parts with the currently used SWAGELOK fittings. A risk of fitting blowout or tube rupture may result.

The tightening of SWAGELOK fittings is accomplished very easily after the tubing has had the ferrules swaged in place. The procedure for tightening a preswaged fittings is as follows:

SWAGELOK Fitting Tightening Instructions

- A. Do not make-up or tighten fitting when the system is pressurized. Reduce pressure to zero before starting.
- B. Use wrenches of the proper size on the SWAGELOK fitting body and nut. Never turn the fitting body, but hold the body stationary and turn the nut.
- C. Insert the end of a tube with pre-swaged ferrules into the fitting body until the front ferrule seats firmly in the fitting body.
- D. Assemble and tighten the nut by hand.
- E. Use a wrench to tighten the fitting until the original fitting position is obtained. If the original position is not known. Tighten the fitting a minimum of a 1/4 turn or until a firm resistance is met. Never turn small diameter fittings (3/8" or less) greater than 1/3 of a turn.
- F. Check tube for proper alignment in fittings.
- G. After all fittings are assembled, pressurize starting at a low pressure (100-200 psig) and check for leaks with a soap solution or leak detecting fluid. If any leaks are evident and the fitting is tight, replace the fitting with a new one following the manufacturers directions for installation.

Other types of high pressure connections in the system are bolted flange joints and NPTF pipe joints. All bolted flange joints should already be pretightened to the proper torque levels. The disassembly of these joints should not be necessary unless a gasket needs replacing. Any removal and replacement of bolted joints should be performed by a qualified technician trained in the use of torque make-up tools. See the system assembly drawing for required bolt torques and tightening sequence. BOLTED JOINTS REQUIRE TIME TO ALLOW THE GASKET TO RELAX. A MINIMUM OF 24 HOURS

SHOULD BE ALLOWED BEFORE RETIGHTENING THE JOINTS TO MINIMIZE THE POSSIBILITY OF CREEP IN THE BOLTED JOINT CONNECTION.

Pipe fittings are use to ensure a pressure tight connection. NPTF dryseal pipe fittings are extensively used in the system and the following procedures should be followed whenever disassembling or assembling these types of fittings.

NPTF Pipe Fitting Assembly Instructions

- A. Always use a suitable extreme pressure thread lubricant and sealant on pipe threads. Galling or seizing of the threads is very common with pipe fittings, especially when stainless steel is used. Never assemble NPTF pipe fittings together without thread lubricant.
- B. NPTF pipe fittings should be tightened with lubricant/sealant on the threads using the proper box, crescent or pipe wrench. Pipe fittings require more torque to attain a seal than do pre-swaged compression fittings. A trial and error approach is usually performed to attain a proper seal. Tightening of pipe joints should be performed by experienced technicians and pressure checked with leak detecting solution before being put into service.
- C. Never back out a NPTF pipe fitting to make alignment of the piping possible. Always try to turn the fitting tighter when alignment is necessary.
- D. Disassembly of pipe fittings should not be performed unless absolutely necessary because they are intended to be permanently installed. Always inspect threads for galling upon removal. If the fitting cannot be removed, seizing of the threads has probably occurred and the whole assembly should be replaced or be repaired by a qualified shop.

11.1.2.2 Electrical Systems

The electrical system is composed of various NEMA rated panels and type SO electrical cable. All electrical enclosures with the exception of the 3 ϕ -100A fused disconnect are rated for permanent outdoor wet environment installation and use (per NEMA 12 or 4). The 3 ϕ -100A disconnect is an indoor type enclosure. 3 ϕ -220/240V power can be supplied from available source directly into the controller enclosure without using the disconnect provide a fused power disconnect is provided on the power source.

11.2 Pebble-Bed Evaporator/Superheater Operation

The operation manual for the 1/48th scale pebble-bed evaporator

and superheater was produced. The manual is distributed under a separate report (SPARTA report # LA-88-09-TR; see Reference ⁹).

12. CONCLUSIONS

The conclusions that can be drawn from the results of this program are tabulated below:

1. The LN2 pebble-bed evaporator/superheater concept was experimentally proven to be a practical means of quickly and simultaneously pressurizing and heating gas for the LB/TS drivers.
2. The LN2 pebble-bed evaporator/superheater outlet gas temperature was regulated to a substantially constant 700°F regardless of the pebble-bed temperature.
3. The internal pressure drop of gas flowing through the LN2 pebble-bed evaporator/superheater was almost negligible (in the order of 100 psi at a flow rate of 53 lbs/min).
4. The pebble-bed heat transfer rate was sufficiently large to vaporize and heat a mass flow rate of LN2 for the times of interest.
5. The internal heat transfer predictions that were used in the design of the LN2 pebble-bed evaporator/superheater were very conservative.
6. The calculated predictions of heat transfer to the pressure vessel walls of the LN2 pebble-bed evaporator/superheater were verified in test and are sufficiently low so as not to be a safety issue.
7. The nickel iron (Ni-Resist) pebbles used in the LN2 pebble-bed evaporator/superheater did not produce any debris in the flowing exhaust. This indicates that there was no breakdown of the pebbles during the temperature and pressure cycling of the unit. Therefore, Ni-Resist seems to be a suitable material for the pebble-bed balls.
8. The liquid nitrogen was completely converted to gas in the upper 1/3 part of the pebble-bed. Also liquid nitrogen did not penetrate radially from the injector to the pebble-bed wall. This indicates that a single radial LN2 injector does not adequately utilize the complete diameter of the bed.

13. RECOMMENDATIONS

1. Alternate injectors should be designed, fabricated and tested. Experiments should be conducted with the pebble-bed to obtain more uniform radial distribution of injected LN2

into the upper portion of the pebble-bed, thereby utilizing more of the pebble-bed in the evaporator section.

2. Alternate internal baffles should be designed, fabricated and tested in the pebble-bed to obtain a more uniform radial gas flow distribution throughout the pebble-bed, thereby utilizing more of the pebble-bed heat during the process.
3. Design the pebble-bed and its heating system to operate at temperatures higher than 1,500°F (1,960°R) ranging to 2,000°F (2,460°R) so as to increase the thermal capacity of the pebble-bed in terms of heat stored/unit volume.
4. Design, fabricate and test an automated exit temperature control system which automatically regulates the flow of LN2 into the mixer to maintain the exit gas temperature at a predetermined value.
5. Design, fabricate, instrument and install a short horizontal length of simulated driver. Coat half of the interior of the simulated driver with a thin coating of plasma sprayed ZrO₂. Pressurize the simulated driver with N₂ heated to predetermined temperatures and measure the internal gas temperature and the pressure vessel wall temperatures as a function of time to obtain accurate values of the Grashoff number so that heat loss to the 1/6th scale and full scale LB/TS drivers can be calculated.
6. Investigate and test pebble-bed pebbles of different sizes made from Ni-resist and alternative materials to reduce the internal flow channeling and to reduce the cost of the pebbles.
7. Increase the quantity of flow, pressure and temperature measurements made within the pebble-bed and run additional tests with the LN2 pebble-bed evaporator/superheater so as to obtain sufficient data to revise and correlate the computer prediction model.
8. Test the parameters of operation of the LN2 pebble-bed evaporator/superheater at exit temperatures ranging from 70°F (530°R) to 800°F (1,260°R) and at exit pressures ranging to 2,000 psig. Obtain performance data and upgrade the computer model.

APPENDIX A - TEST REPORT AND GRAPHICAL TEST DATA
DYNAMICS TECHNOLOGY, INCORPORATED
1/48TH SCALE PEBBLE-BED HEATER

INTENTIONALLY LEFT BLANK.

1. INTRODUCTION

Dynamics Technology, Inc. (DTI) personnel supported the BRL/Sparta 1/48th scale pebble bed heater development program by performing heat transfer and transient gas dynamic calculations, assisting in test design, developing a customized data acquisition system, assisting in the installation of instrumentation, power and heating systems, and acquiring, processing and interpreting the test data. The pebble bed heater was built and hydrotested (see DTM-8705-02-DTH) under Sparta direction at the fabricator's facility (Coleman Welding). The pebble bed heater was then transported to DTI by heavy crane where initial tests were conducted and to the Cosmodyne cryogenics facility where the final tests were conducted.

This report documents the equipment and test procedures and provides the test data. Because of the extensive amount of data being reported, the information is presented in two volumes. Volume I discusses the procedures, presents the data graphically and provides a preliminary interpretation; Volume II contains the data acquisition software listing, the operators' notes and the tabular data.

2. PEBBLE BED HEATER DESCRIPTION

The 1/48th scale unit tested performs both liquid nitrogen evaporation and heating; for simplicity the unit is referred to as a heater.

The pebble bed heater is a cylindrical pressure vessel containing 3/4 inch diameter nickel iron (Niresist) balls inside a 1 foot diameter stainless steel basket which is in turn surrounded by 1 inch of zirconium oxide insulation (Figure 1). Nine Watlow heaters are arranged circumferentially 4 inches from the centerline, the heaters are 60 inches long and the pressure vessel is 80 inches in height. An inlet port admits the fluid to be heated (nitrogen gas or water at DTI and liquid nitrogen at Cosmodyne) and an exhaust port

ducts the flow for disposal (a valve in the disposal line allows the back pressure to be controlled). A bypass arrangement (not shown in Figure 1) allows a portion of the incoming flow to be diverted and mixed with the exhaust flow to precisely control the exhaust temperature. Figure 2 shows the pebble bed heater installed at the DTI facility and Figure 3 shows the installation at Cosmodyne.

Considerable wiring and piping was necessary to operate the pebble bed heater (Figures 4 to 7). Two phase power (15 amps/phase, 210 volts) was brought to each of the nine heater rods. The heater power and control system included three heater breaker boxes (three heaters per breaker box each with individual breakers) each connected to a controller box. The controller was operated by establishing setpoints for the desired heater rod temperature; measurements from thermocouples mounted on two of the heater rod sheaths were displayed on the controller and the controller would open relays to automatically shut off the heaters when the setpoints were reached. Three manual switches were available to override the power to the three heater breaker boxes and an overall manual switch could terminate power to all of the heater breaker boxes. As a further safety precaution, a safety disconnect box (with 70 amp/phase fuses) was available for emergency shutdown.

3. INSTRUMENTATION

Omega model 1729 Chromel Alumel thermocouples and Omega model PX-302-5 KV G pressure gauges were installed throughout the pebble bed heater (Figure 8). Chromel alumel wiring brought the thermocouple signals to individual Omega TAC signal conversion boxes whose output was 1 mv per degree F. Thirty seven thermocouples were installed; of these, 11 were attached to TAC boxes and made available for automatic data acquisition. The remainder were recorded manually at intervals throughout each test. External temperatures of the pebble bed inlet, body and exhaust were monitored with an Omega portable temperature sensor, as well as the permanently mounted thermocouples shown in Figure 8. The pressure transducers (mounted at the ends of 1 foot long, 3/8ths inch ID tubes to avoid temperature extremes) were powered by 20 volt power supplies and had nominal calibrations of 5 mv/psi. All five of the

available pressure transducers were attached to the data acquisition system via a power supply/interface box which provided nominal calibrations of 2.5 mv/psi.

A DTI digital Data Acquisition System (DAS) was used to acquire and process test data during the pebble bed heater tests. The DAS consists of an HP9920 computer with a Trans Era MDAS-7000 16 channel digitizer. Custom software was written (Appendix A) to acquire data upon user interrupt. The data was sampled (at 10 Hz for 5 seconds sweeping across the 16 channels) and averaged to suppress the considerable noise on the thermocouple signals.

In the present software configuration, there occurs occasional time misregistrations (caused by initialization of a run sequence whose start was then delayed by the test engineer). These minor glitches in no way compromise the interpretation of the test data.

Processed data was printed out for each data line (acquisition time) in reduced form. The first data line contains the calibration coefficients. Each data line is identified by a filename of the form LB_XXXXYY where XXXX is an experiment identifier (e.g., DTIB is the second test conducted at DTI and COSA is the first test conducted at Cosmodyne) and YY is the numeric index of the data line.

4. TEST PROCEDURES

Tests run at DTI and at Cosmodyne are discussed separately for the rest of the report.

4.1 DTI Shakedown Tests

A short power up and system test was run to check out system performance.

A full day of shakedown testing followed, whose results are tabulated in Appendix B. Seven of the nine pebble bed heaters were turned on about 9:20 a.m. (power was only

available to handle seven heaters); the pebble bed had retained heat from the previous day's power up so the initial bed conditions were not ambient. The controllers were set to 750 F and this rod sheath temperature was reached in about 25 minutes. The controllers were then set to 1400 F; at 3 hours and 13 minutes into the test the setpoints were changed to 1200 F in an effort to equilibrate the bed temperature in sufficient time to complete the cool down tests within the day.

At 2:30 p.m. a six pack of nitrogen gas was used as the test fluid; gas injected into the pebble bed for periods of about 5 minutes each with successive back pressures of 50, 100 and 150 psi. A second, short nitrogen injection was conducted at 3:13 p.m. and at approximately 3:45 p.m. water was injected into the pebble bed through the inlet piping to further cool the facility and to get some experience with two phase flow. Initially, a cloud of water vapor was observed at the exhaust exit; later, as the exhaust piping sufficiently cooled the vapor, considerable condensation was observed at the exit. In fact, as water continued to be added to the pebble bed heater, water collected in the horizontal exhaust piping.

4.2 Cosmodyne Cryogenic Tests

A week of testing ensued at the Cosmodyne facility. While the first day had been expected to be a shakedown test period, the system worked from the beginning and test data was acquired. Tabular results are presented in Appendix C along with the raw notes compiled by the DTI DAS operator.

Liquid nitrogen was supplied by a constant displacement pump (Figure 9) at flow rates of 4, 6 and 8 GPM from a liquid nitrogen storage tank (Figure 10); pebble bed operating pressures were atmospheric (short start ups), 500, 1000 and 1500 psig. Pebble bed

heaters were nominally powered up about 7:00 a.m. and the bed temperature brought up to test temperatures (about 1300 F) in about 4 hours. The flow of liquid nitrogen into the pebble bed was initiated by opening the pebble bed valve and closing down the bypass valve on the liquid nitrogen supply line.

After the flow was established and a few atmospheric data points were taken, the bed was pressurized by manually closing down the exhaust valve. If the exhaust temperature significantly exceeded the design goal of 700 F, a portion of the liquid nitrogen supply was diverted to the mixer by manually opening the diverter valve. Both of these procedures were relatively easy to perform and simple adjustments maintained the desired values. The liquid nitrogen injection tests nominally lasted 5 to 15 minutes depending primarily on the flow rate; the criteria for terminating the test was the exhaust gas dropping below 700 F.

The exhaust gas exiting the pipe produced an extremely loud noise, most assuredly due to the fact that the flow was sonic at the pipe end. A Cosmodyne supplied muffler was placed over the end of the exhaust pipe but its effect was minimal.

If sufficient time remained to complete a second test during the day, the heaters were turned on to raise the bed temperature back up to the desired test temperature (~1300 F).

5. TEST RESULTS

Test results from each facility are discussed separately.

5.1 DTI Shakedown Tests

Computer generated plots of various data channels are presented here in their engineering form. Comments are made here in staccato keyed to each data plot:

- Upon heatup the upper bed radial temperatures differed by a maximum of 200 F with the highest temperature being near the heater rod. After adjusting the setpoint to 1200 F the radial temperature became quite uniform (Figure 11).
- During nitrogen gas injection at 50 psi the upper bed center temperature dropped from 1100 F to about 100 F; meanwhile the bed temperature near the heater element dropped to 400 F and the outside of the bed changed little. During the 100 psi and 150 psi purges the internal bed temperatures rose about 100 F while the outside temperature of the bed changed little (Figure 12, expanded time scale). A second nitrogen gas injection and water injection did not greatly change the bed temperature.
- The axial portion of the lower bed did not heat up as much as the outer portions (Figure 13); the maximum temperature reached in the outer bed region was 200 F less than in the upper region.
- During nitrogen gas injection the axial portion of the lower bed heated up 500 F while the outer portion heated up about 150 F (Figure 14, expanded time scale).
- During heatup the upper section liner temperature trailed the bed temperature by about 200 F (Figure 15); the upper liner temperature dropped about 200 F during the nitrogen injection while the lower liner temperature did not drop significantly until water was injected into the pebble bed (Figure 16).

- The middle bed temperature heated up a bit faster ($T \sim 200$ F) than the upper and lower bed temperature (Figure 17); during nitrogen injection the middle bed temperature dropped far less rapidly than the upper bed temperature and continued to decay slowly during subsequent nitrogen and water injection (Figure 18). As previously noted, the lower bed temperature was forced up by the nitrogen purging and did not drop significantly until water injection at which time the bed temperature dropped to ~ 200 F.
- Exhaust gas temperatures were ambient until nitrogen injection (Figure 19). The bed temperature exit temperature rose to 500 F during the first nitrogen gas injection and over 800 F during the second nitrogen purge (Figure 20). When water was injected into the bed, the bed exit temperature dropped to about 200 F. The respective mixer exhaust temperatures were 200 F, 650 F and 200 F.
- Pressure transducer output are provided in Figure 21.

5.2 Cosmodyne Cryogenic Tests

Again computer generated plots are presented here in engineering form. Comments are provided for the first test point (4 GPM, 500 psi) since this was the first time that liquid nitrogen had been injected into the pebble bed heater. Subsequent tests produced similar results to this test.

TESTS AT 4 GPM

500 PSI Backpressure

- The bed temperature was brought up to 1300 F in about three hours (Figure 22); the maximum temperature difference between the radial locations was about 200 F with the axial location being the coolest. This behavior was observed throughout the test series.

- During liquid nitrogen injection at 500 psi the upper bed axial temperature dropped about 1400 F while the outer radial locations dropped about 500 F and 200 F (Figure 23). This indicates that the nitrogen is not efficiently transferring heat from the outer portion of the upper bed, presumably due to the injector and/or baffle design.
- The axial portion of the lower bed did not heat up as much as the outer portions (Figure 24) as in the DTI tests. The maximum temperature reached was several hundred degrees lower than in the upper bed.
- The temperature of the lower bed initially heated up during liquid nitrogen injection (due to hot gases forced down from the upper two chambers) and then cooled approximately 1000 F as bed heat was transferred to the nitrogen (Figure 25). Here the radial temperatures dropped further than the axial bed temperature and remained steady after injection was terminated.
- During heatup the upper section liner temperature trails the bed temperature by about 200 F (Figure 26). During liquid nitrogen injection, the liner temperatures drop about 600 F (Figure 27).
- The middle section of the bed heats up a bit faster than the upper section (Figure 28) although they equilibrate after about 3 hours of heating. The upper and middle bed sections lose heat rapidly during liquid nitrogen injection whereas the lower bed temperature initially rises (Figure 29). When injection is terminated, the middle and lower section temperatures equilibrate.
- Exhaust temperatures were near ambient until liquid nitrogen injection forced heated gases through them (Figure 30); exhaust temperatures reached 700 F for about 5 minutes and then decreased to about 300 F at the time the injection was terminated (Figure 31).

- Pressure transducer readings during injection are included in Figure 32. Throughout the test program the pressure transducers verified that the desired bed pressure had been reached and held steady throughout injection.

1000 PSI Backpressure

Plots of the test data are included in Figures 33 through 43 in the same format as the previous test. The results are similar to those observed with the following exceptions: the initial bed temperatures were a bit higher (~100 F) and the bed exit temperature was also a bit higher and held up a bit longer. The exhaust temperature was controlled by bypassing liquid nitrogen to the mixing chamber and was held at 700 F for about 10 minutes.

1500 Psi Backpressure

Plots of the test data are included in Figures 44 through 54 in the same format. The results are similar with the following exceptions. The initial bed temperatures reached about 1400 F. Exhaust temperature reached as much as 900 F; bypass flow to the mixer was manipulated several times so that a steady temperature was not achieved during a shortened test period. This test was shut down to eliminate excessive vibrations (~5 to 10 Hz) on the liquid nitrogen feeder pipe. The test was then restarted and better control of the exhaust gas temperature was achieved.

TESTS AT 6 GPM

500 Psi Backpressure

Plots of the test data are included in Figures 55 through 65 and the results are similar to those observed in previous tests. Note that the test bed temperature was relatively high just before liquid nitrogen injection. Gas temperature at the mixer exit climbed to 800 F before the bypass line was activated; about ten minutes of data were taken during liquid nitrogen injection and the exhaust temperature was actively controlled (limited to 700 F) during about 5 minutes of testing.

1000 Psi Backpressure

Plots of the test data are included in Figures 66 through 76 with the results being similar to previous tests. Near the end of the test the bed pressure was raised to 1500 psi; no effects of the pressure change were immediately obvious.

1500 Psi Backpressure

Plots of the test data are included in Figures 77 through 87 with the results being similar to previous tests. The mixer exit temperature was brought down to 700 F by activating the bypass line and then allowed to return to about 900 F.

TESTS AT 8 GPM

500 Psi Backpressure

Plots of the test data are included in Figures 88 through 98 with the results being similar to the previous tests.

1000 Psi Backpressure

Plots of the test data are included in Figures 99 through 109 with the results being similar to the previous tests.

1500 Psi Backpressure

Plots of the test data are included in Figures 110 through 120 with the results being similar to the previous tests. This is the most stressing test planned and there were no anomalies. Near the end of the test, the bed pressure was raised to ~ 2000 psi to check the pressure vessel; safety pressure relief valves set for 2000 psi at room temperature released several times at a pressure of about 1900 psi as read manually from a pressure gauge in the exhaust line just prior to the backpressure valve. This early release may be due to the pressure drop across the bed.

Increasing Backpressure

A final test was run with the backpressure varying from zero to 2000 psi (nearly) in increments of 500 psi throughout the test. The backpressure was limited by the safety relief valves as before. Plots of the test data are included in Figures 121 to 131 with the results being similar to the previous tests. This test was run to simulate the conditions that the prototype will encounter.

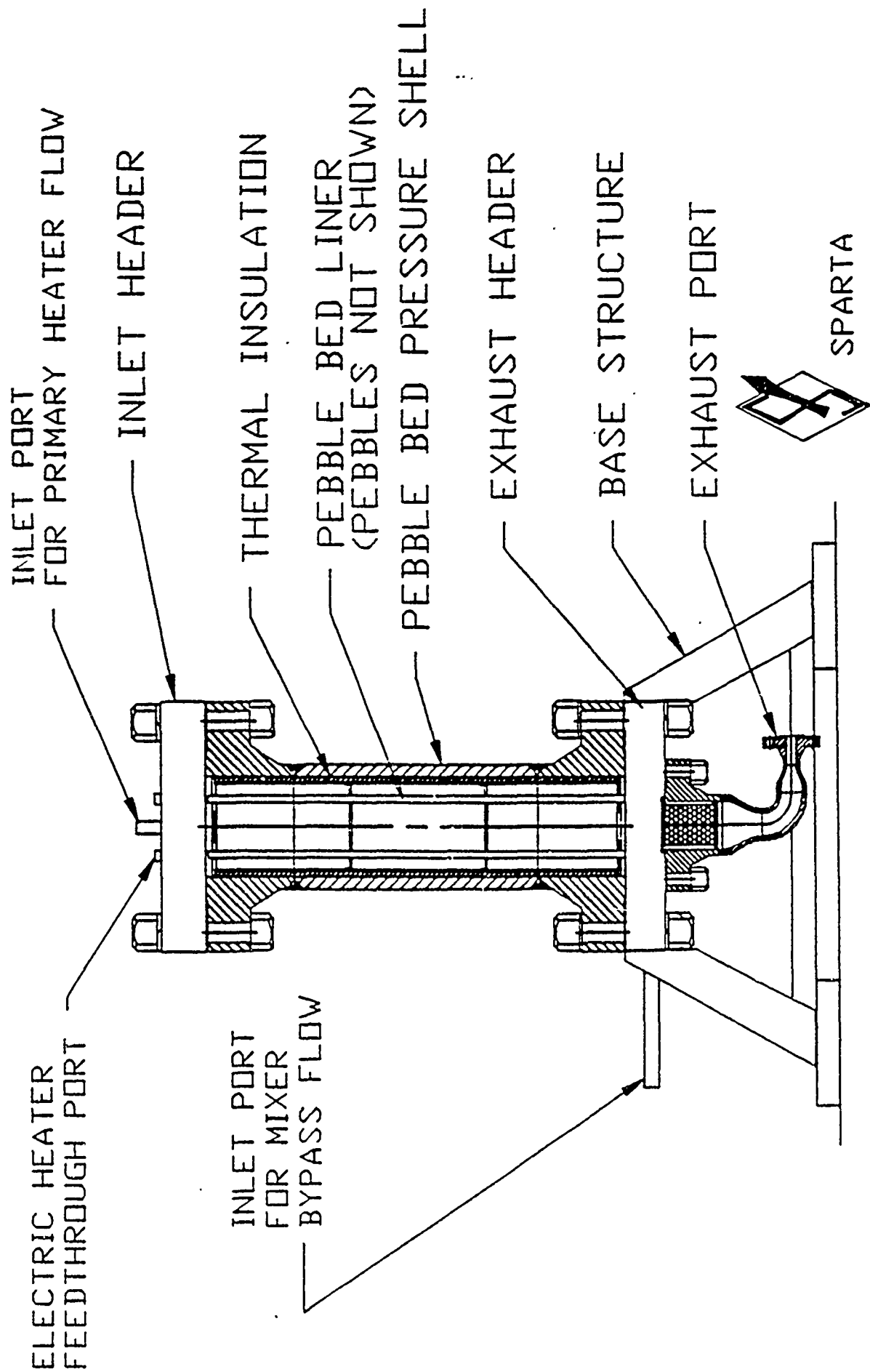
SUMMARY

Tests of the 1/48th scale heater were run and data acquired for shakedown tests and cryogenic proof tests. A DTI data acquisition system collected the data, processed it, displayed the results on a monitor in near real time, and printed out plots and tabular results in post test.

The tests at DTI were highly successful with the instrumentation, the data acquisition system and the pebble bed heater responding very much as expected. The test data should be examined in detail to assess the efficiency of the pebble bed heater and our ability to predict its flowfields and heat transfer. It appears from the tests that the lower section of the pebble bed heater did not heat up as uniformly as desired and that a more uniform nitrogen flowfield could be achieved by a different injection and/or baffle arrangement.

Tests at Cosmodyne were the first to our knowledge to flash heat a liquified gas to elevated temperatures in one pass. The pebble bed heater behaved very much like it did at DTI with nitrogen gas injection. There exist a few questions of improving the pebble bed efficiency but no question of proof of principle. An important secondary achievement is that the mixer exhaust temperature could be controlled by introducing liquid nitrogen directly into the pebble bed exhaust using the bypass line.

FIGURE 1. SCHEMATIC OF SUPERHEATER DESIGN



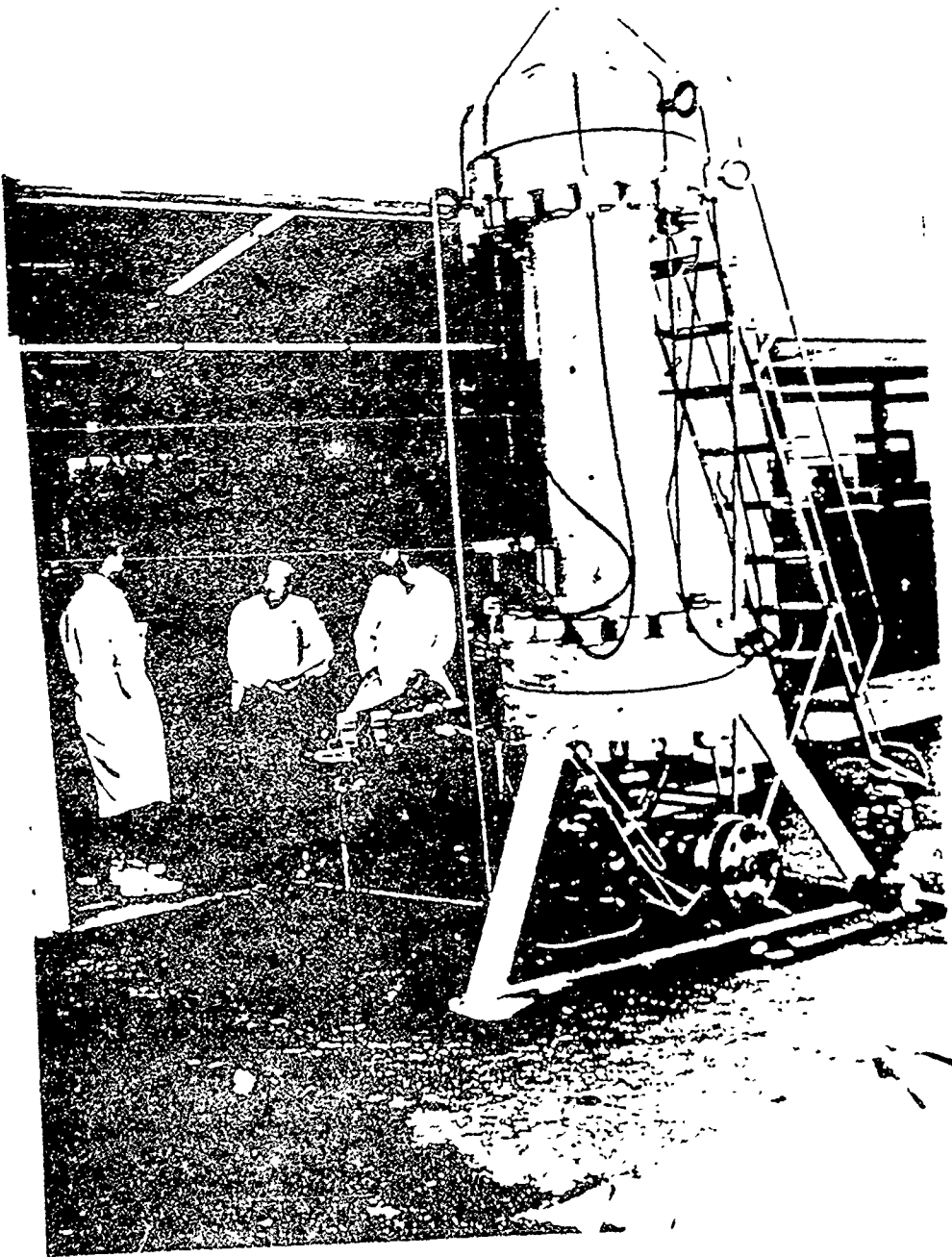


FIGURE 2. LBTS PEBBLE BED HEATER BEING TESTED AT DTI

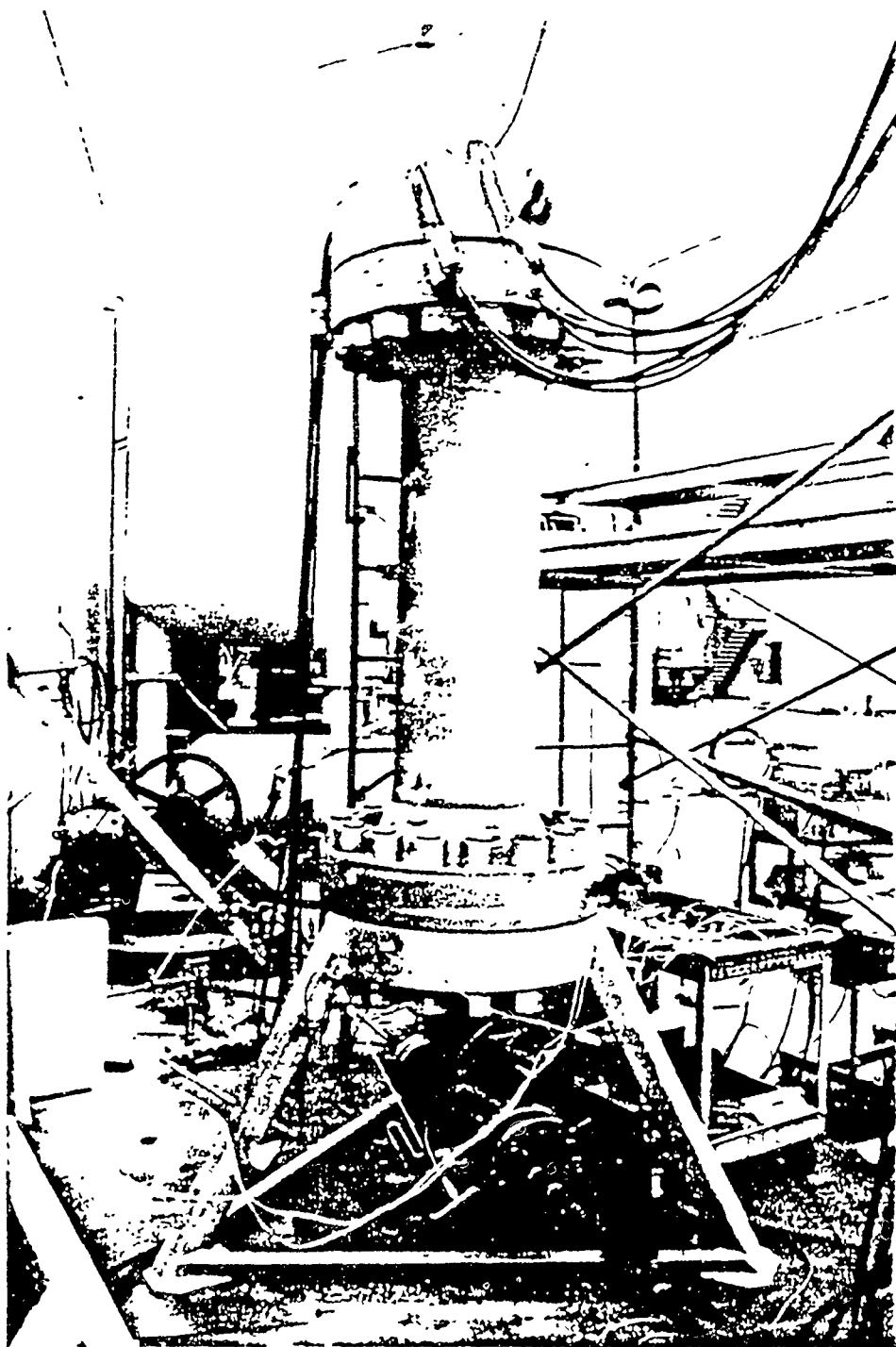


FIGURE 3 LBTS PEBBLE BED HEATER BEING TESTED AT COSMODYNE

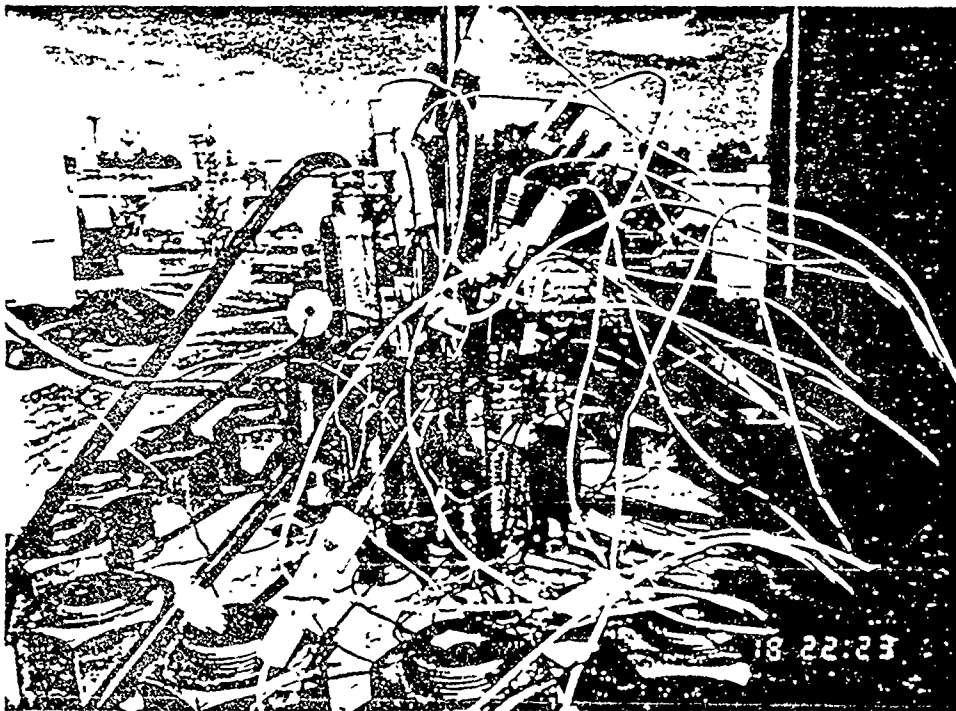


FIGURE 4. HEATING AND INSTRUMENTATION WIRING ON TOP OF THE PEBBLE BED HEATER

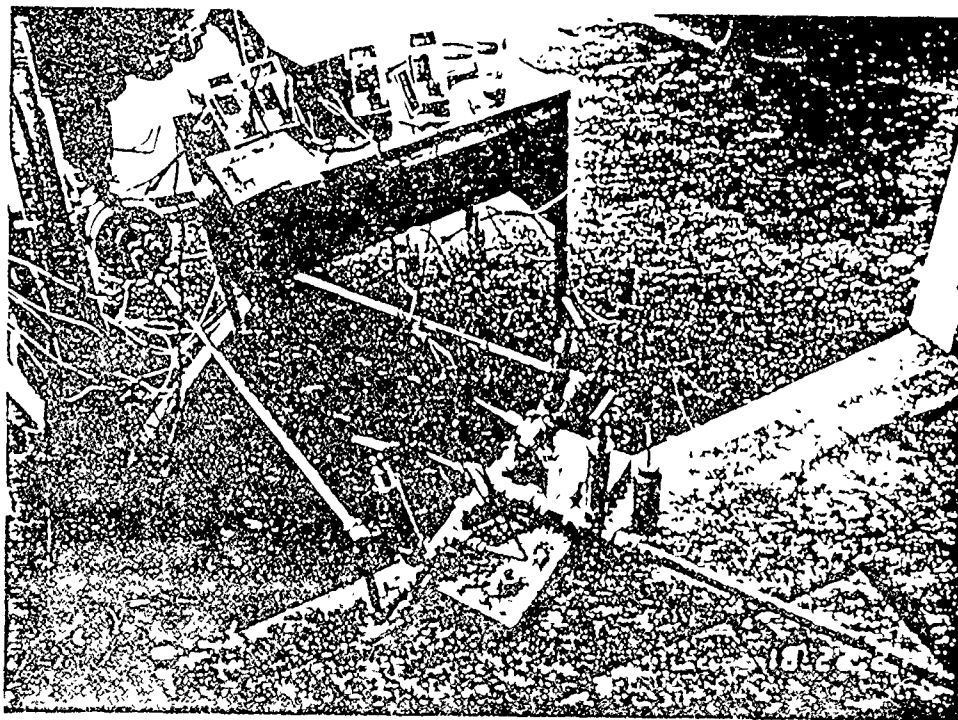


FIGURE 5. INLET AND BYPASS PIPING AND VALVE CONTROL ARRANGEMENT



FIGURE 6. INSTRUMENTATION AND DATA ACQUISITION SYSTEM

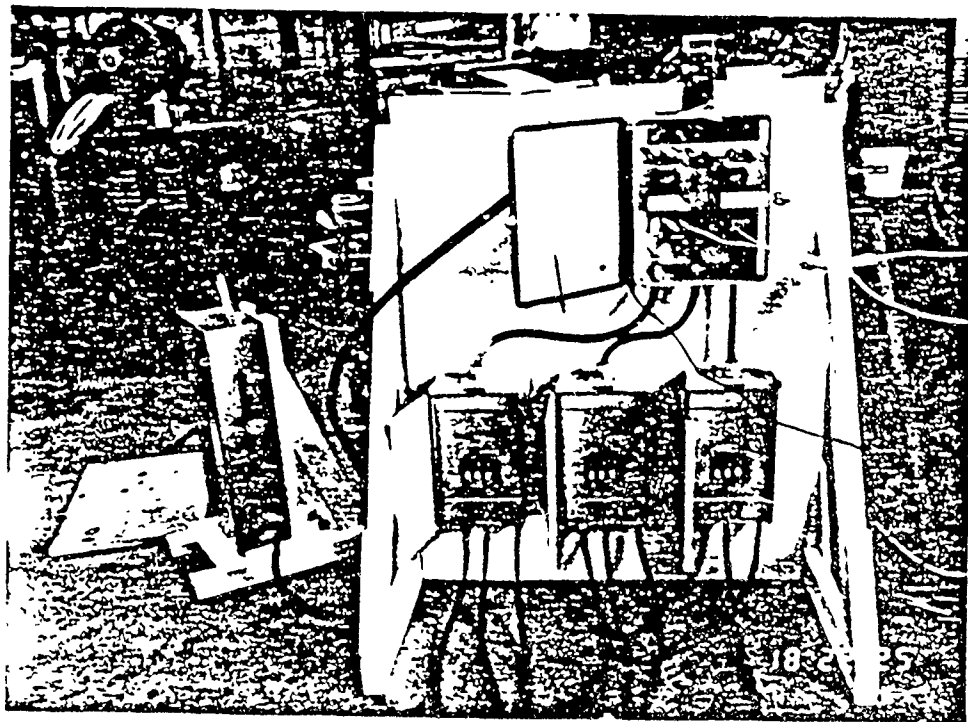
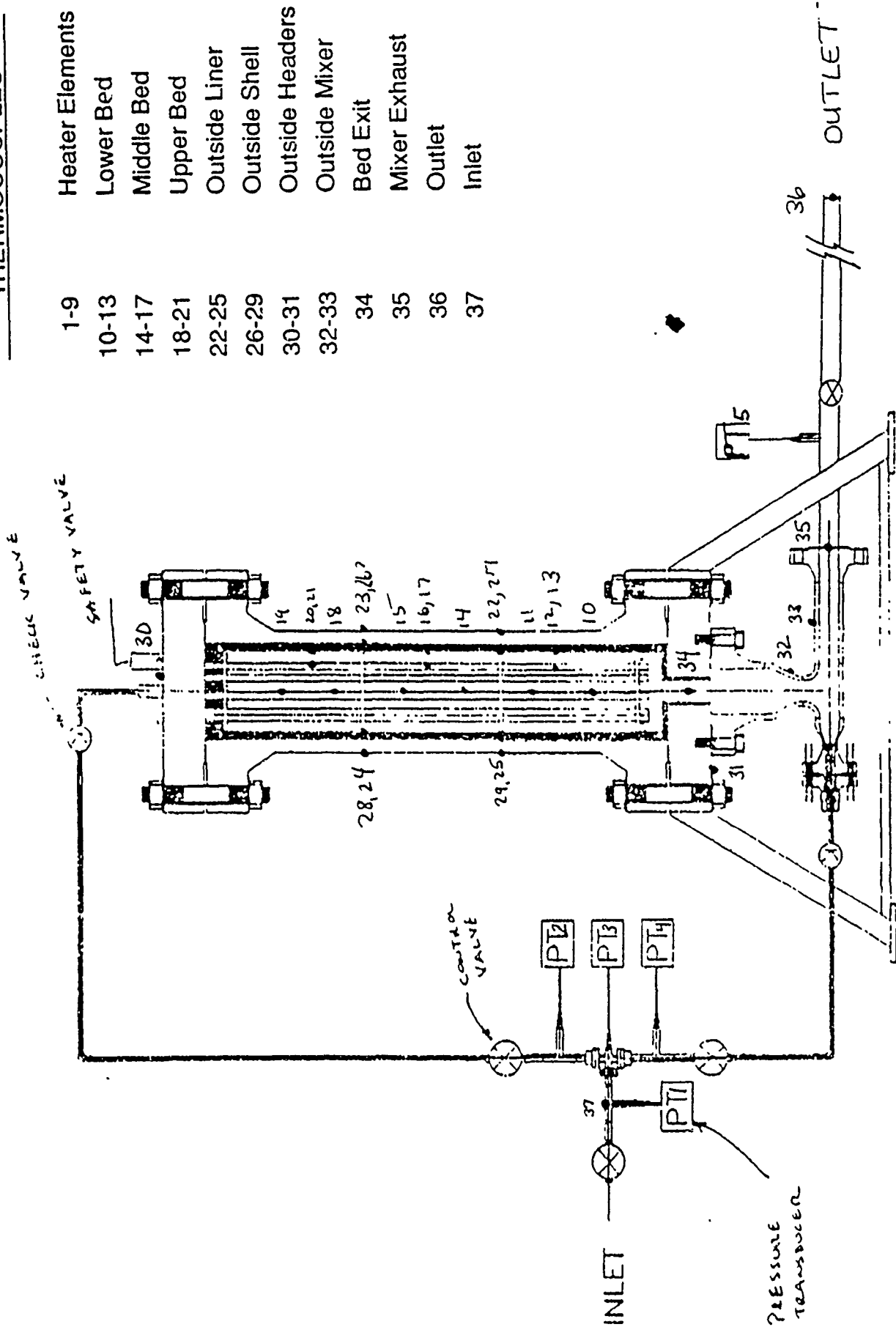


FIGURE 7. HEATER POWER AND CONTROL SYSTEM

THERMOCOUPLES



Heater Elements	
Lower Bed	1-9
Middle Bed	10-13
Upper Bed	14-17
Outside Liner	18-21
Outside Shell	22-25
Outside Headers	26-29
Outside Mixer	30-31
Bed Exit	32-33
Mixer Exhaust	34
Outlet	35
Inlet	36
	37

FIGURE 8. SENSOR LOCATIONS

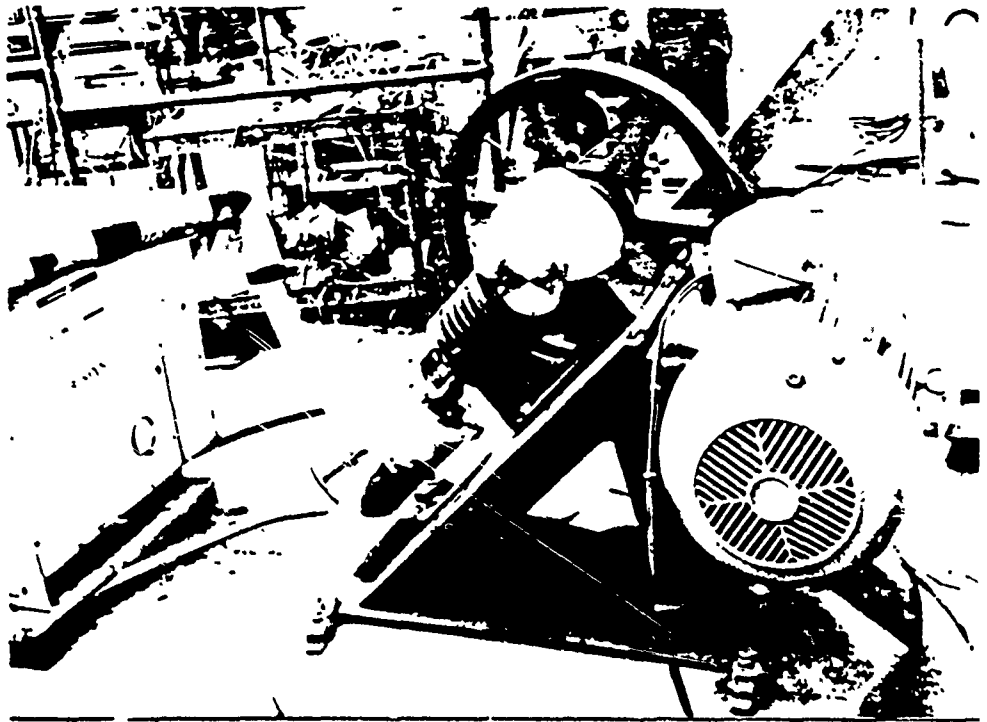


FIGURE 9 CRYOGENIC PUMP

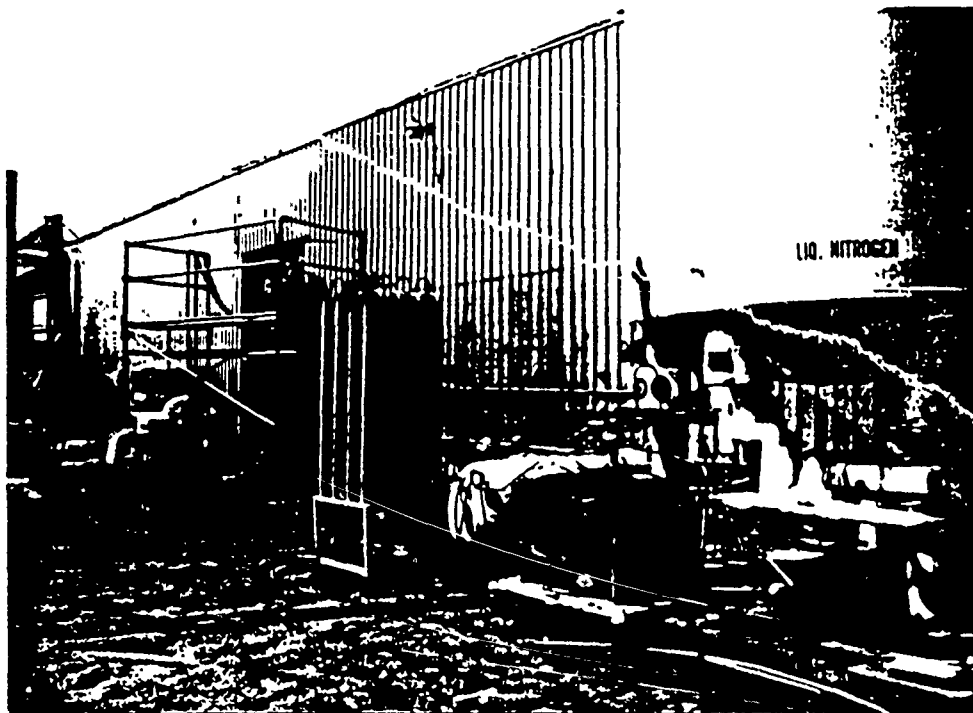


FIGURE 10 LIQUID NITROGEN STORAGE TANK

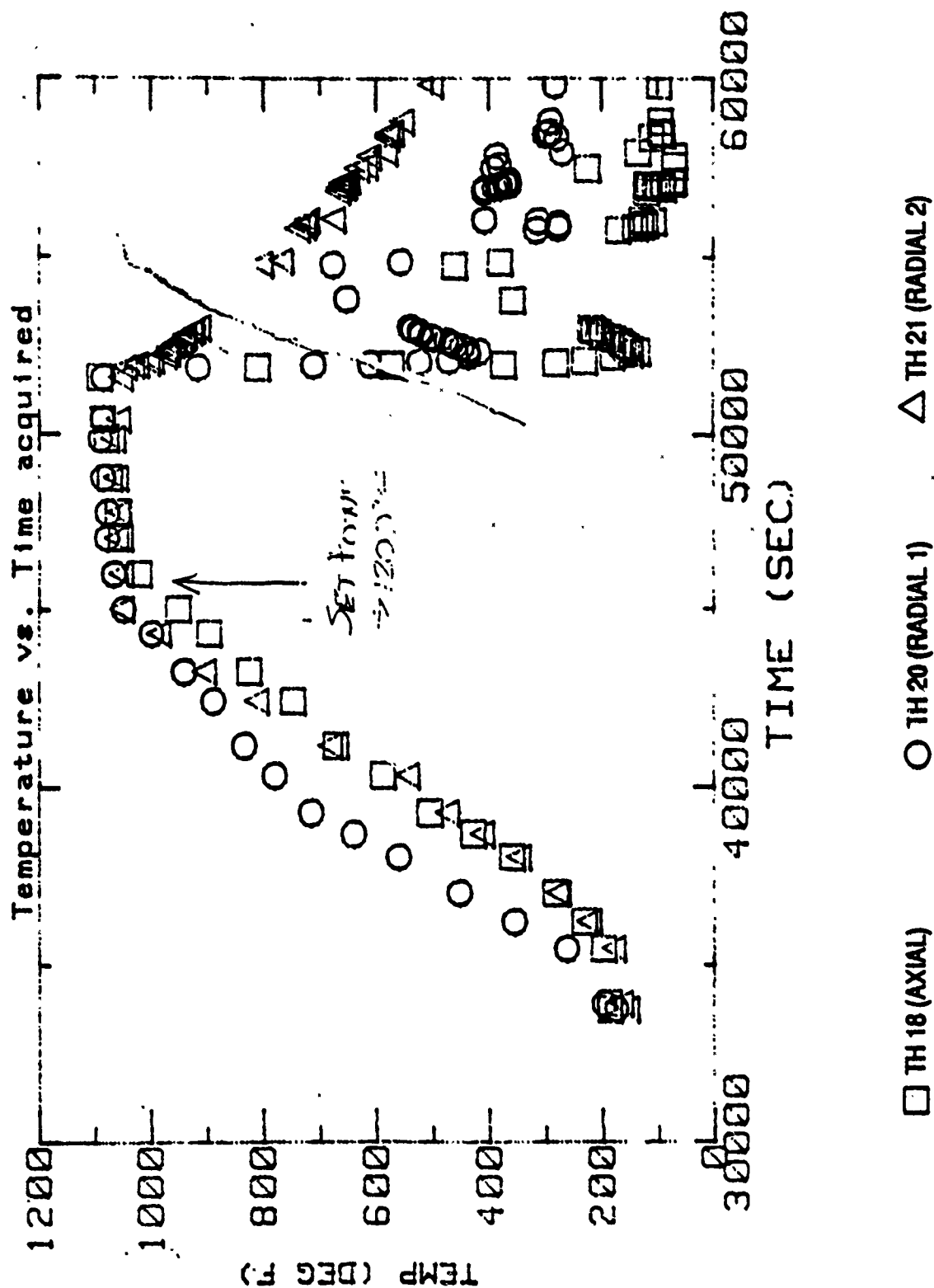


FIGURE 11. UPPER BED RADIAL TEMPERATURE DISTRIBUTION
FULL TEST

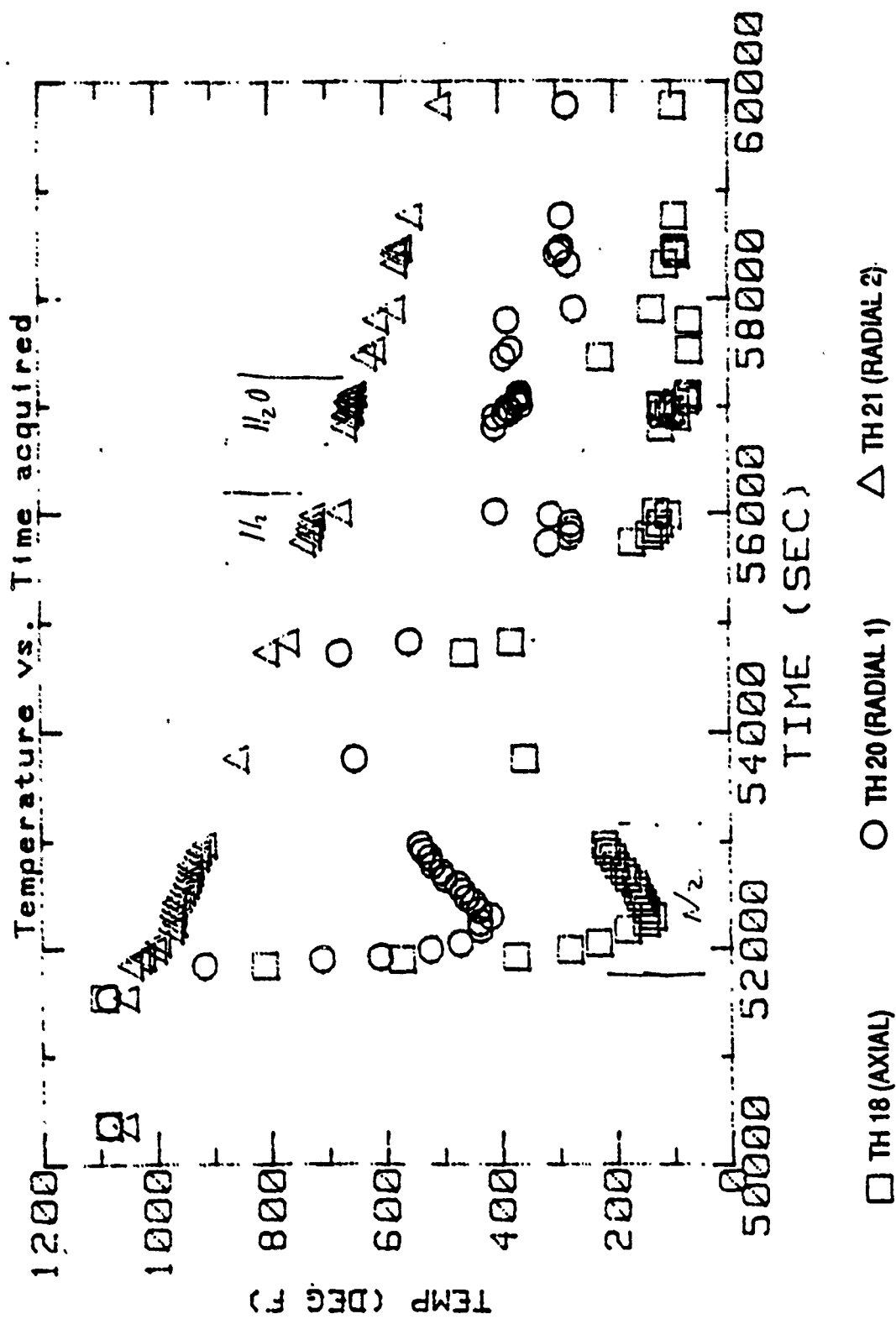


FIGURE 12. UPPER BED RADIAL TEMPERATURE DISTRIBUTION
EXPANDED TIME SCALE DURING INJECTION

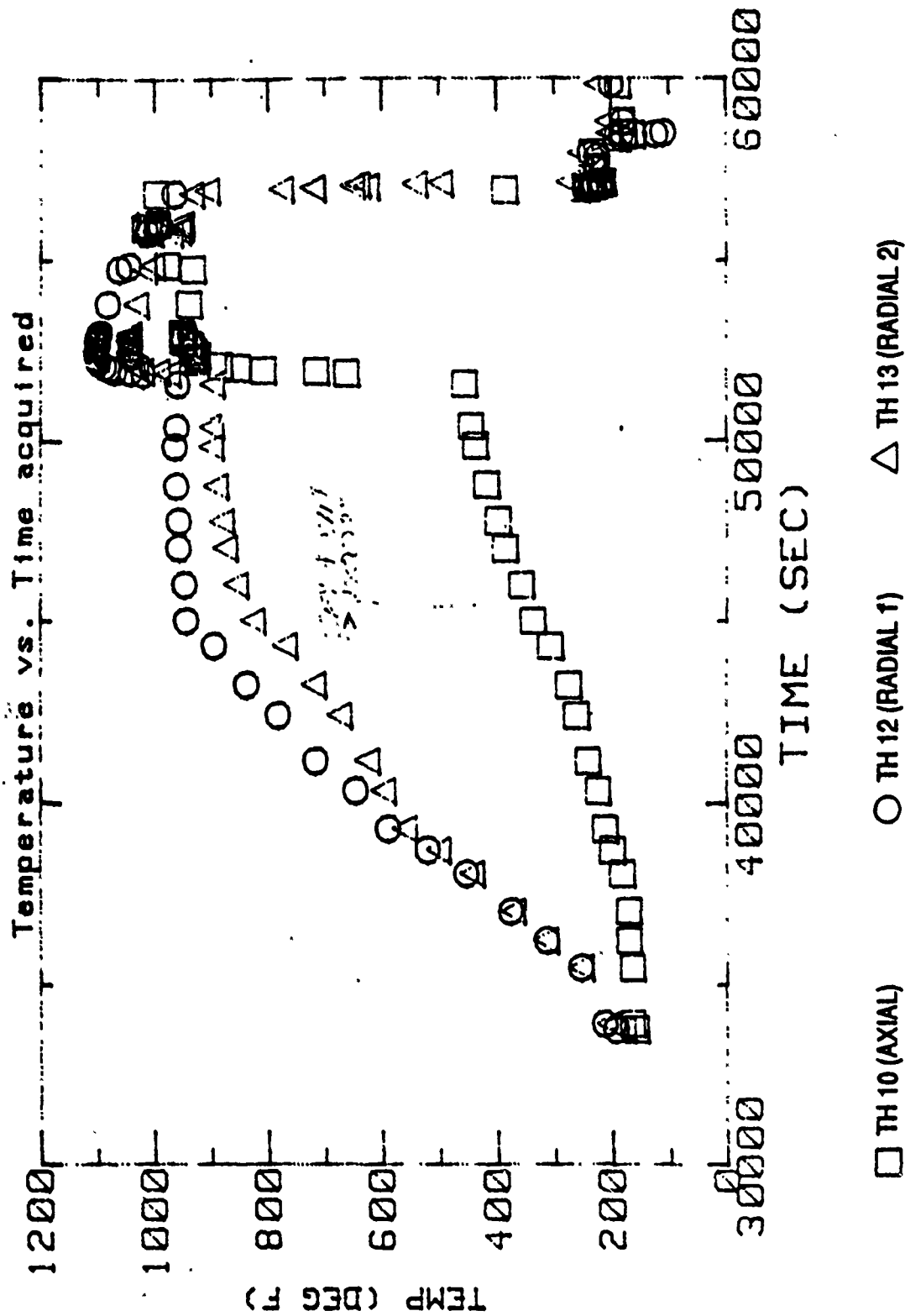


FIGURE 13. LOWER BED RADIAL TEMPERATURE DISTRIBUTION
FULL TEST

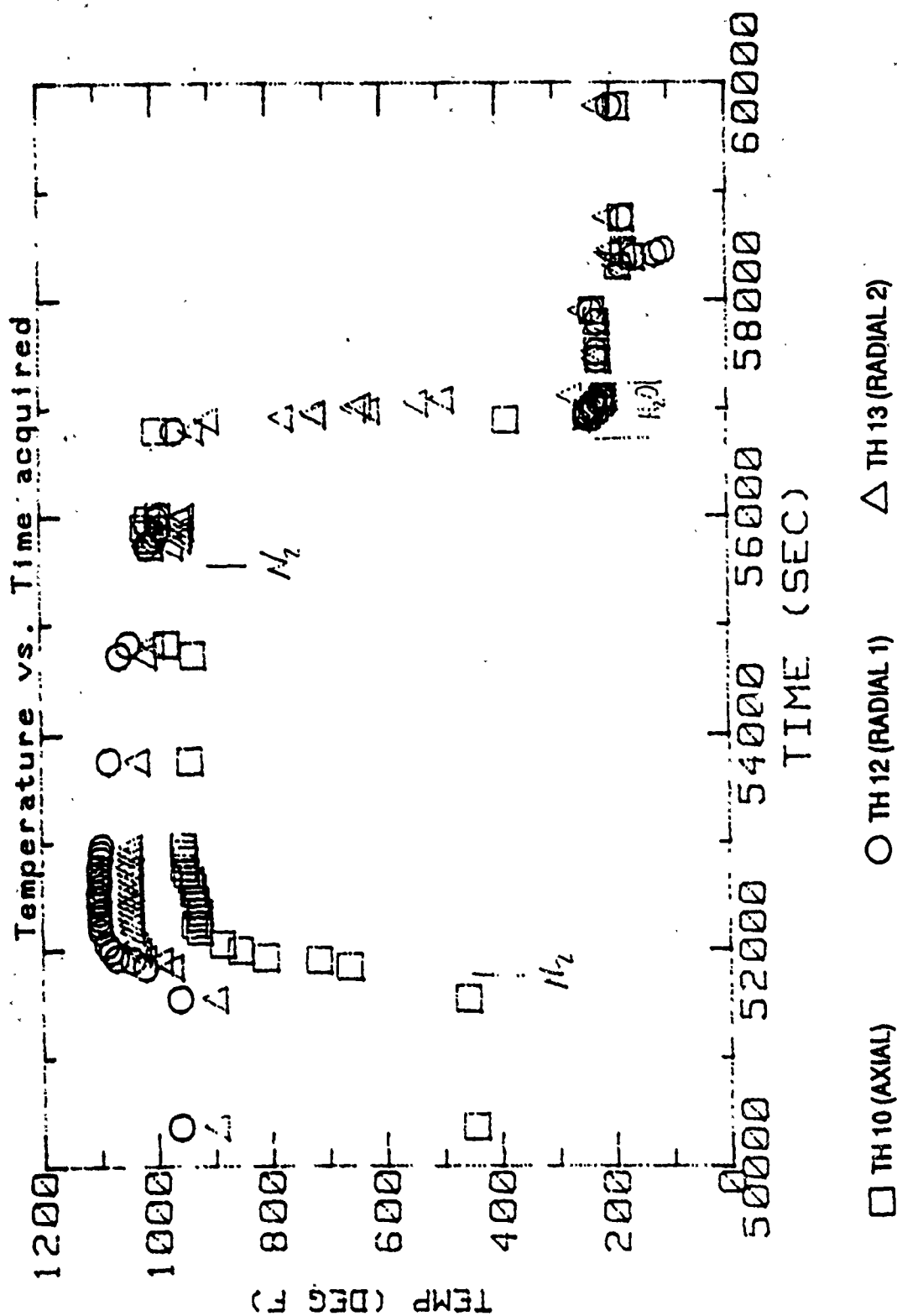


FIGURE 14. LOWER BED RADIAL TEMPERATURE DISTRIBUTION
EXPANDED TIME SCALE

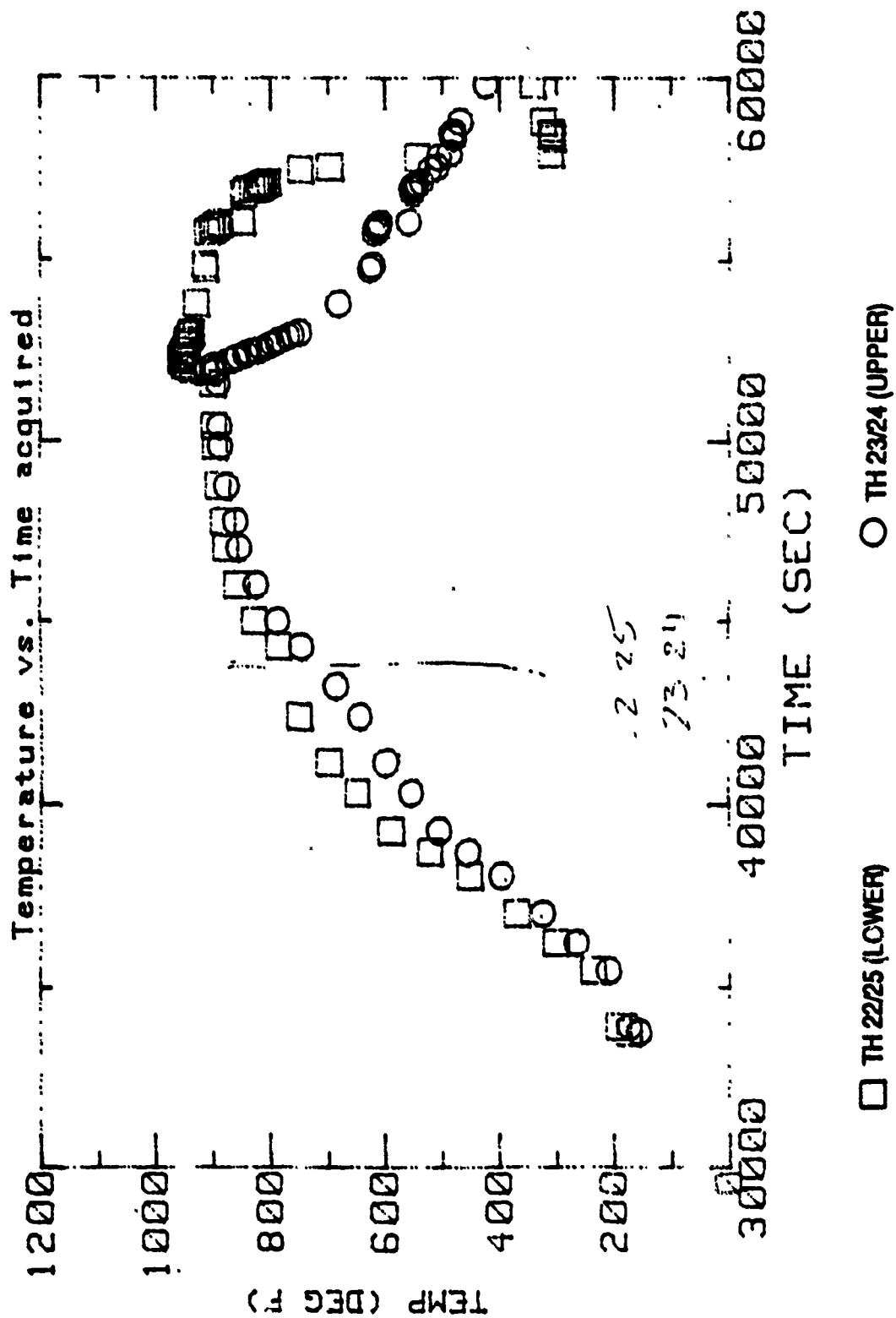


FIGURE 15. OUTSIDE LINER TEMPERATURES
FULL TEST

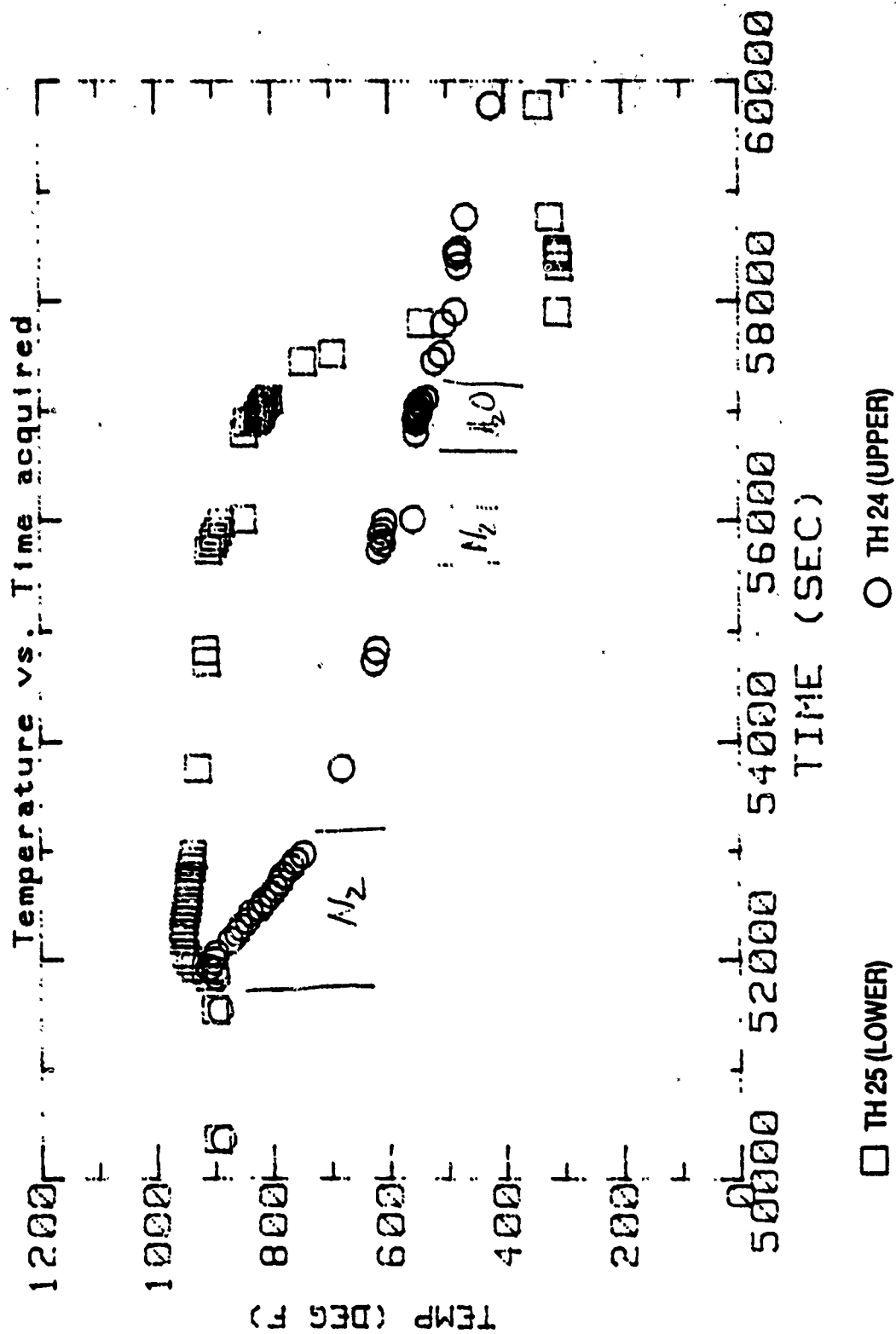


FIGURE 16. OUTSIDE LINER TEMPERATURE
EXPANDED TIME SCALE

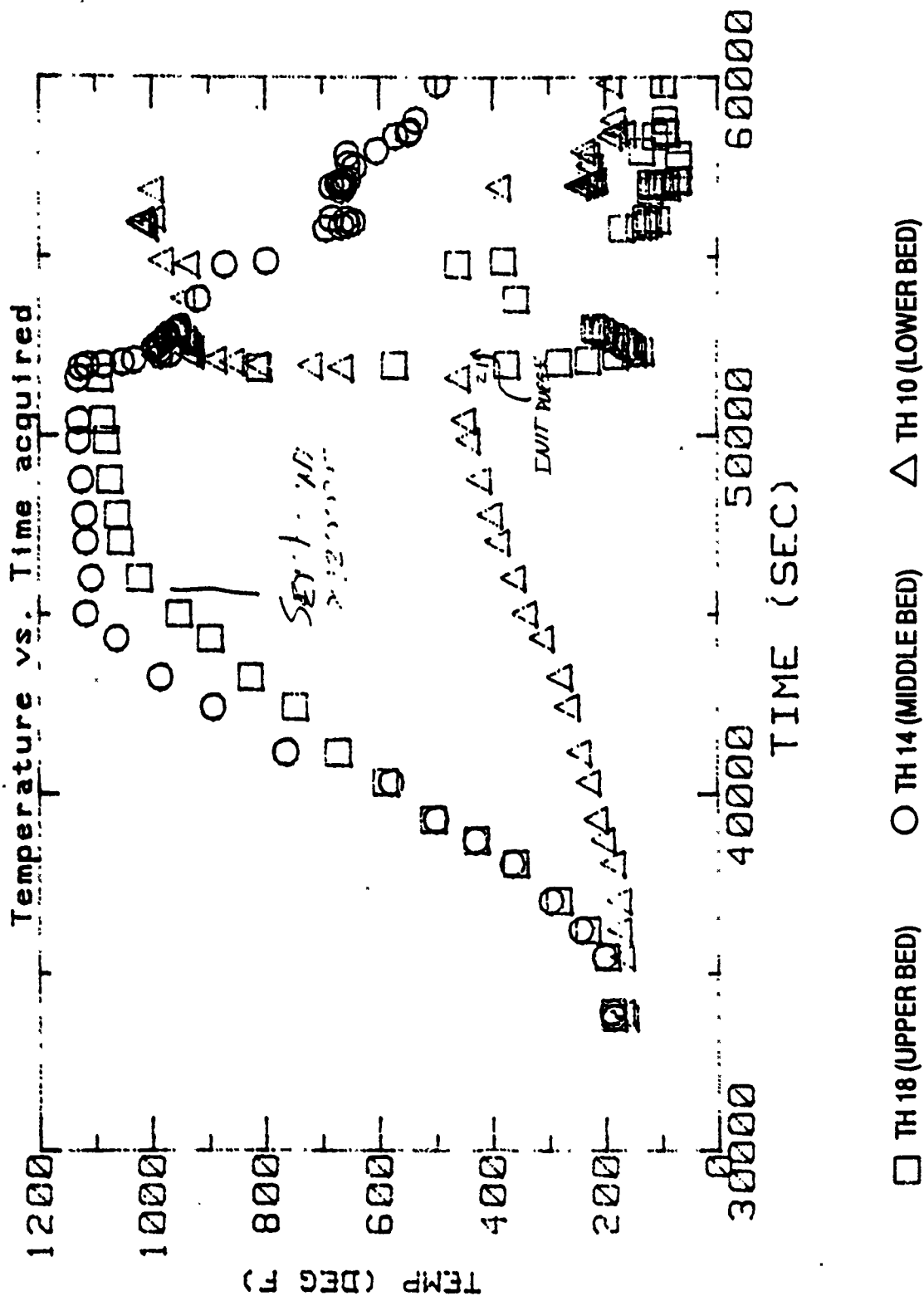


FIGURE 17. AXIAL TEMPERATURE DISTRIBUTION
FULL TEST

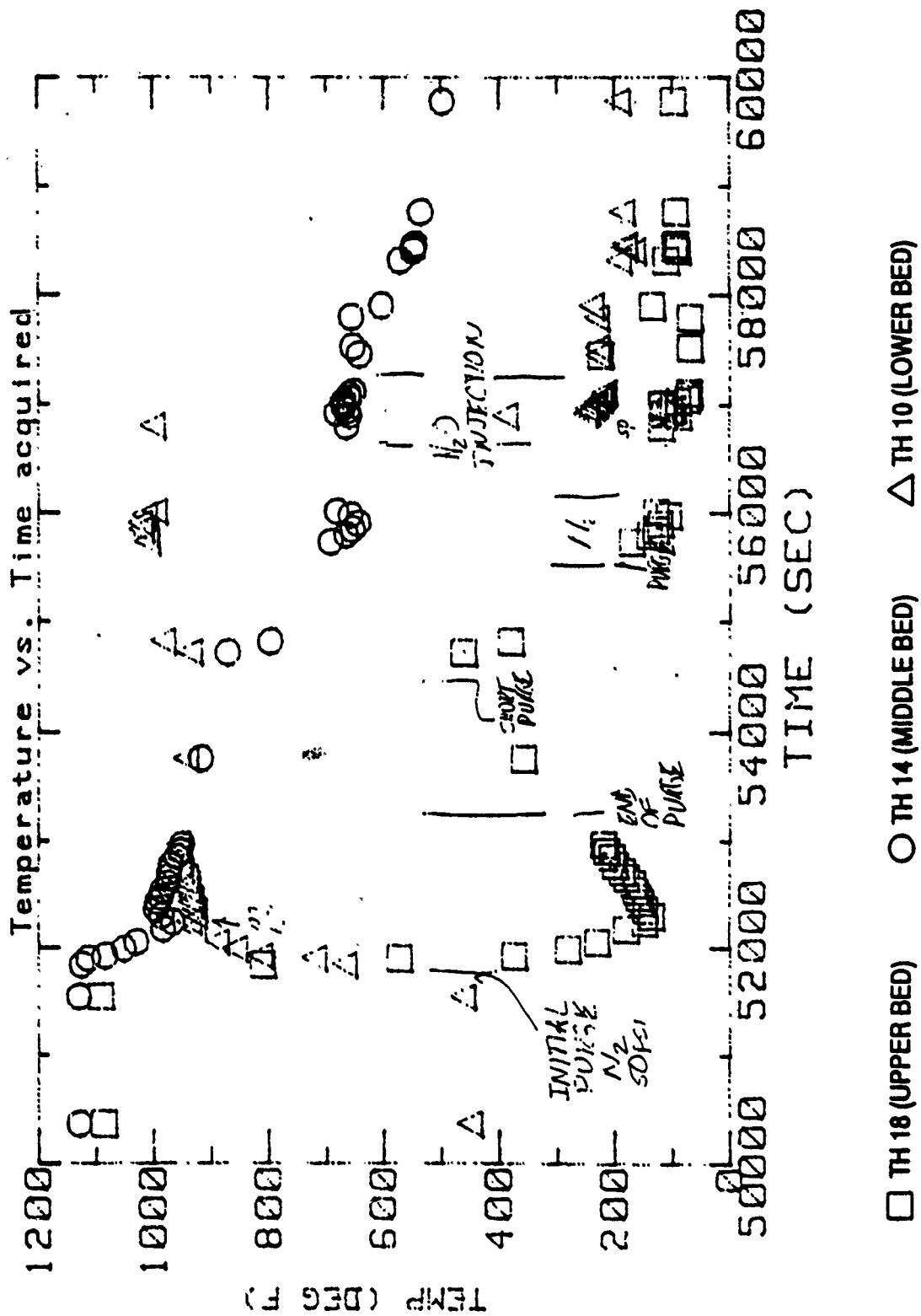


FIGURE 18. AXIAL TEMPERATURE DISTRIBUTION
EXPANDED TIME SCALE

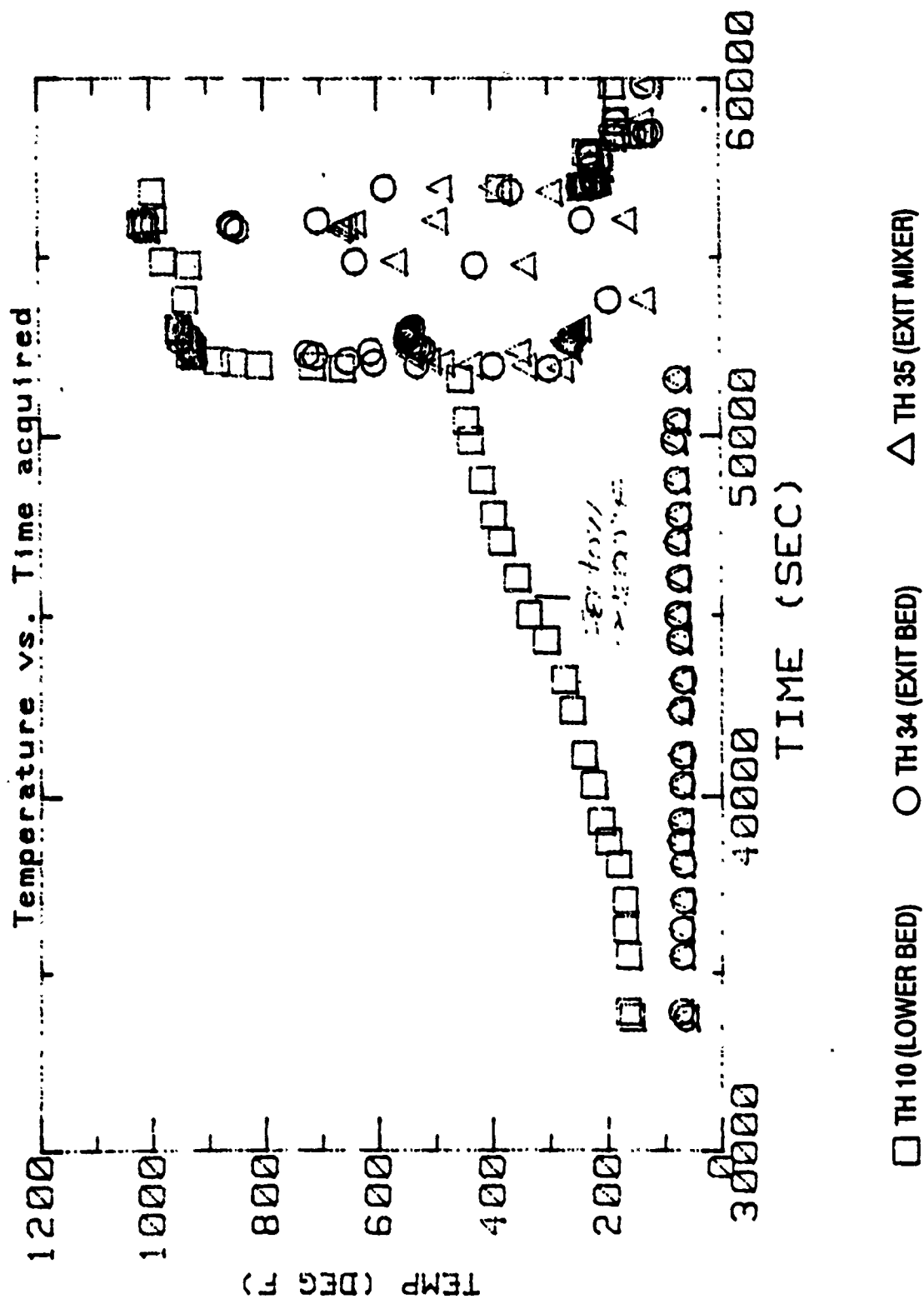


FIGURE 19. EXHAUST TEMPERATURES - FULL TEST

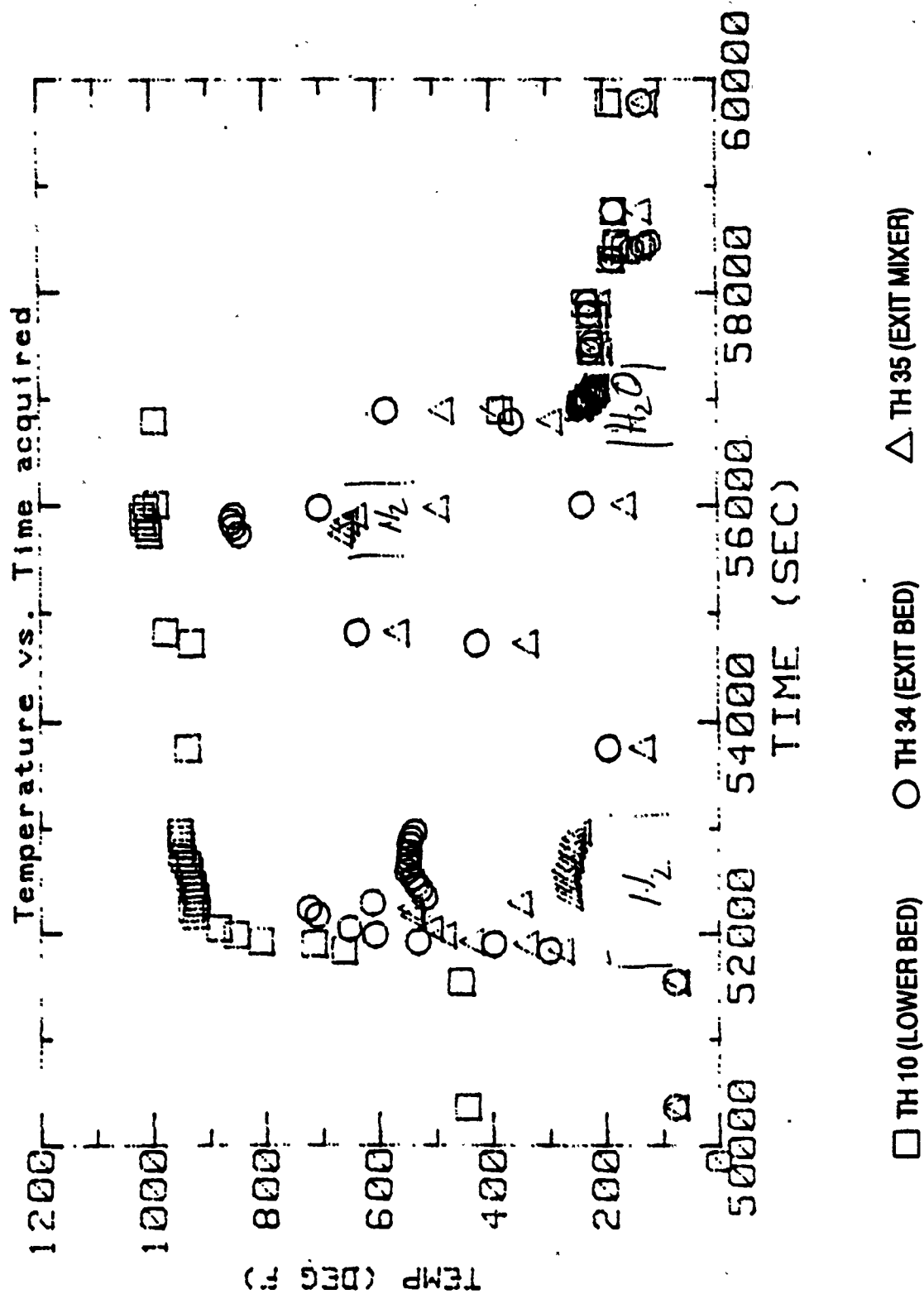


FIGURE 20. EXHAUST TEMPERATURES - EXPANDED TIME SCALES

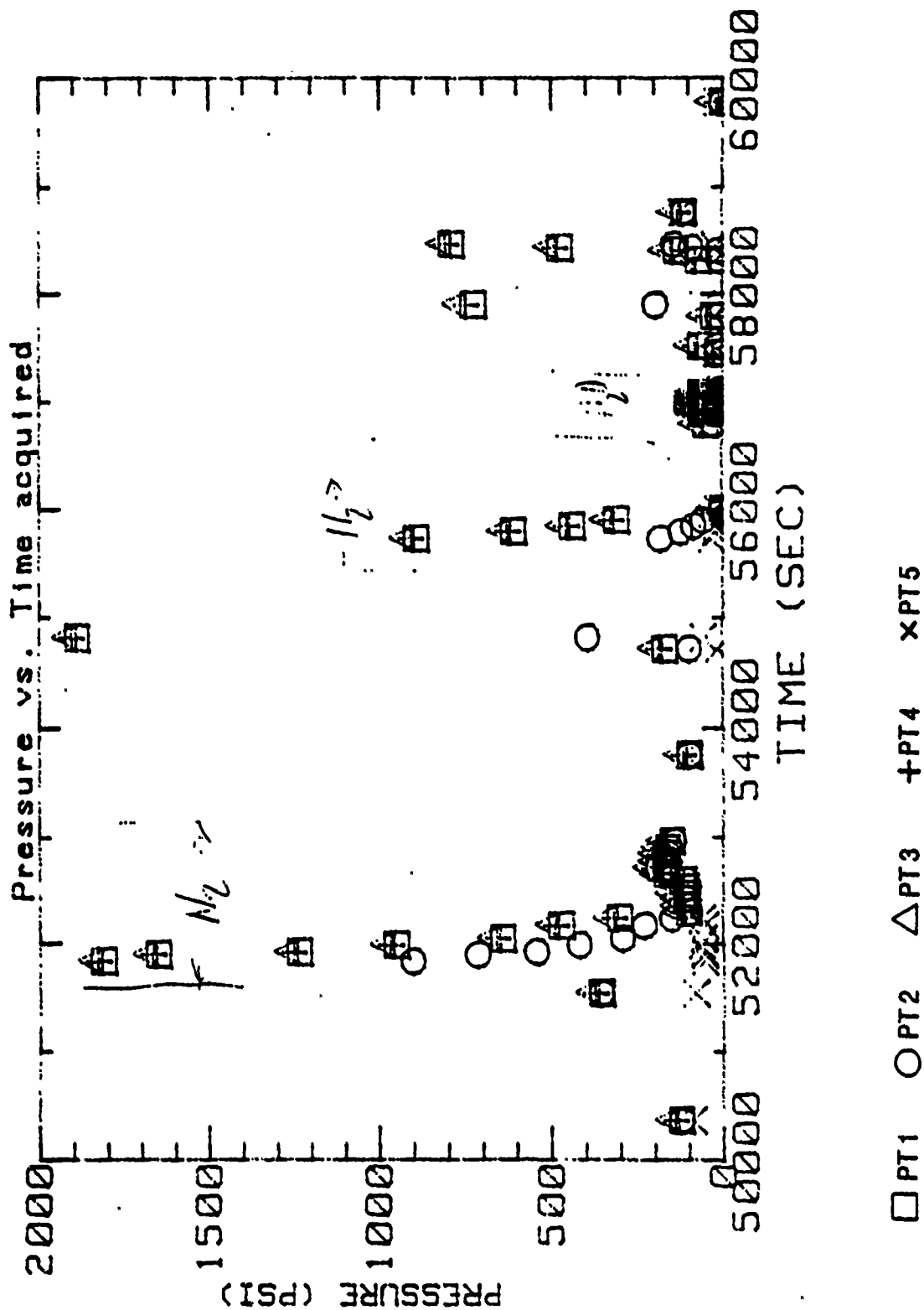
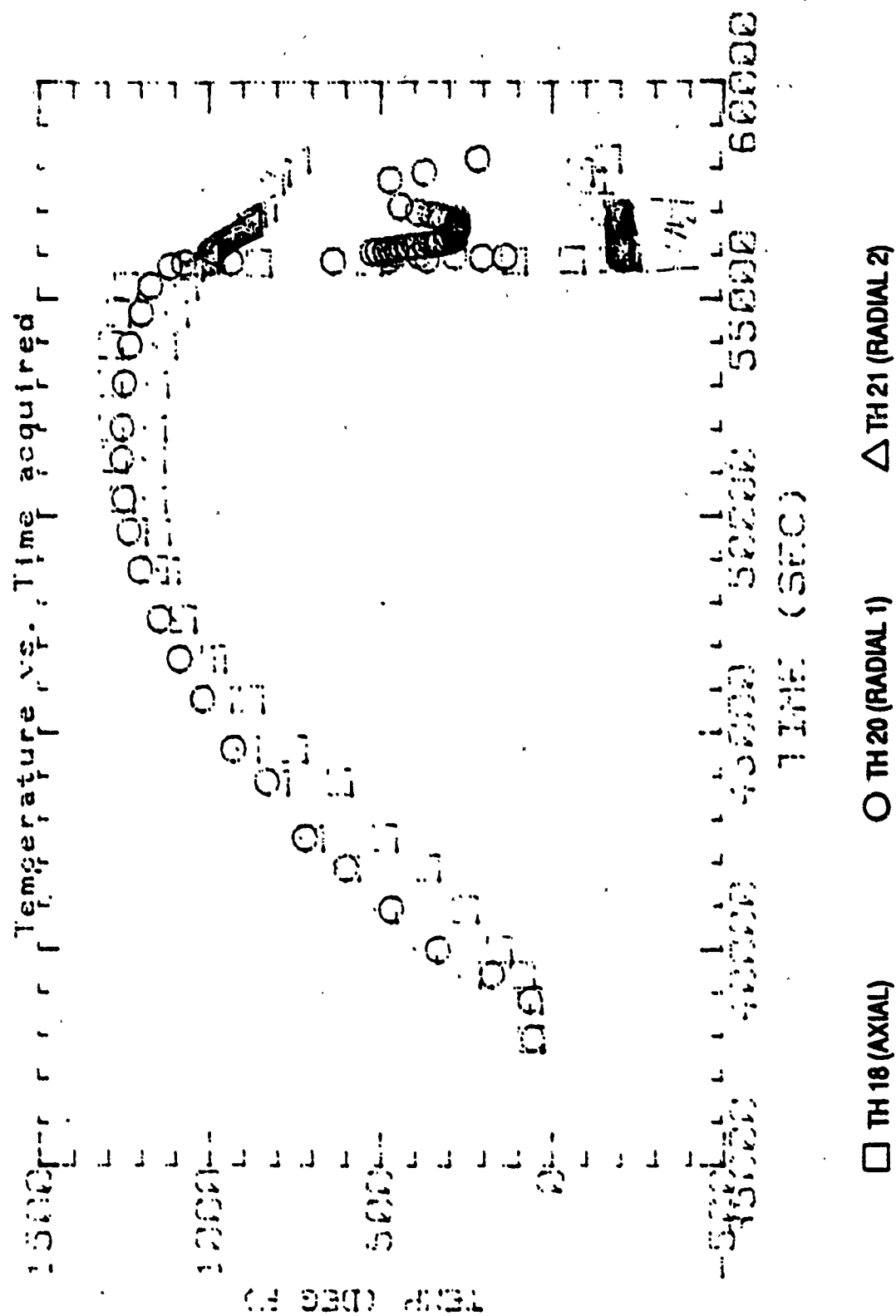


FIGURE 21. BED PRESSURE - EXPANDED TIME SCALE



**FIGURE 22. UPPER BED RADIAL TEMPERATURE DISTRIBUTION
FULL TEST**

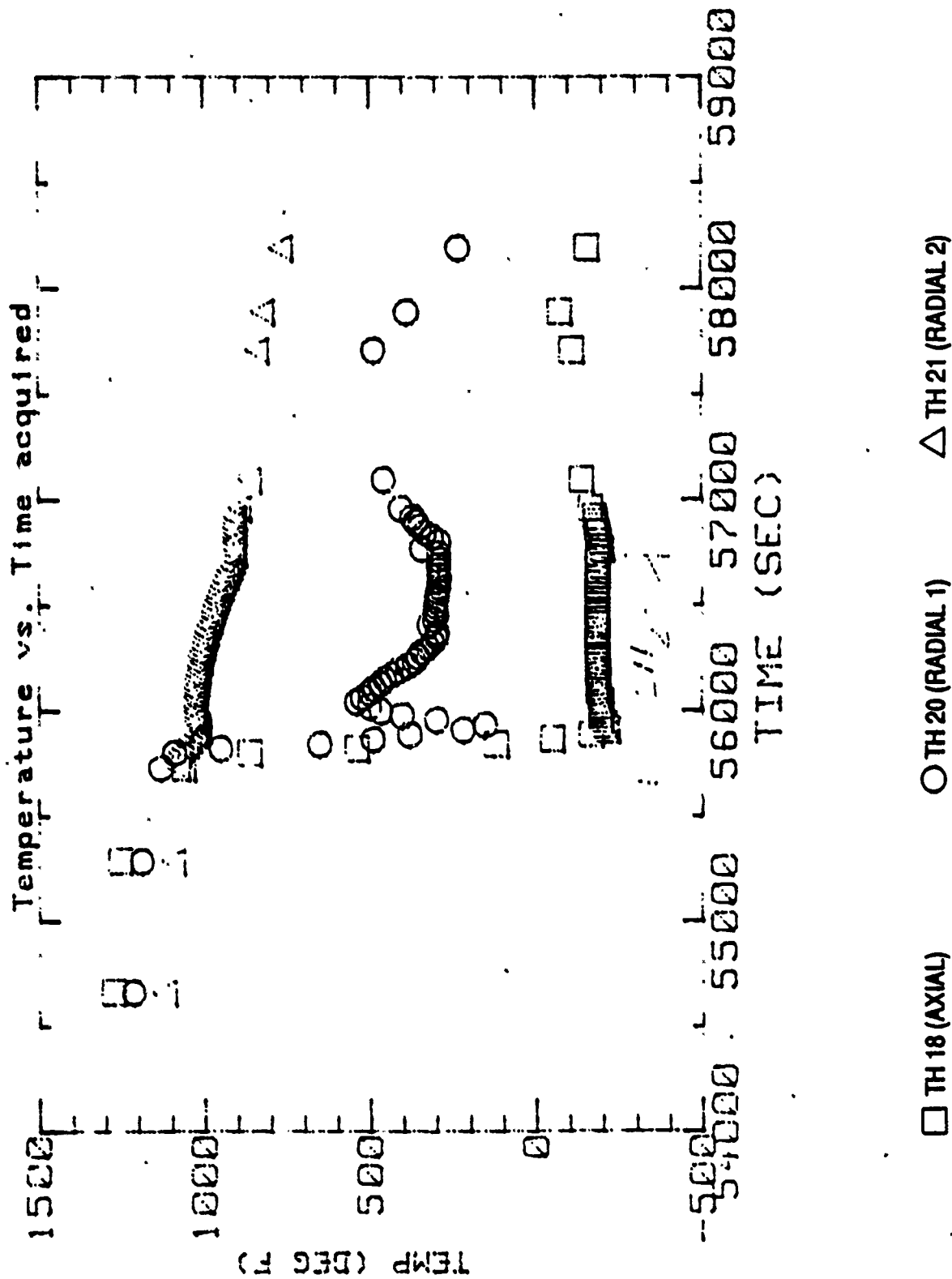


FIGURE 23. UPPER BED RADIAL TEMPERATURE DISTRIBUTION
EXPANDED TIME SCALE DURING INJECTION

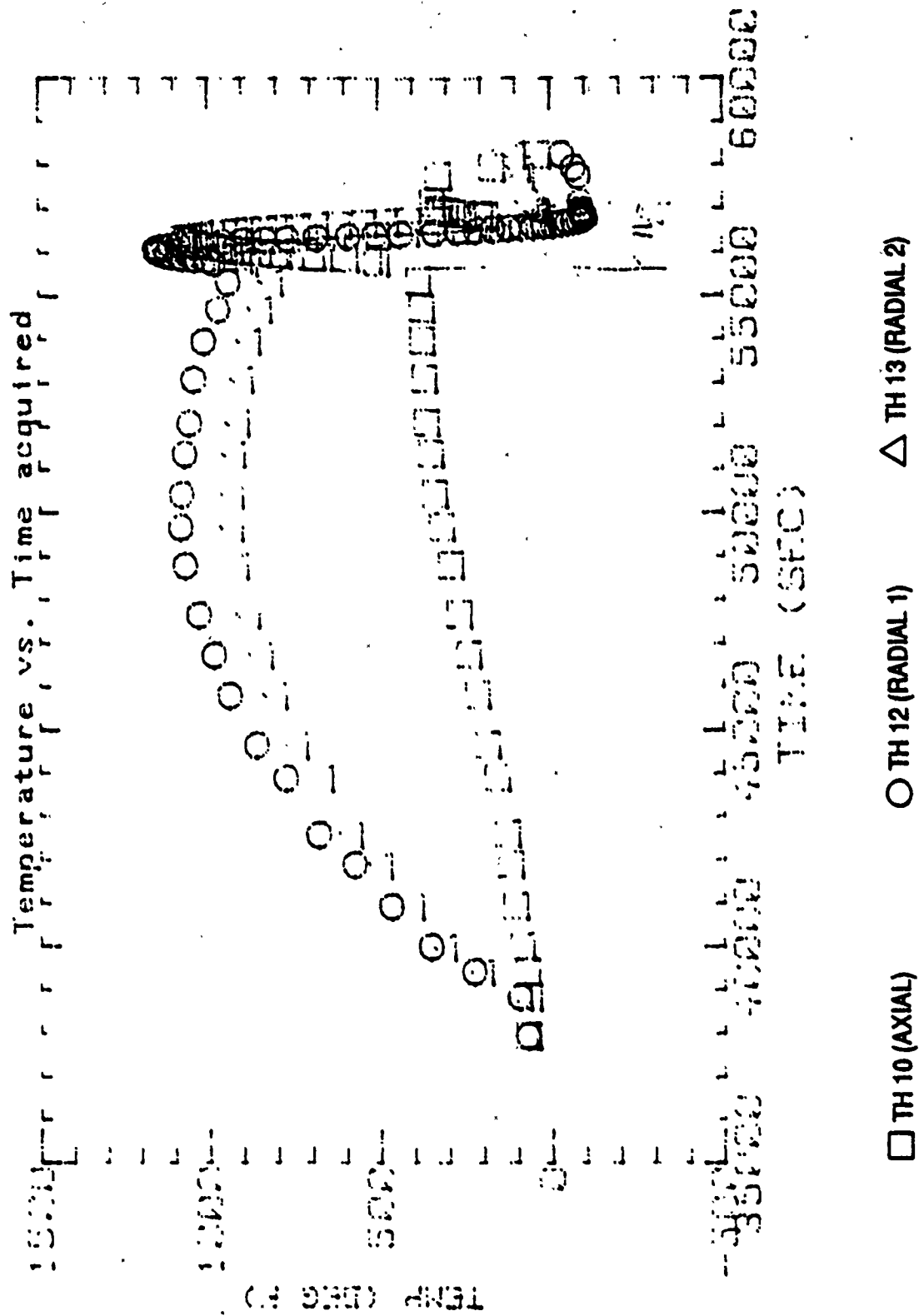


FIGURE 24. LOWER BED RADIAL TEMPERATURE DISTRIBUTION
FULL TEST

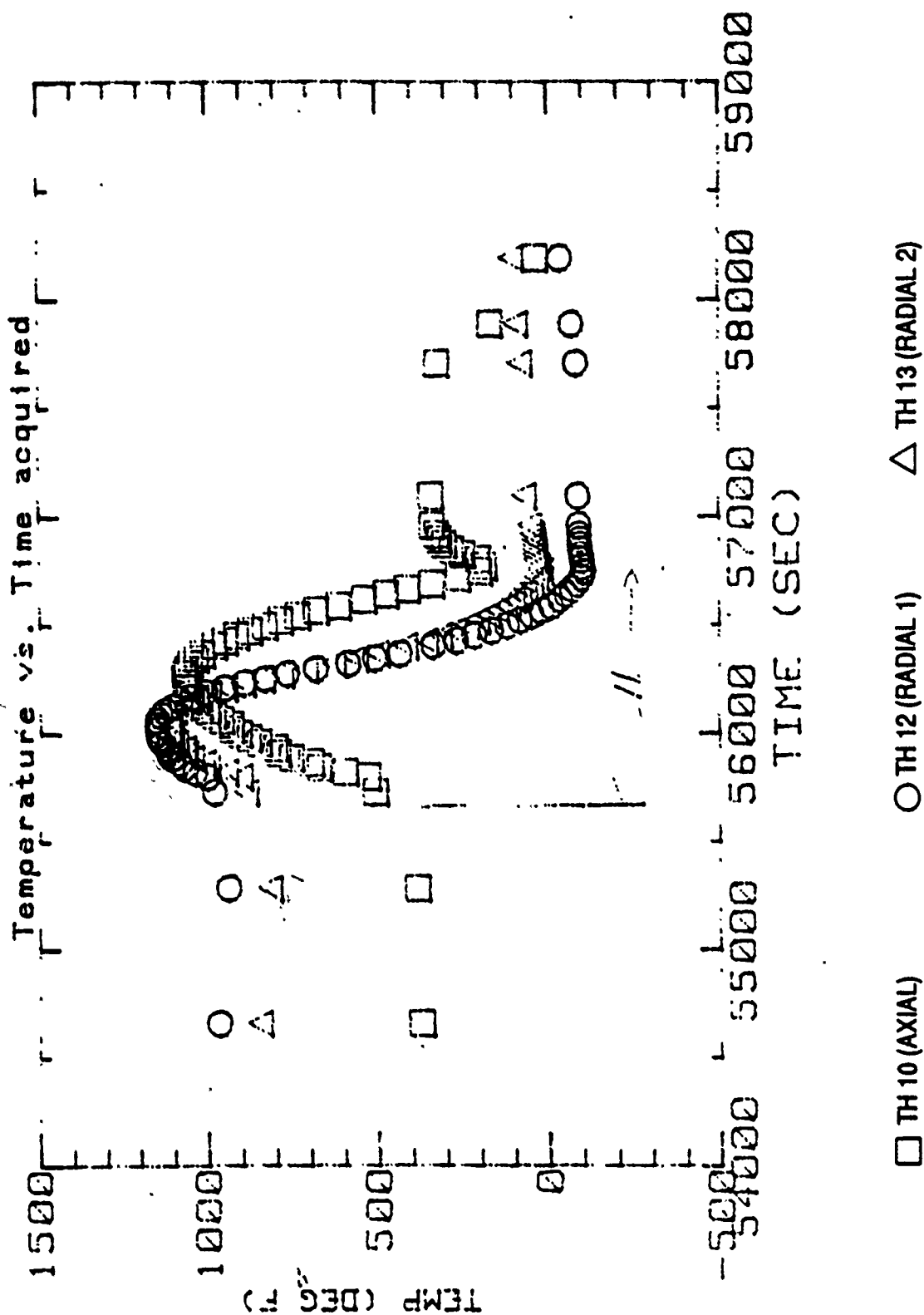
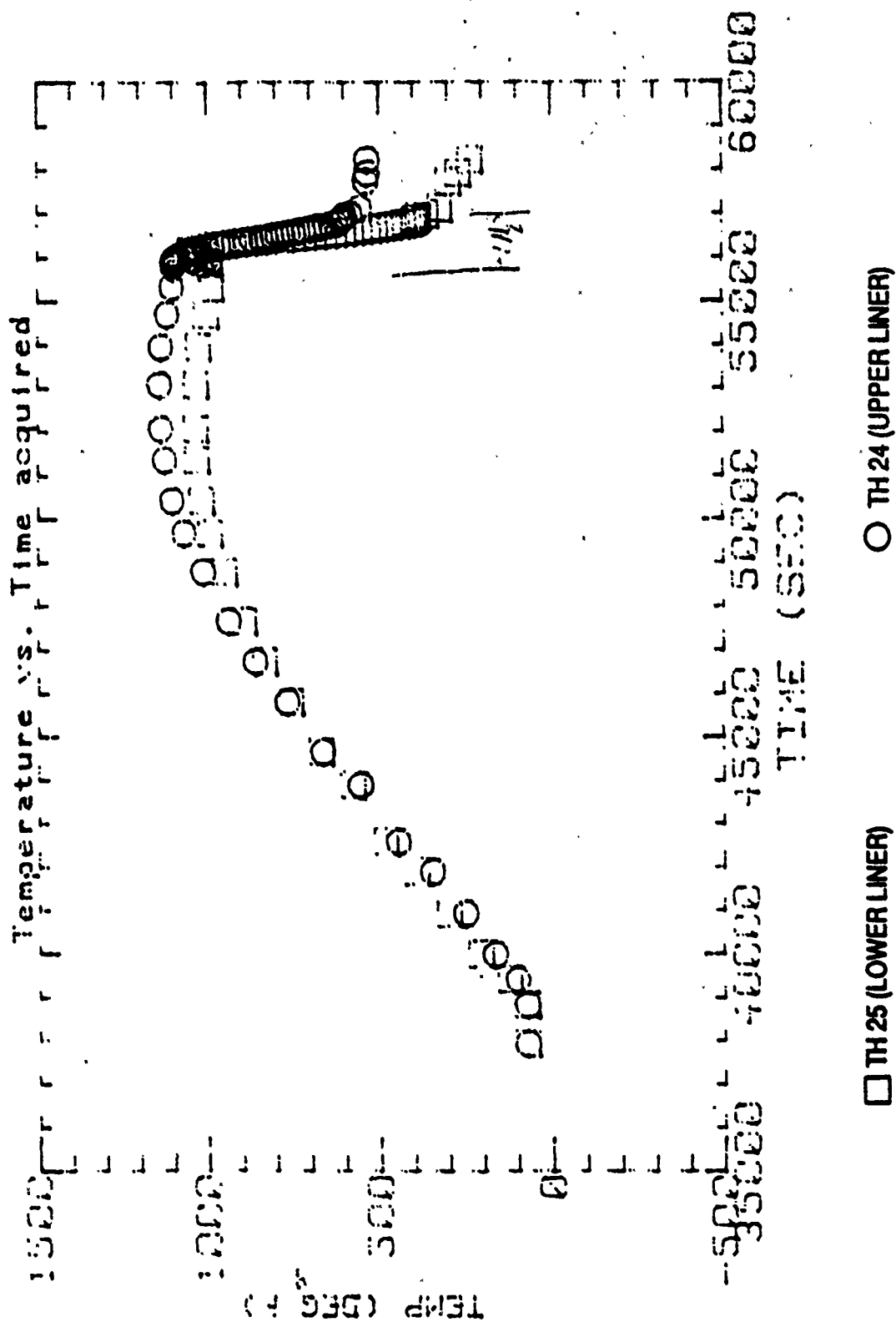


FIGURE 25. LOWER BED RADIAL TEMPERATURE DISTRIBUTION
EXPANDED TIME SCALE DURING INJECTION



**FIGURE 26. OUTSIDE LINER TEMPERATURES
FULL TEST**

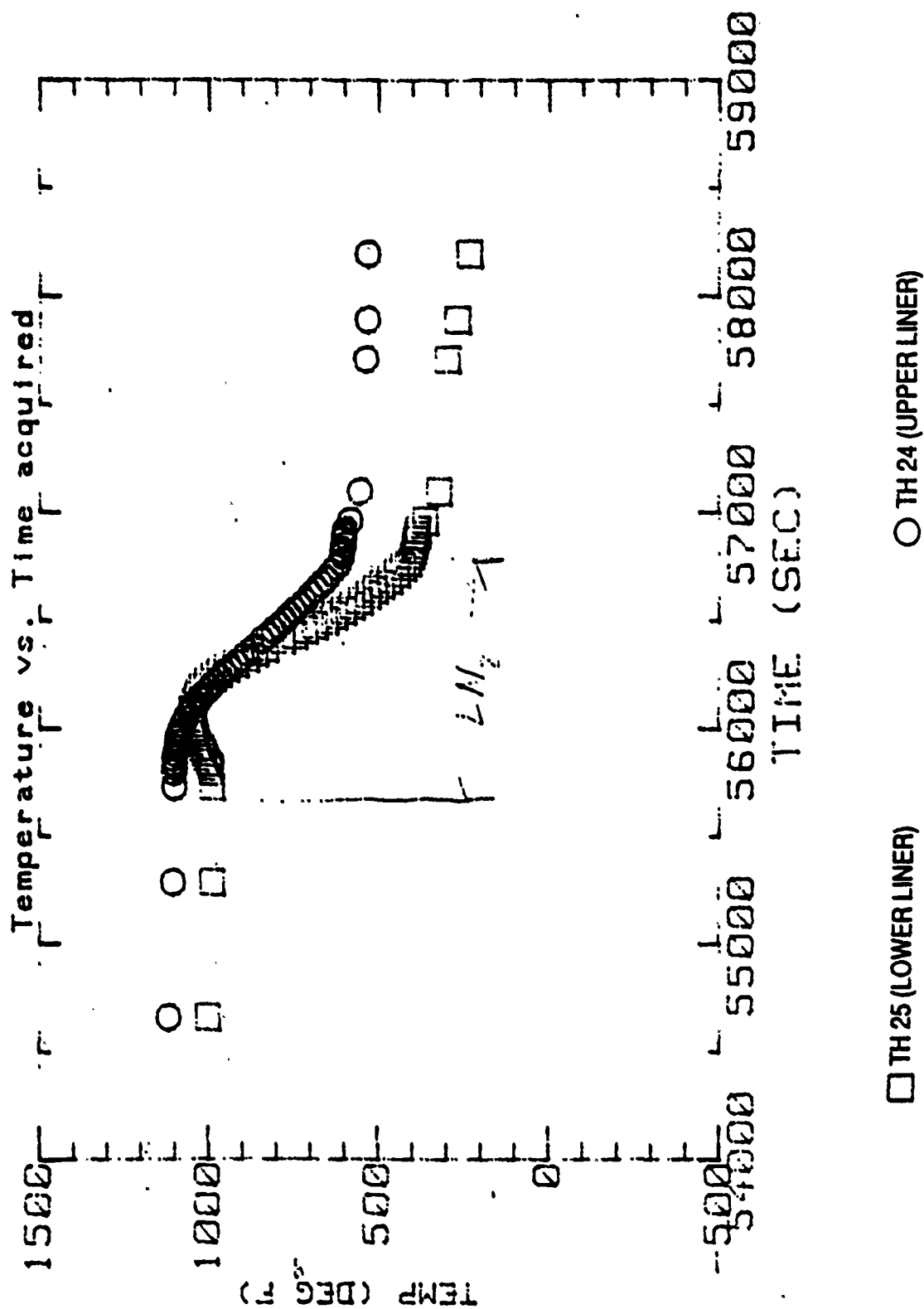


FIGURE 27. OUTSIDE LINER TEMPERATURE
EXPANDED TIME SCALE

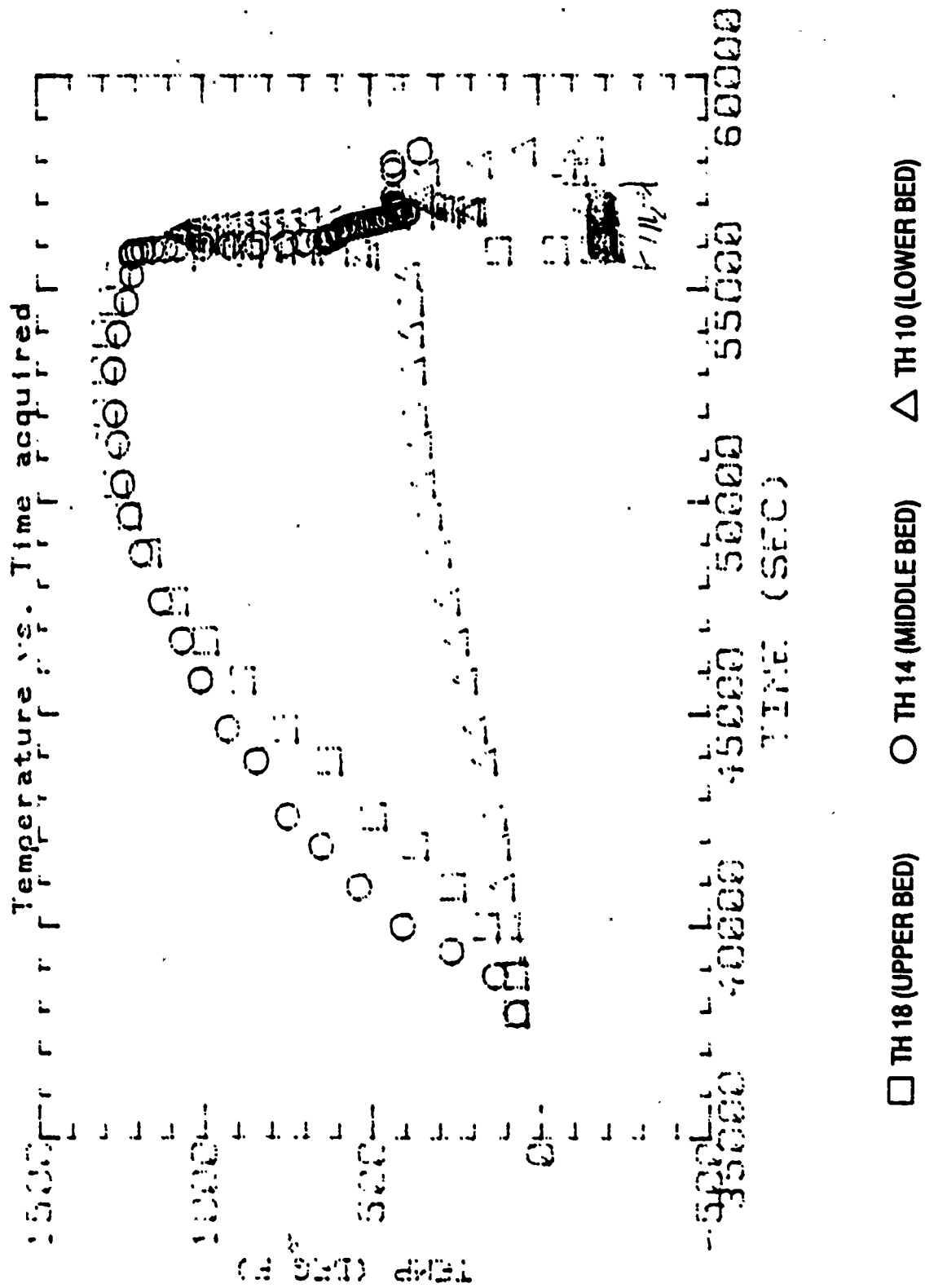


FIGURE 28. AXIAL TEMPERATURE DISTRIBUTION

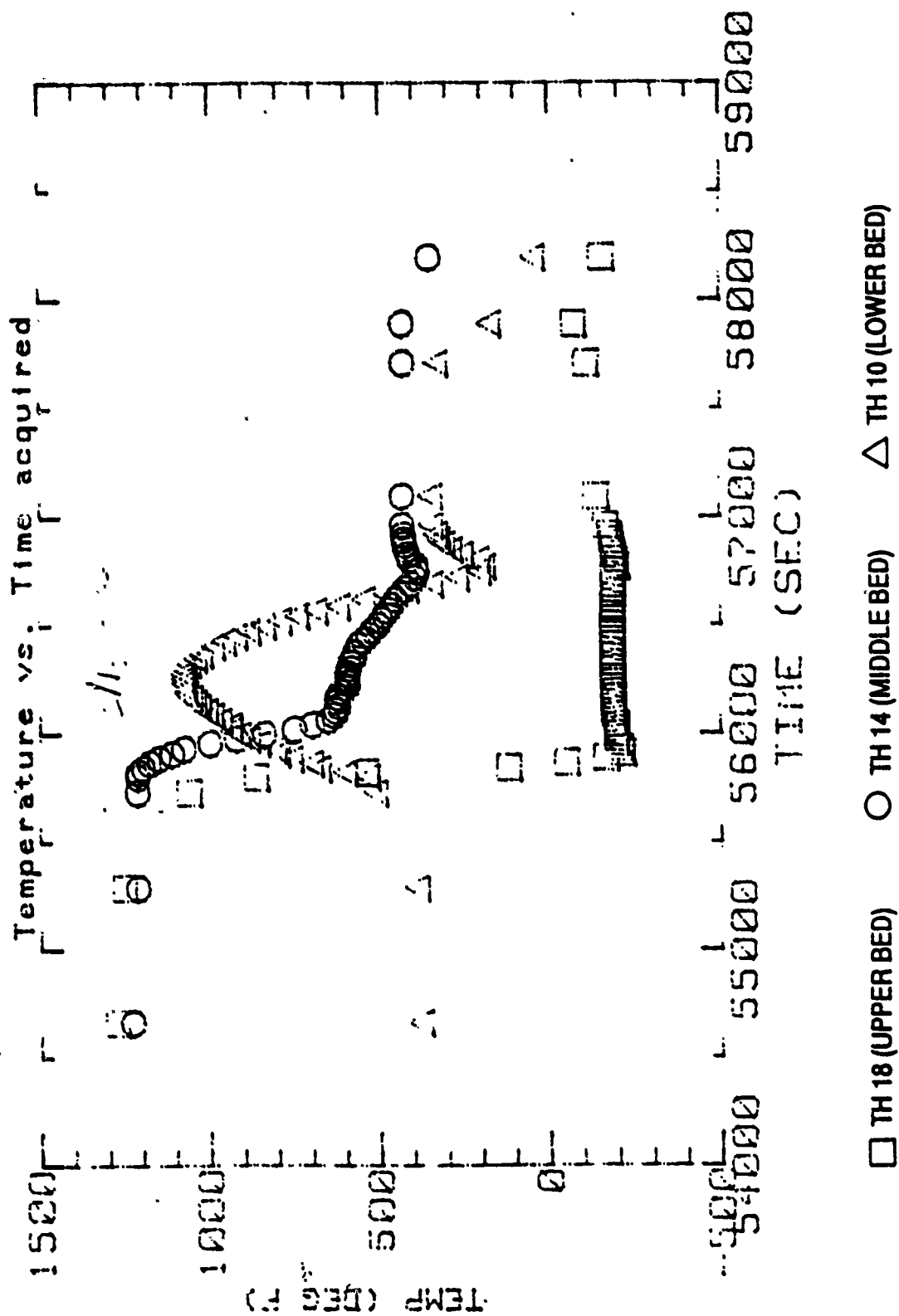


FIGURE 29. AXIAL TEMPERATURE DISTRIBUTION
EXPANDED TIME SCALE DURING INJECTION

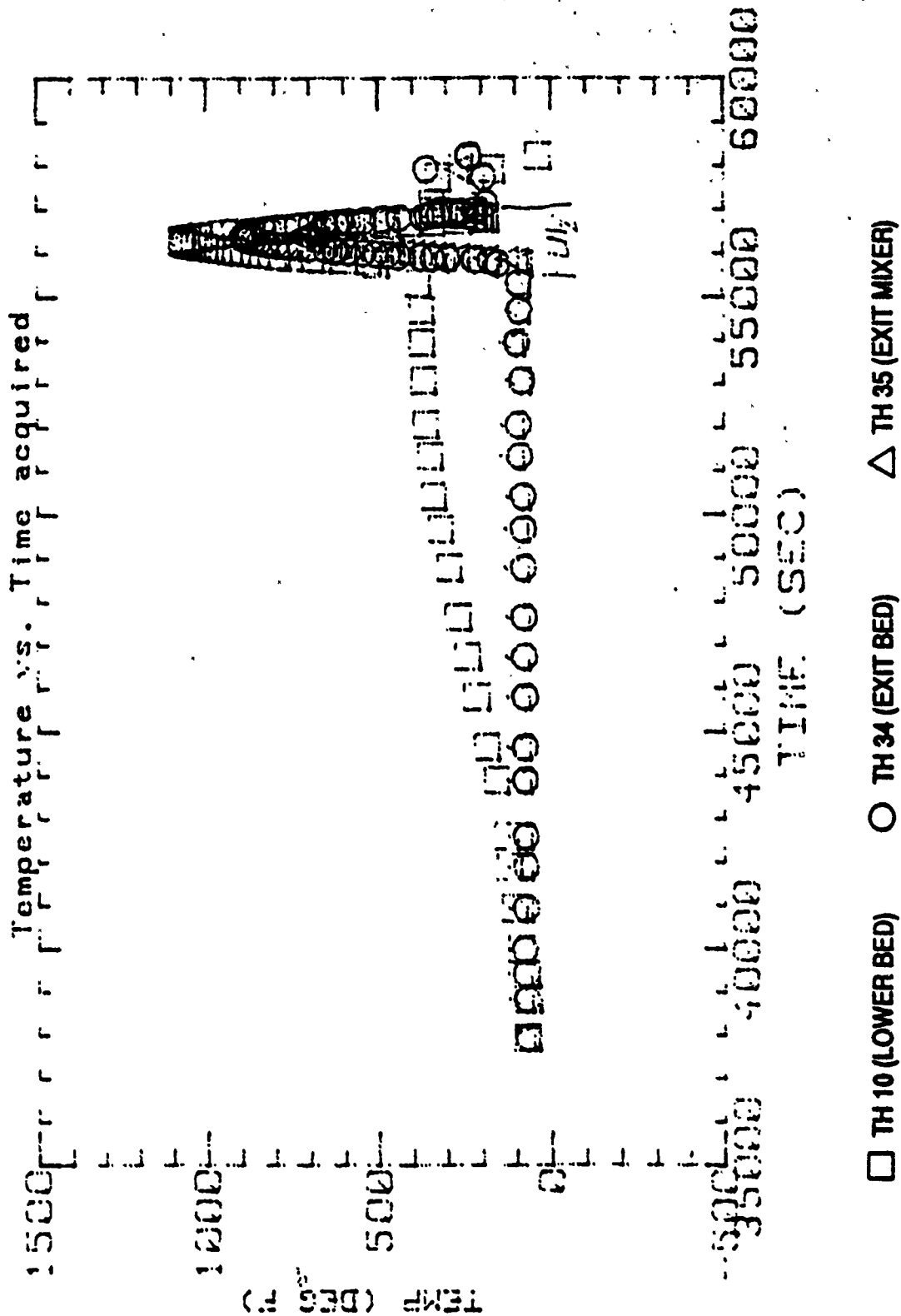


FIGURE 30. EXHAUST TEMPERATURES - FULL TEST

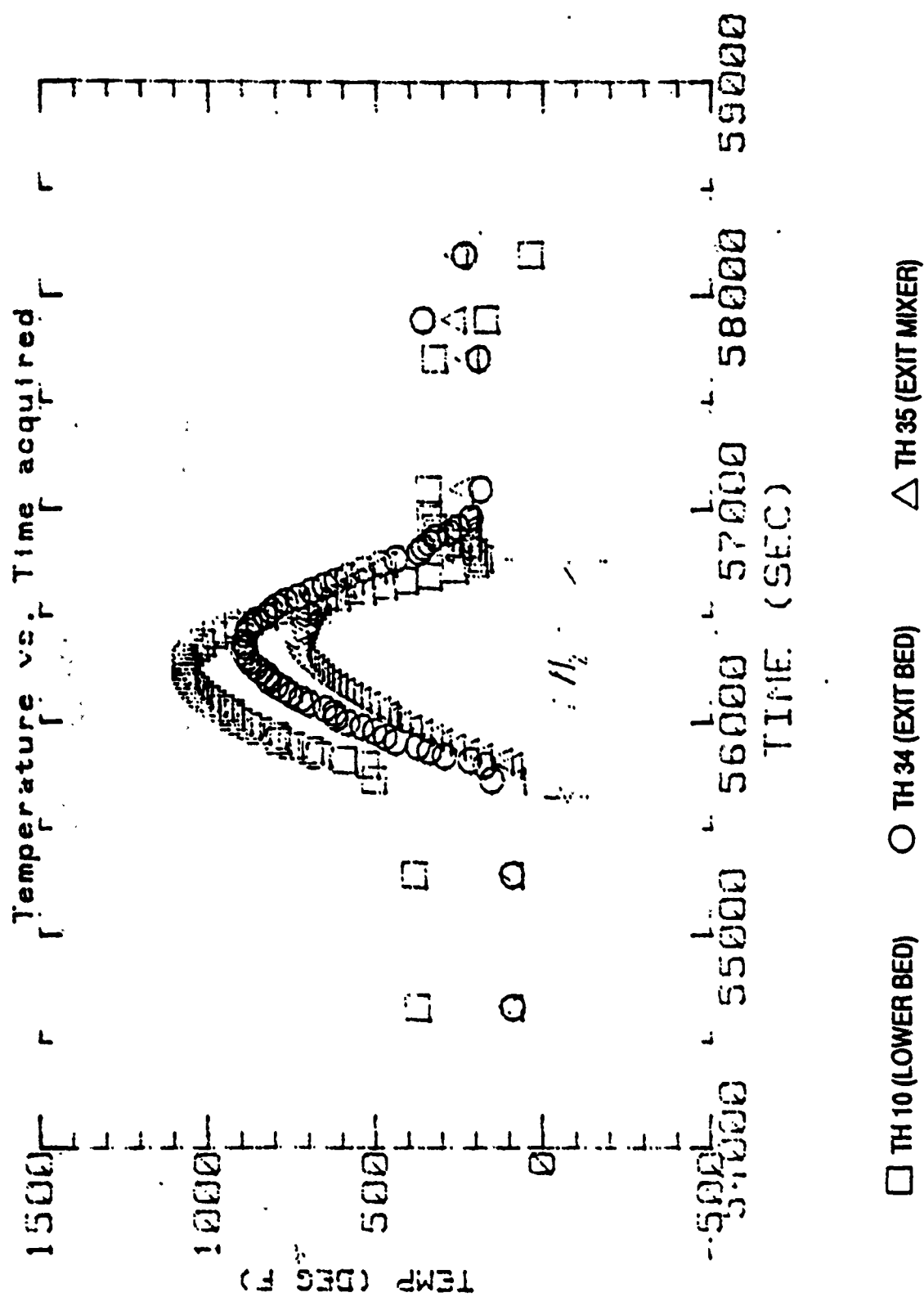


FIGURE 31. EXHAUST TEMPERATURES
EXPANDED TIME SCALES DURING INJECTION

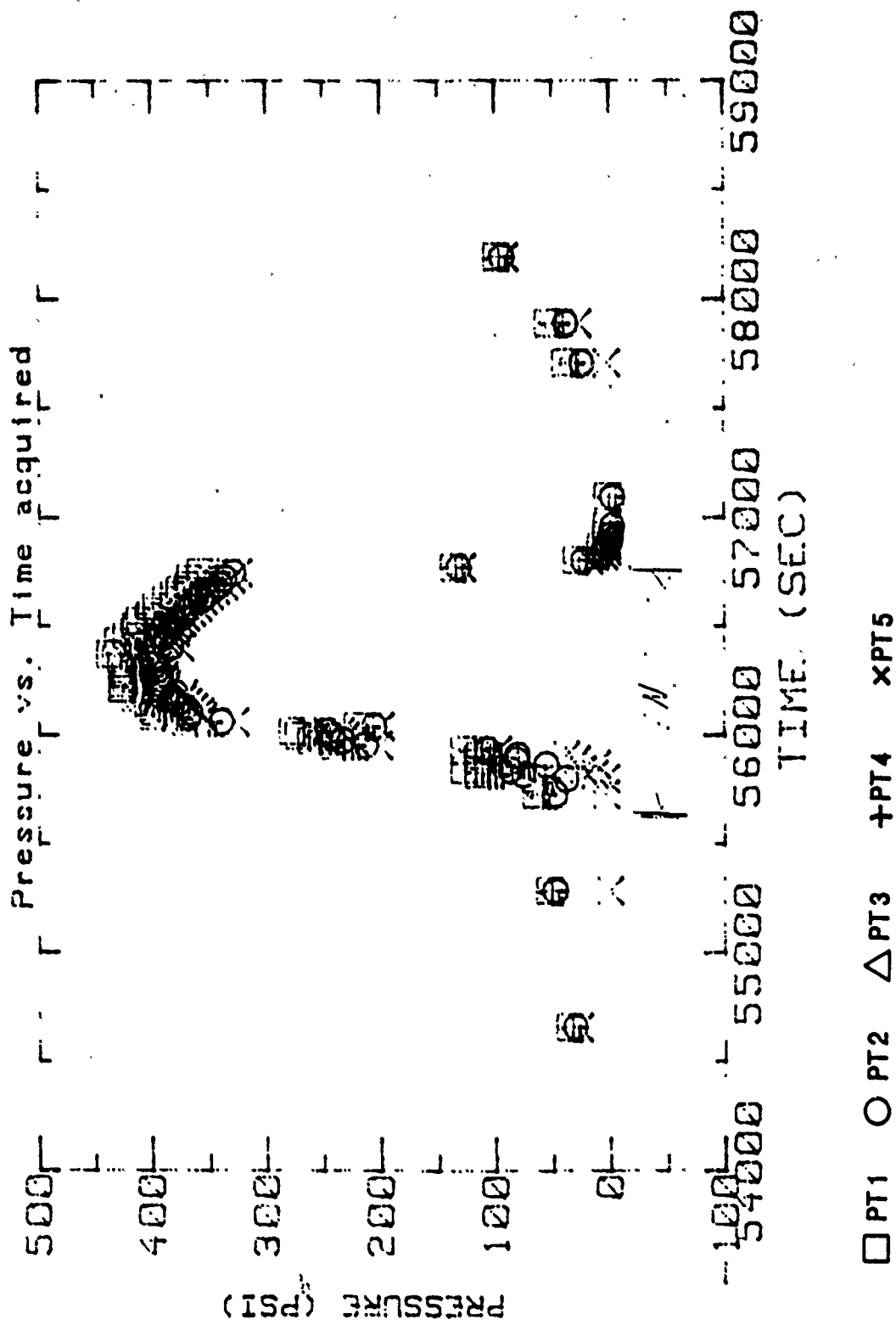


FIGURE 32. BED PRESSURE

EXPANDED TIME SCALE DURING INJECTION

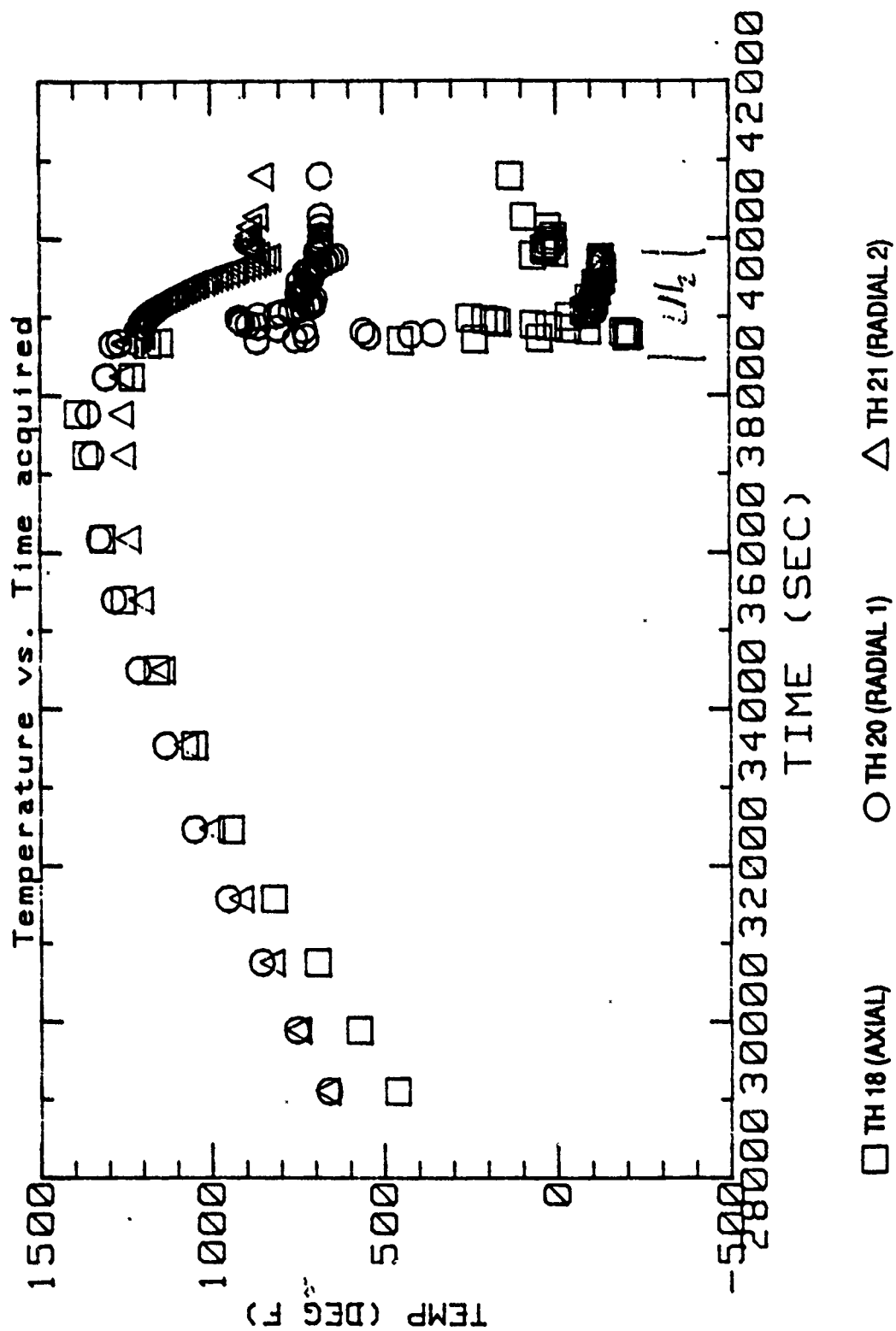
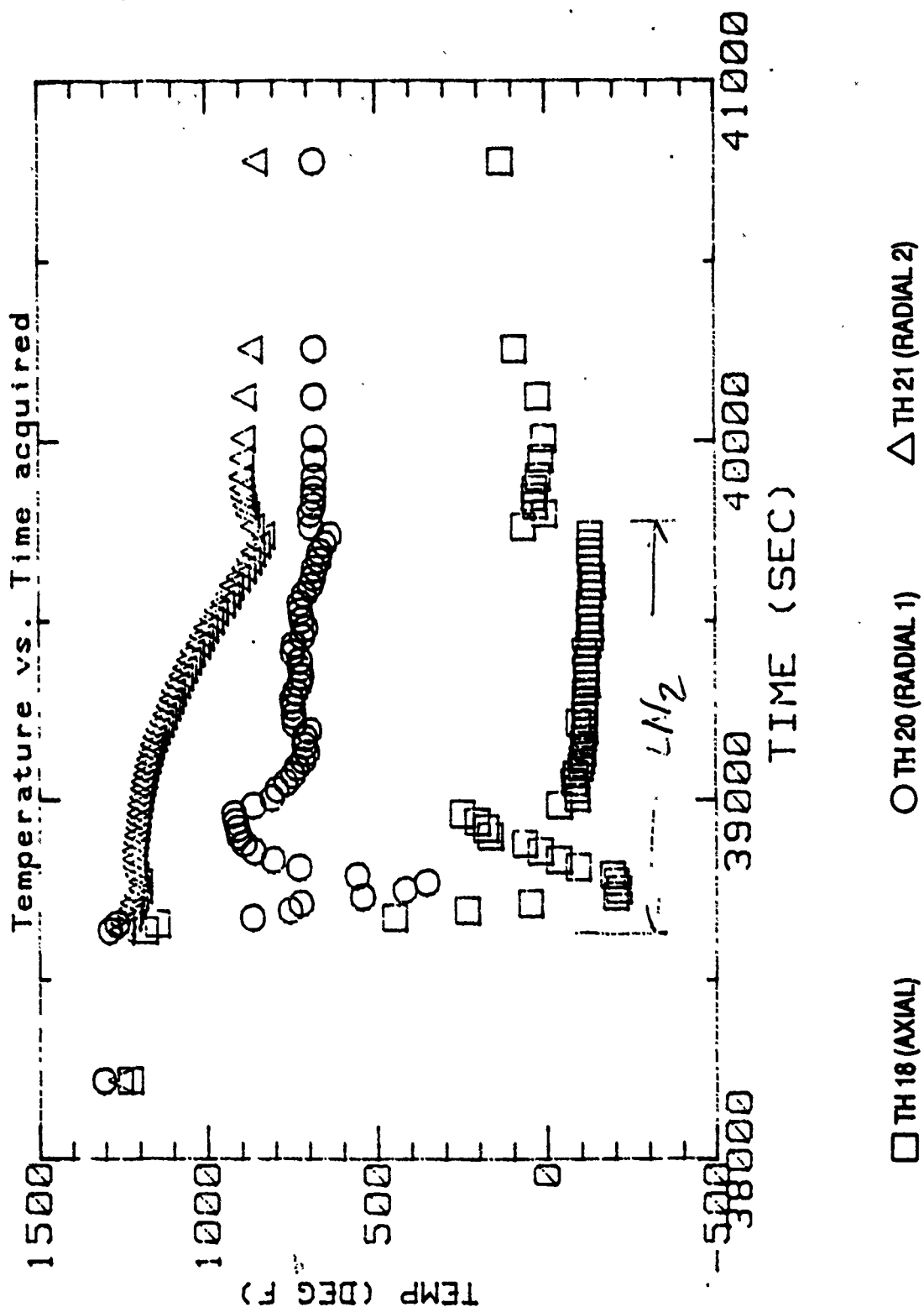


FIGURE 33. UPPER BED RADIAL TEMPERATURE DISTRIBUTION
FULL TEST



**FIGURE 34. UPPER BED RADIAL TEMPERATURE DISTRIBUTION
EXPANDED TIME SCALE DURING INJECTION**

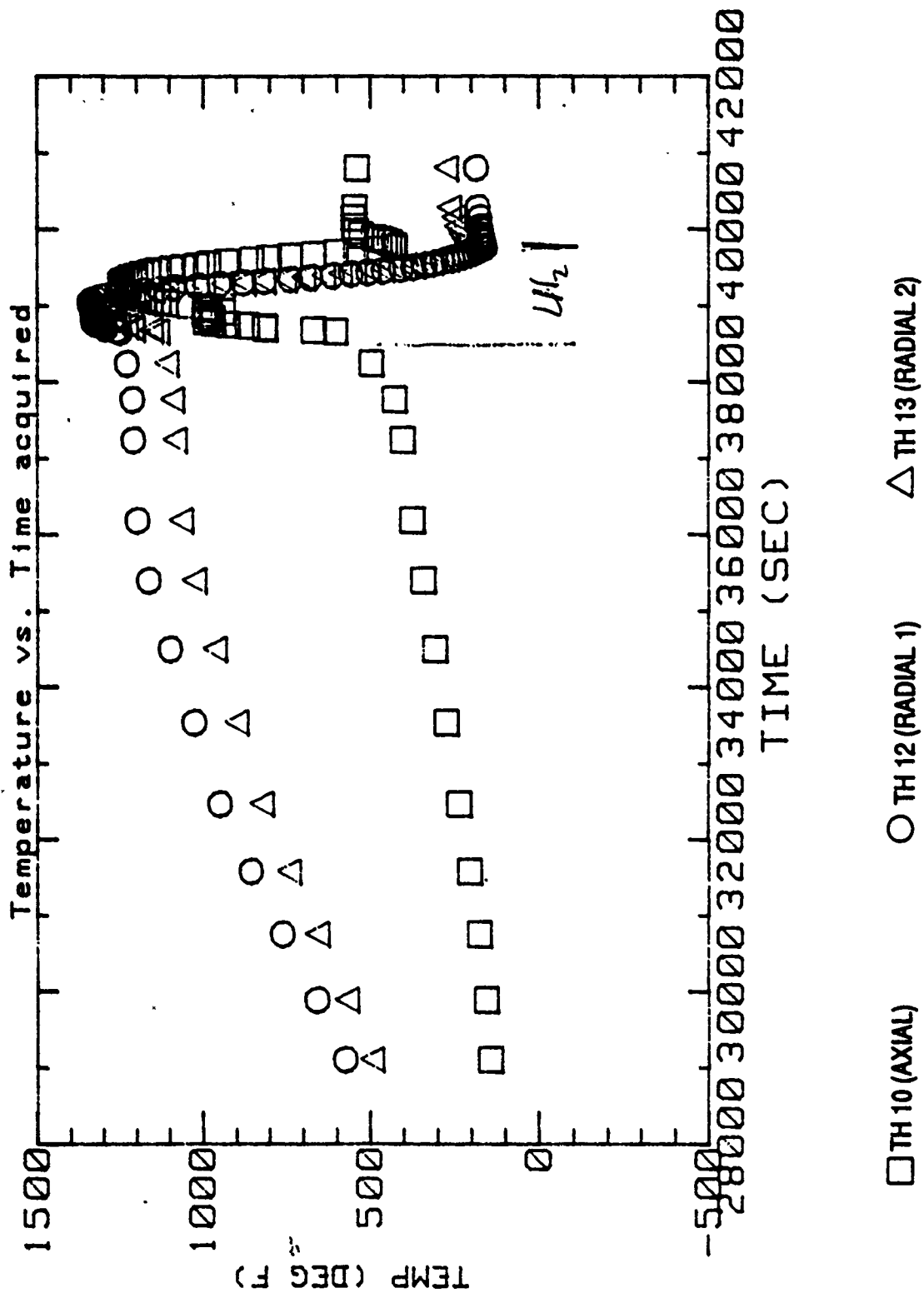


FIGURE 35. LOWER BED RADIAL TEMPERATURE DISTRIBUTION
FULL TEST

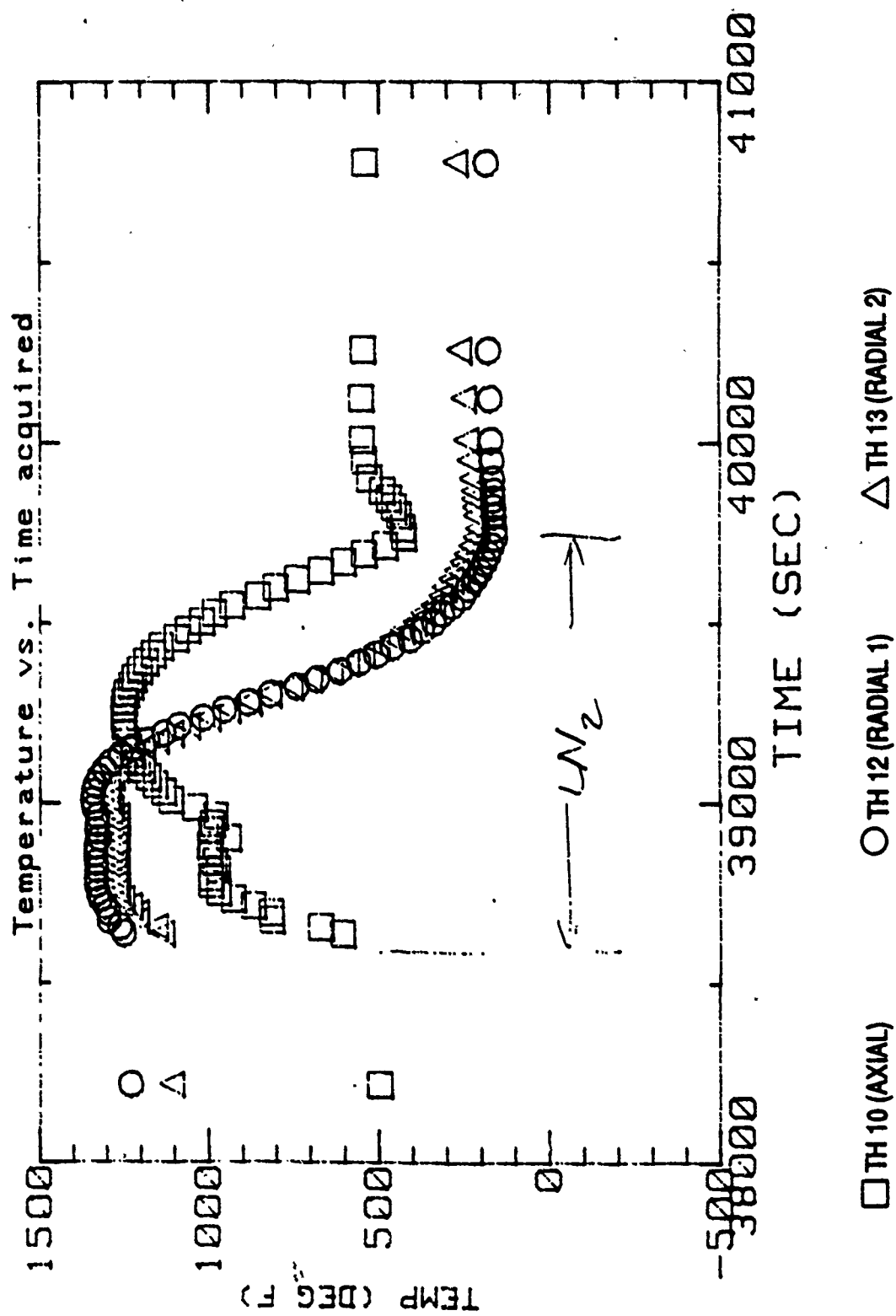
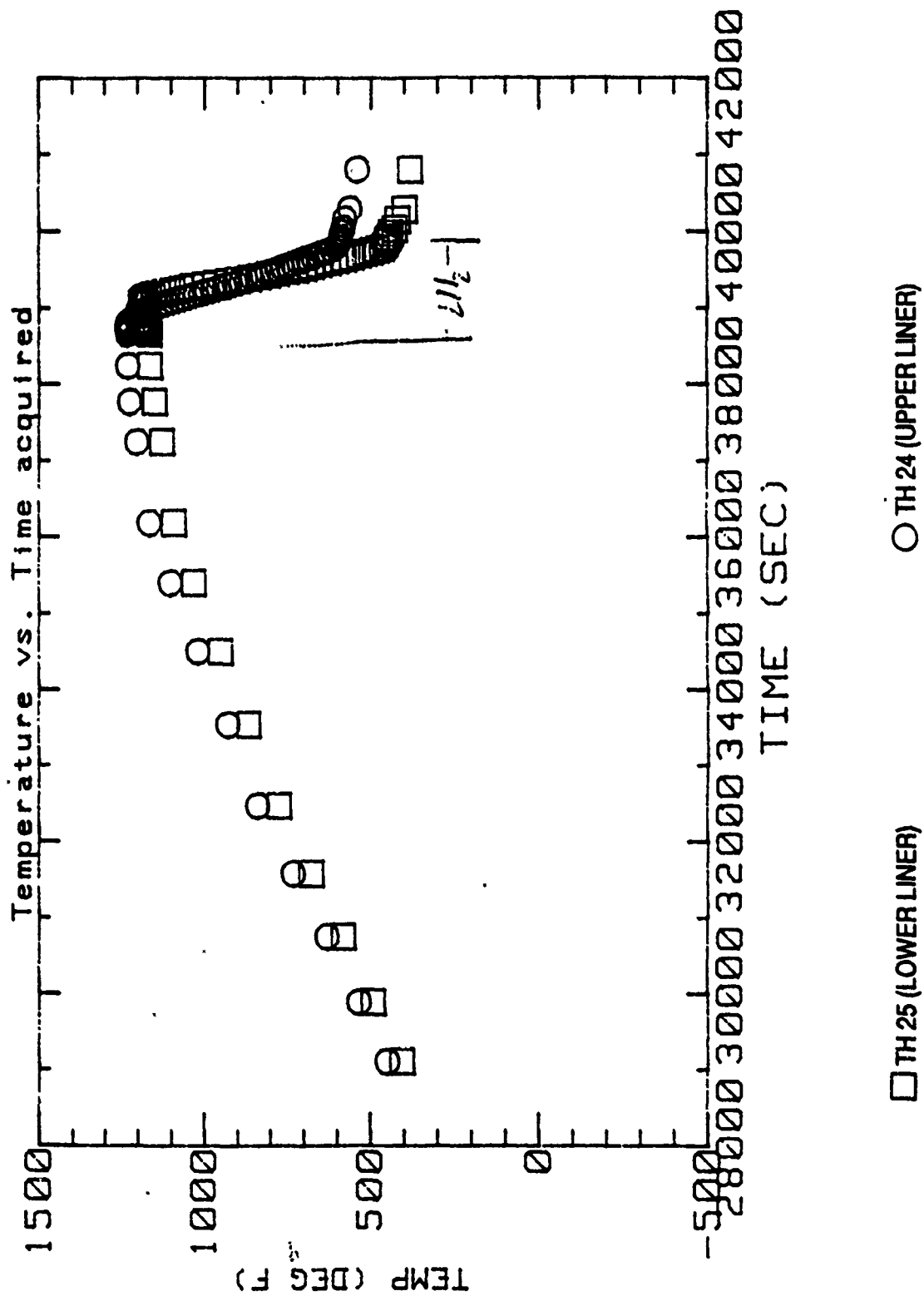


FIGURE 36. LOWER BED RADIAL TEMPERATURE DISTRIBUTION
EXPANDED TIME SCALE



**FIGURE 37. OUTSIDE LINER TEMPERATURE
FULL TEST**

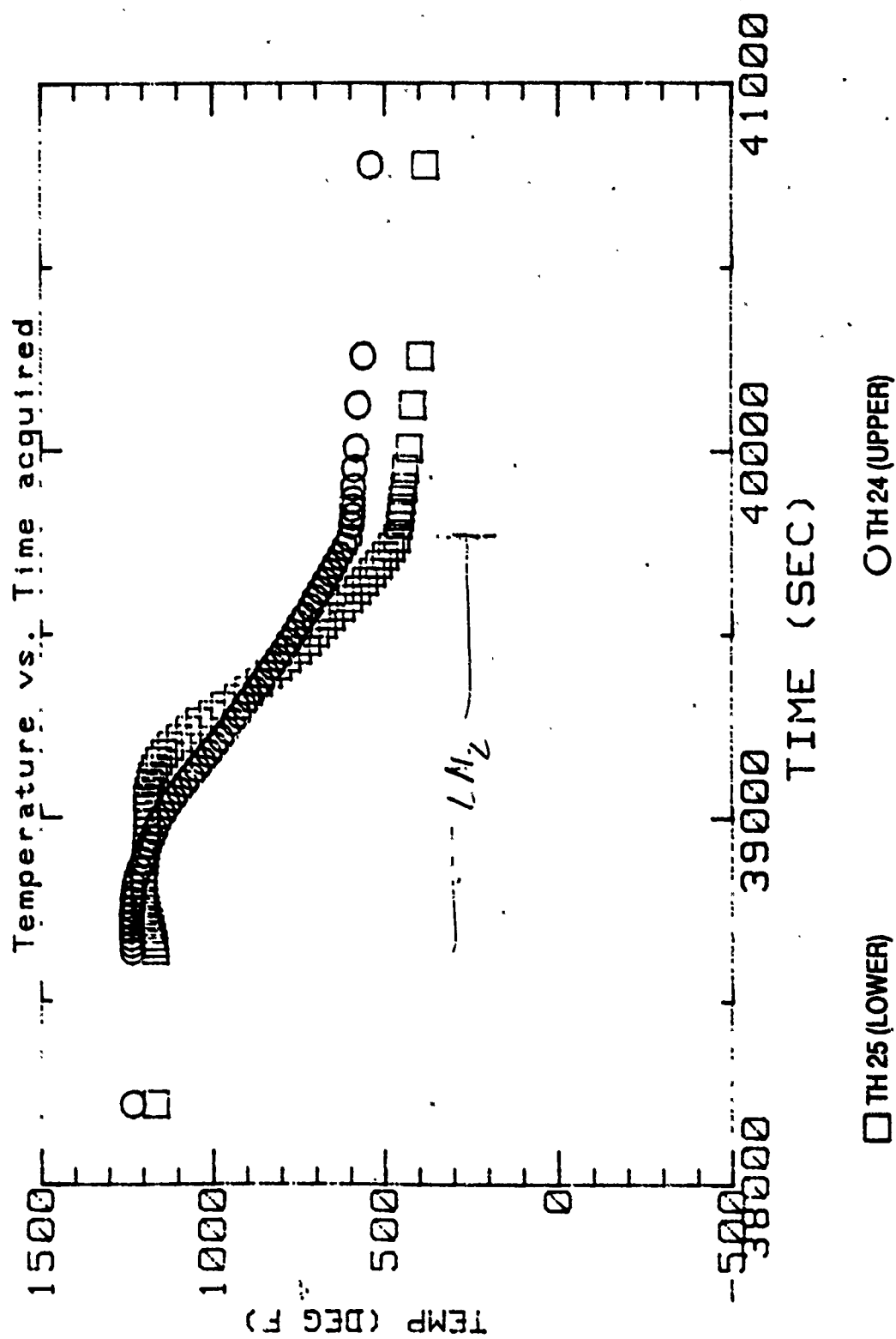


FIGURE 38. OUTSIDE LINER TEMPERATURE
EXPANDED TIME SCALE DURING INJECTION

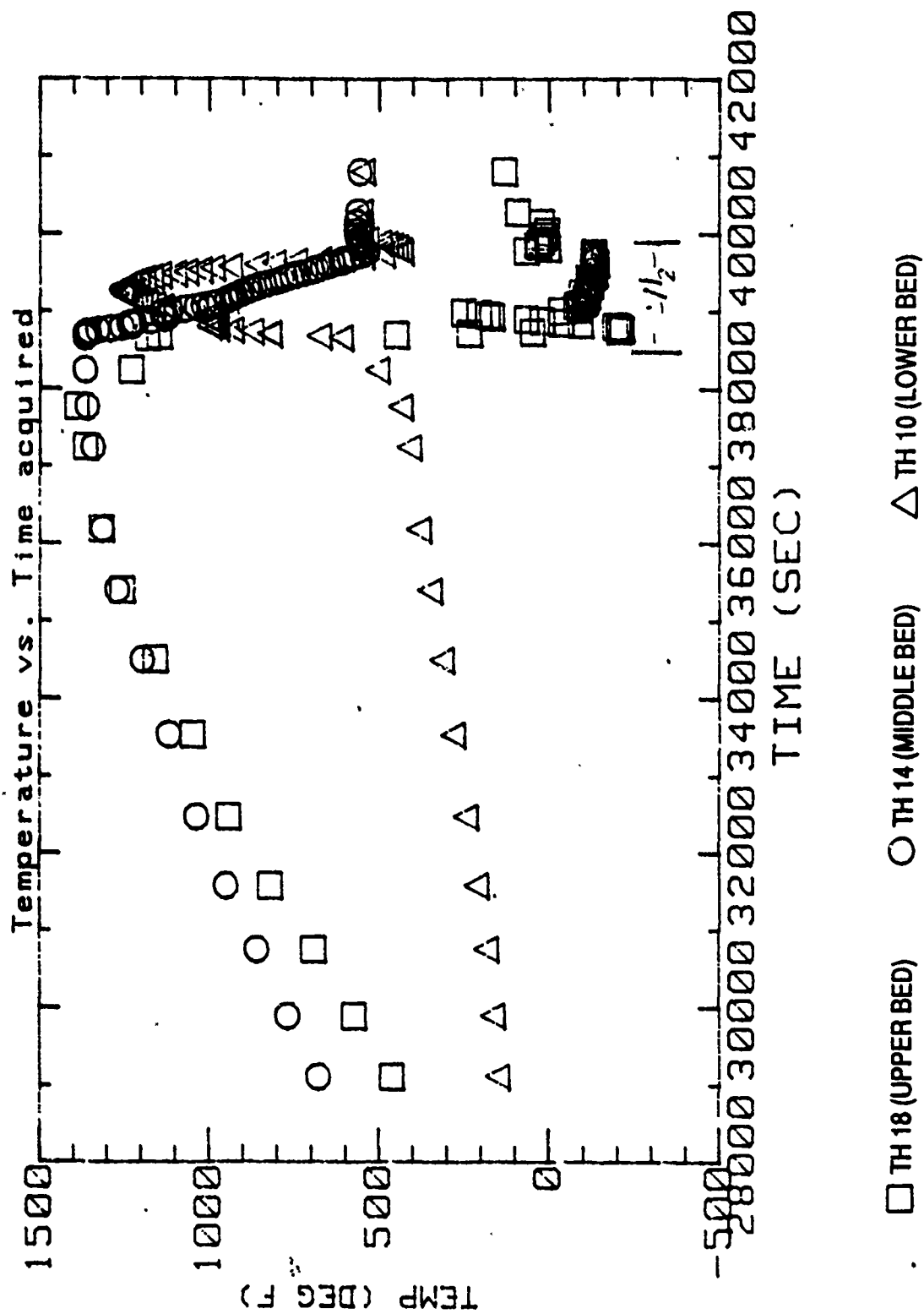
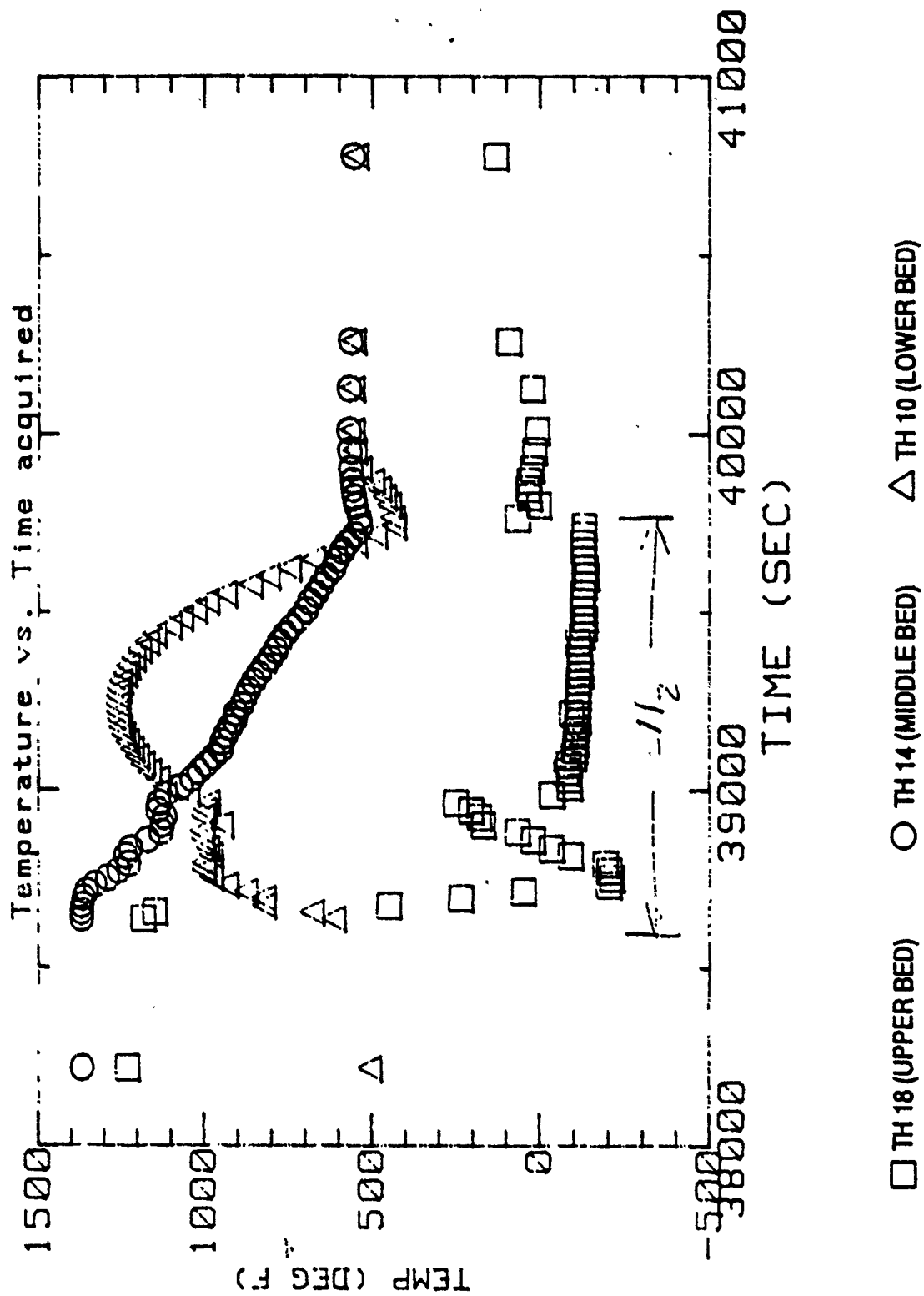


FIGURE 39. AXIAL TEMPERATURE DISTRIBUTION
FULL TEST



**FIGURE 40. AXIAL TEMPERATURE DISTRIBUTION
EXPANDED TIME SCALE DURING INJECTION**

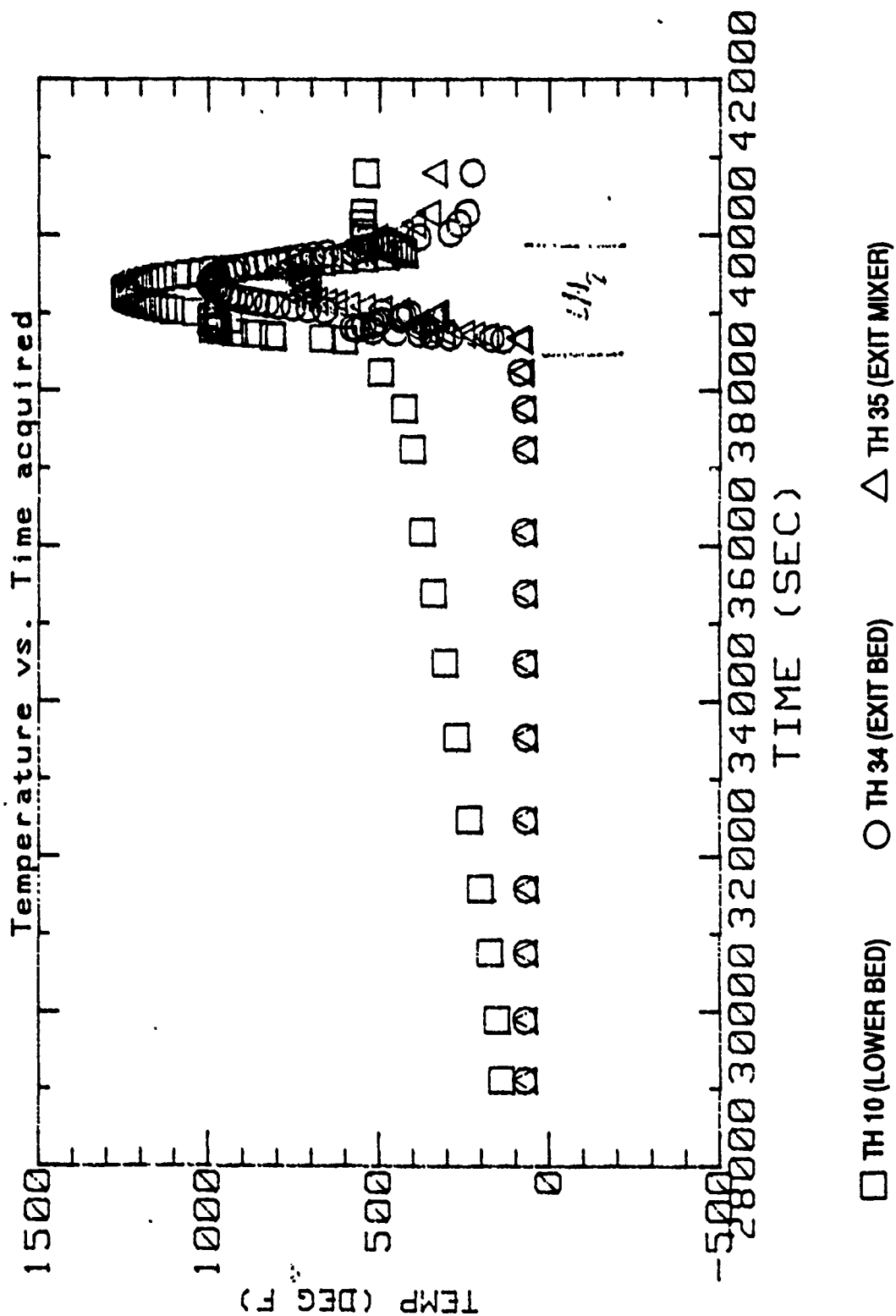
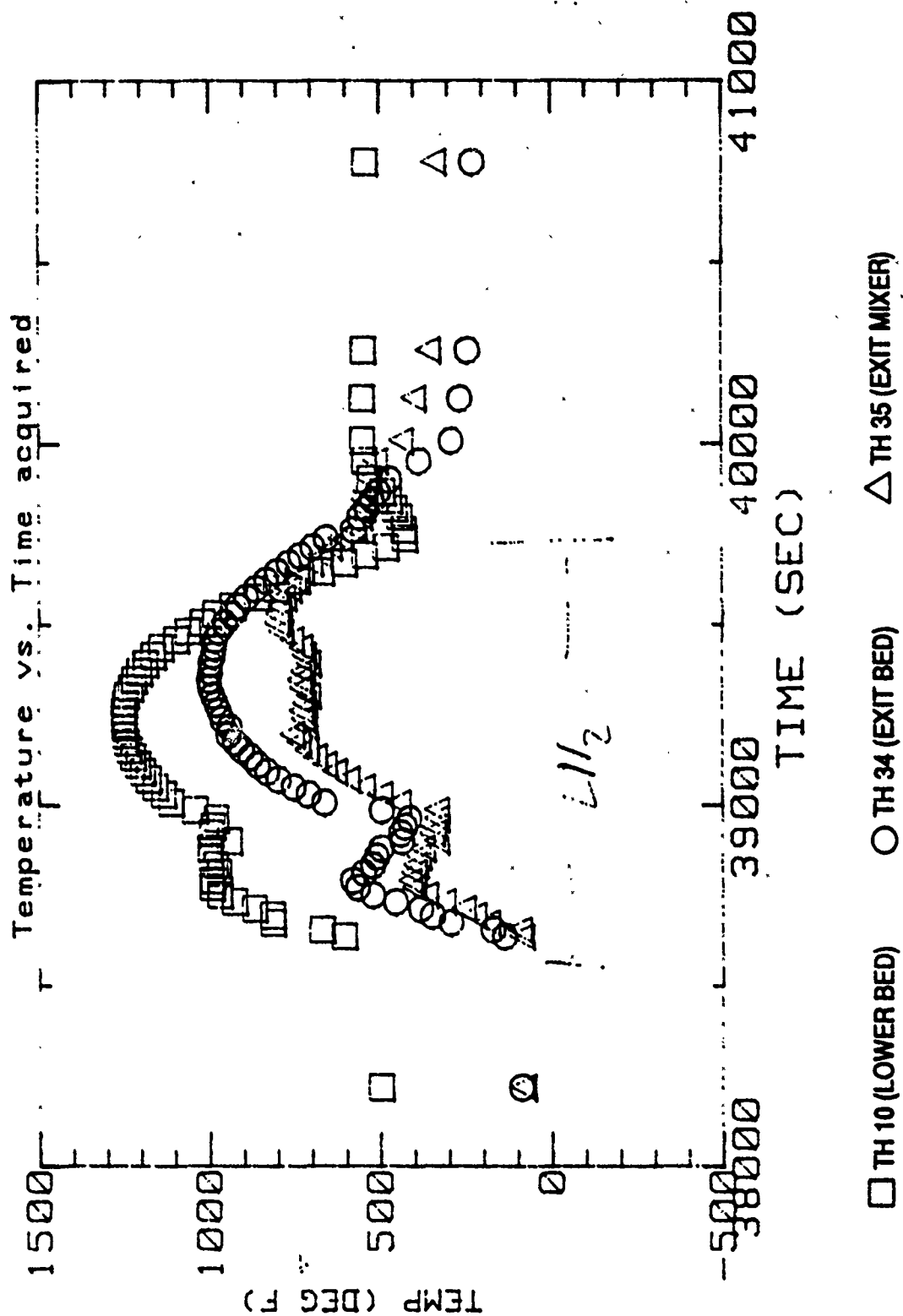


FIGURE 41. EXHAUST TEMPERATURES - FULL TEST



**FIGURE 42. EXHAUST TEMPERATURES
EXPANDED TIME SCALE DURING INJECTION**

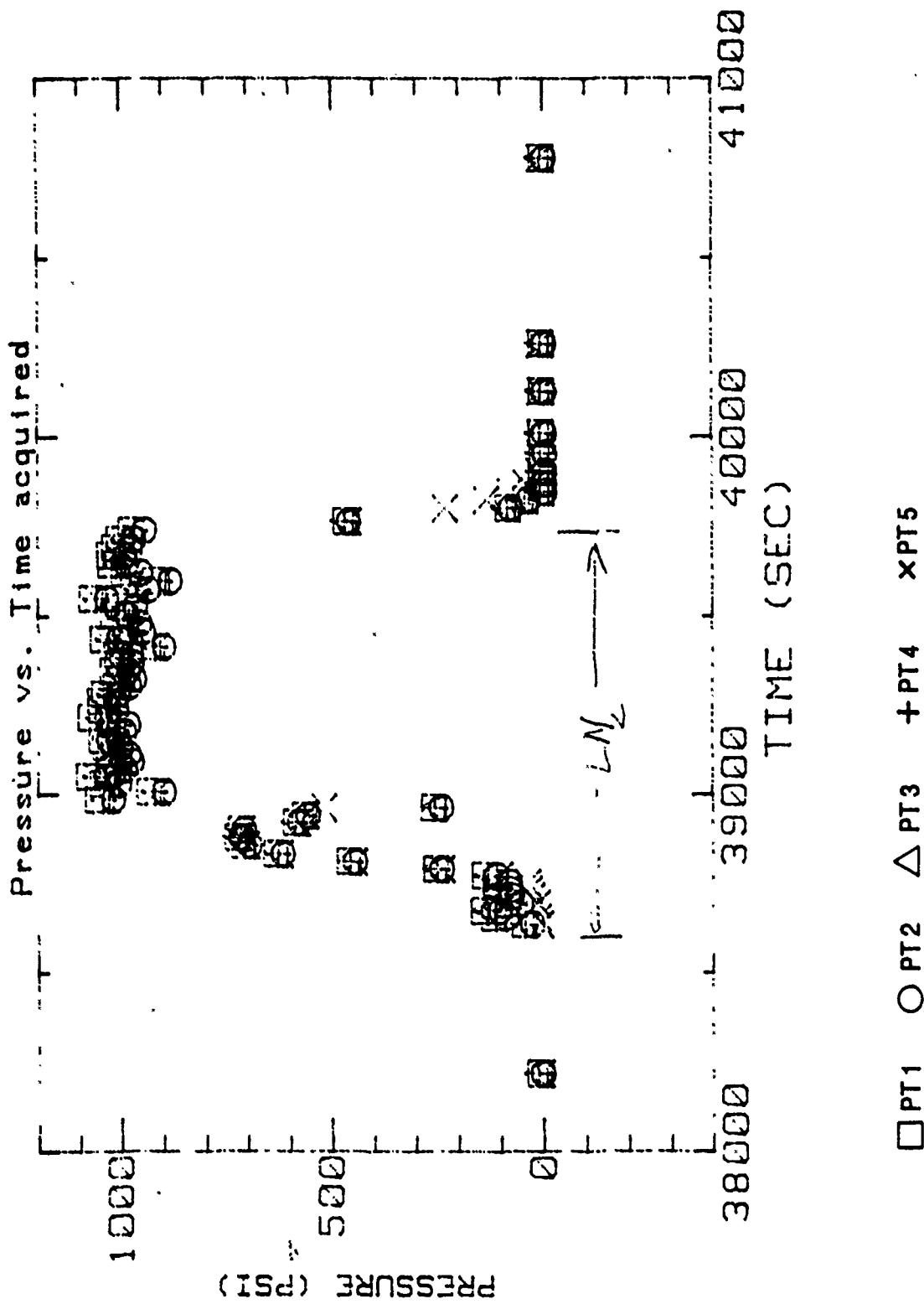
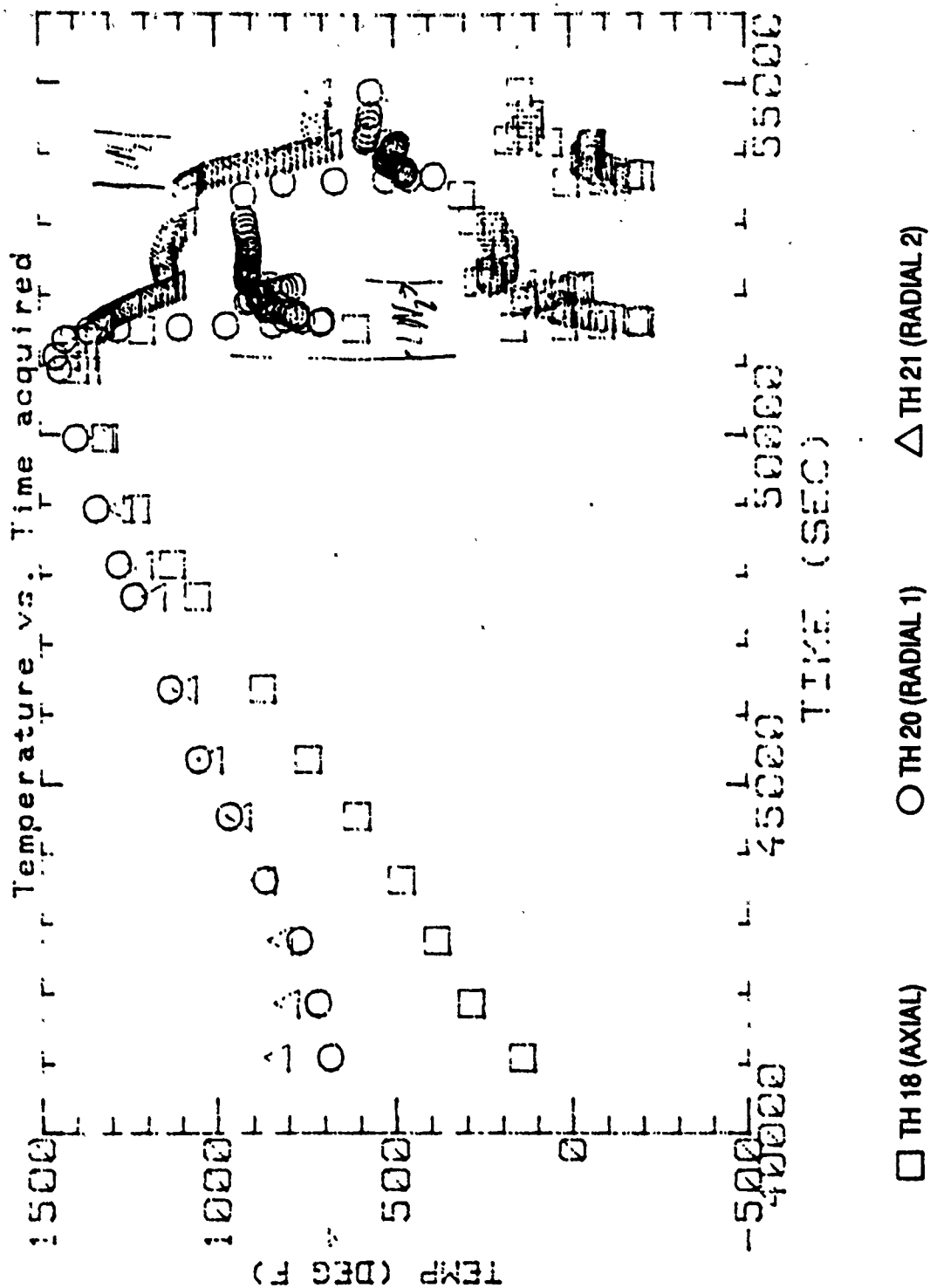
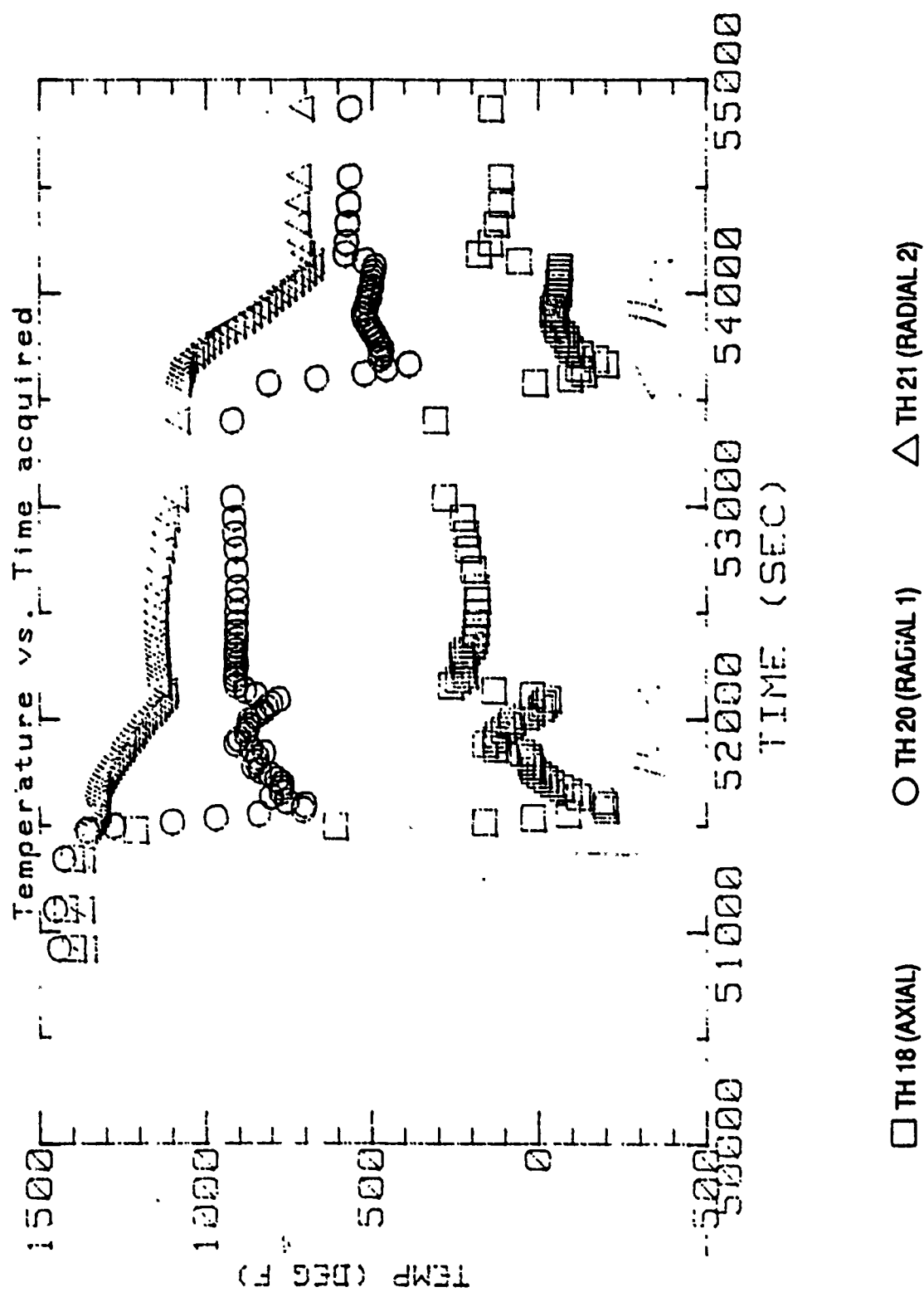


FIGURE 43. BED PRESSURE
EXPANDED TIME SCALE DURING INJECTION



**FIGURE 44. UPPER BED RADIAL TEMPERATURE DISTRIBUTION
FULL TEST**



**FIGURE 45. UPPER BED RADIAL TEMPERATURE DISTRIBUTION
EXPANDED TIME SCALE DURING INJECTION**

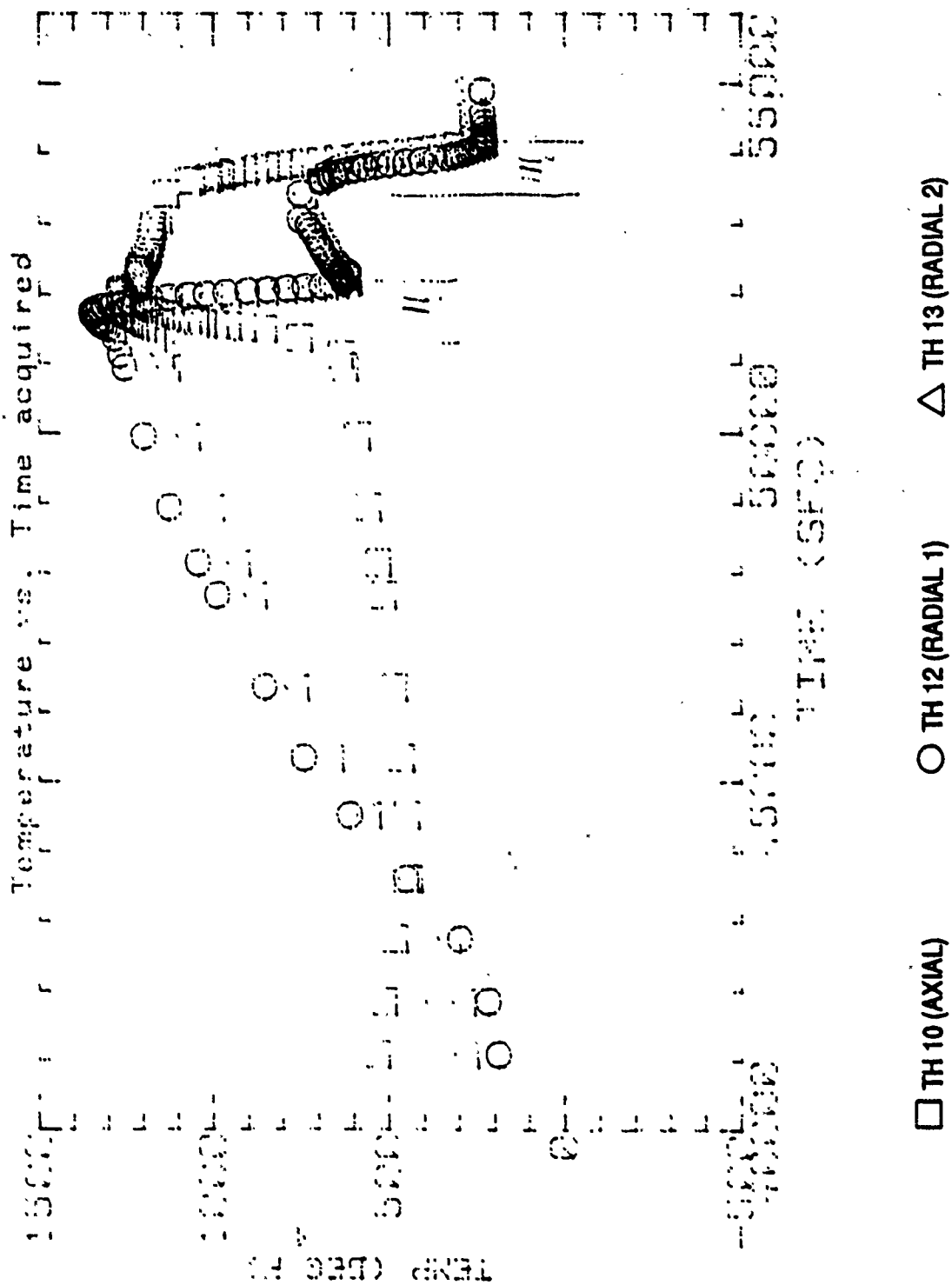


**FIGURE 46. LOWER BED RADIAL TEMPERATURE DISTRIBUTION
FULL TEST**

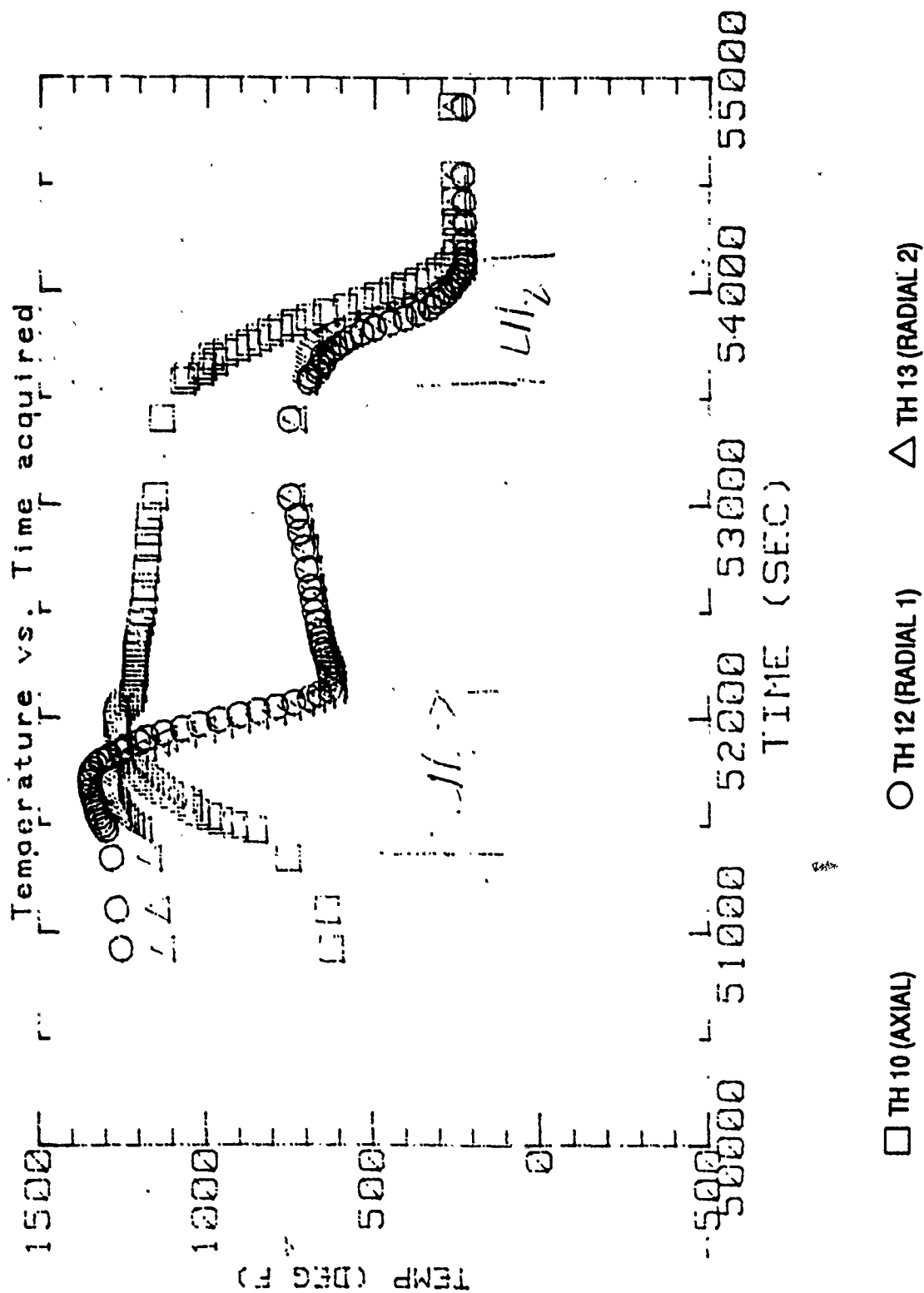


**FIGURE 47. LOWER BED RADIAL TEMPERATURE DISTRIBUTION
EXPANDED TIME SCALE DURING INJECTION**

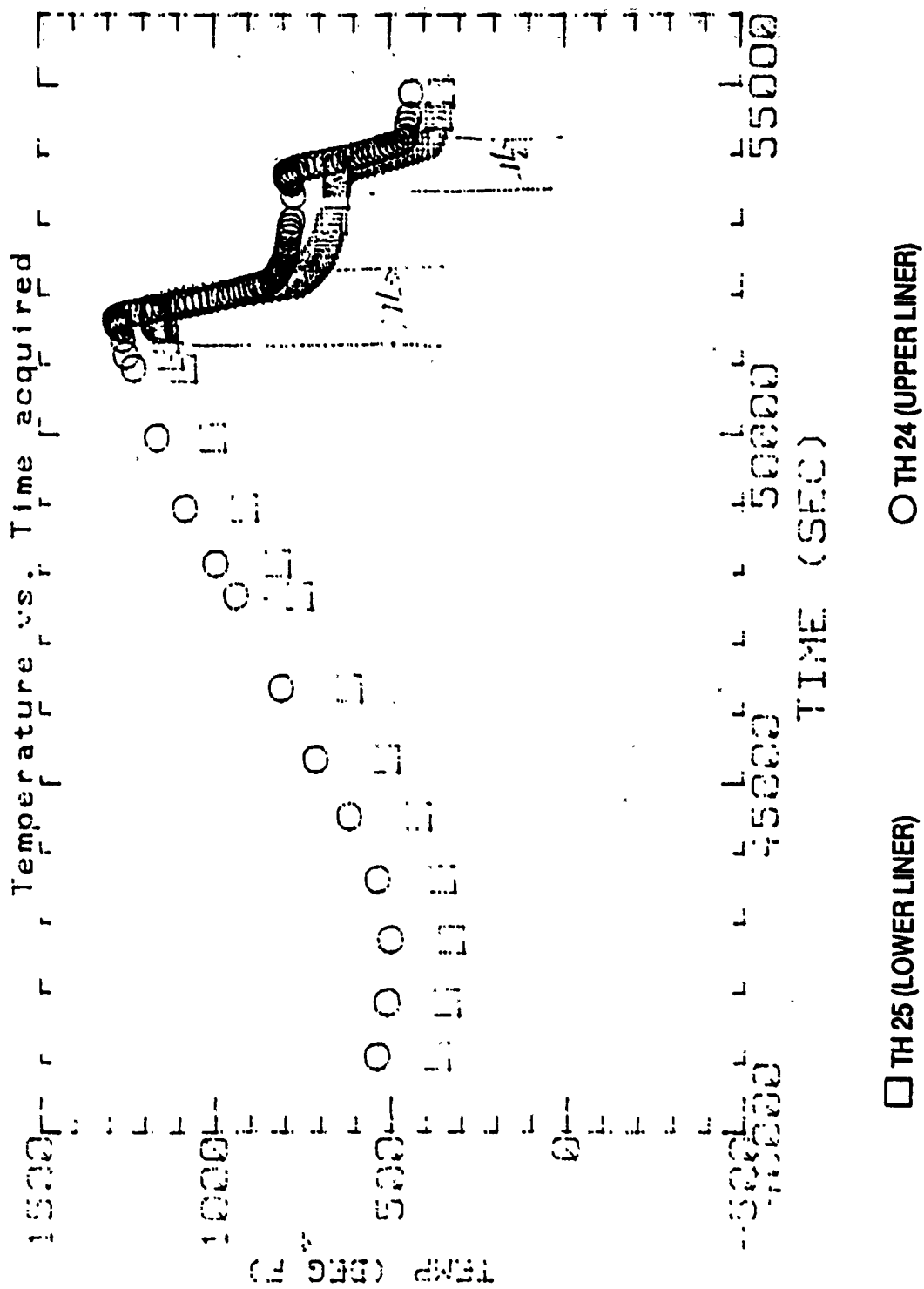


**FIGURE 48. OUTSIDE LINER TEMPERATURES
FULL TEST**

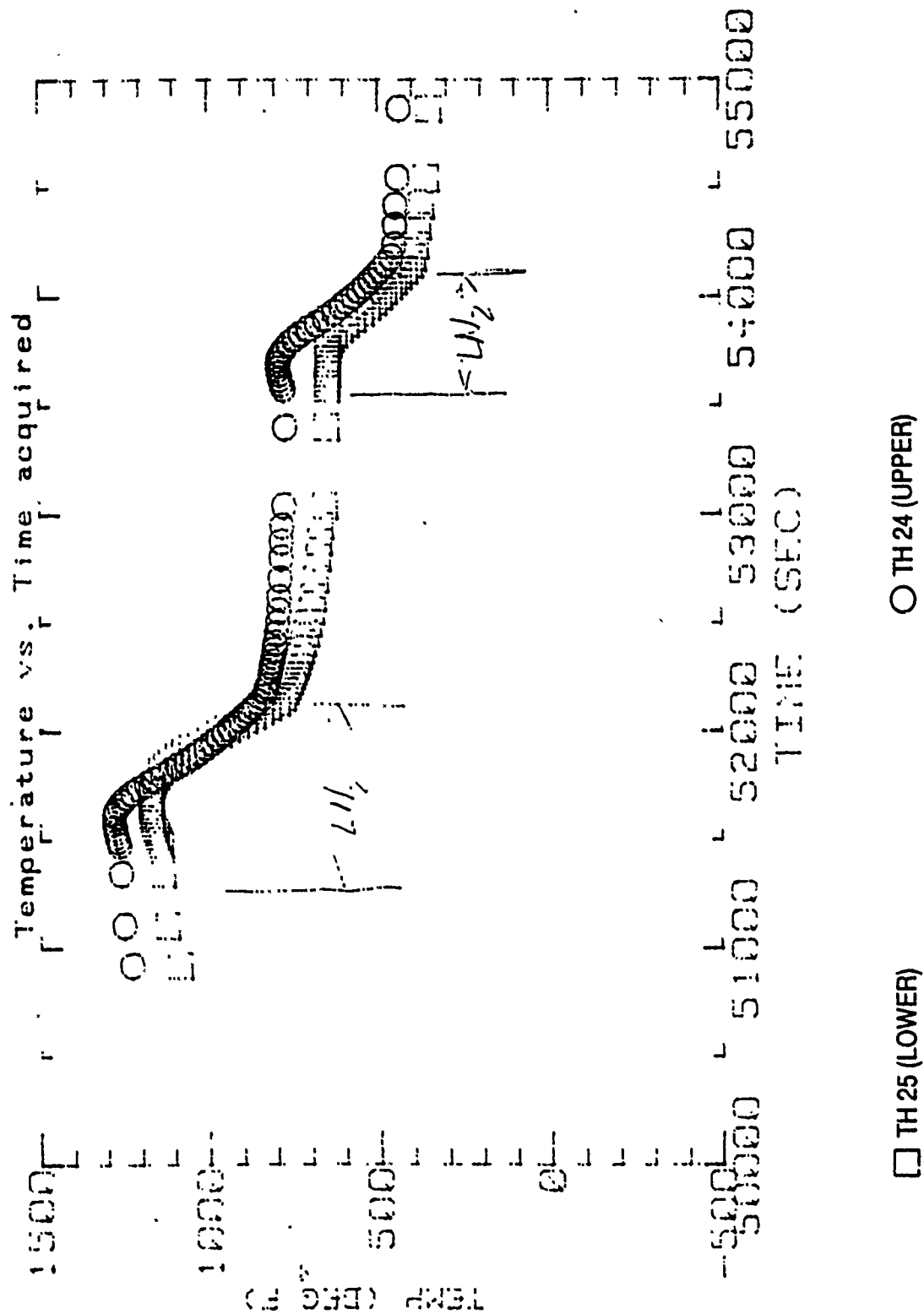
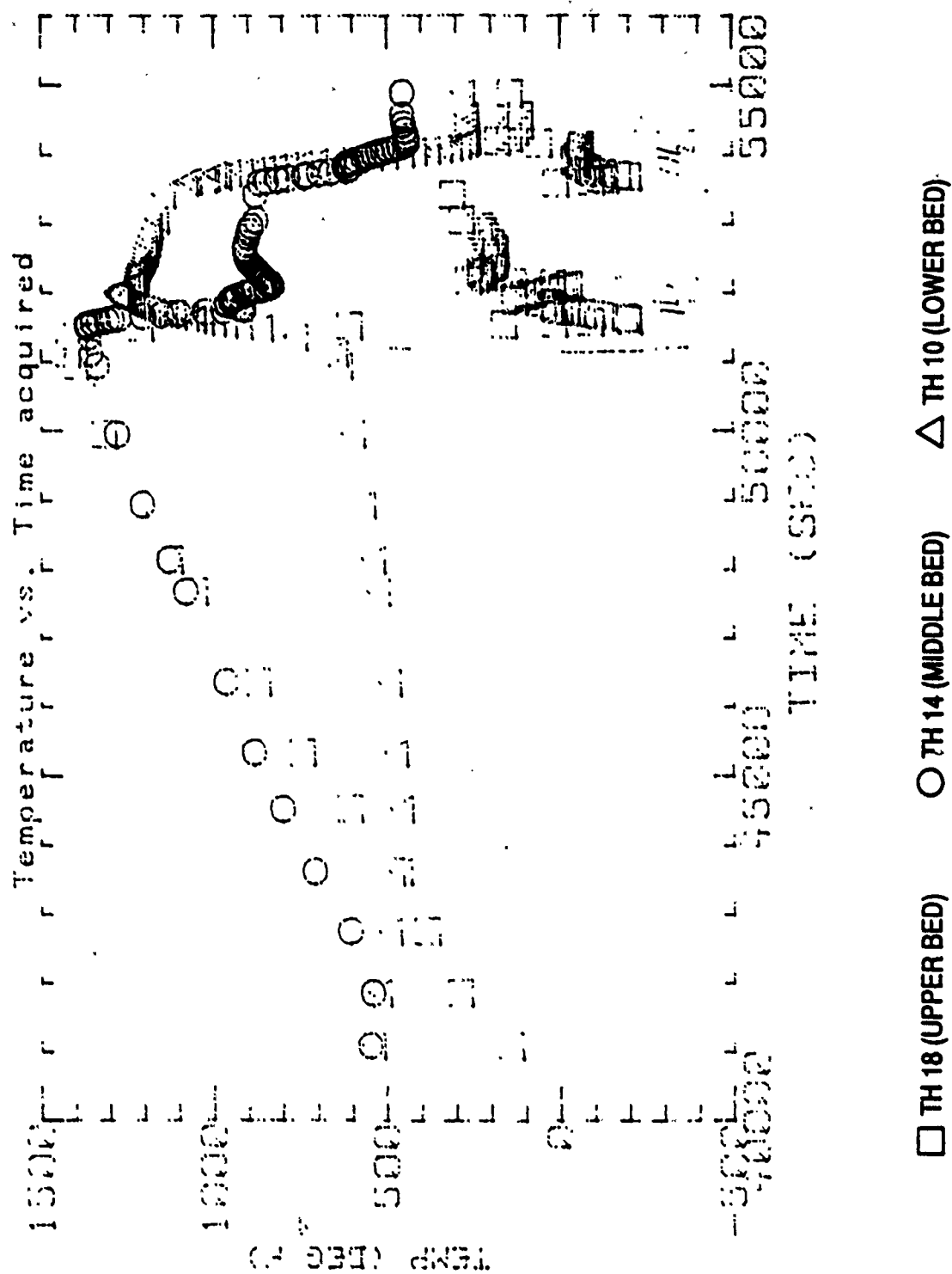


FIGURE 49. OUTSIDE LINER TEMPERATURE
EXPANDED TIME SCALE DURING INJECTION



**FIGURE 50. AXIAL TEMPERATURE DISTRIBUTION
FULL TEST**

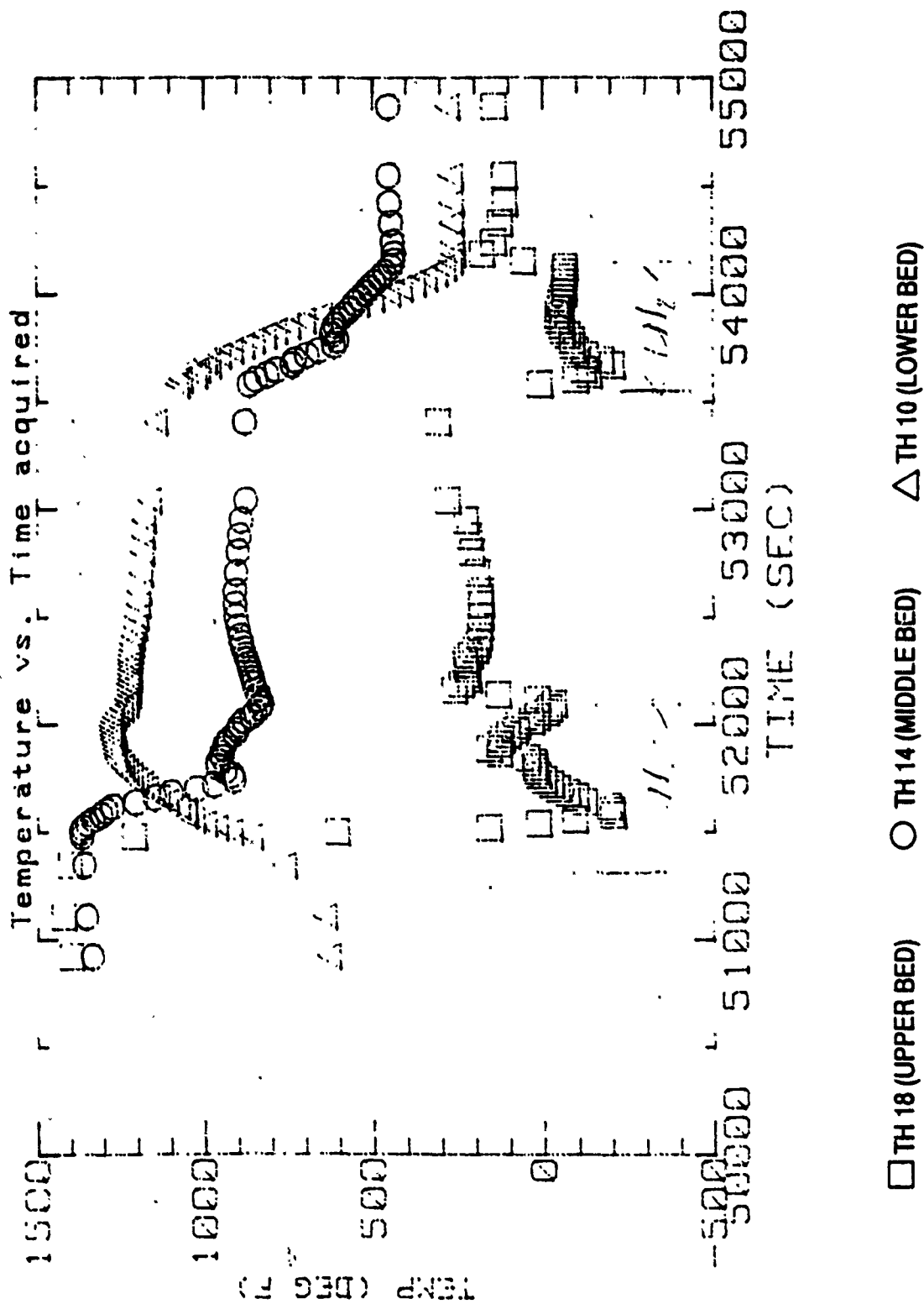


FIGURE 51. AXIAL TEMPERATURE DISTRIBUTION
EXPANDED TIME SCALE DURING INJECTION

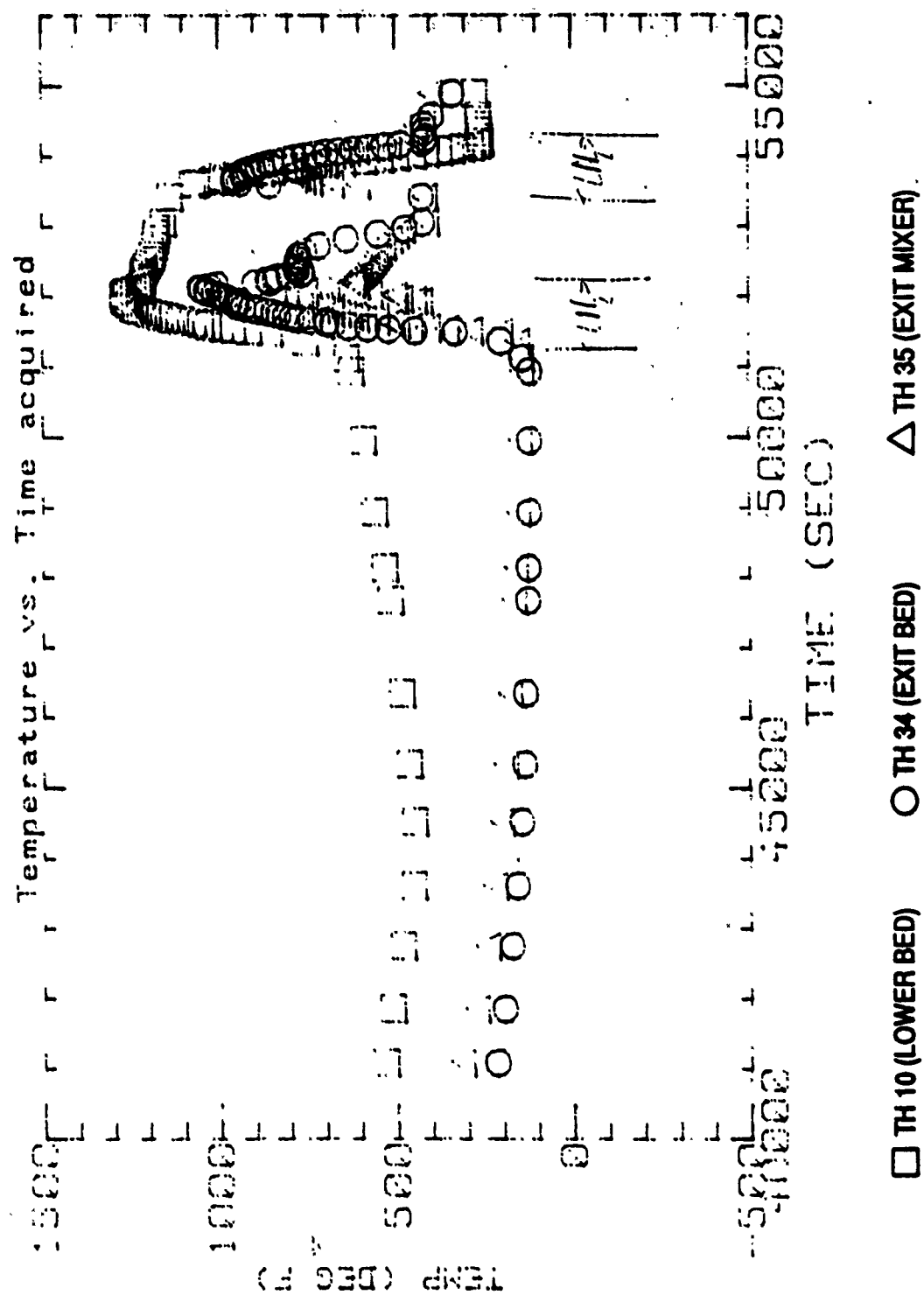
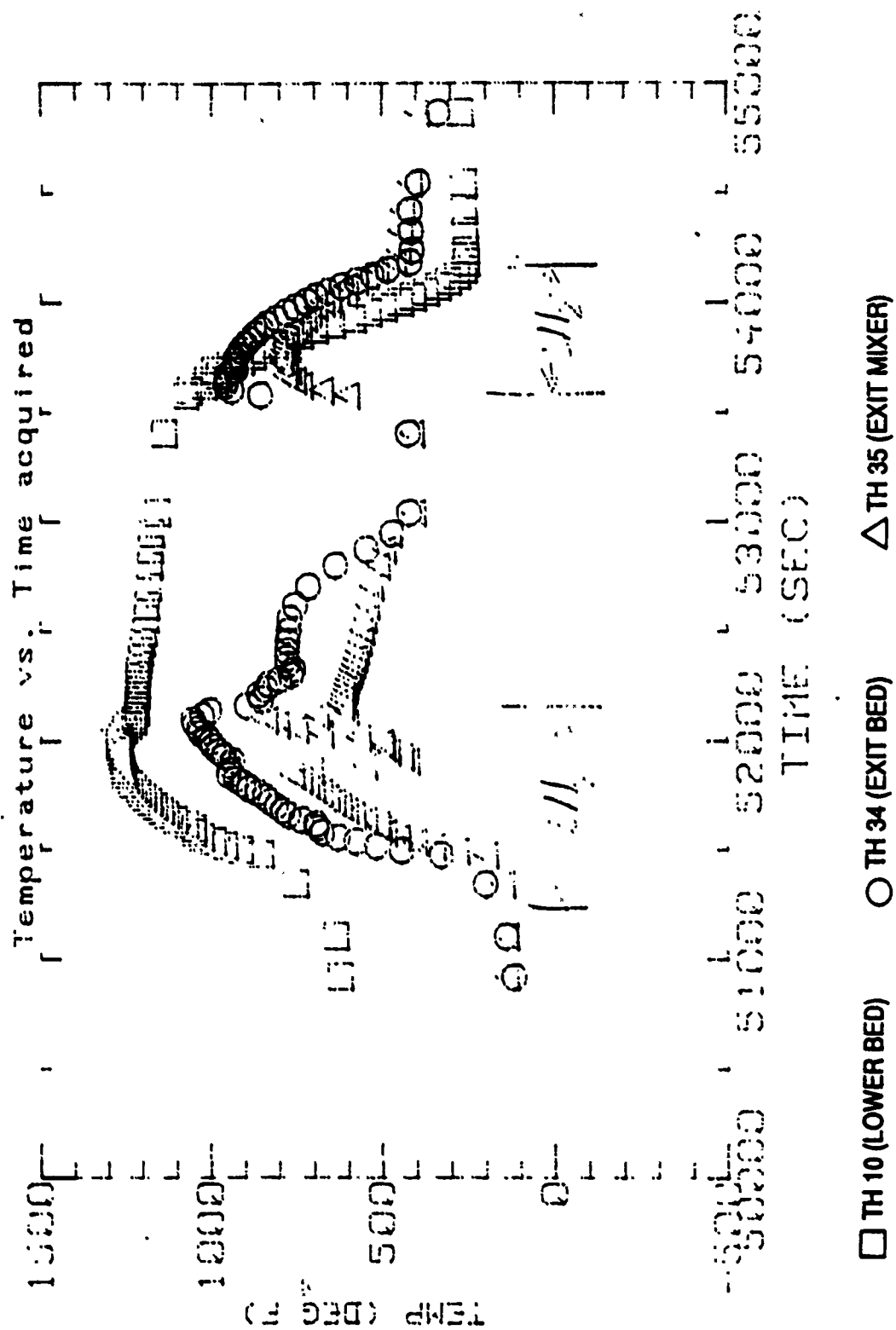
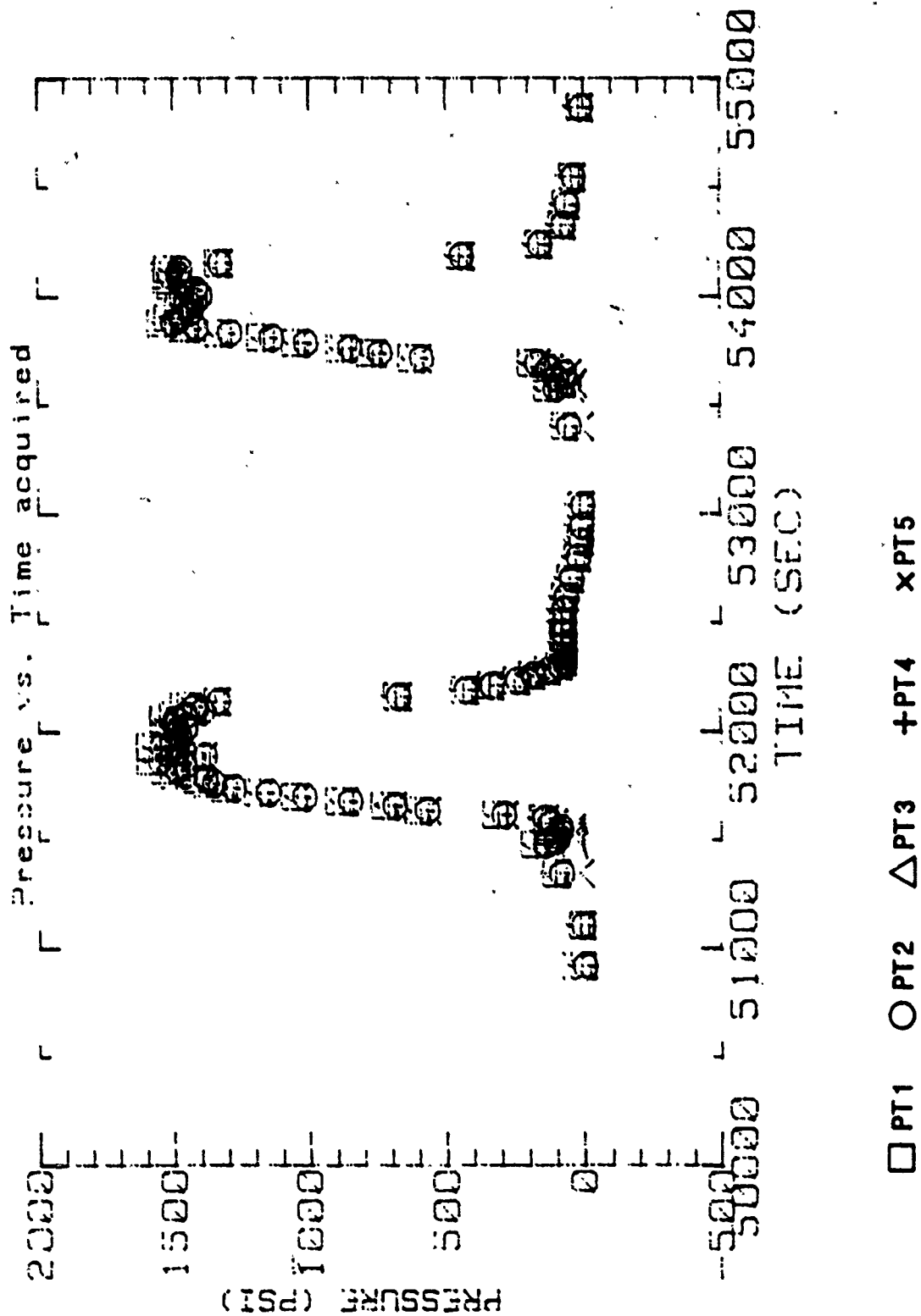


FIGURE 52. EXHAUST TEMPERATURES - FULL TEST



**FIGURE 53. EXHAUST TEMPERATURES
EXPANDED TIME SCALES DURING INJECTION**



**FIGURE 54. PRESSURE TRANSDUCER READINGS
EXPANDED TIME SCALE DURING INJECTION**

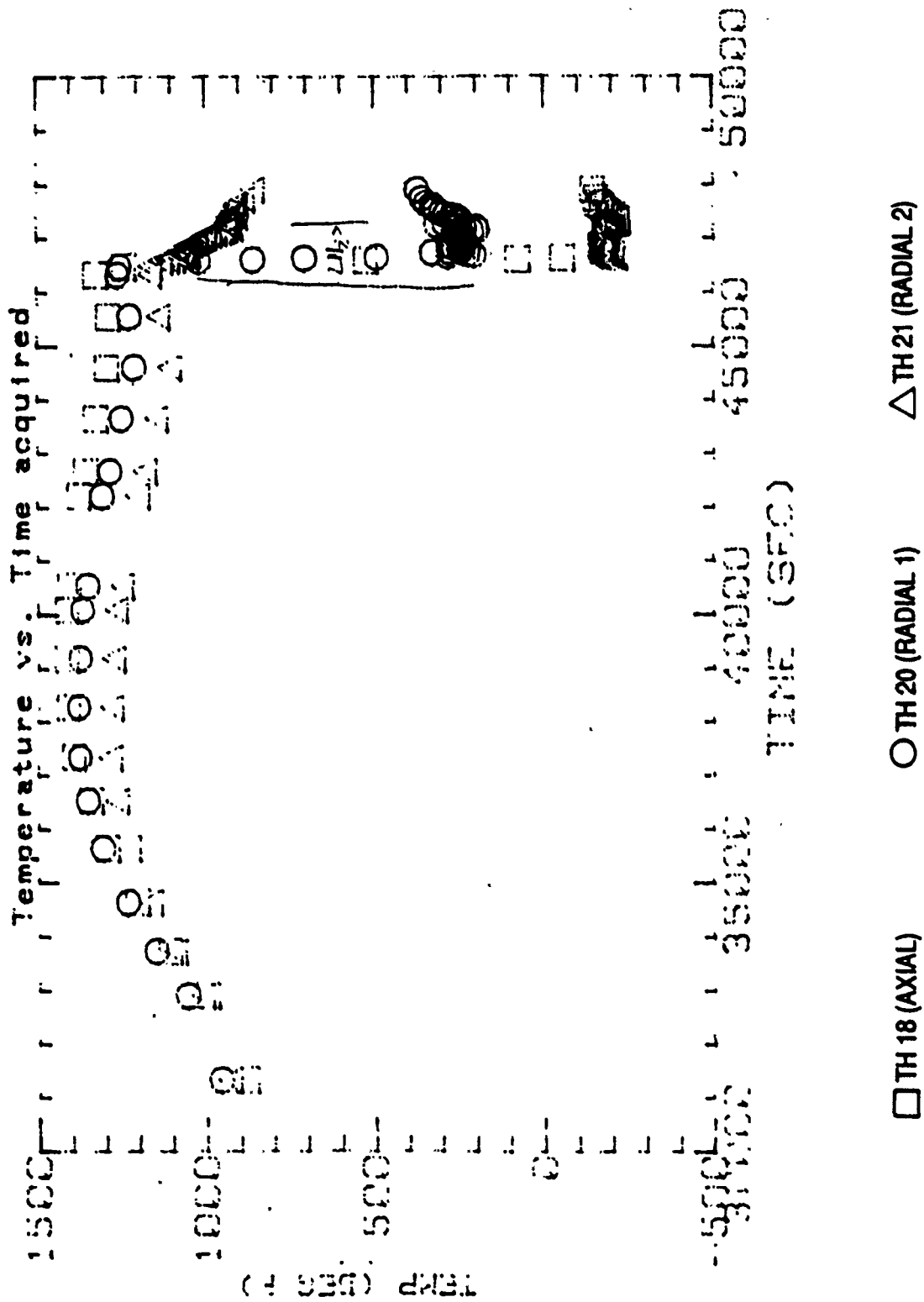


**FIGURE 55. UPPER BED RADIAL TEMPERATURE DISTRIBUTION
FULL TEST**

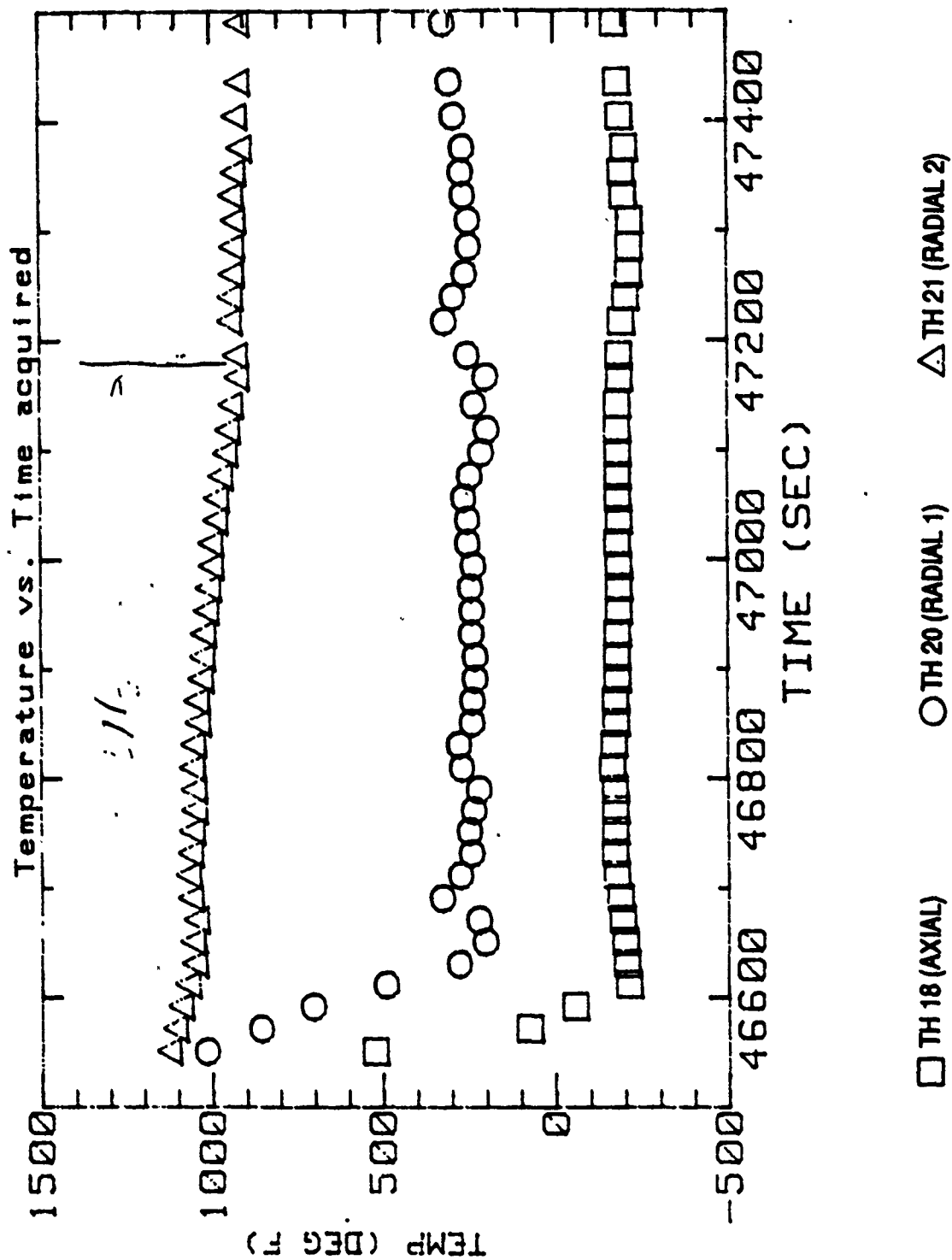


FIGURE 56. UPPER BED RADIAL TEMPERATURE DISTRIBUTION
EXPANDED TIME SCALE DURING INJECTION

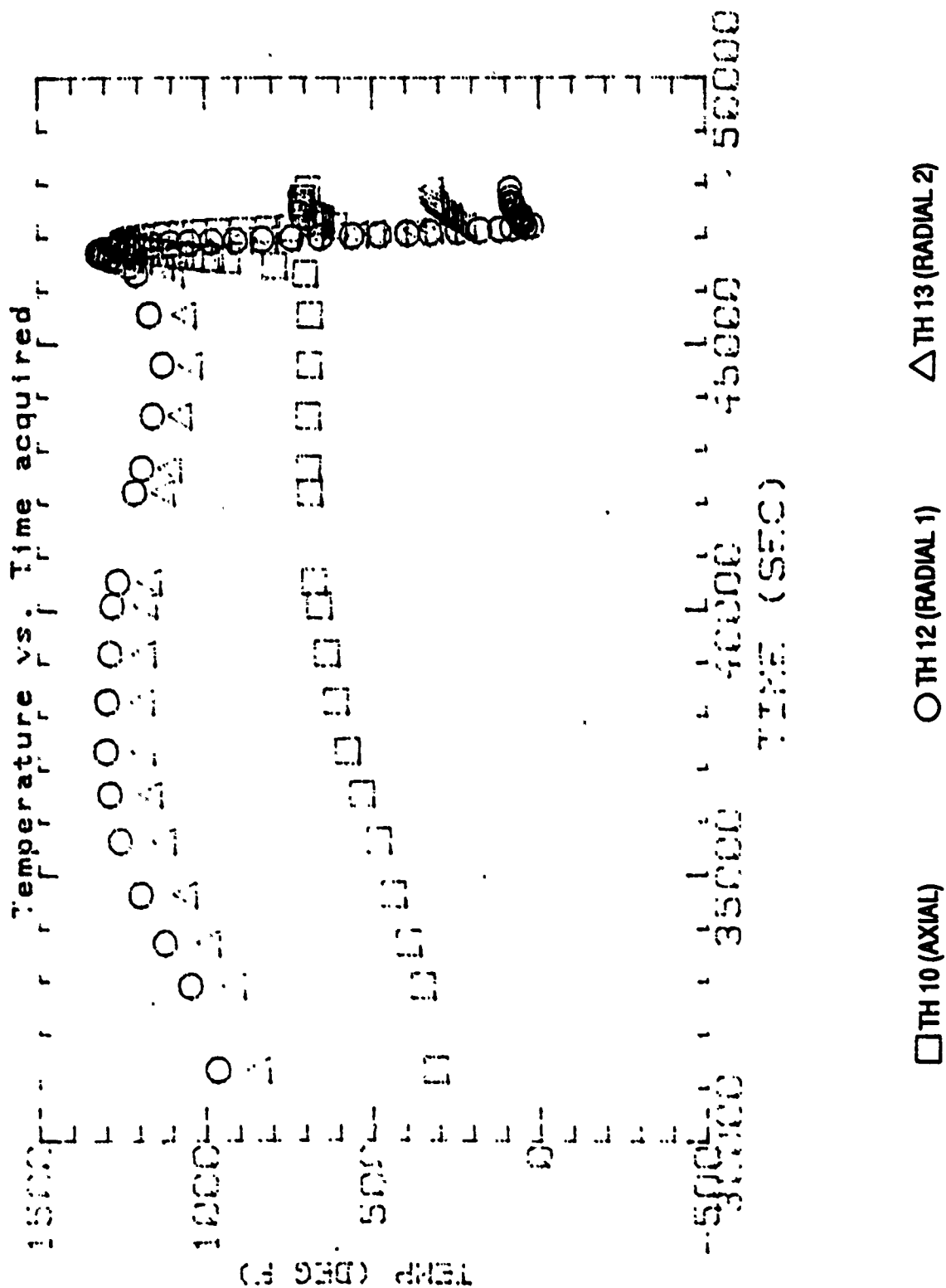
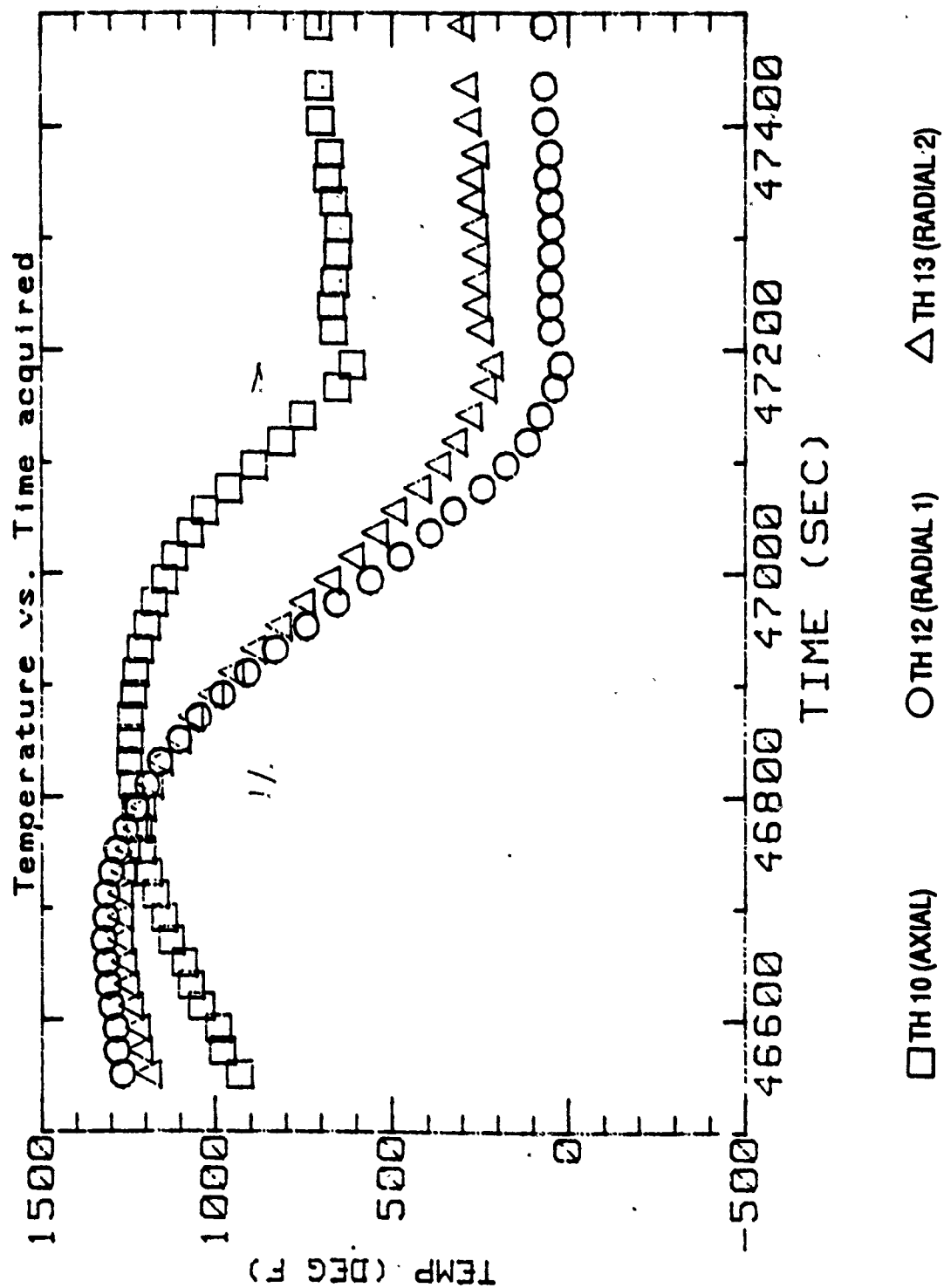
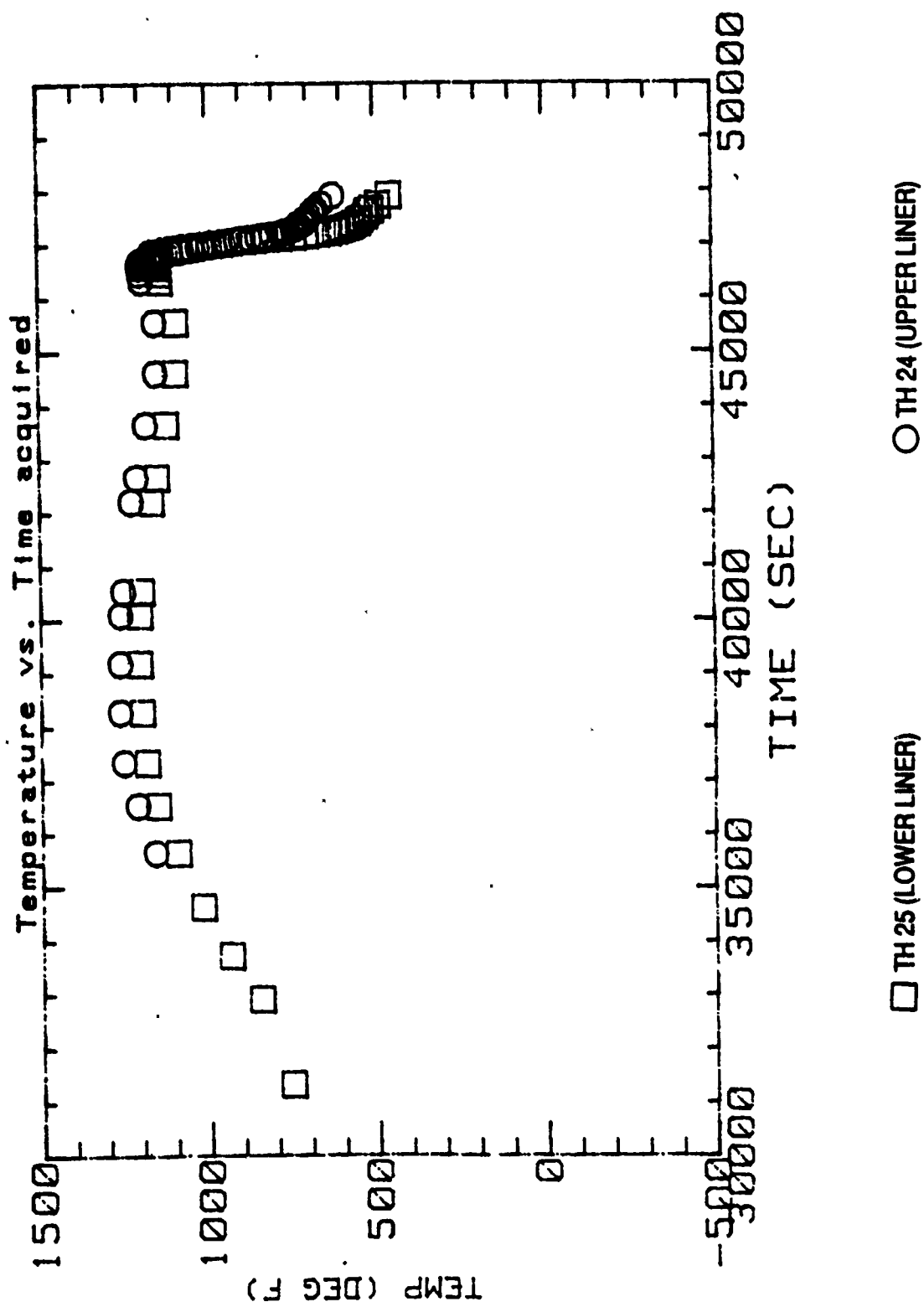


FIGURE 57. LOWER BED RADIAL TEMPERATURE DISTRIBUTION
FULL TEST



**FIGURE 58. LOWER BED RADIAL TEMPERATURE DISTRIBUTION
EXPANDED TIME SCALE DURING INJECTION**



**FIGURE 59. OUTSIDE LINER TEMPERATURES
FULL TEST**

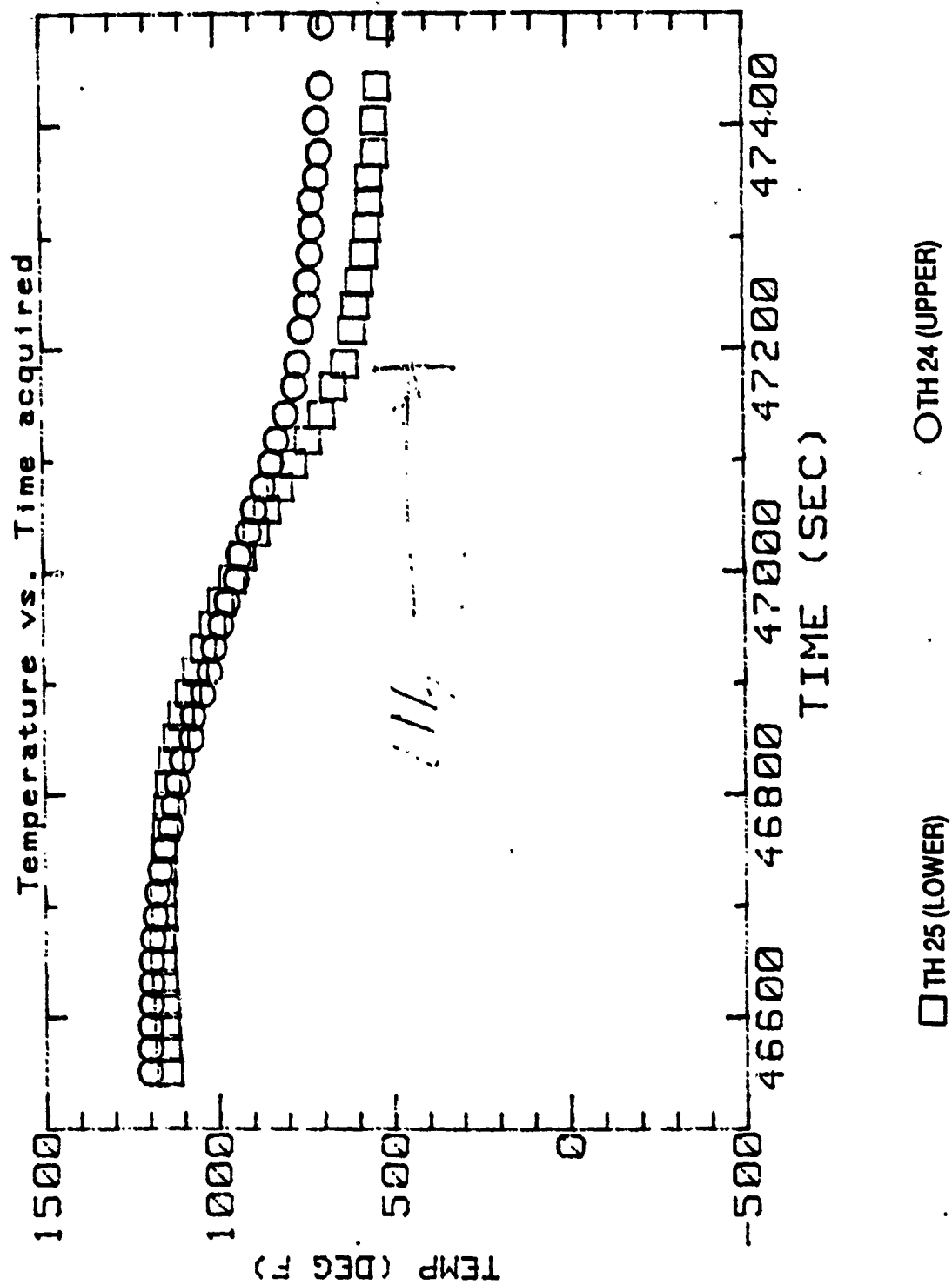


**FIGURE 60. OUTSIDE LINER TEMPERATURE
EXPANDED TIME SCALE DURING INJECTION**

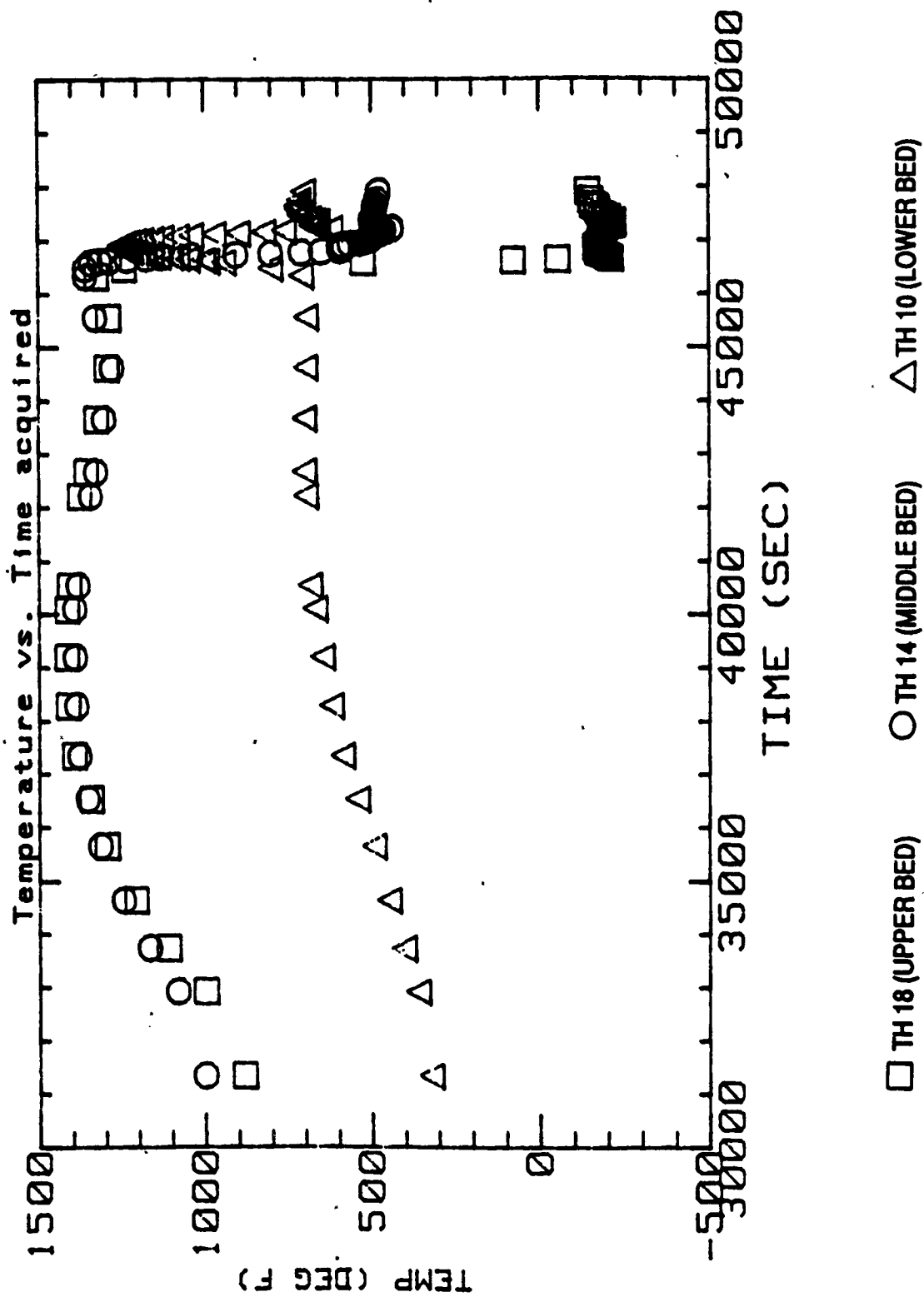
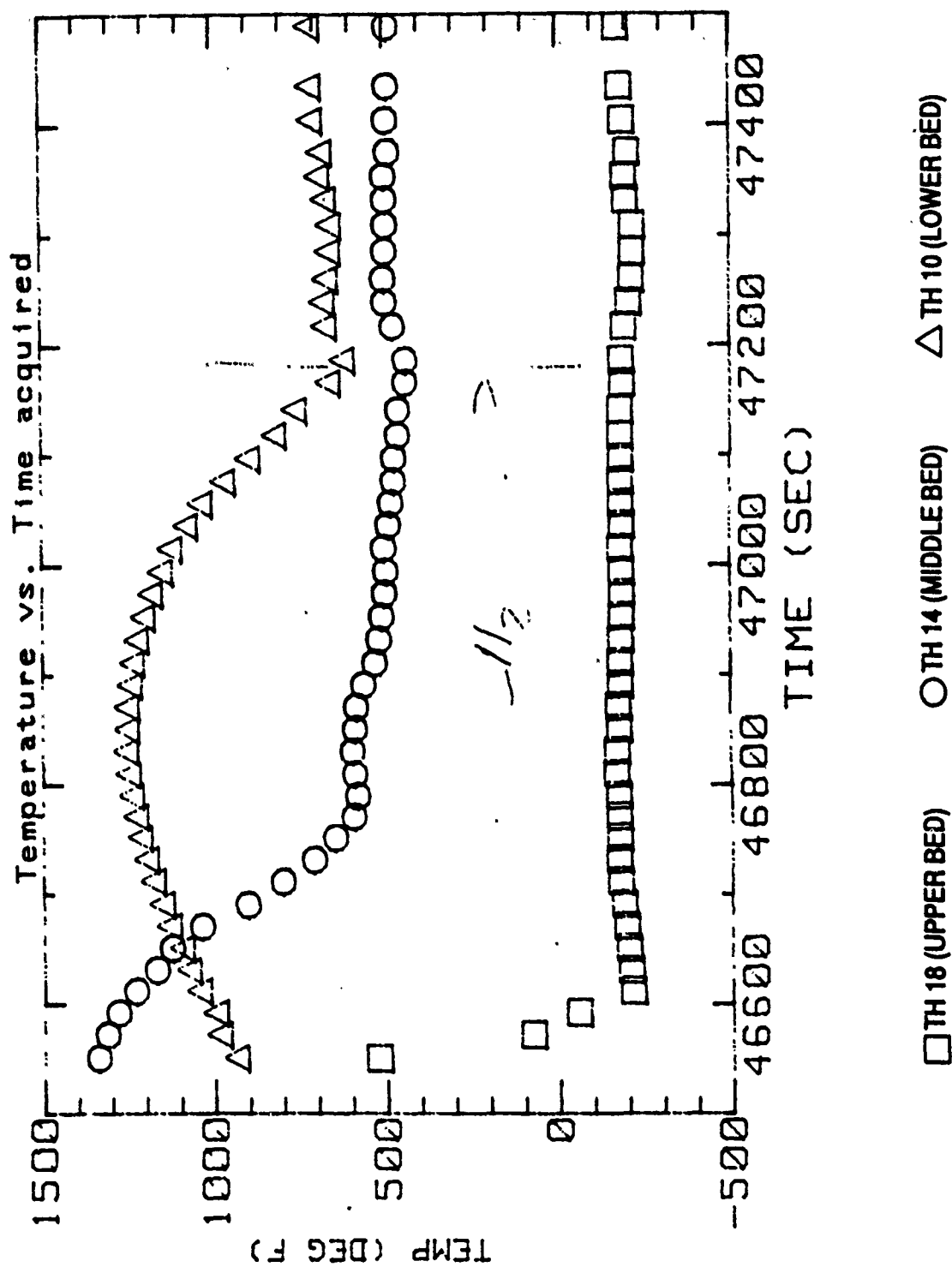


FIGURE 61. AXIAL TEMPERATURE DISTRIBUTION
FULL TEST



**FIGURE 62. AXIAL TEMPERATURE DISTRIBUTION
EXPANDED TIME SCALE DURING INJECTION**

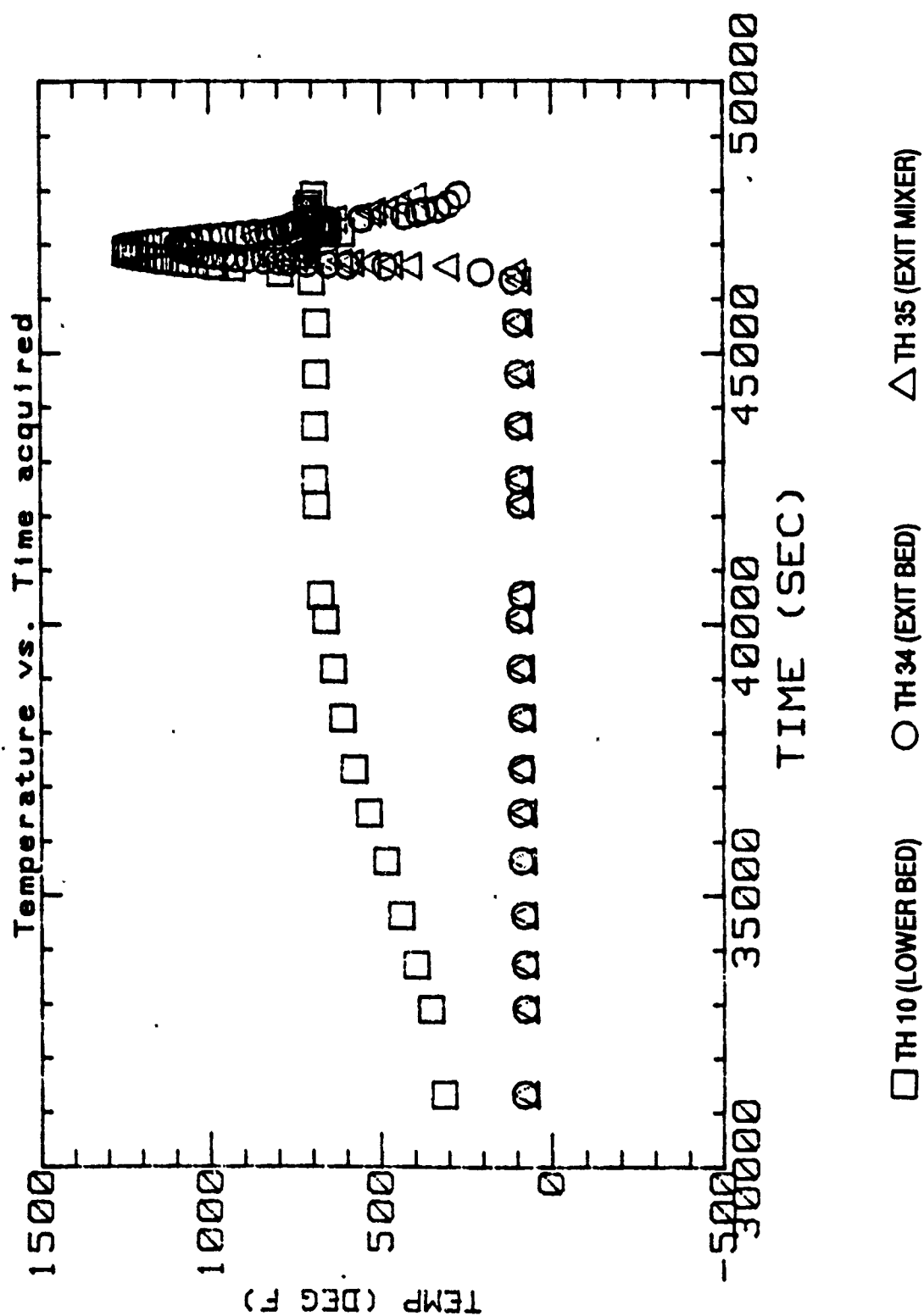
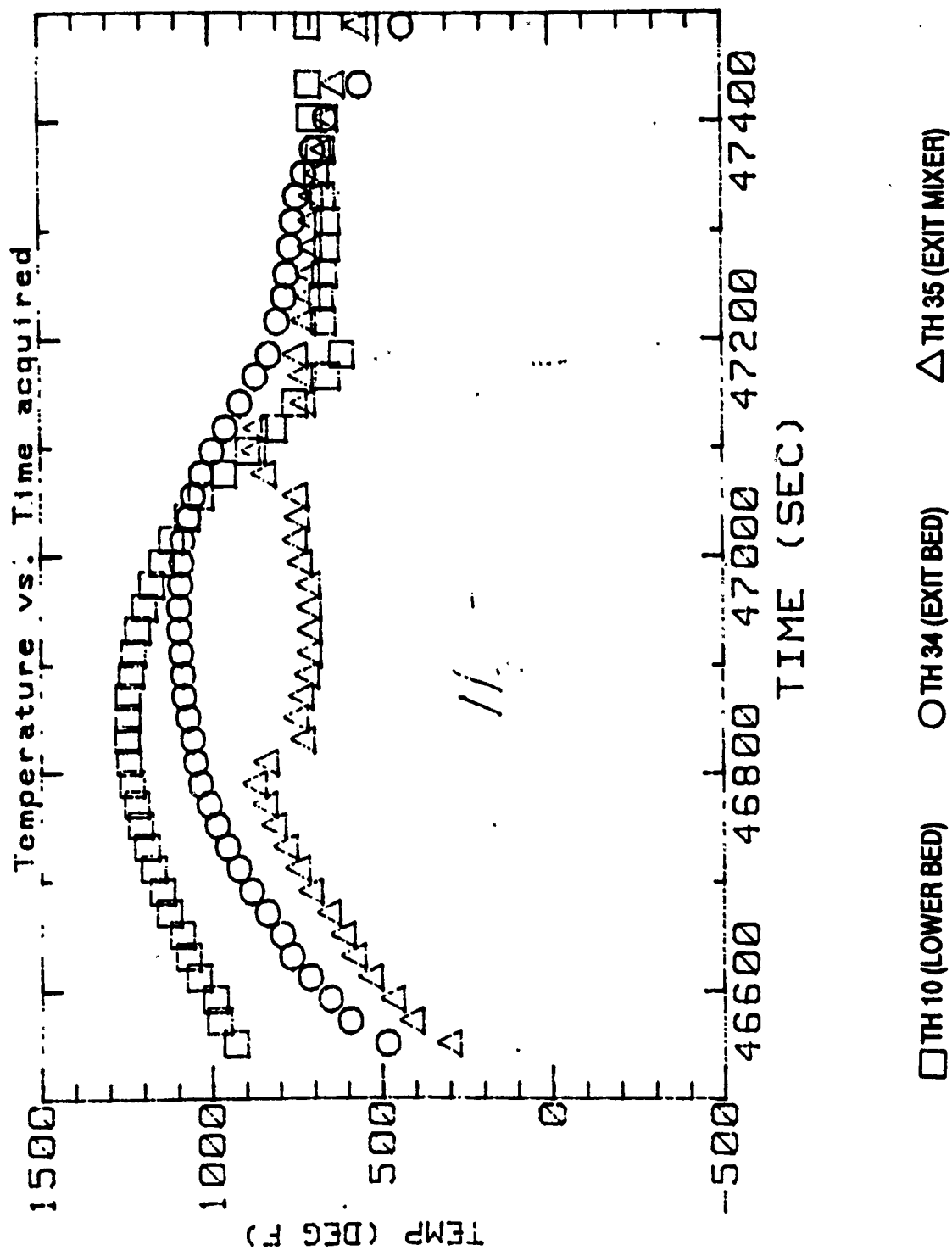
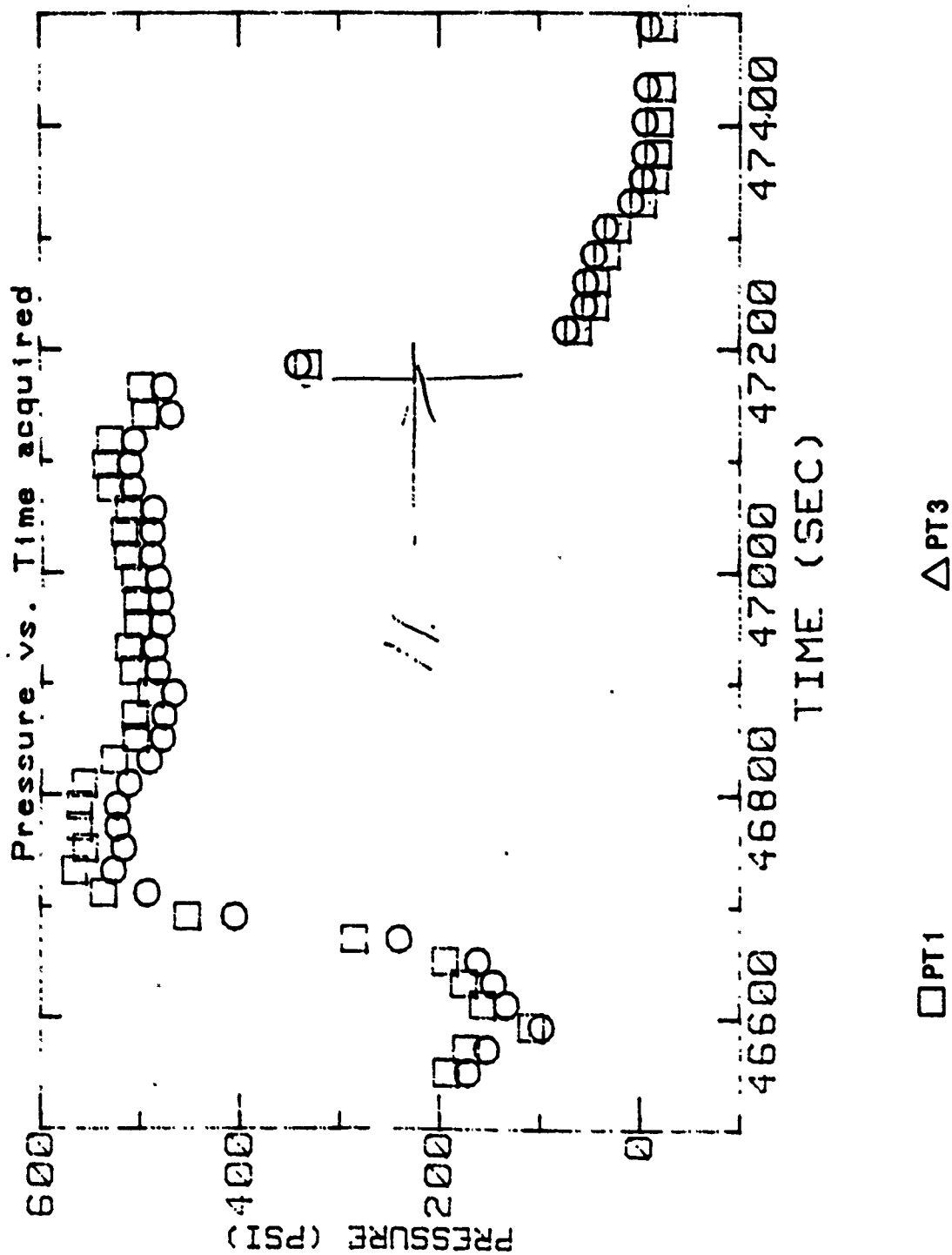


FIGURE 63. EXHAUST TEMPERATURES - FULL TEST



**FIGURE 64. EXHAUST TEMPERATURES
EXPANDED TIME SCALES DURING INJECTION**



**FIGURE 65. BED PRESSURE
EXPANDED TIME SCALE DURING INJECTION**

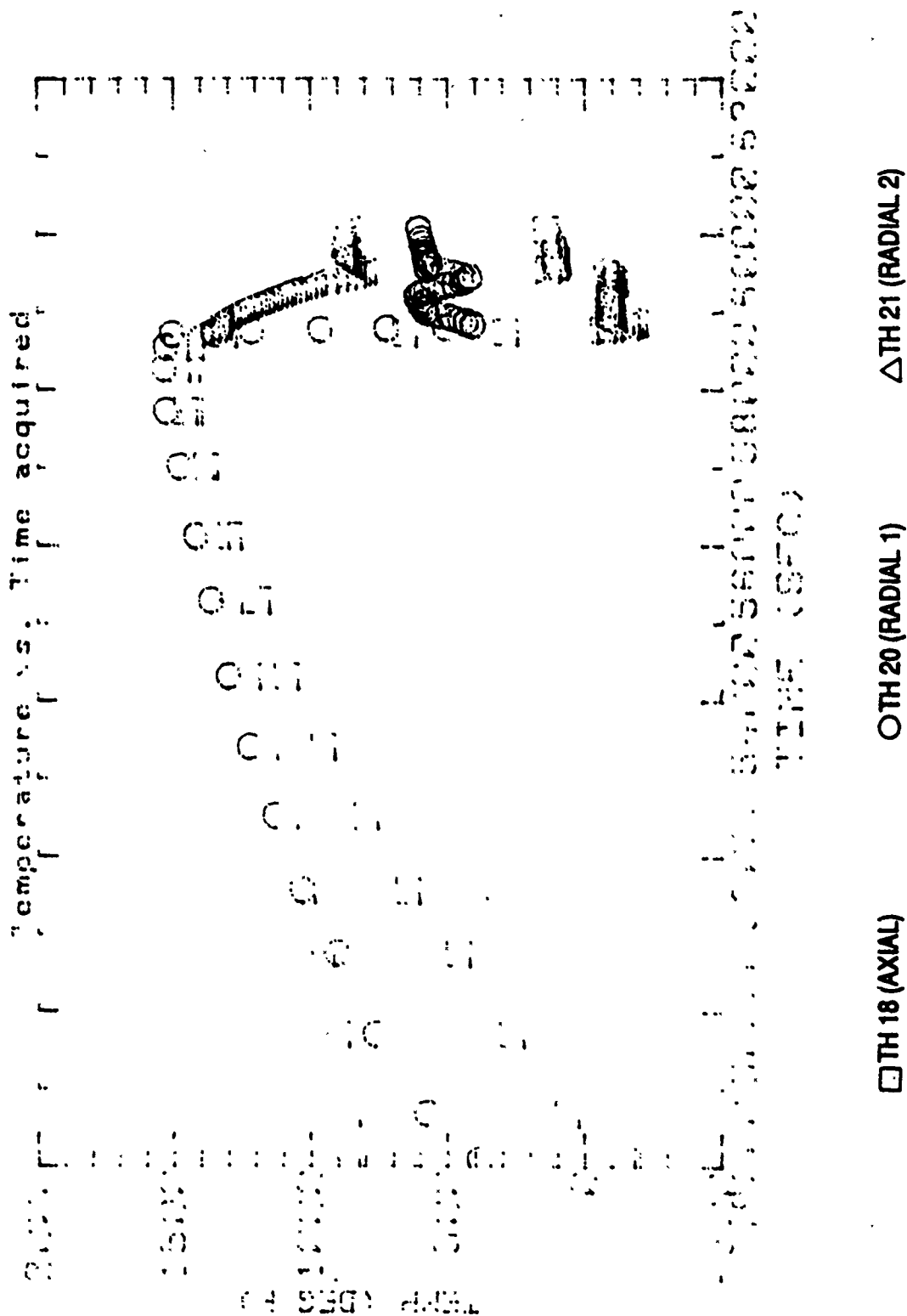


**FIGURE 66. UPPER BED RADIAL TEMPERATURE DISTRIBUTION
FULL TEST**

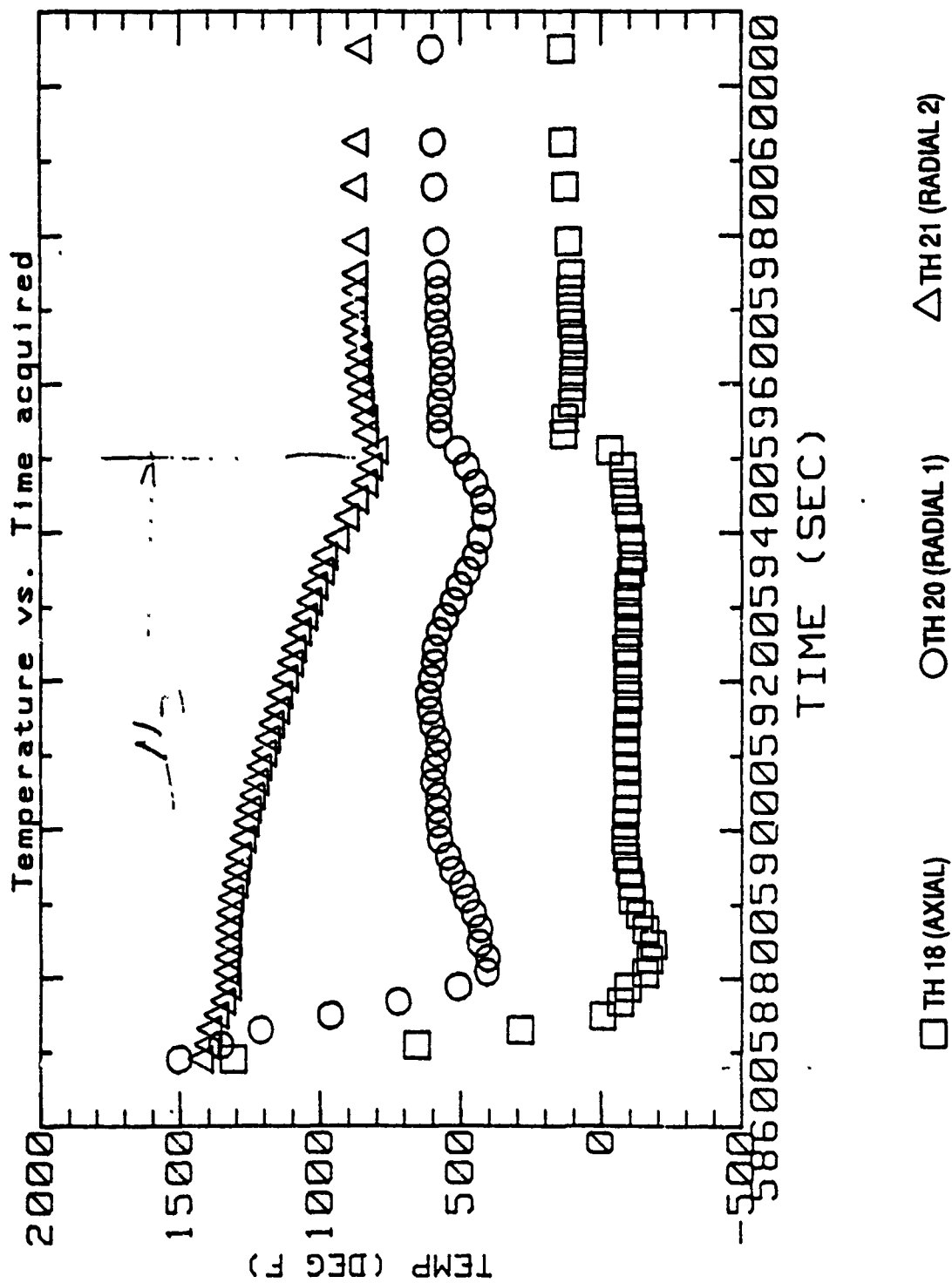


**FIGURE 67. UPPER BED RADIAL TEMPERATURE DISTRIBUTION
EXPANDED TIME SCALE DURING INJECTION**

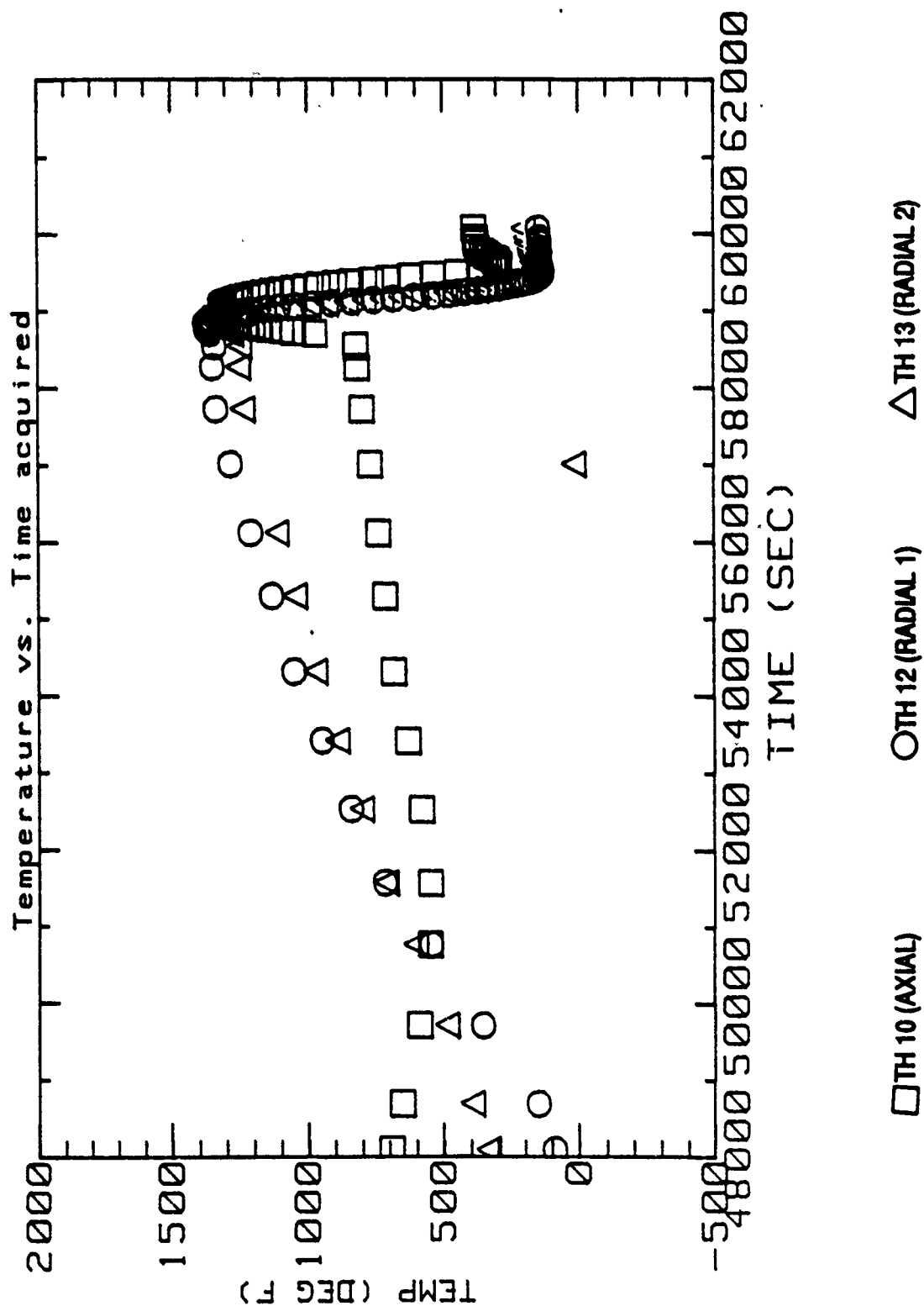


FIGURE 68. LOWER BED RADIAL TEMPERATURE DISTRIBUTION
EHH I TEST

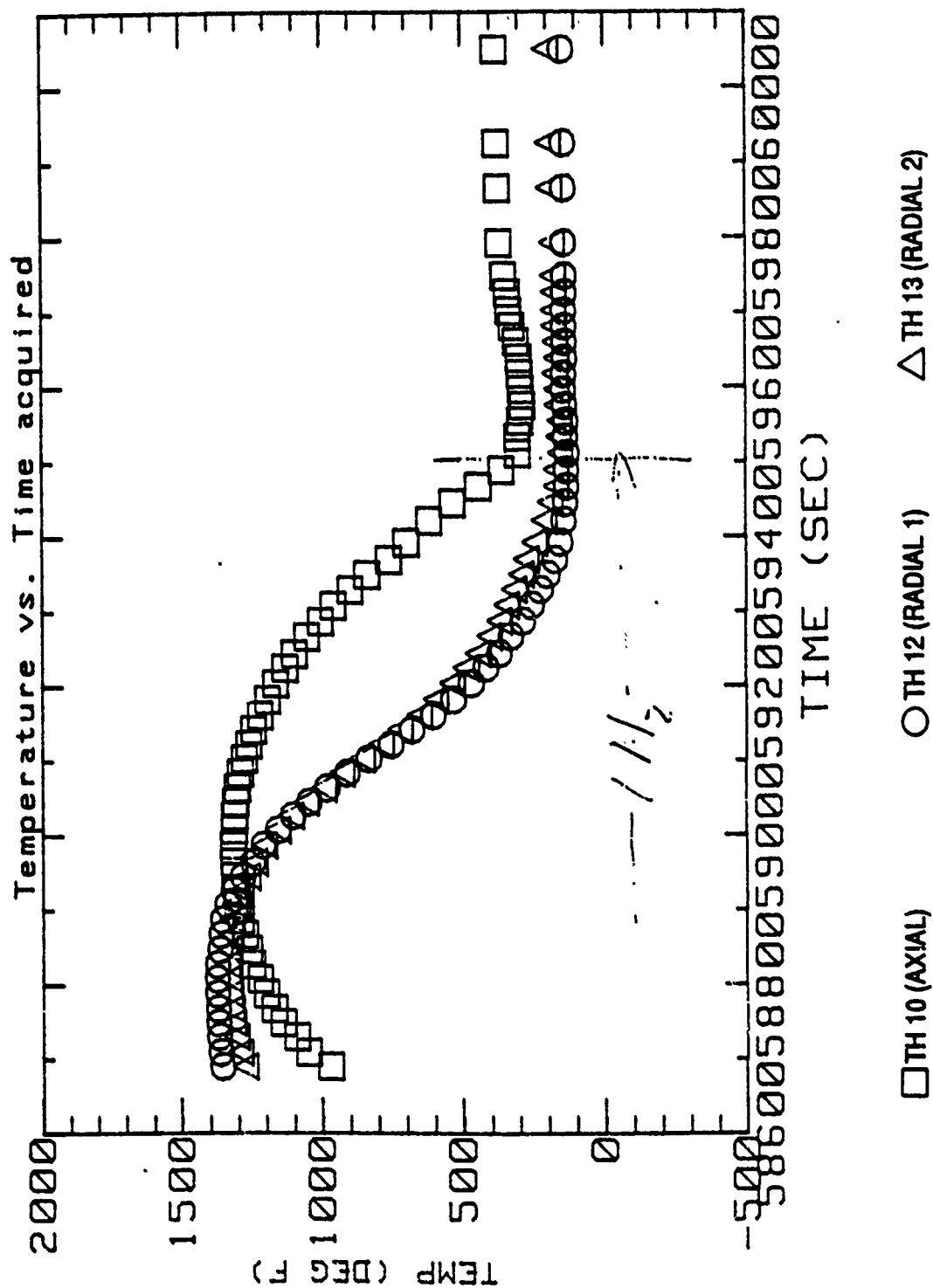
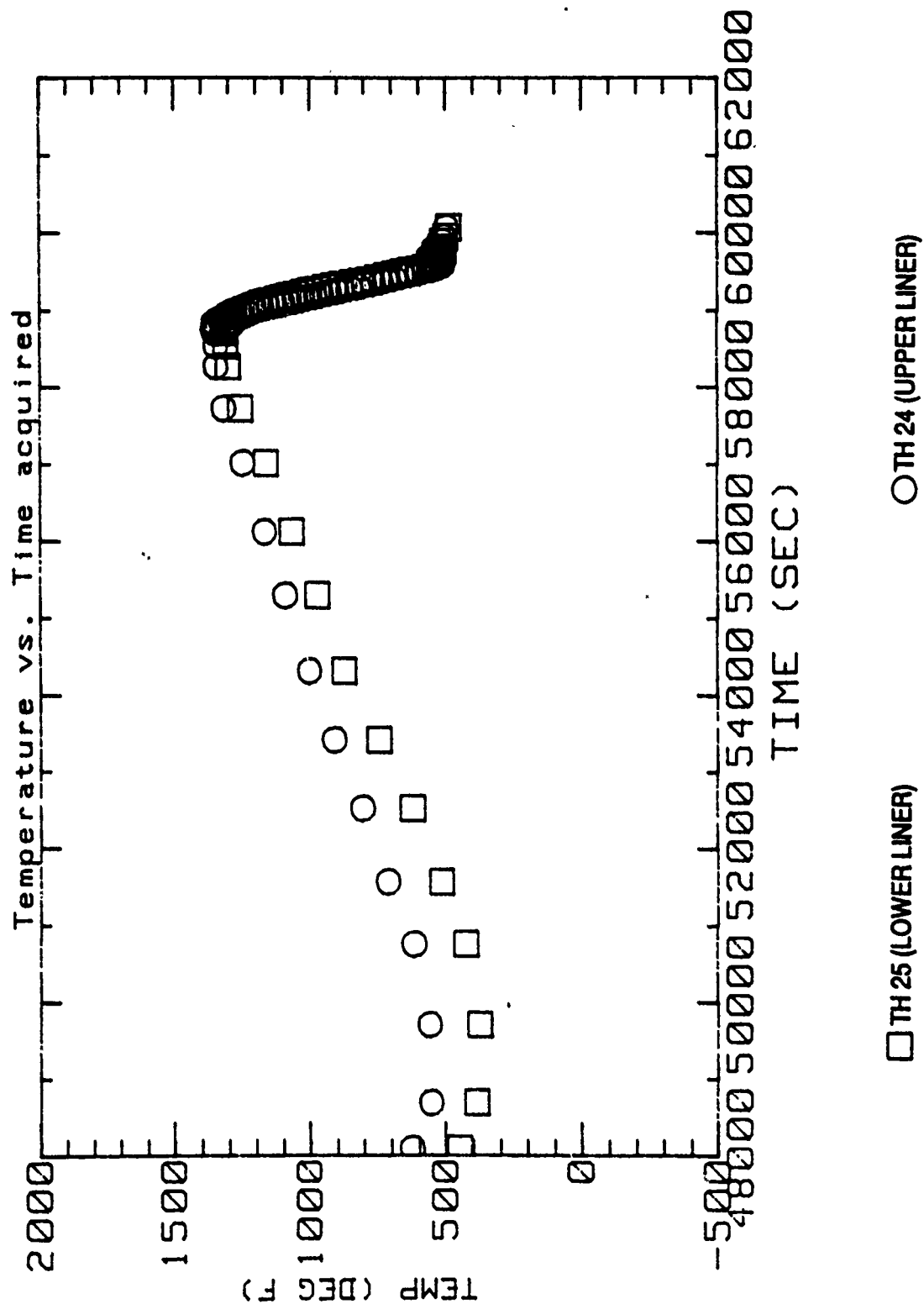


FIGURE 69. LOWER BED RADIAL TEMPERATURE DISTRIBUTION
EXPANDED TIME SCALE DURING INJECTION



**FIGURE 70. OUTSIDE LINER TEMPERATURES
FULL TEST**

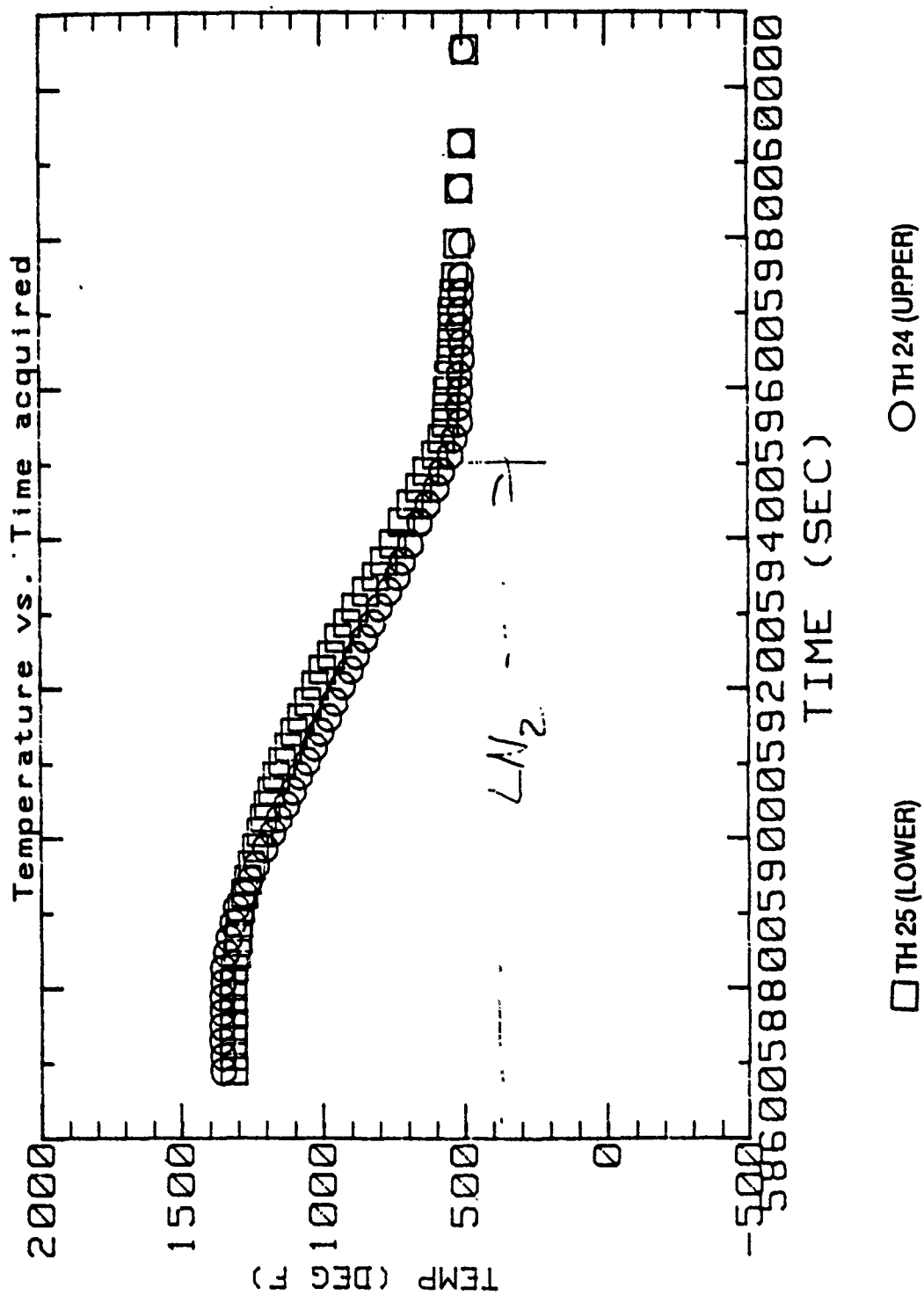
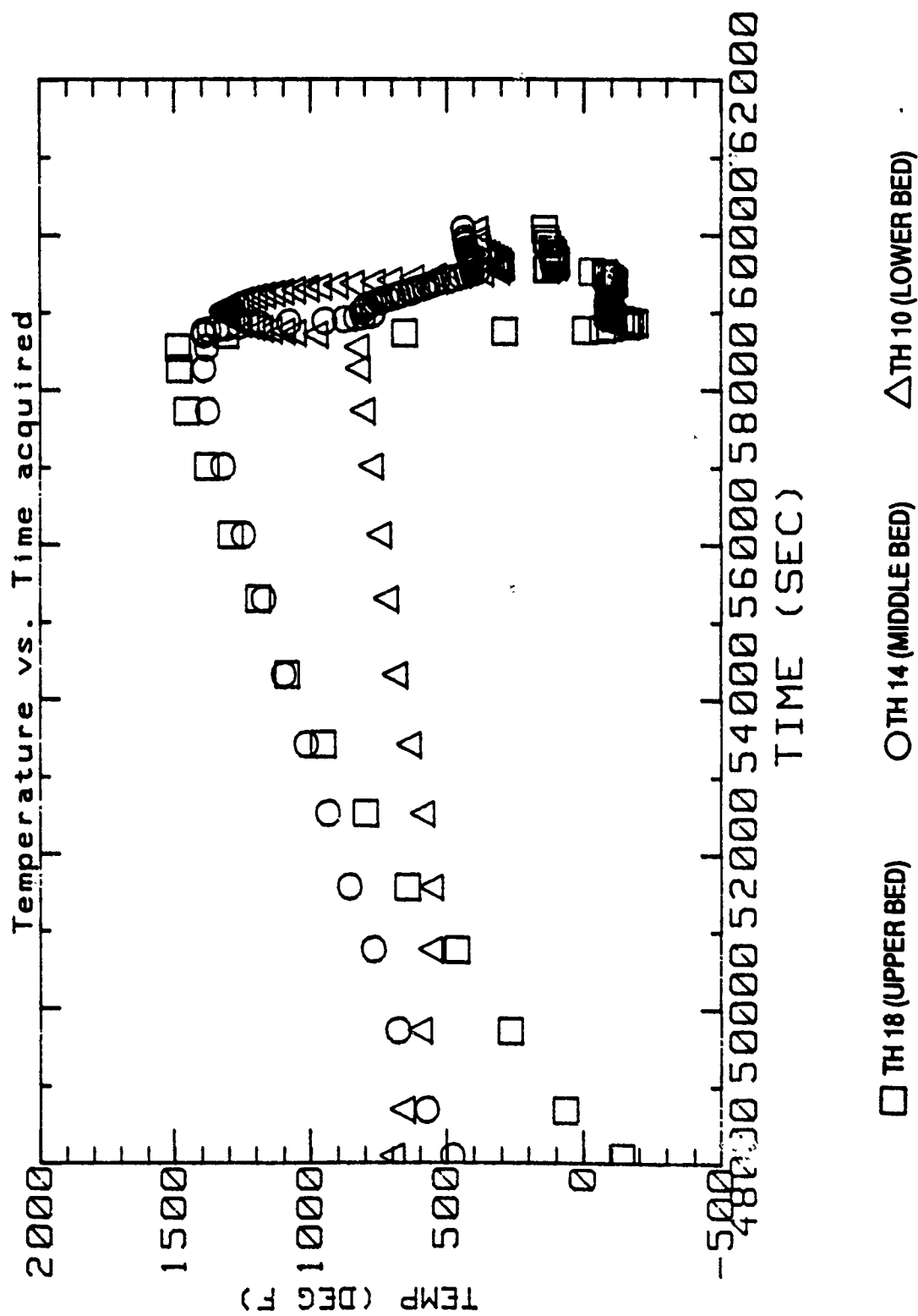
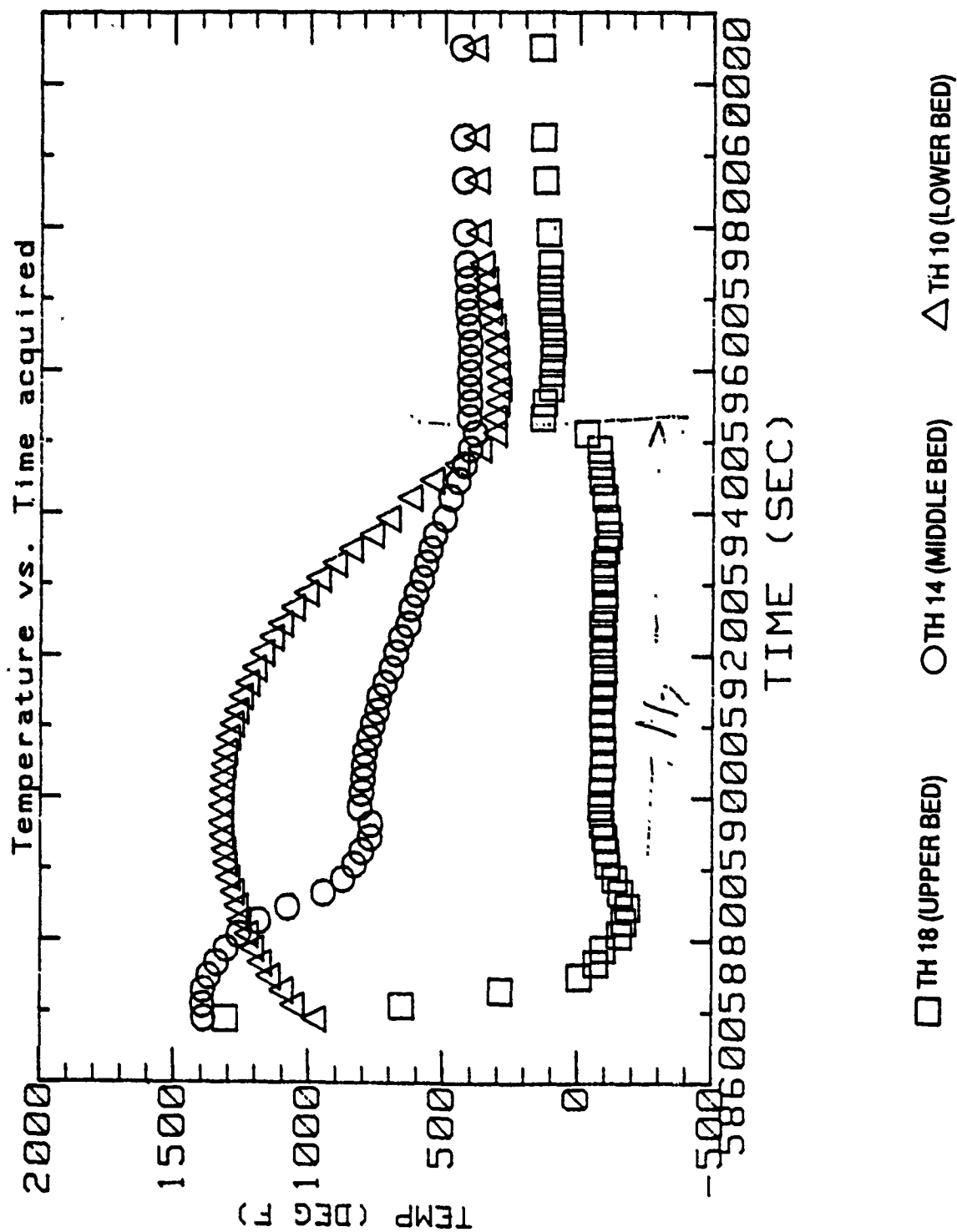


FIGURE 71. OUTSIDE LINER TEMPERATURE
EXPANDED TIME SCALE DURING INJECTION



**FIGURE 72. AXIAL TEMPERATURE DISTRIBUTION
FULL TEST**



**FIGURE 73. AXIAL TEMPERATURE DISTRIBUTION
EXPANDED TIME SCALE DURING INJECTION**

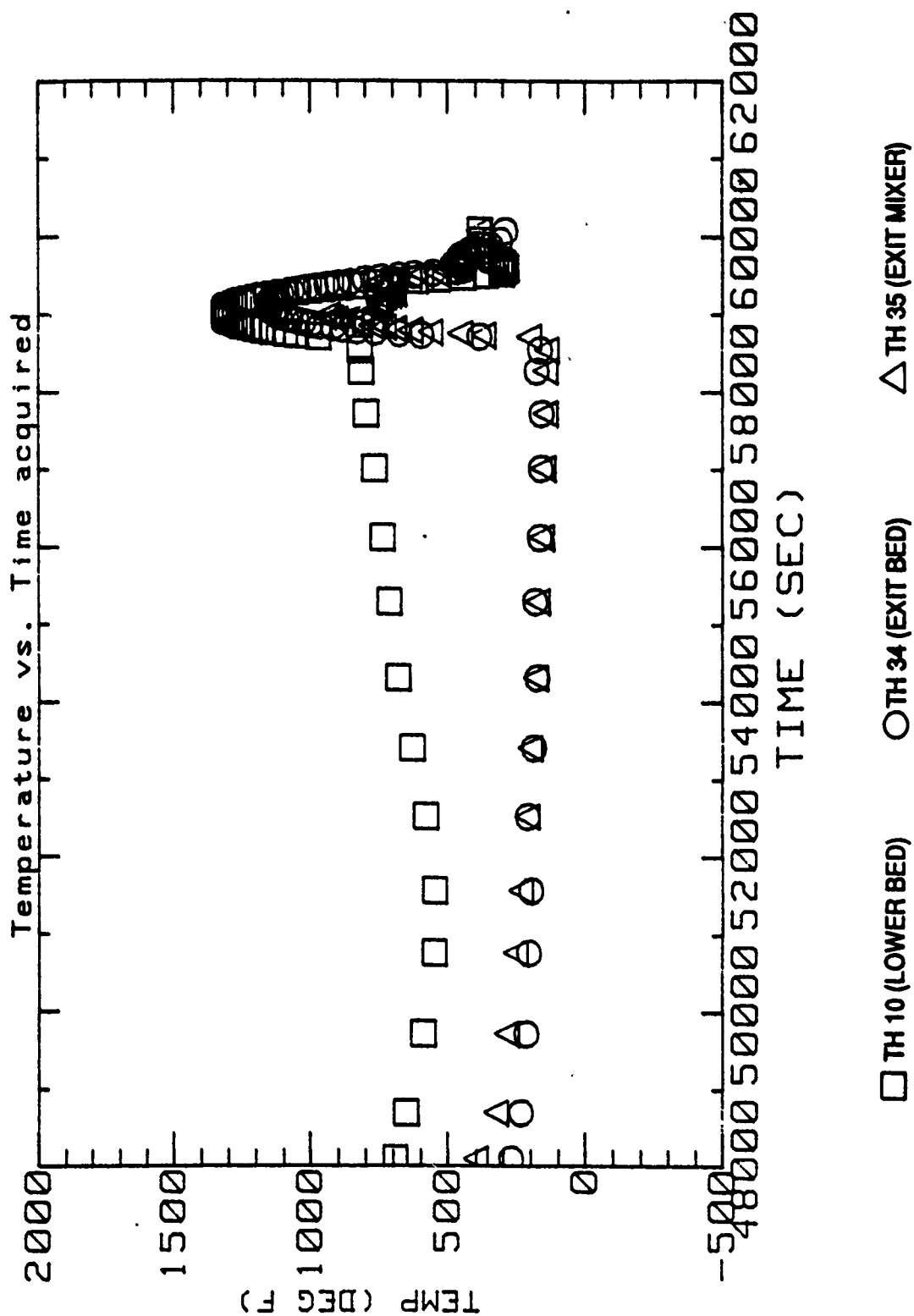


FIGURE 74. EXHAUST TEMPERATURES - FULL TEST

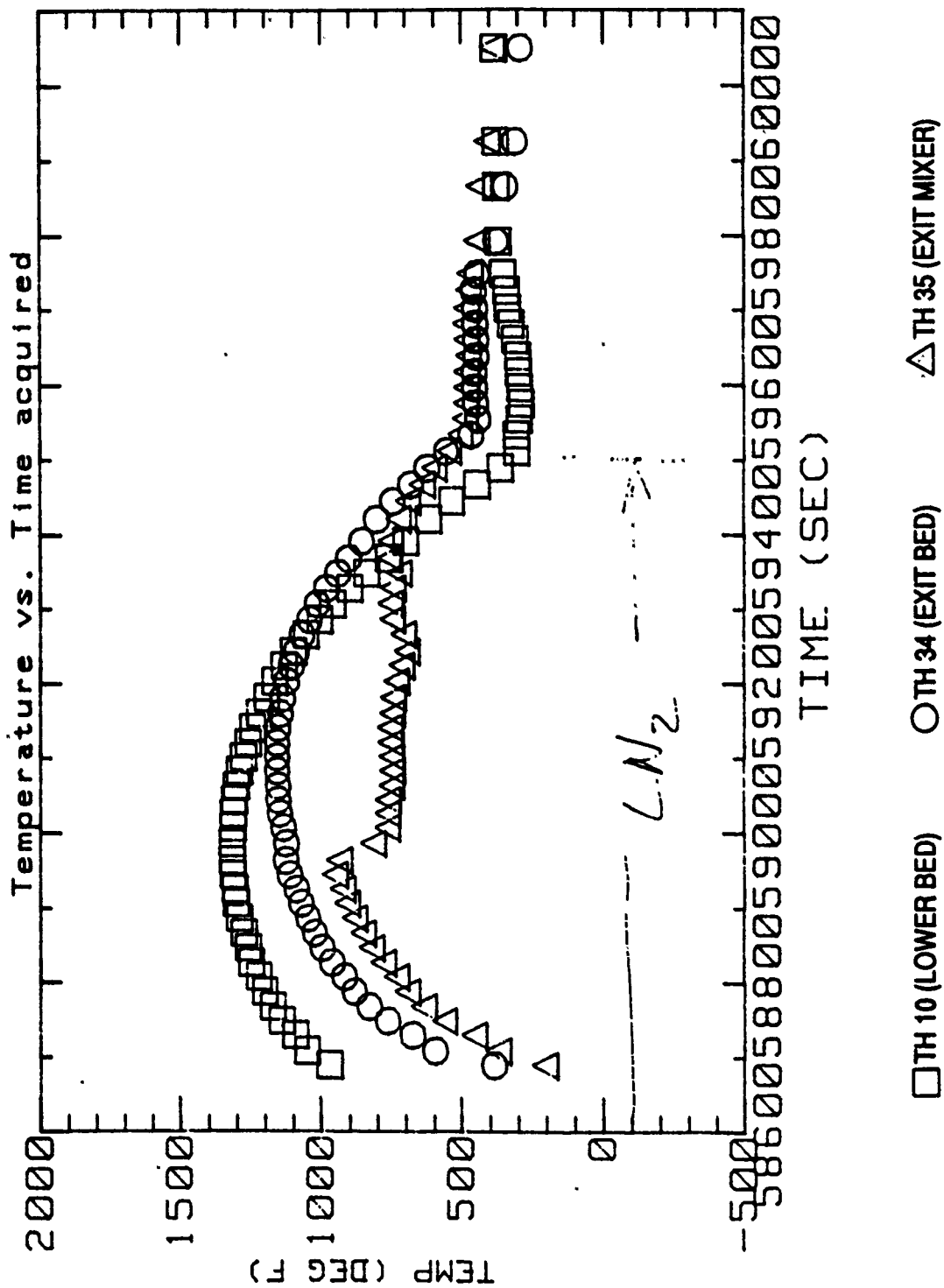


FIGURE 75. EXHAUST TEMPERATURES
EXPANDED TIME SCALES DURING INJECTION

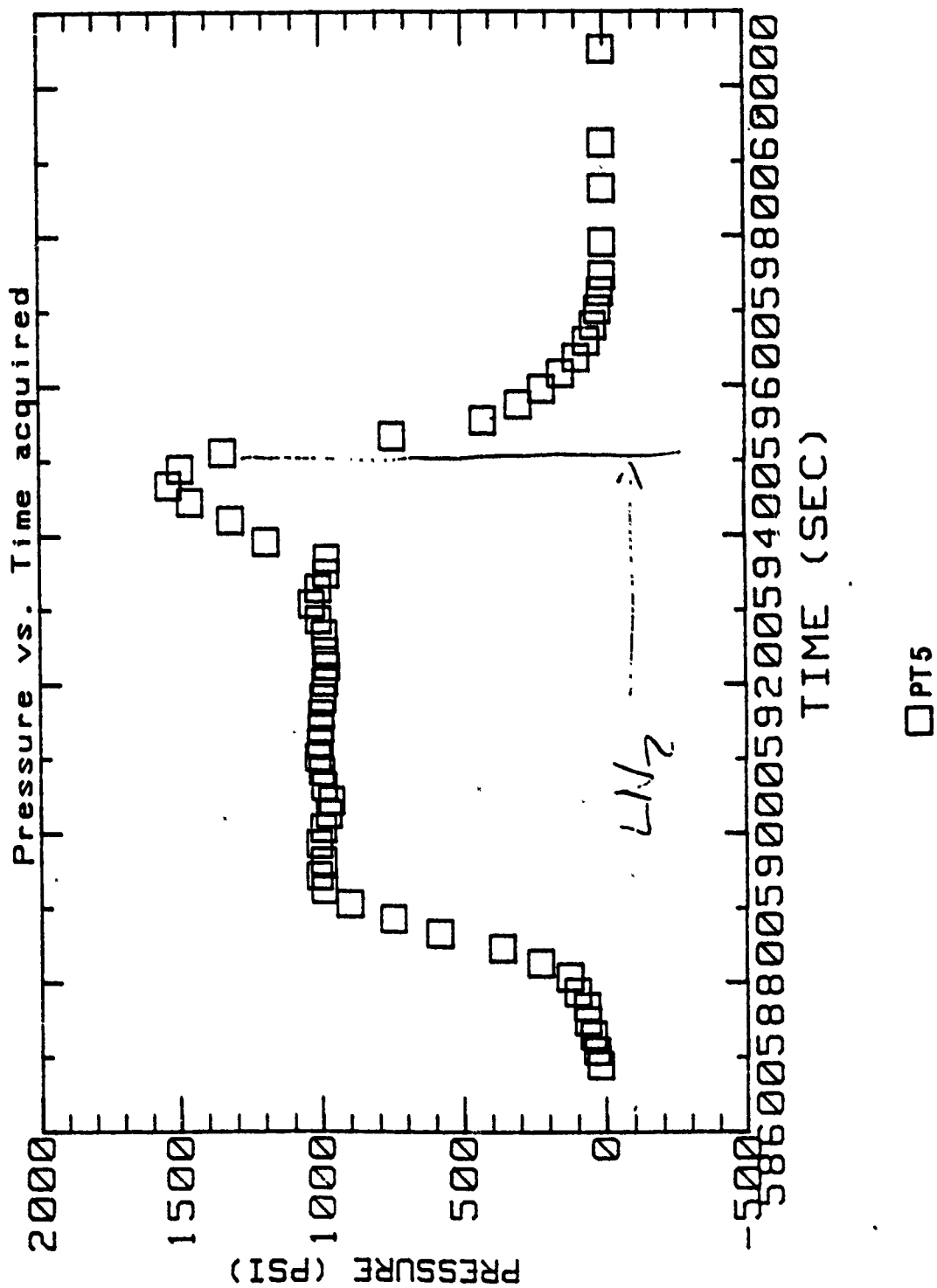
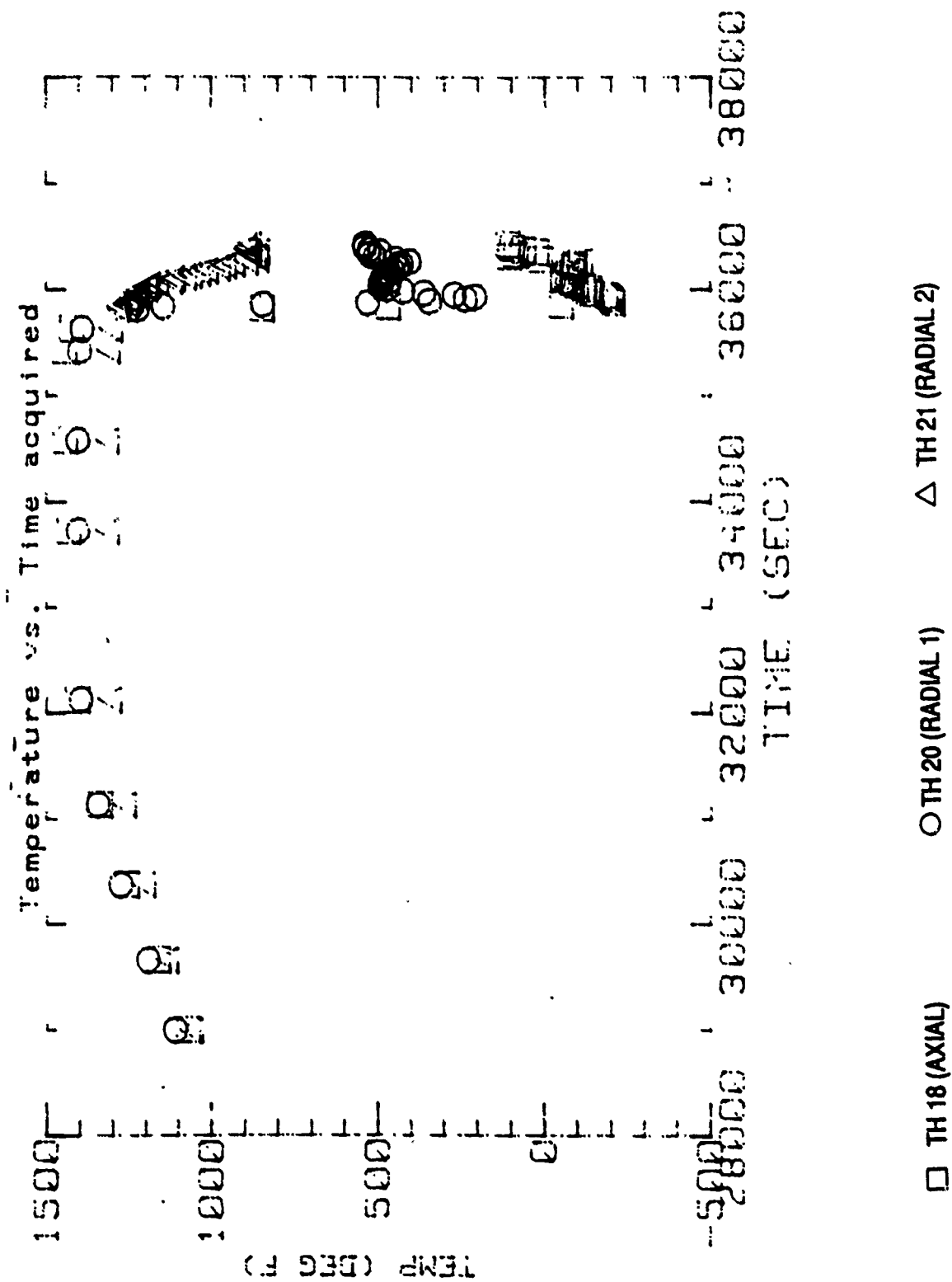
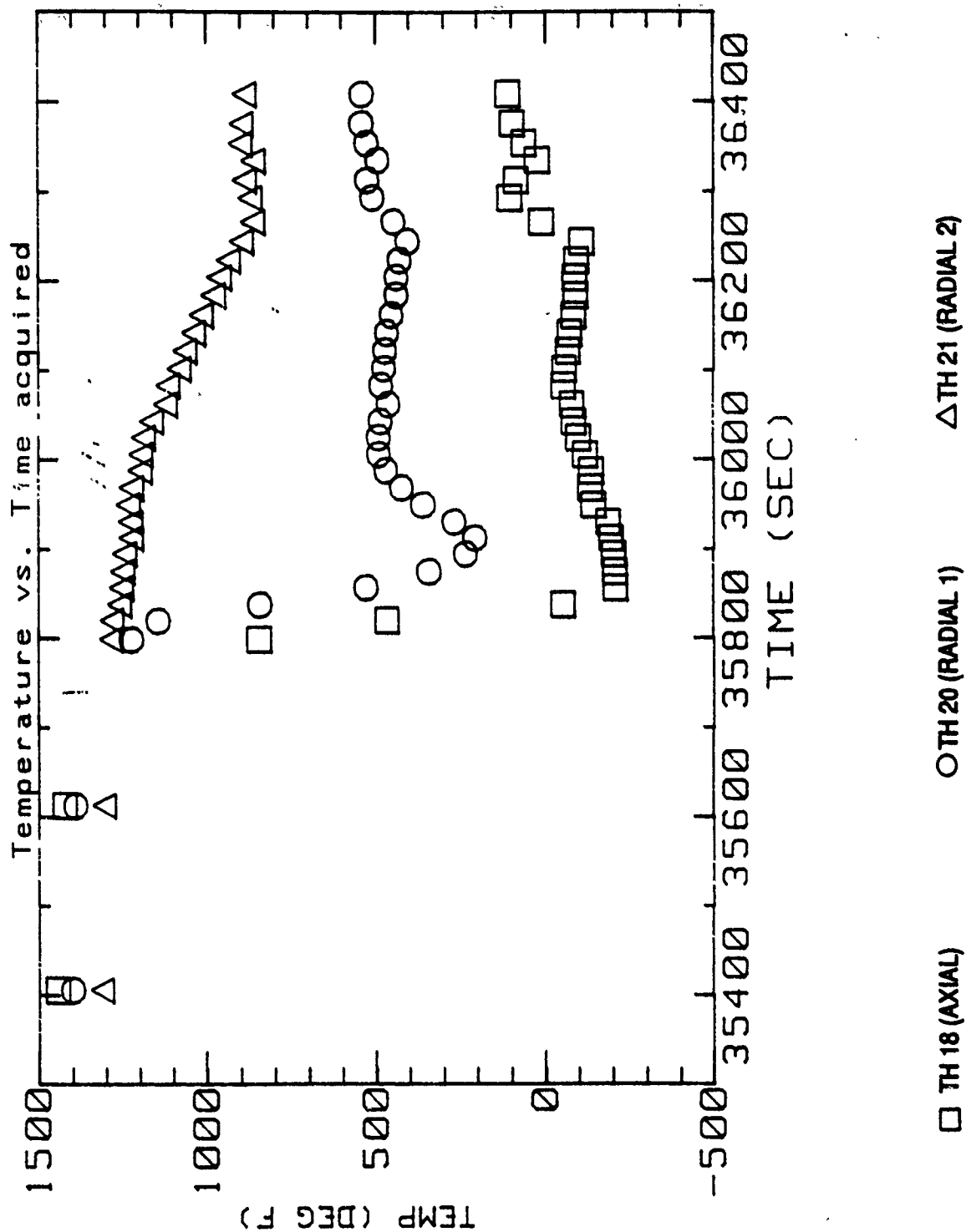


FIGURE 76. BED PRESSURE
EXPANDED TIME SCALE DURING INJECTION



**FIGURE 77. UPPER BED RADIAL TEMPERATURE DISTRIBUTION
FULL TEST**



**FIGURE 78. UPPER BED RADIAL TEMPERATURE DISTRIBUTION
EXPANDED TIME SCALE DURING INJECTION**

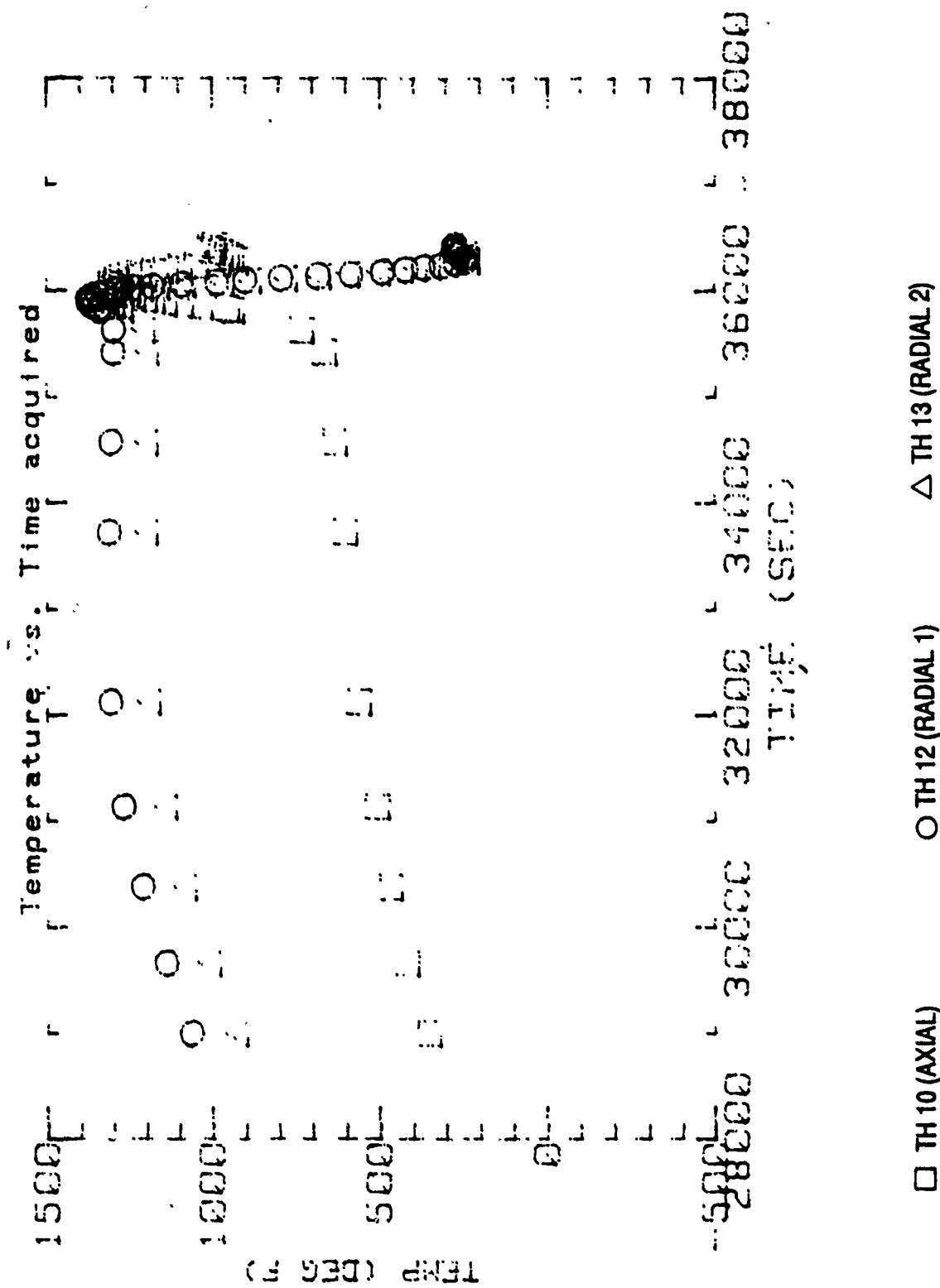
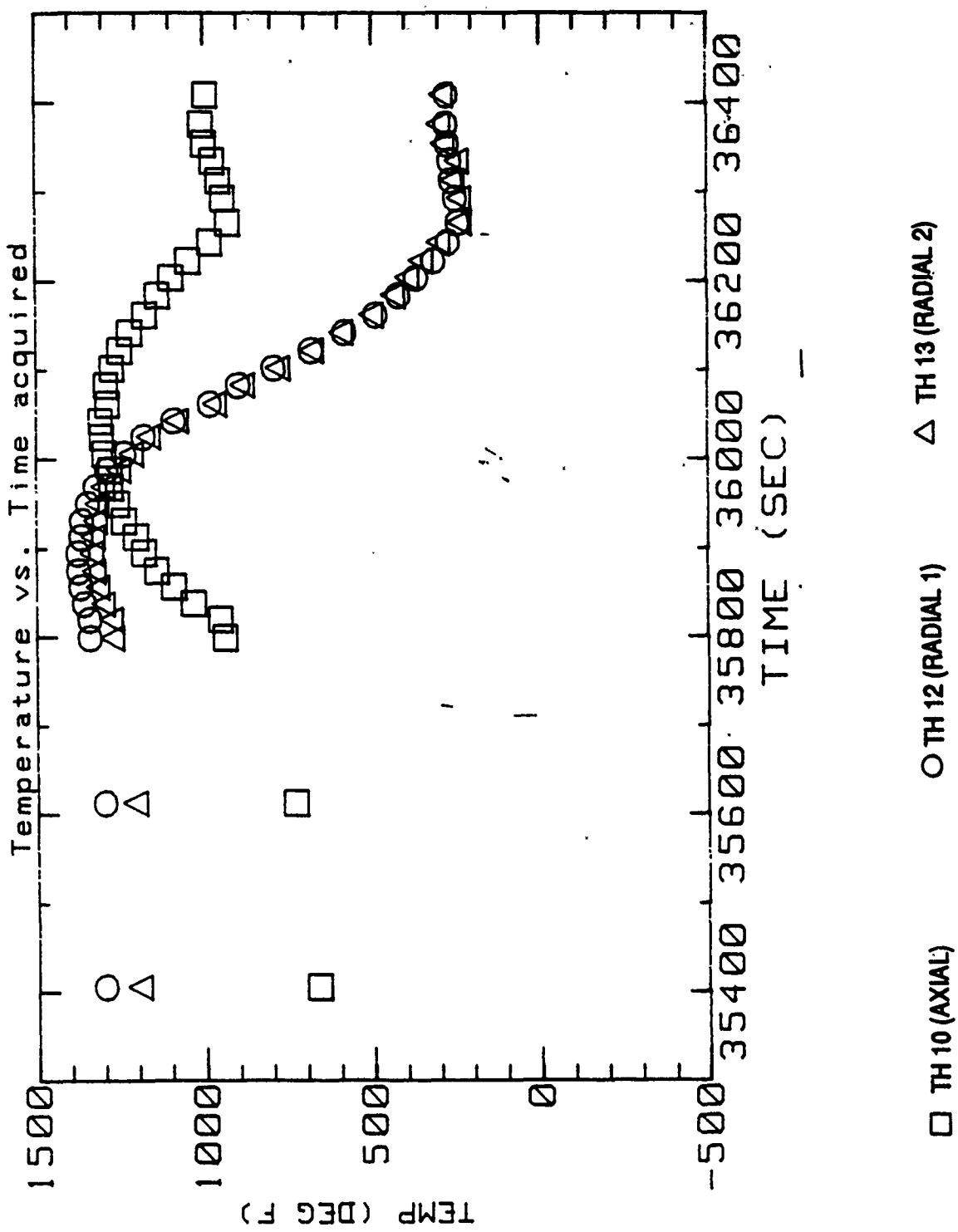
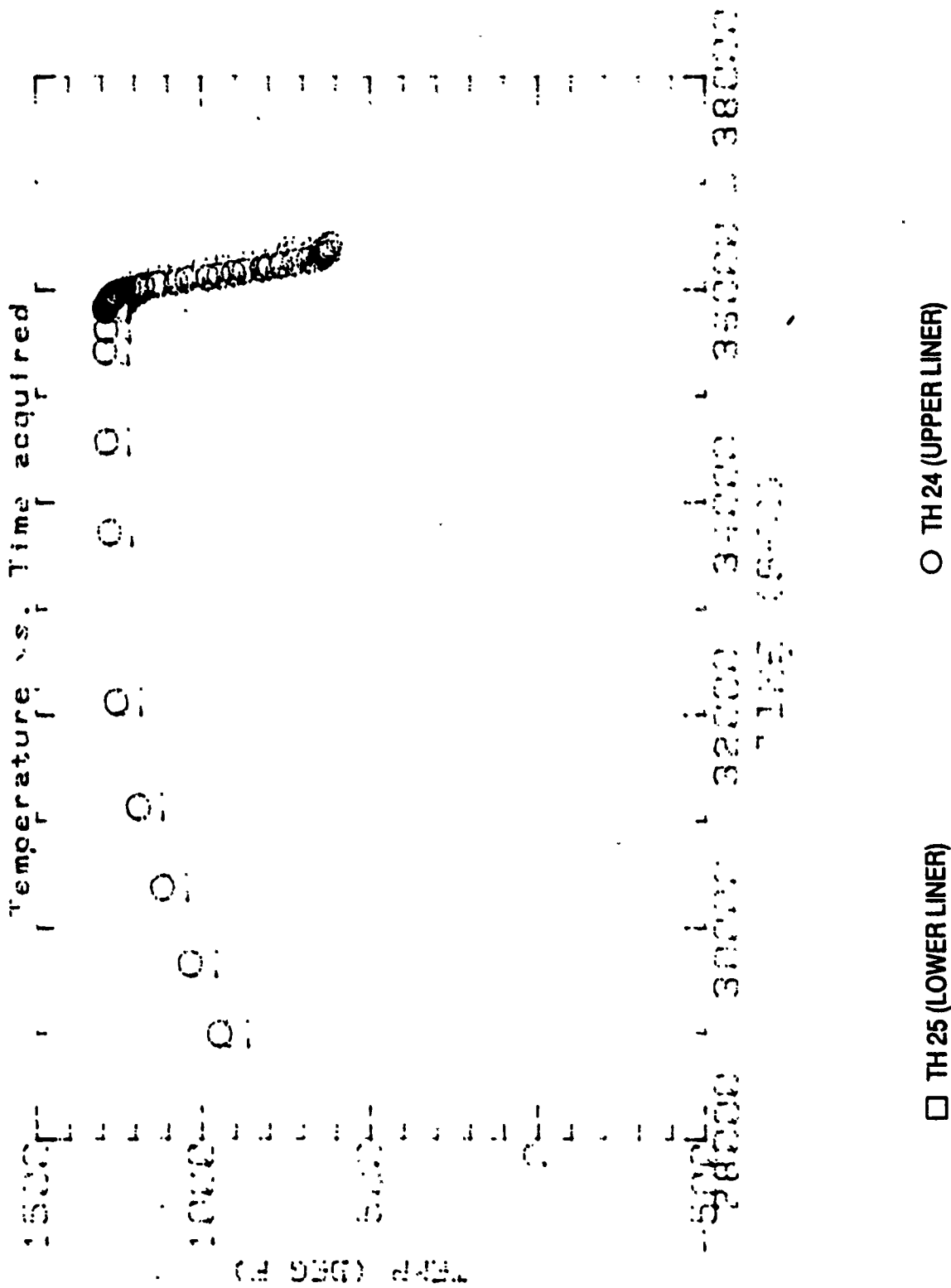


FIGURE 79. LOWER BED RADIAL TEMPERATURE DISTRIBUTION
FULL TEST



**FIGURE 80. LOWER BED RADIAL TEMPERATURE DISTRIBUTION
EXPANDED TIME SCALE DURING INJECTION**



**FIGURE 81. OUTSIDE LINER TEMPERATURES
FULL TEST**

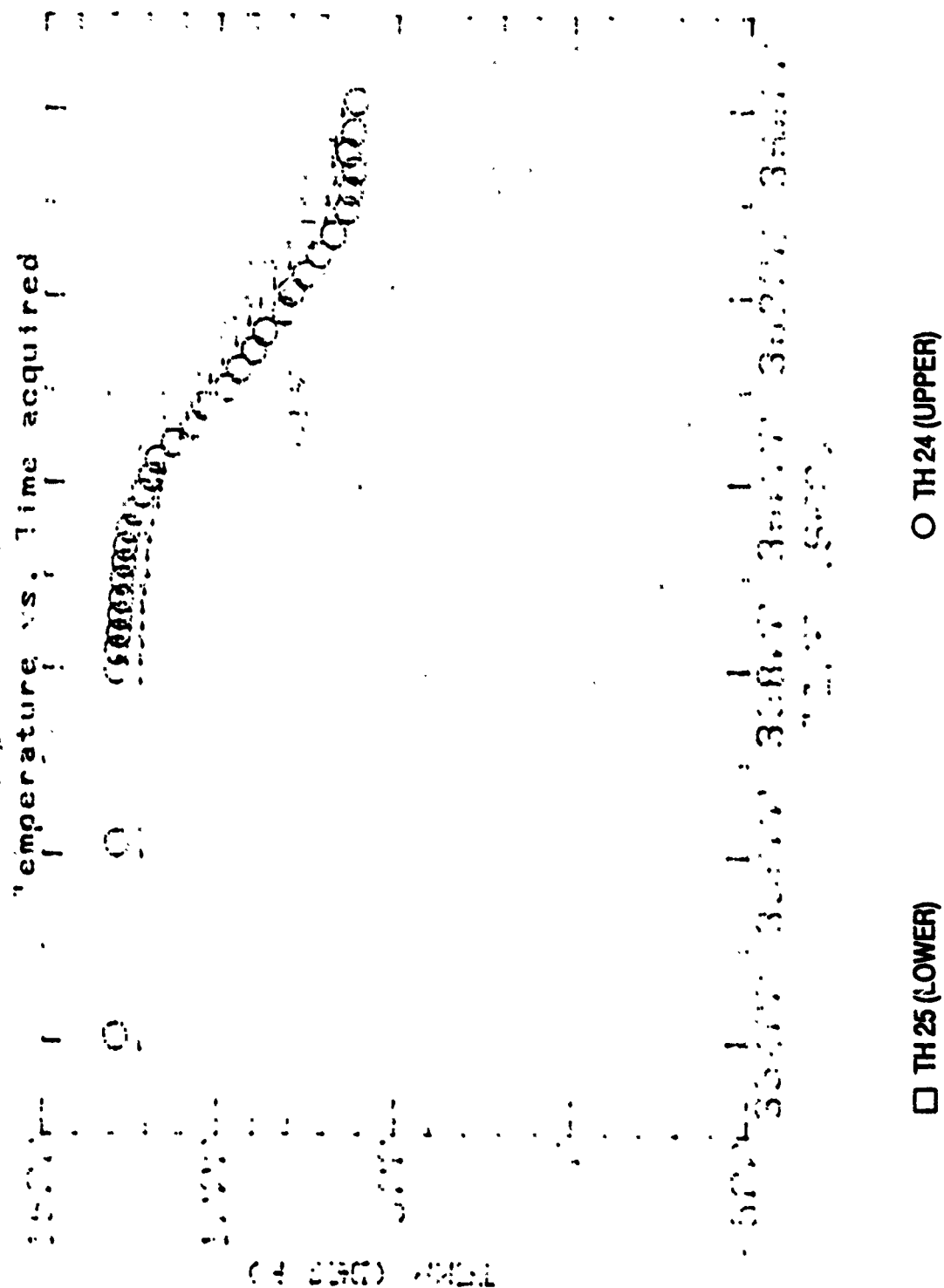


**FIGURE 82. OUTSIDE LINER TEMPERATURE
EXPANDED TIME SCALE DURING INJECTION**

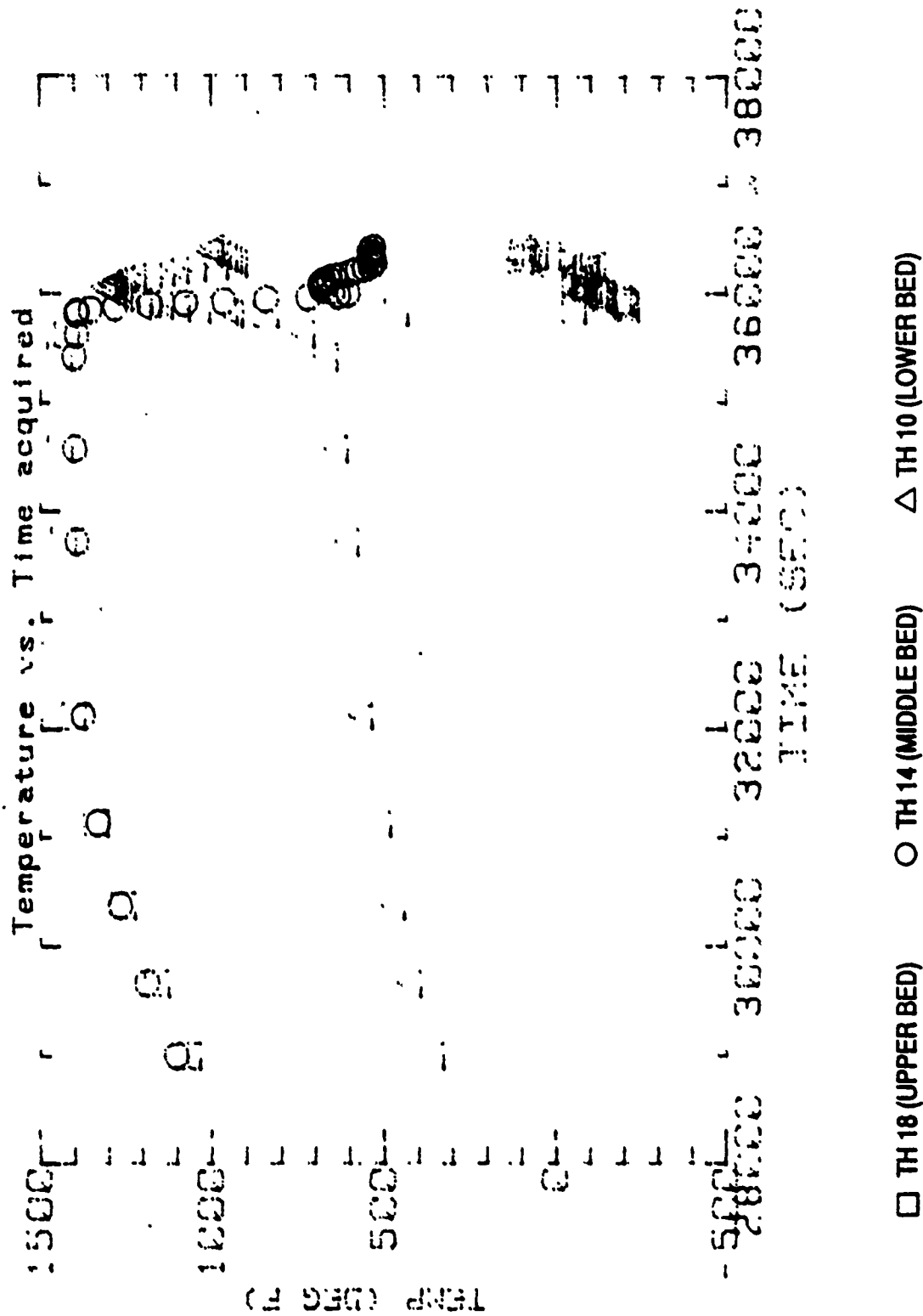


**FIGURE 83. AXIAL TEMPERATURE DISTRIBUTION
FULL TEST**

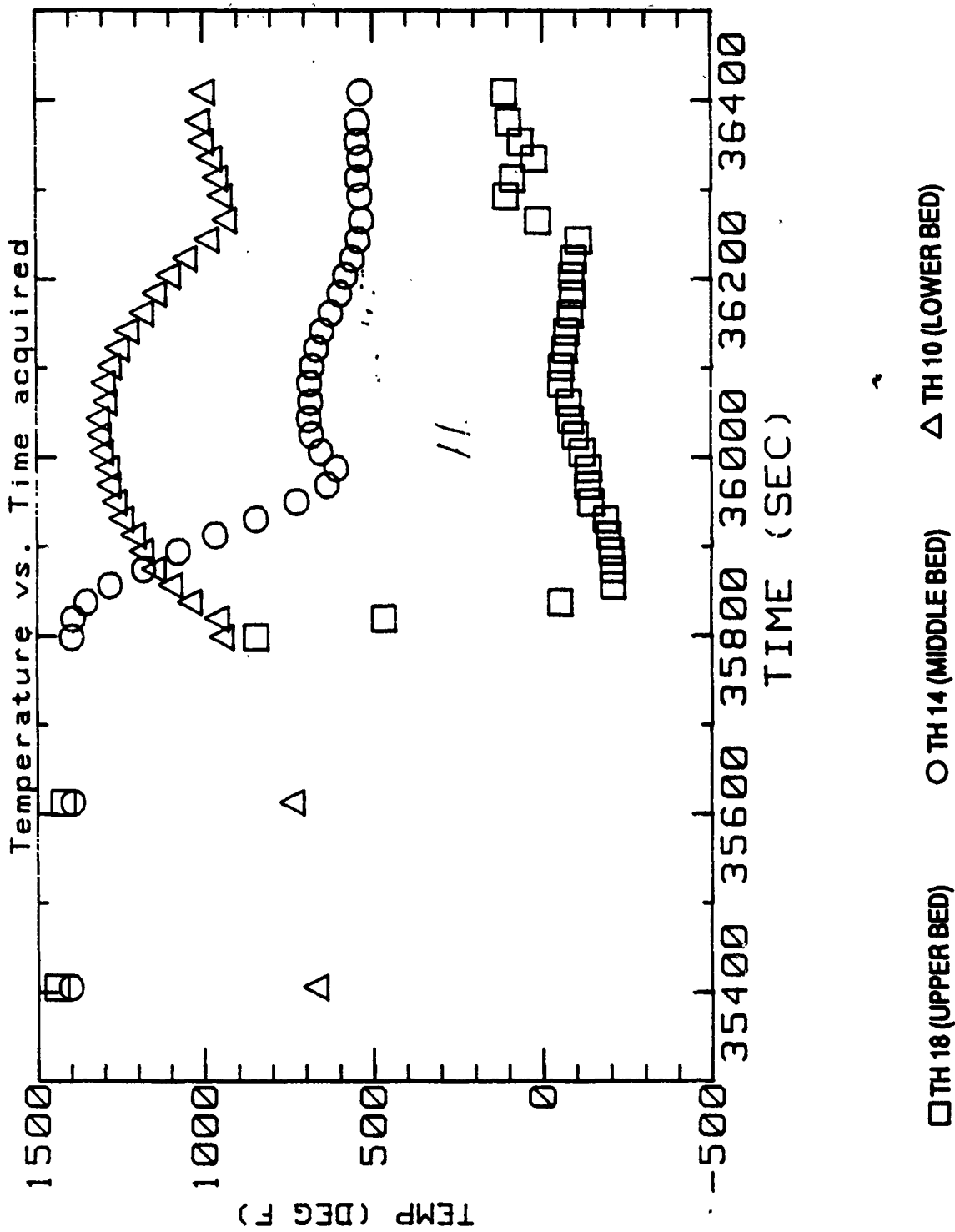


**FIGURE 84. AXIAL TEMPERATURE DISTRIBUTION
EXPANDED TIME SCALE DURING INJECTION**

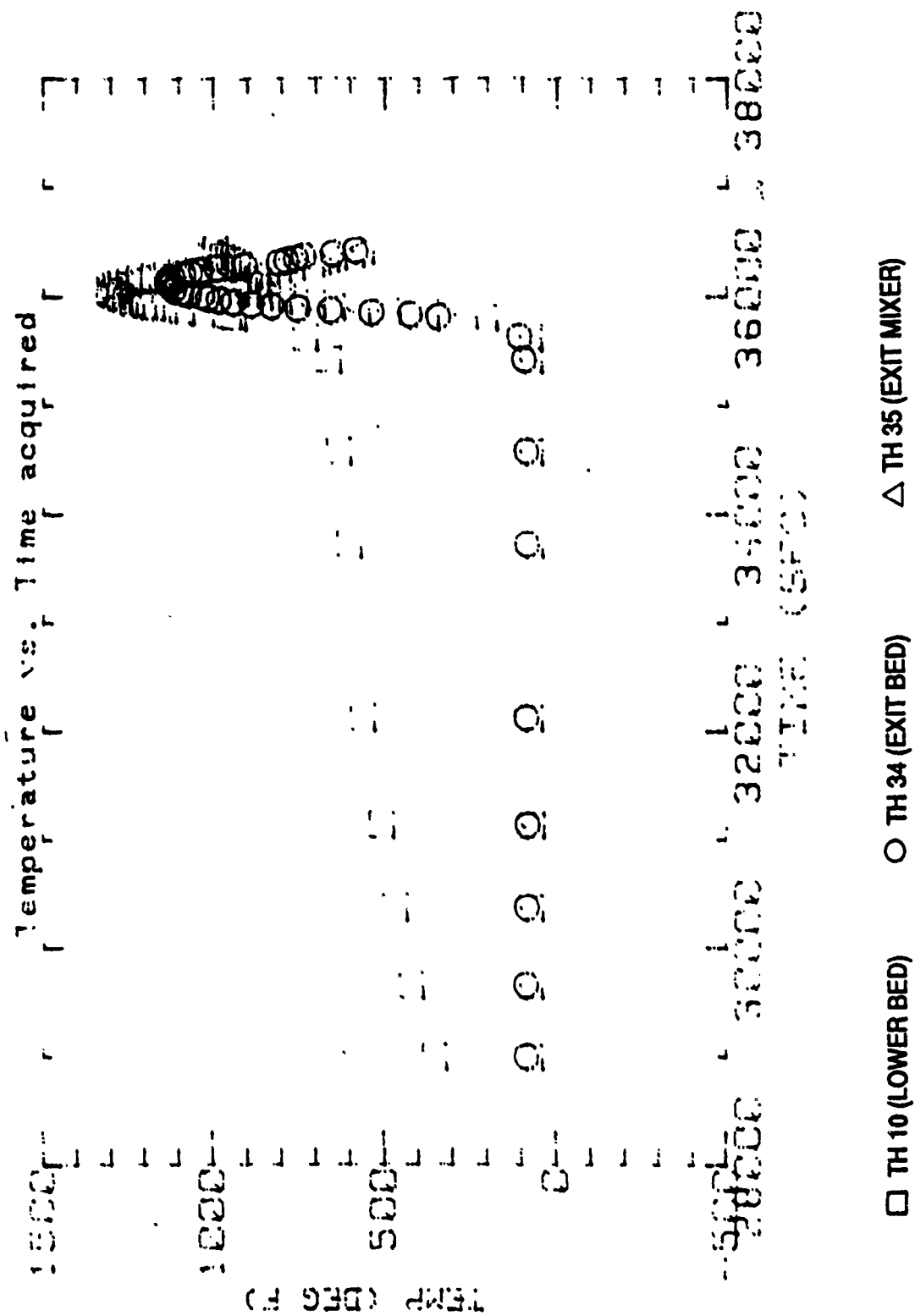
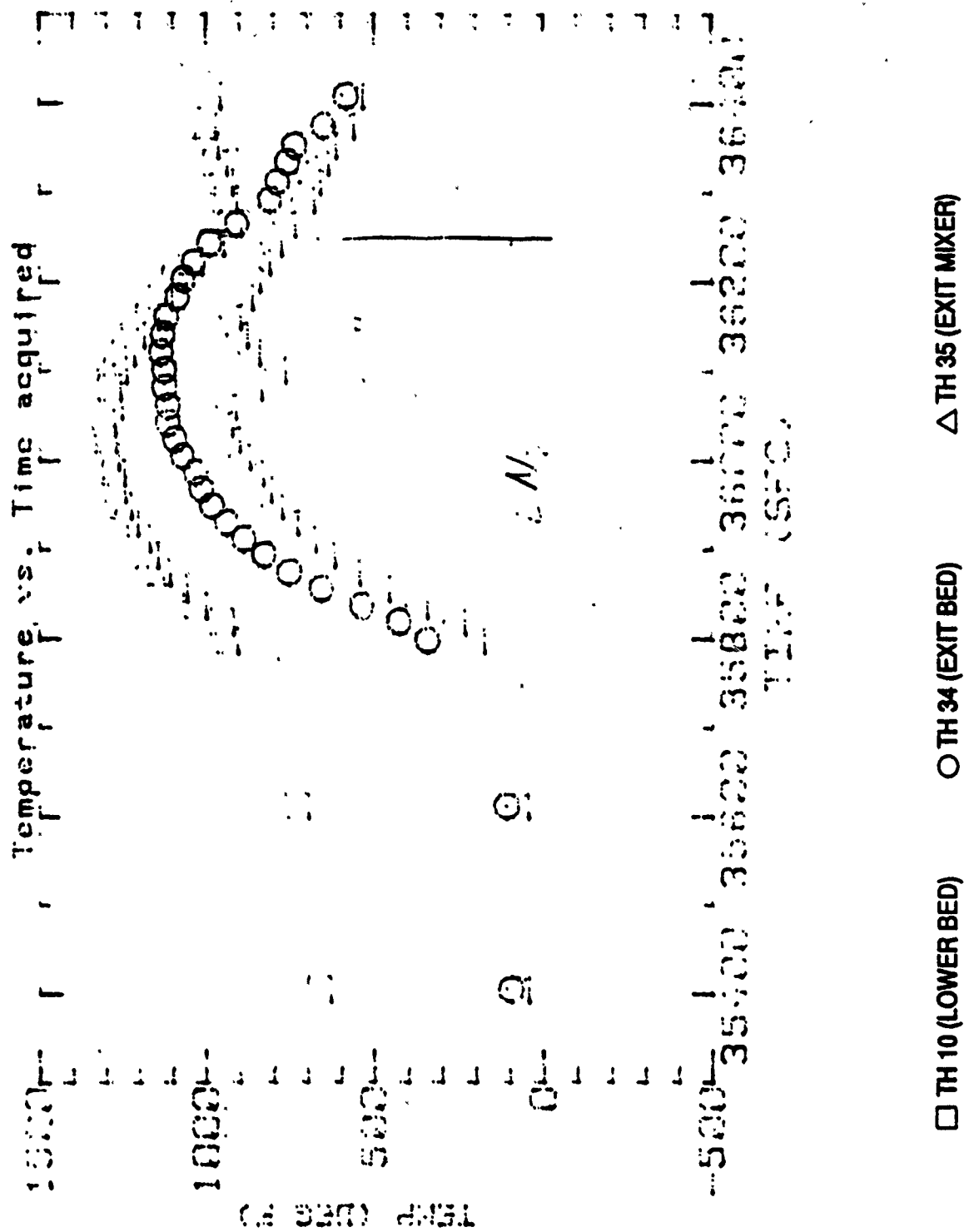


FIGURE 85. EXHAUST TEMPERATURES - FULL TEST



**FIGURE 86. EXHAUST TEMPERATURES
EXPANDED TIME SCALES DURING INJECTION**

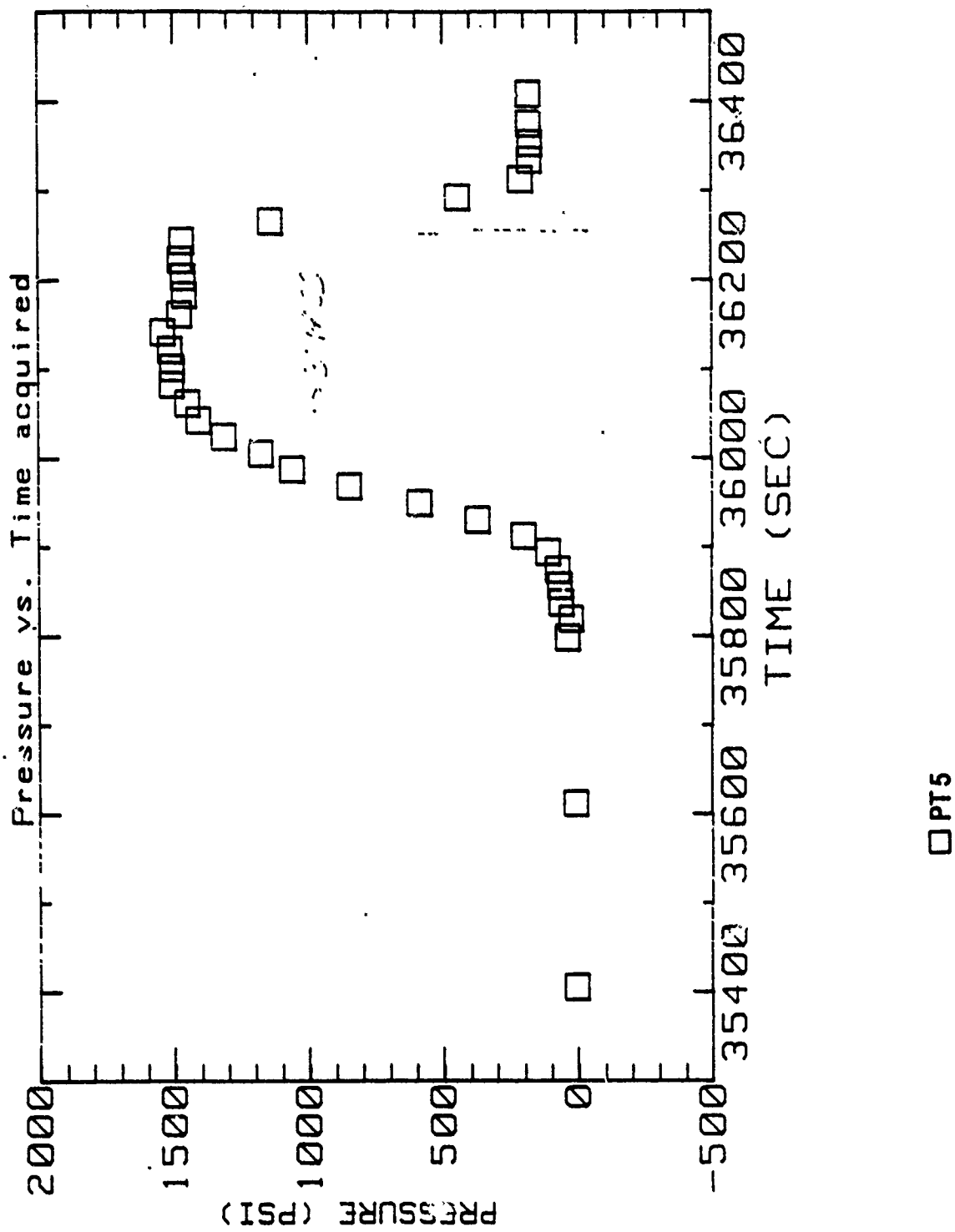


FIGURE 87. BED PRESSURE
EXPANDED TIME SCALE DURING INJECTION

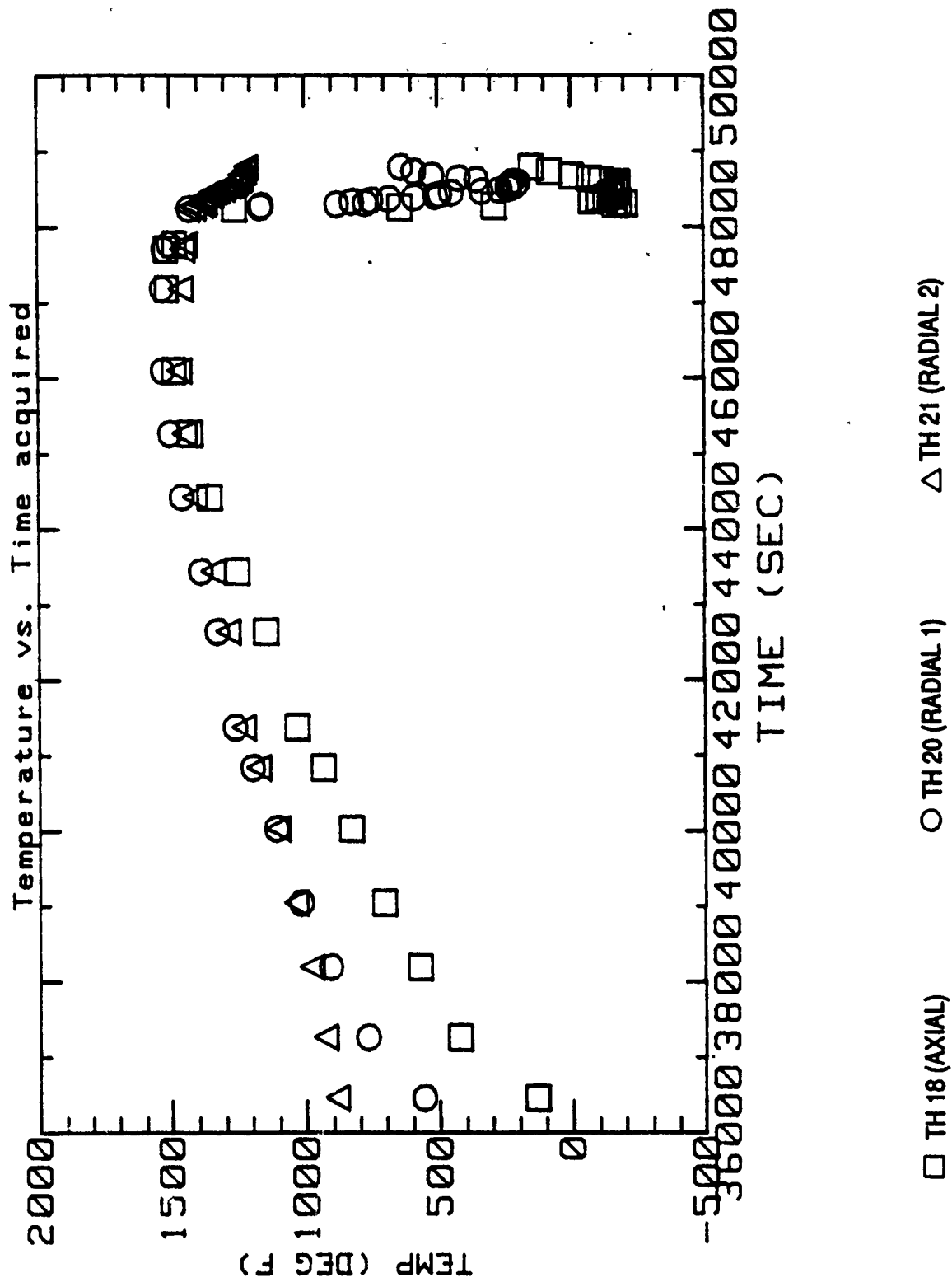
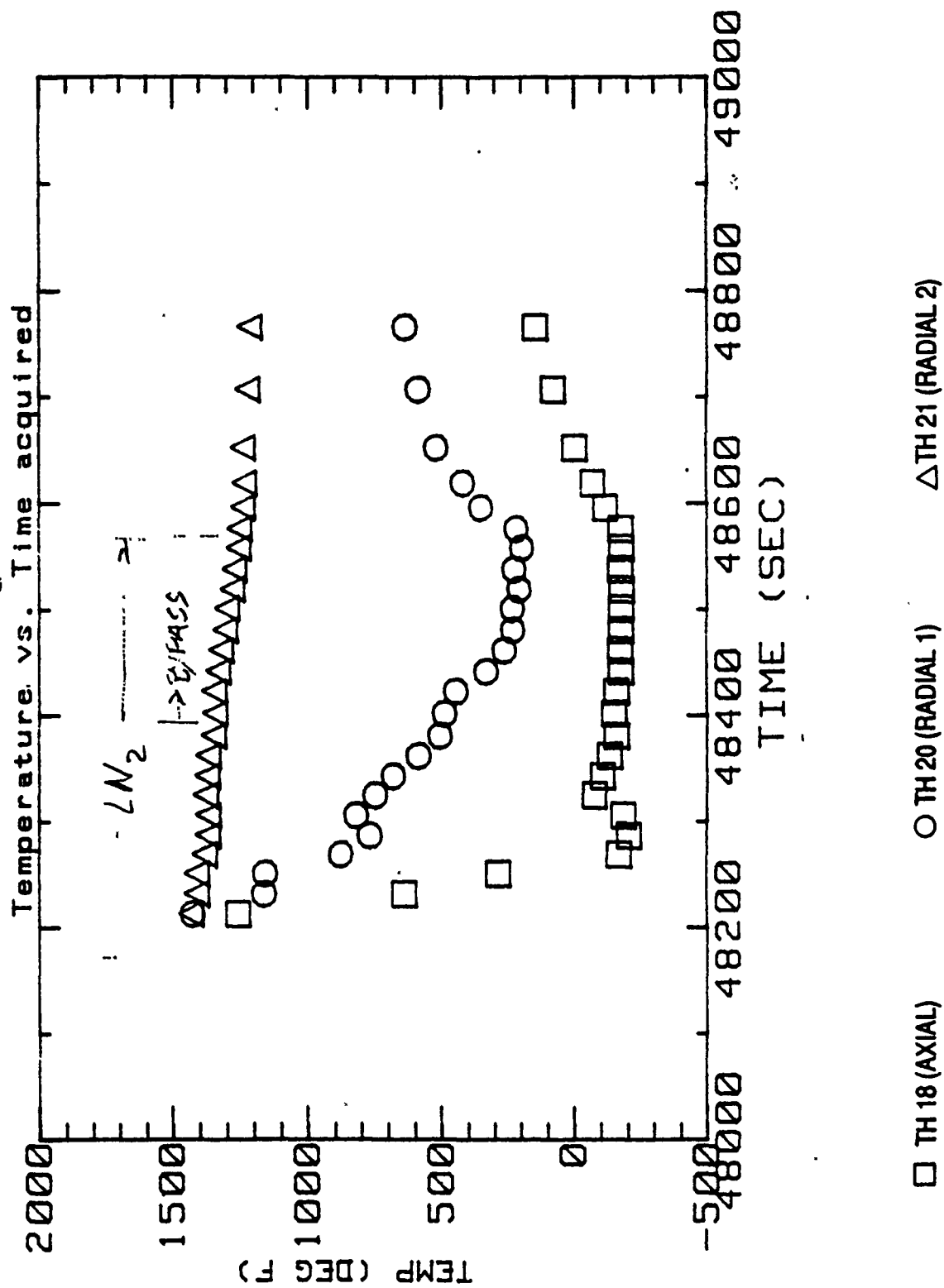
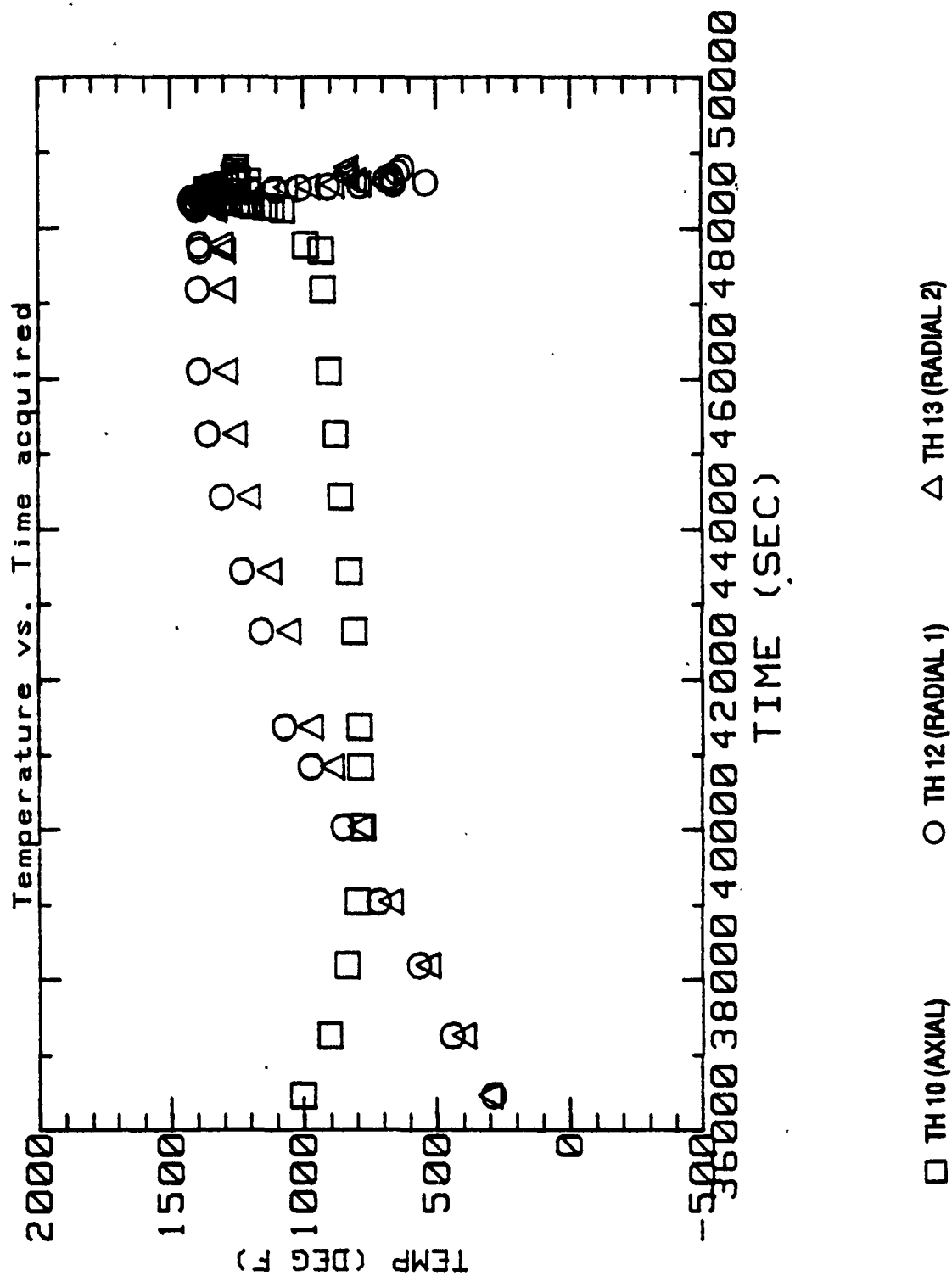


FIGURE 88. UPPER BED RADIAL TEMPERATURE DISTRIBUTION
FUEL TEST



**FIGURE 89. UPPER BED RADIAL TEMPERATURE DISTRIBUTION
EXPANDED TIME SCALE DURING INJECTION**



**FIGURE 90. LOWER BED RADIAL TEMPERATURE DISTRIBUTION
FULL TEST**

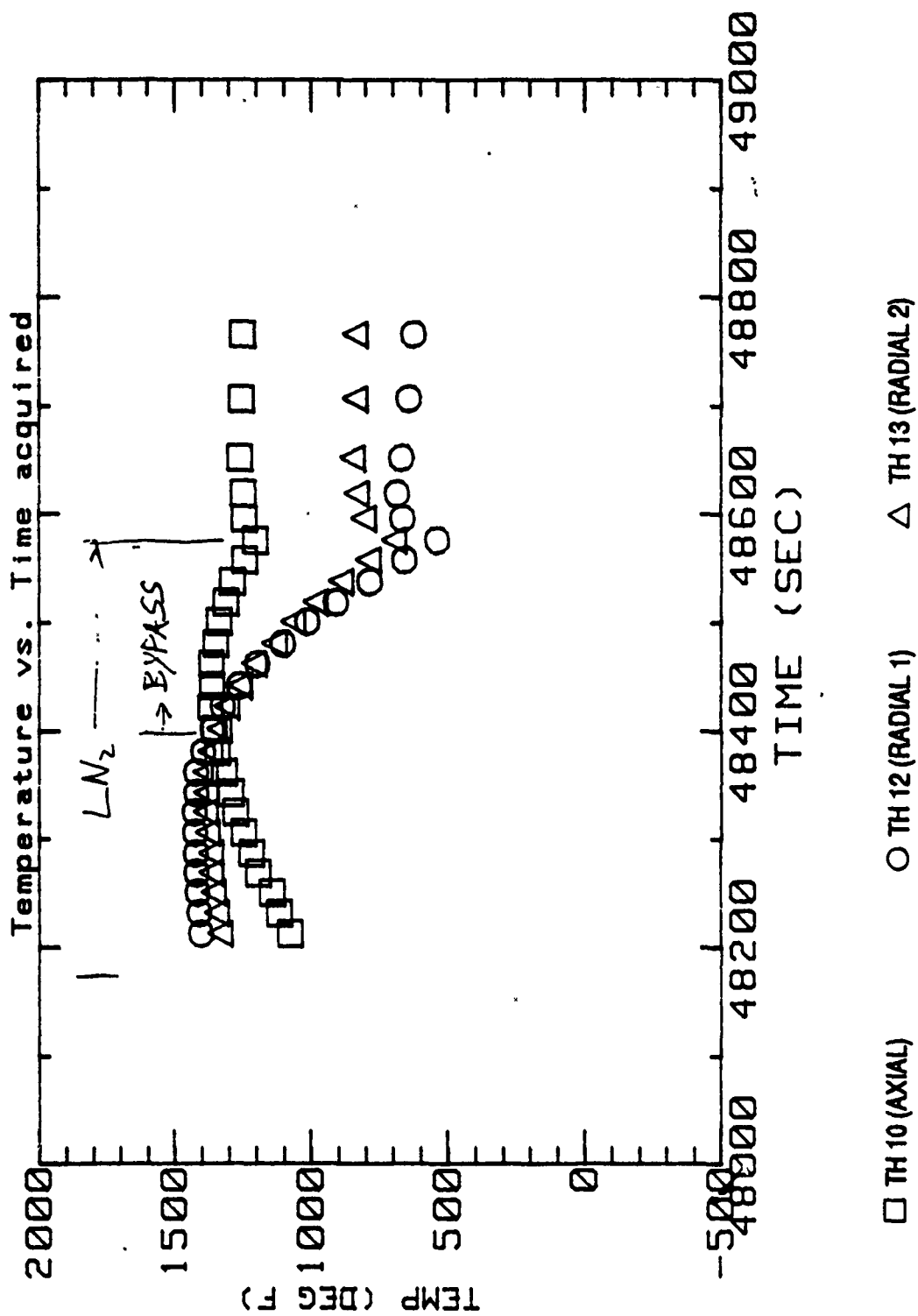


FIGURE 91. LOWER BED RADIAL TEMPERATURE DISTRIBUTION
EXPANDED TIME SCALE DURING INJECTION

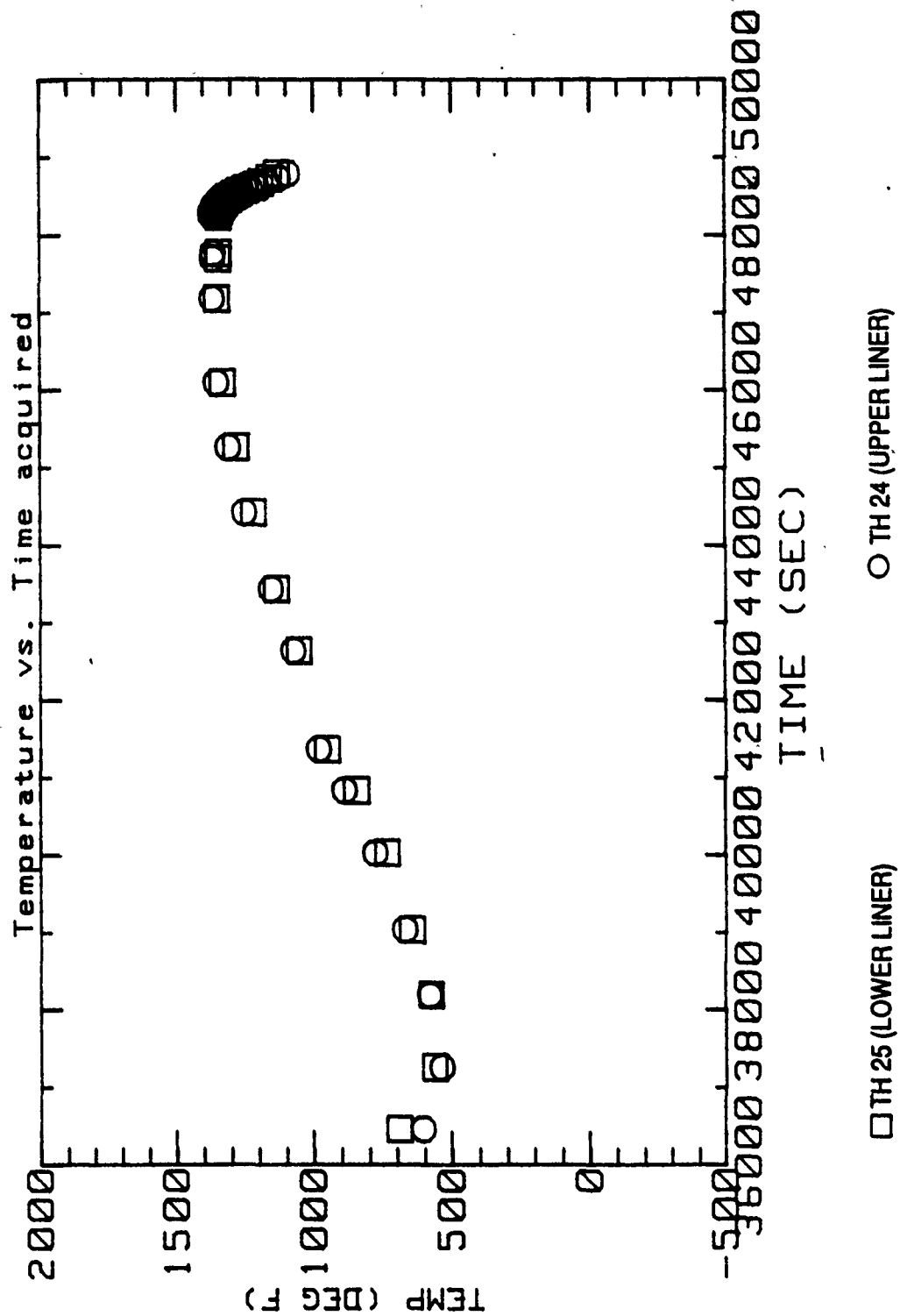


FIGURE 92. OUTSIDE LINER TEMPERATURES
FULL TEST

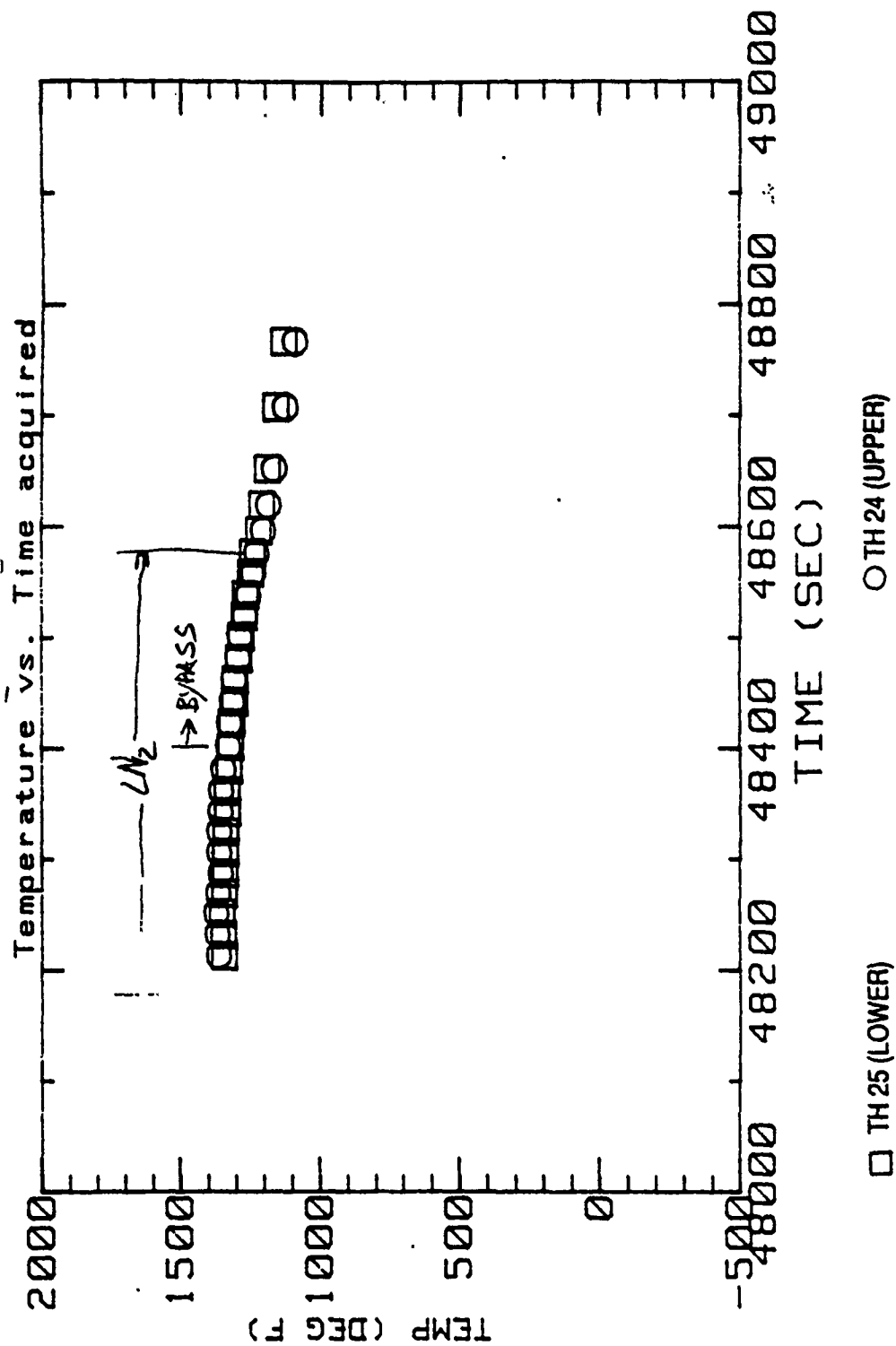
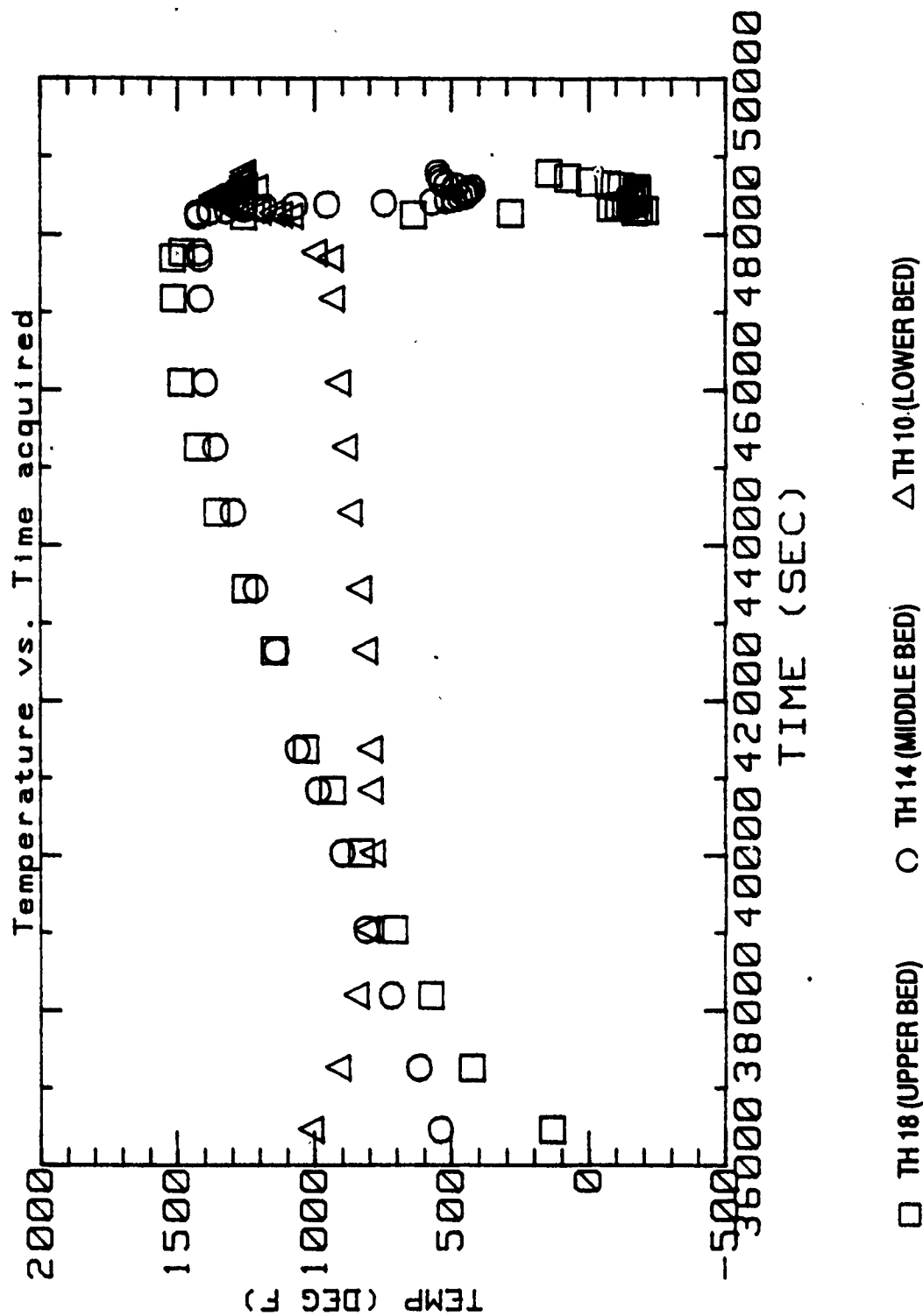


FIGURE 93. OUTSIDE LINER TEMPERATURE
EXPANDED TIME SCALE DURING INJECTION



**FIGURE 94. AXIAL TEMPERATURE DISTRIBUTION
FULL TEST**

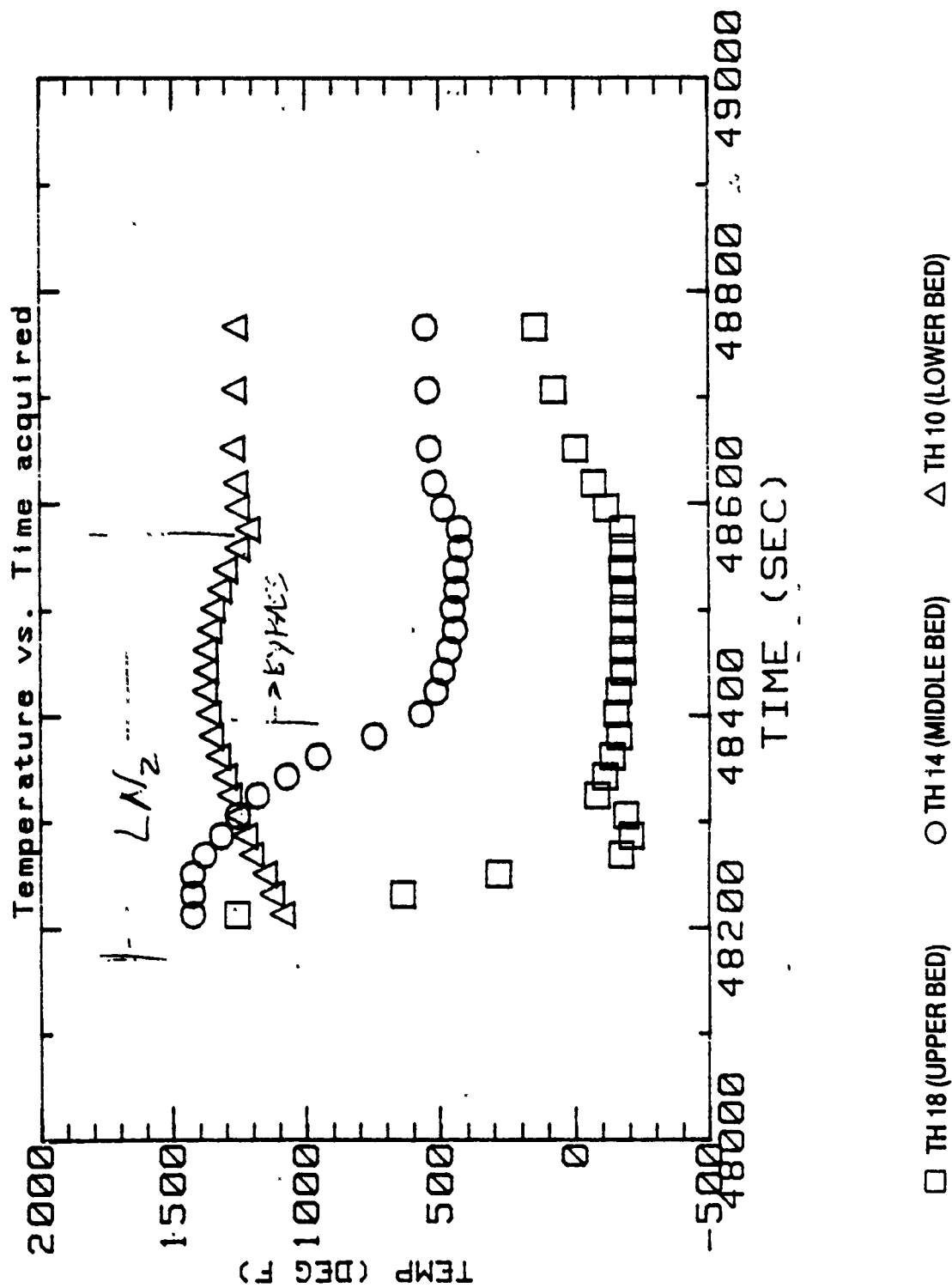


FIGURE 95. AXIAL TEMPERATURE DISTRIBUTION
EXPANDED TIME SCALE DURING INJECTION

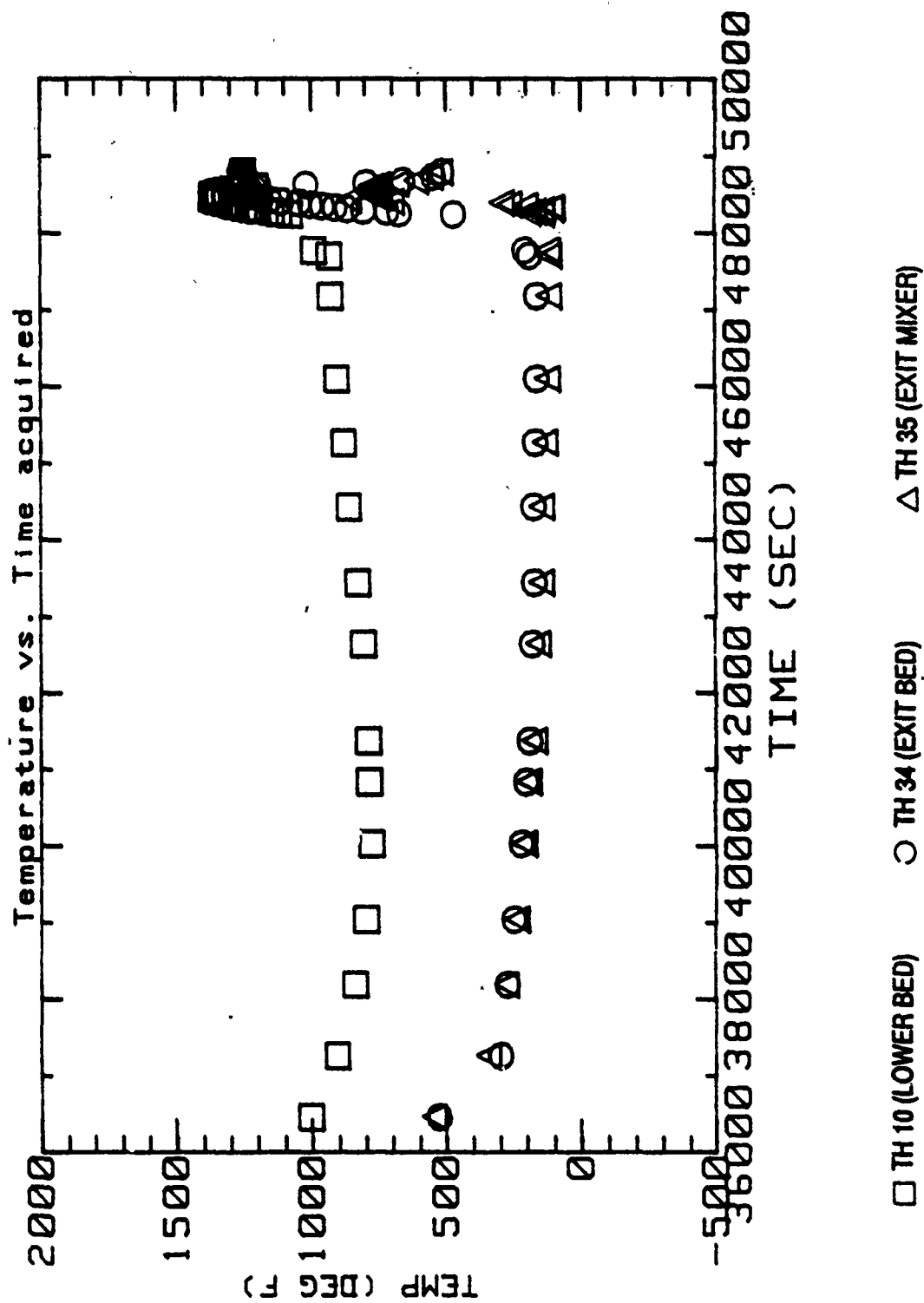
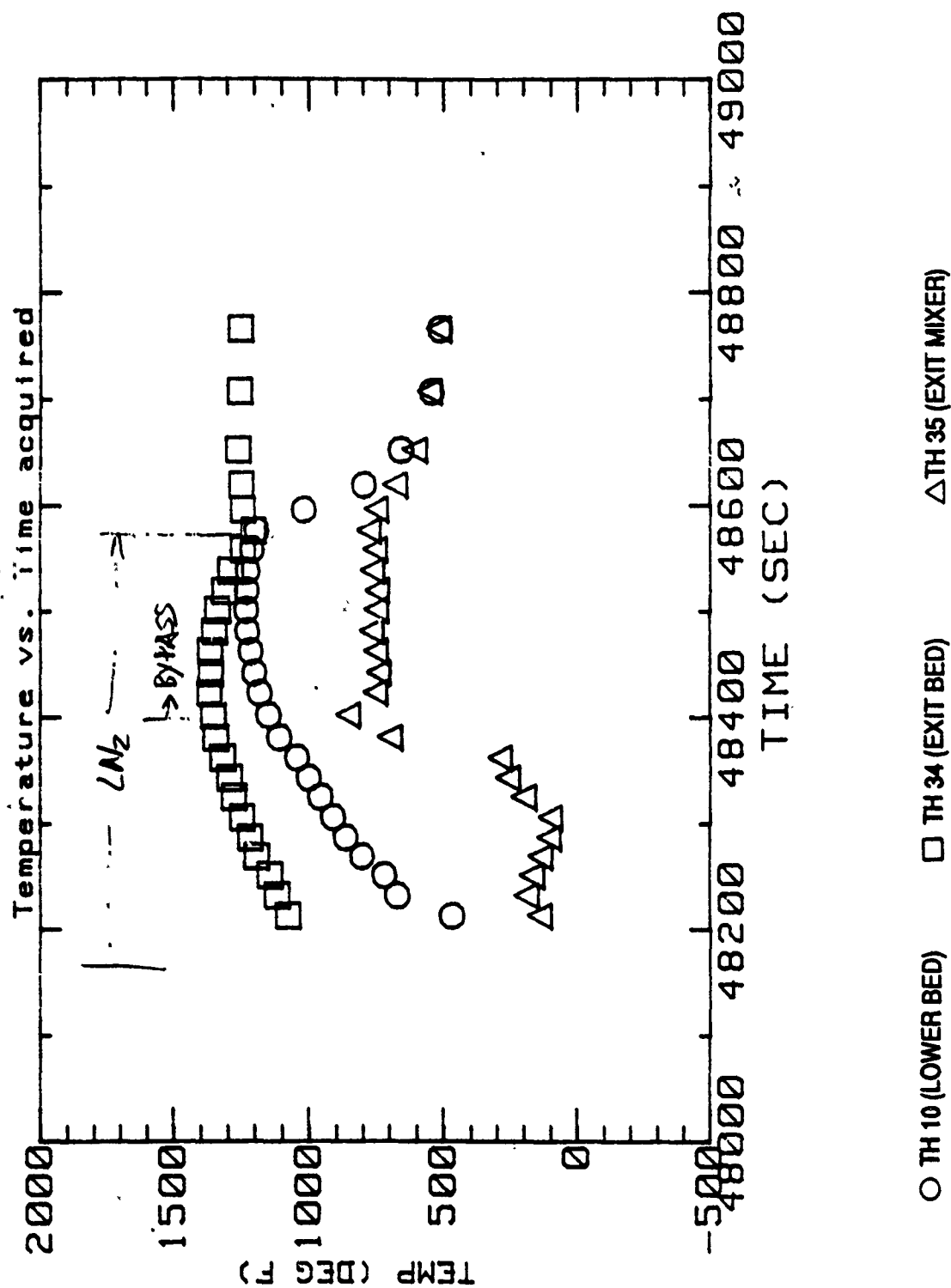


FIGURE 96. EXHAUST TEMPERATURES - FULL TEST



**FIGURE 97. EXHAUST TEMPERATURES
EXPANDED TIME SCALES DURING INJECTION**

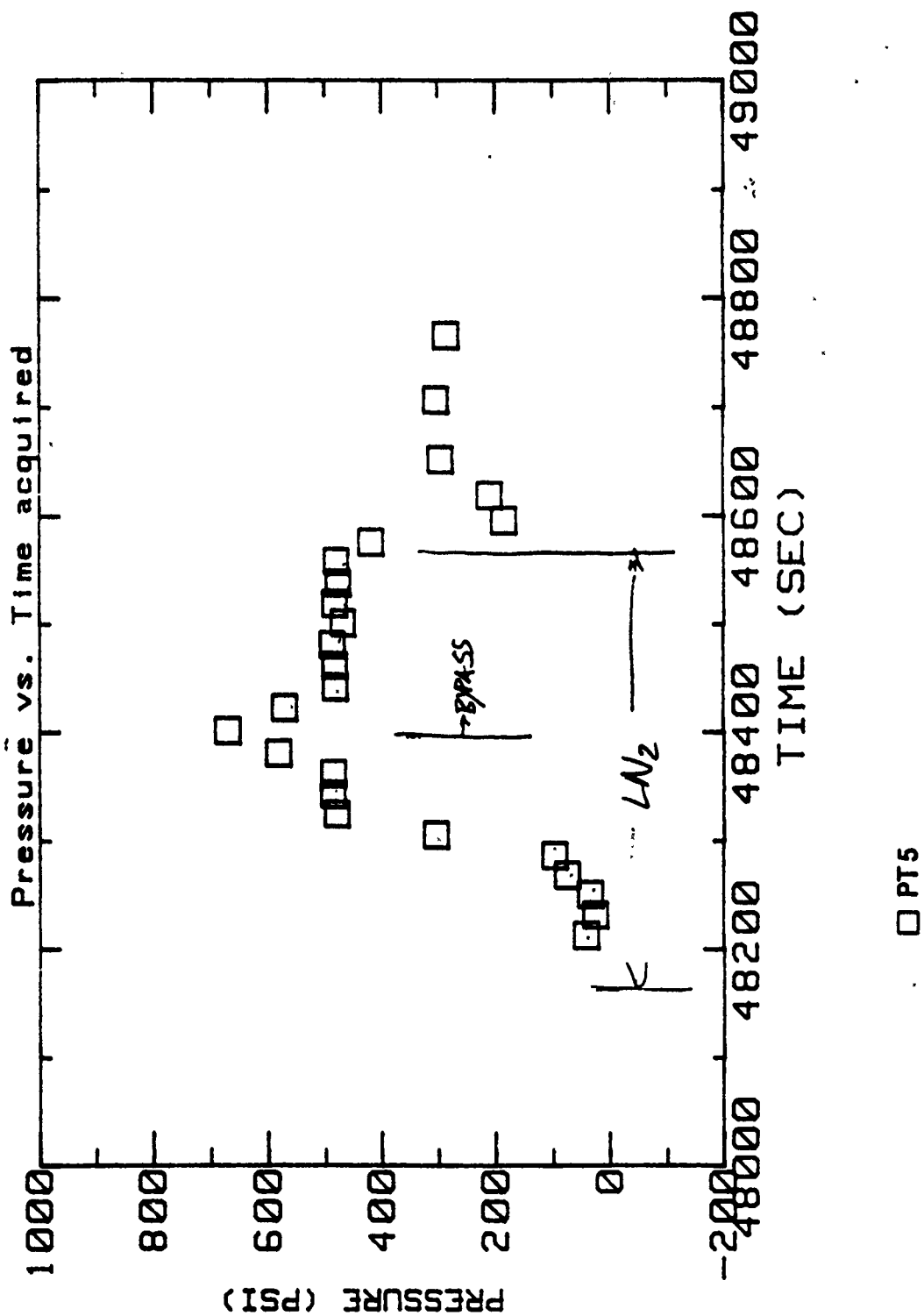
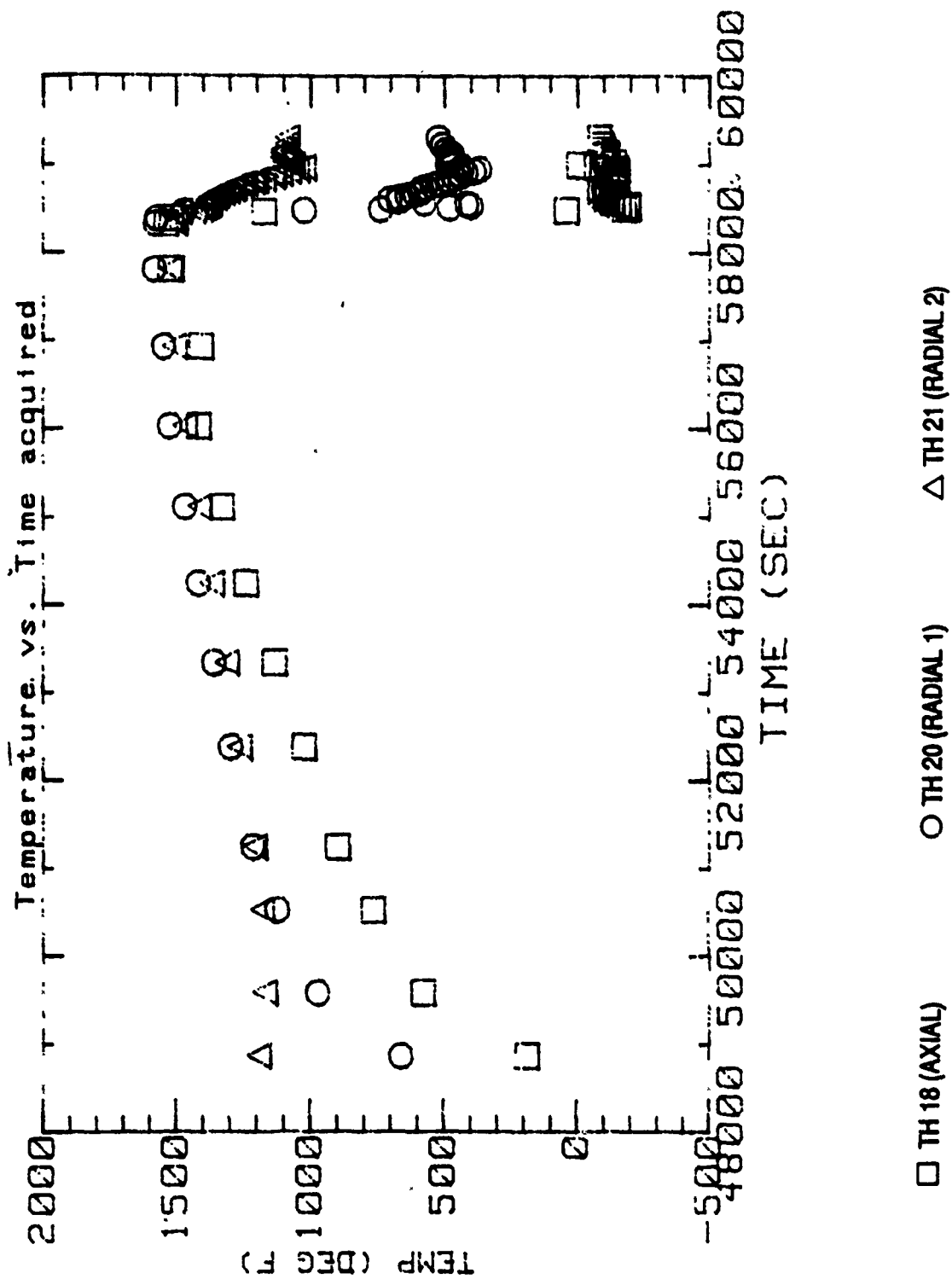


FIGURE 98. BED PRESSURE
EXPANDED TIME SCALE DURING INJECTION



**FIGURE 99. UPPER BED RADIAL TEMPERATURE DISTRIBUTION
FULL TEST**

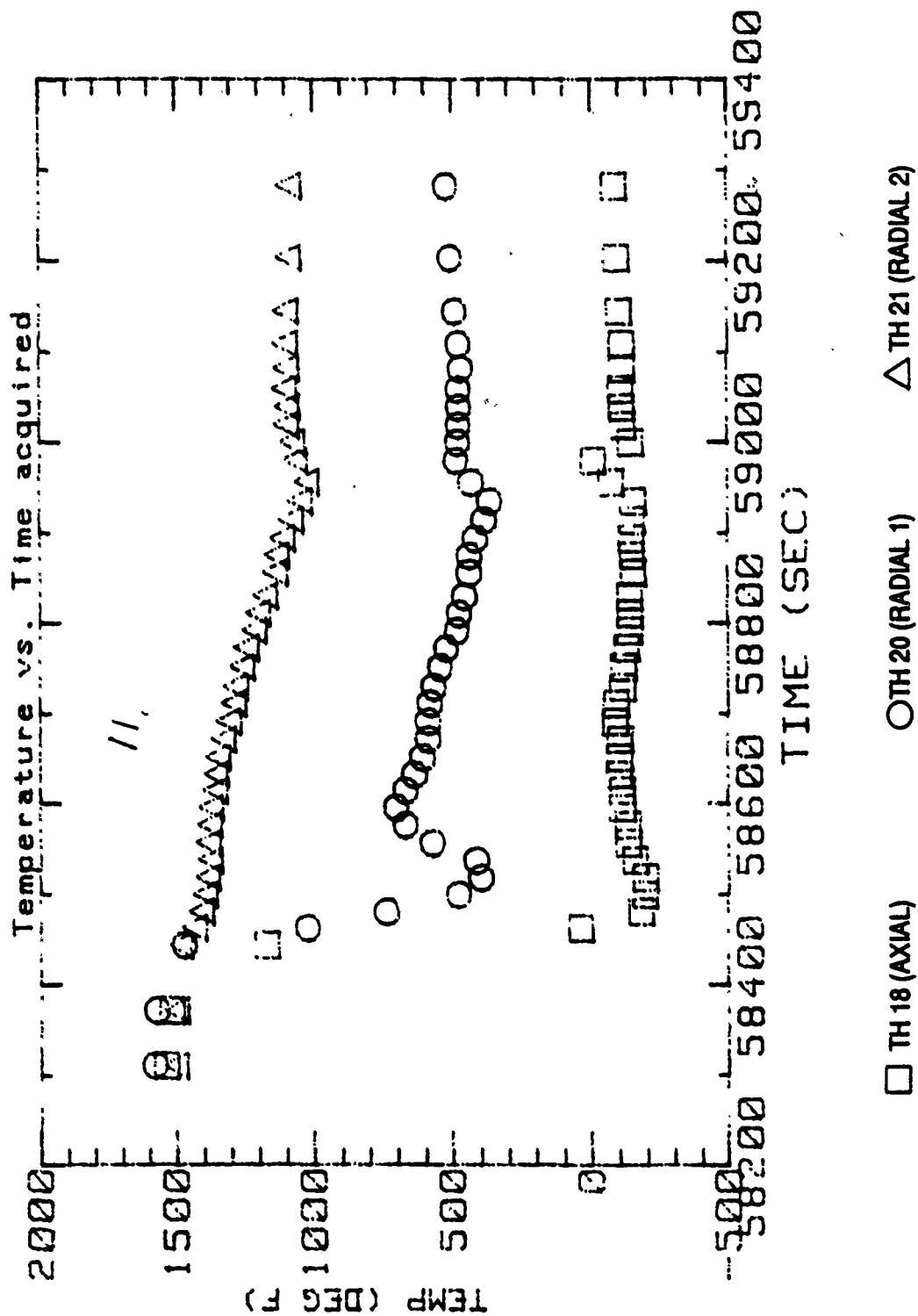


FIGURE 100. UPPER BED RADIAL TEMPERATURE DISTRIBUTION
EXPANDED TIME SCALE DURING INJECTION

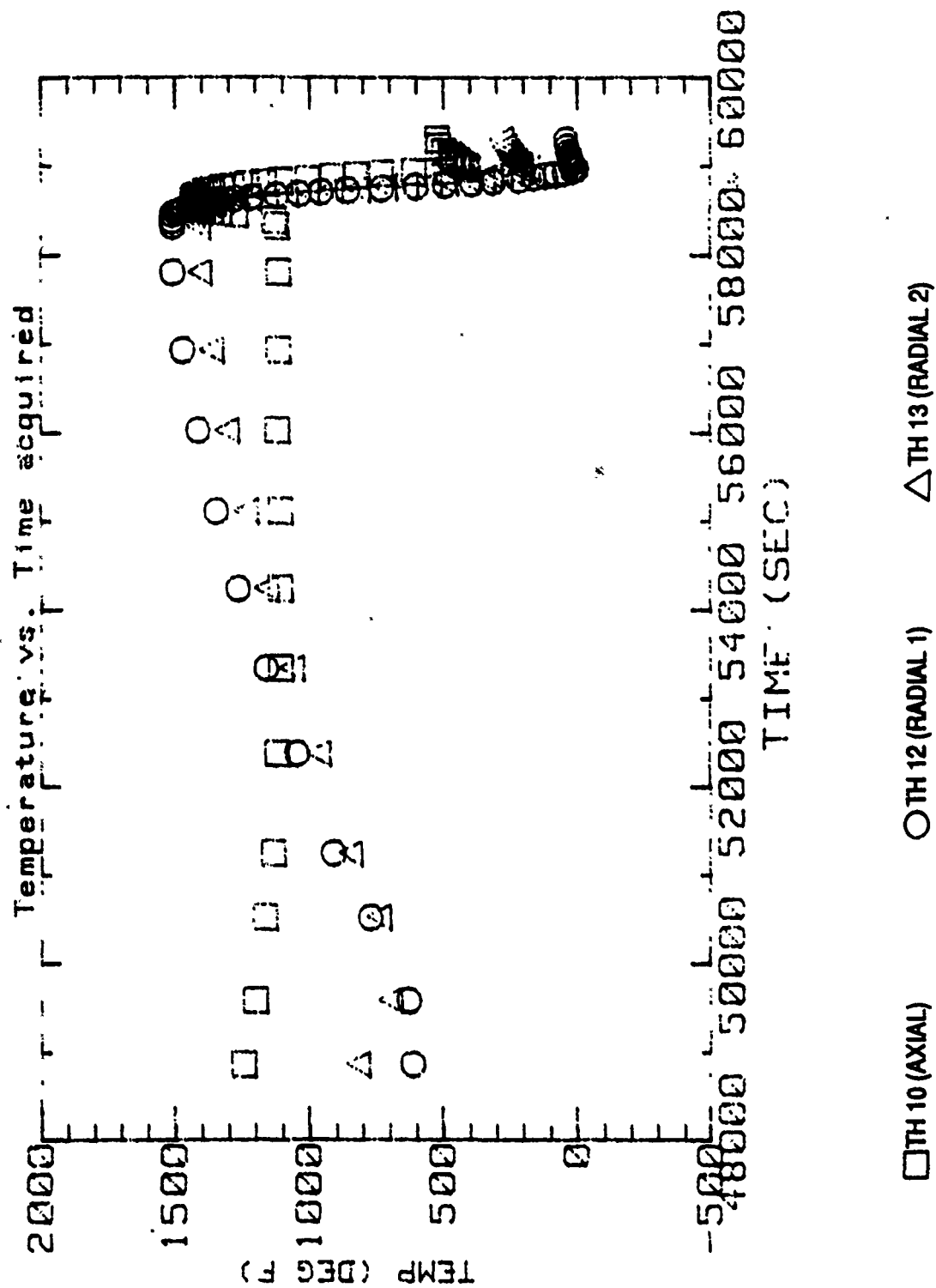


FIGURE 101. LOWER BED RADIAL TEMPERATURE DISTRIBUTION
FULL TEST

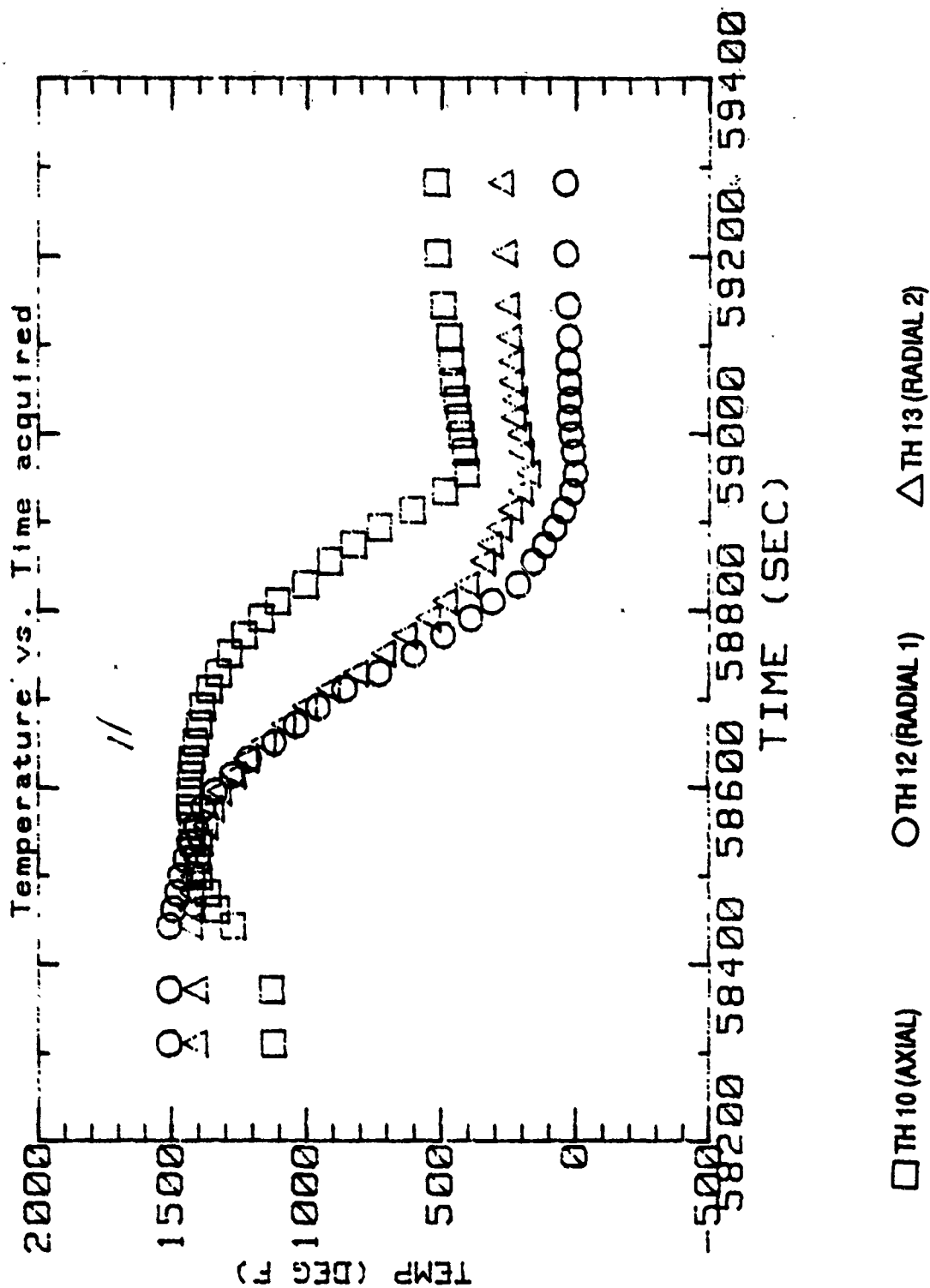


FIGURE 102. LOWER BED RADIAL TEMPERATURE DISTRIBUTION
EXPANDED TIME SCALE DURING INJECTION

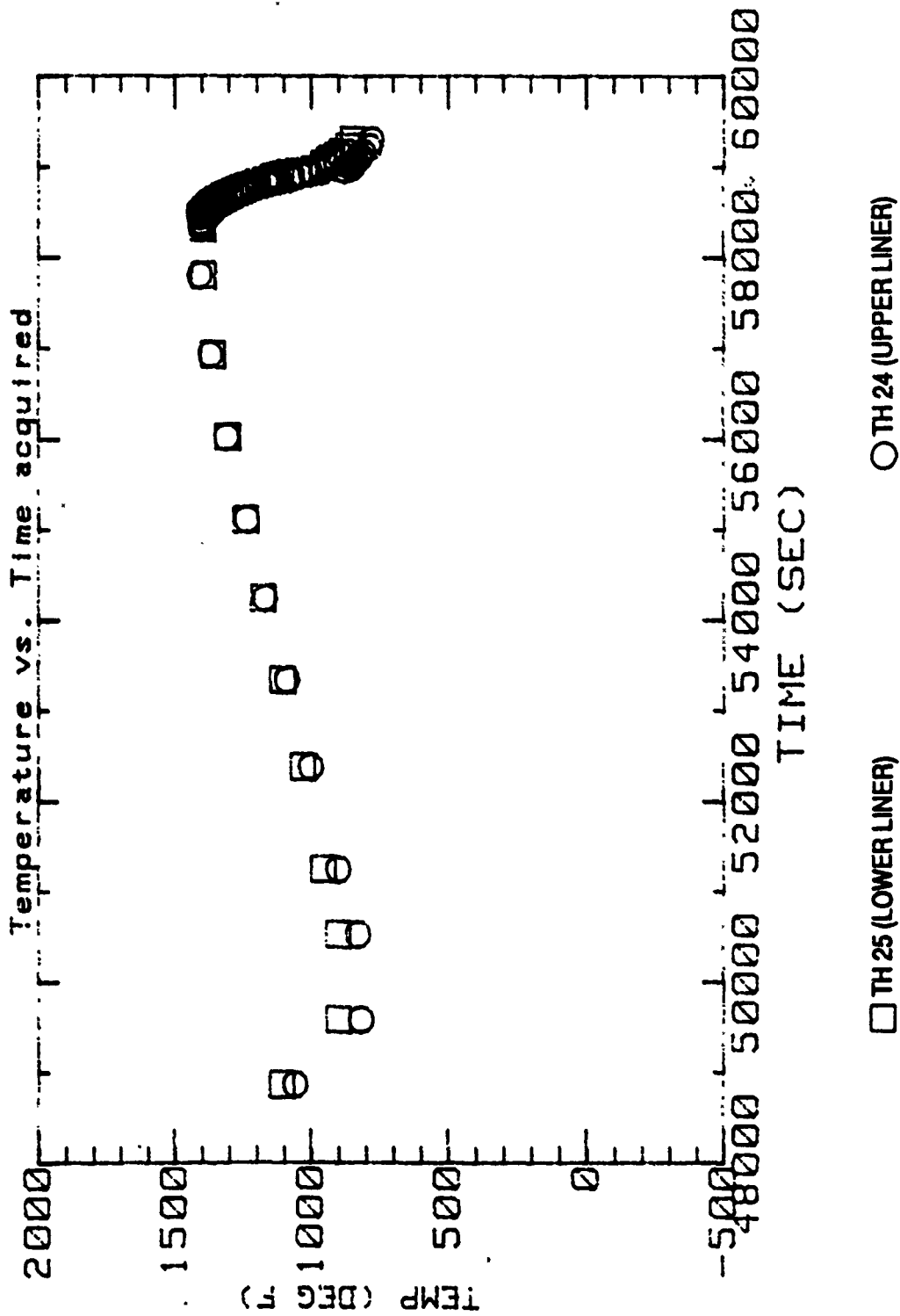


FIGURE 103. OUTSIDE LINER TEMPERATURES
FULL TEST

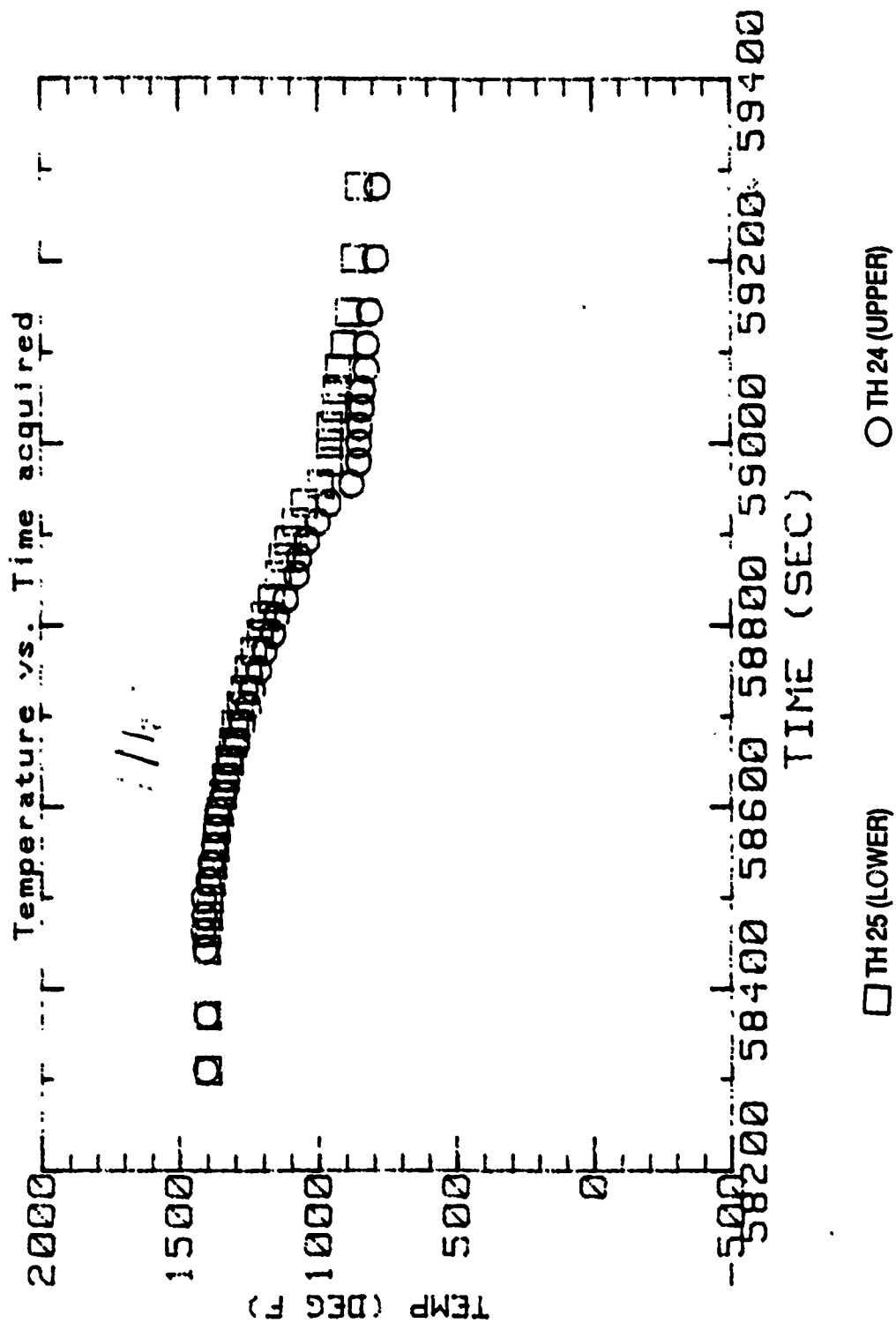
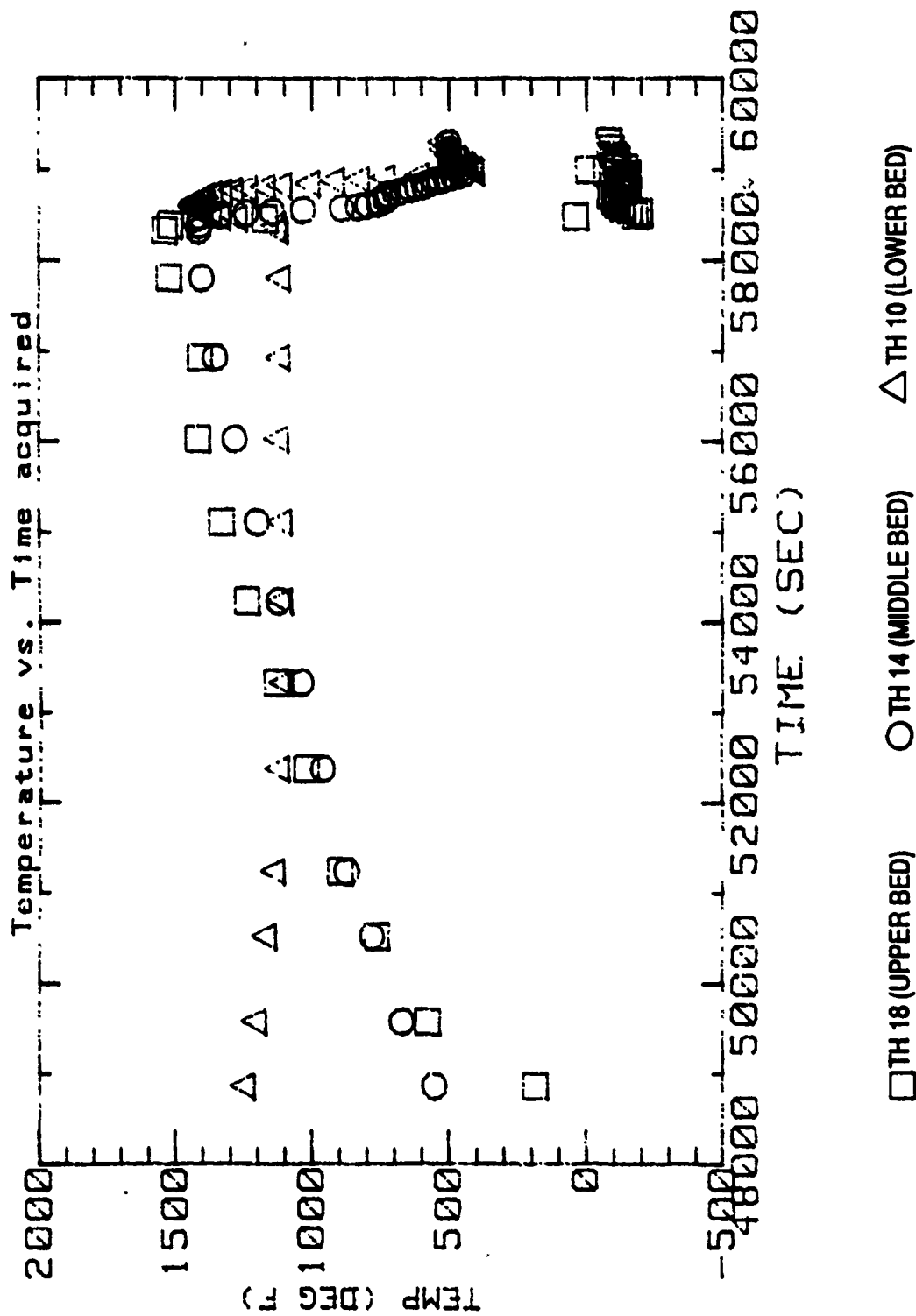


FIGURE 104. OUTSIDE LINER TEMPERATURE
EXPANDED TIME SCALE DURING INJECTION



**FIGURE 105. AXIAL TEMPERATURE DISTRIBUTION
FULL TEST**

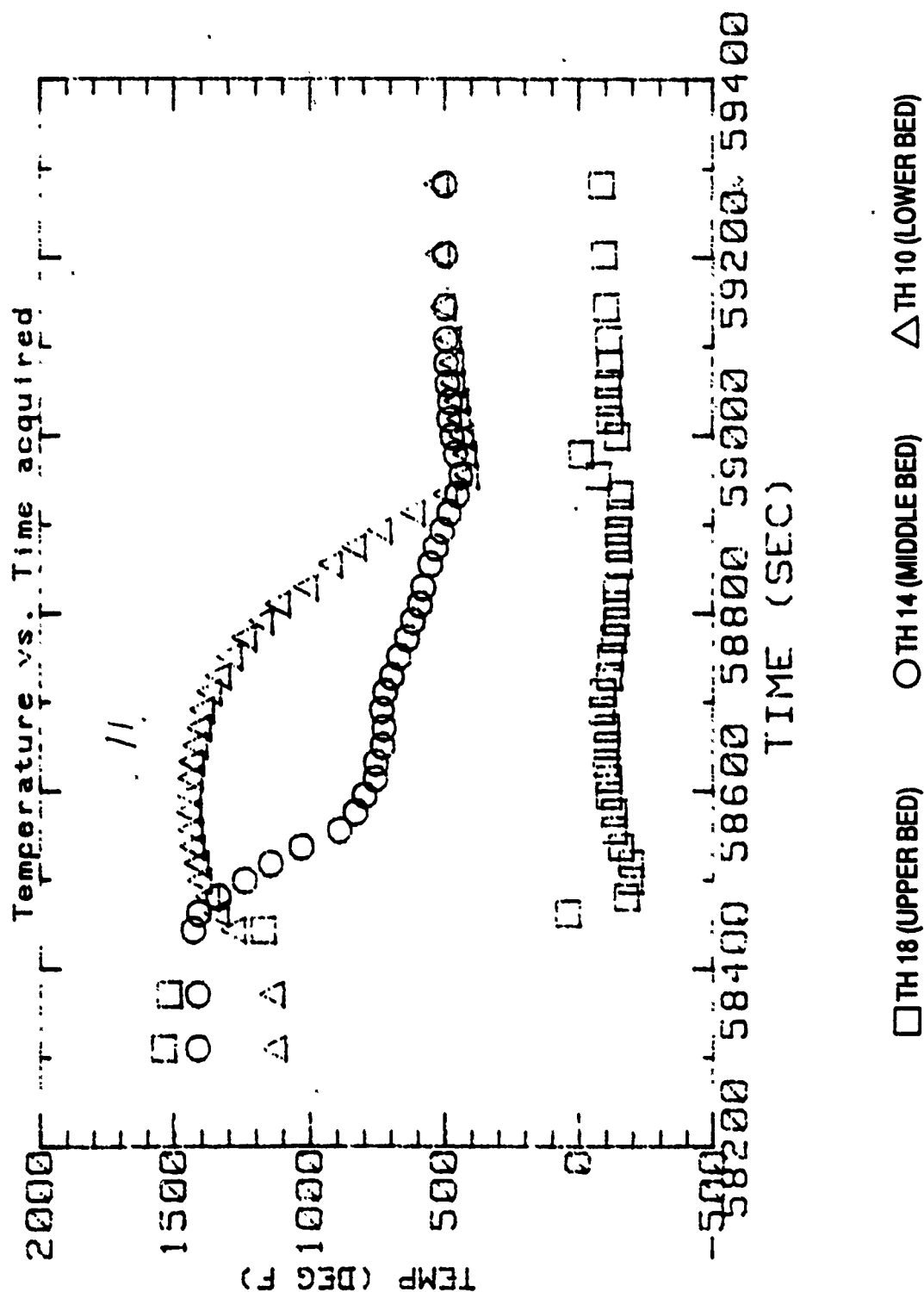


FIGURE 106. AXIAL TEMPERATURE DISTRIBUTION
EXPANDED TIME SCALE DURING INJECTION

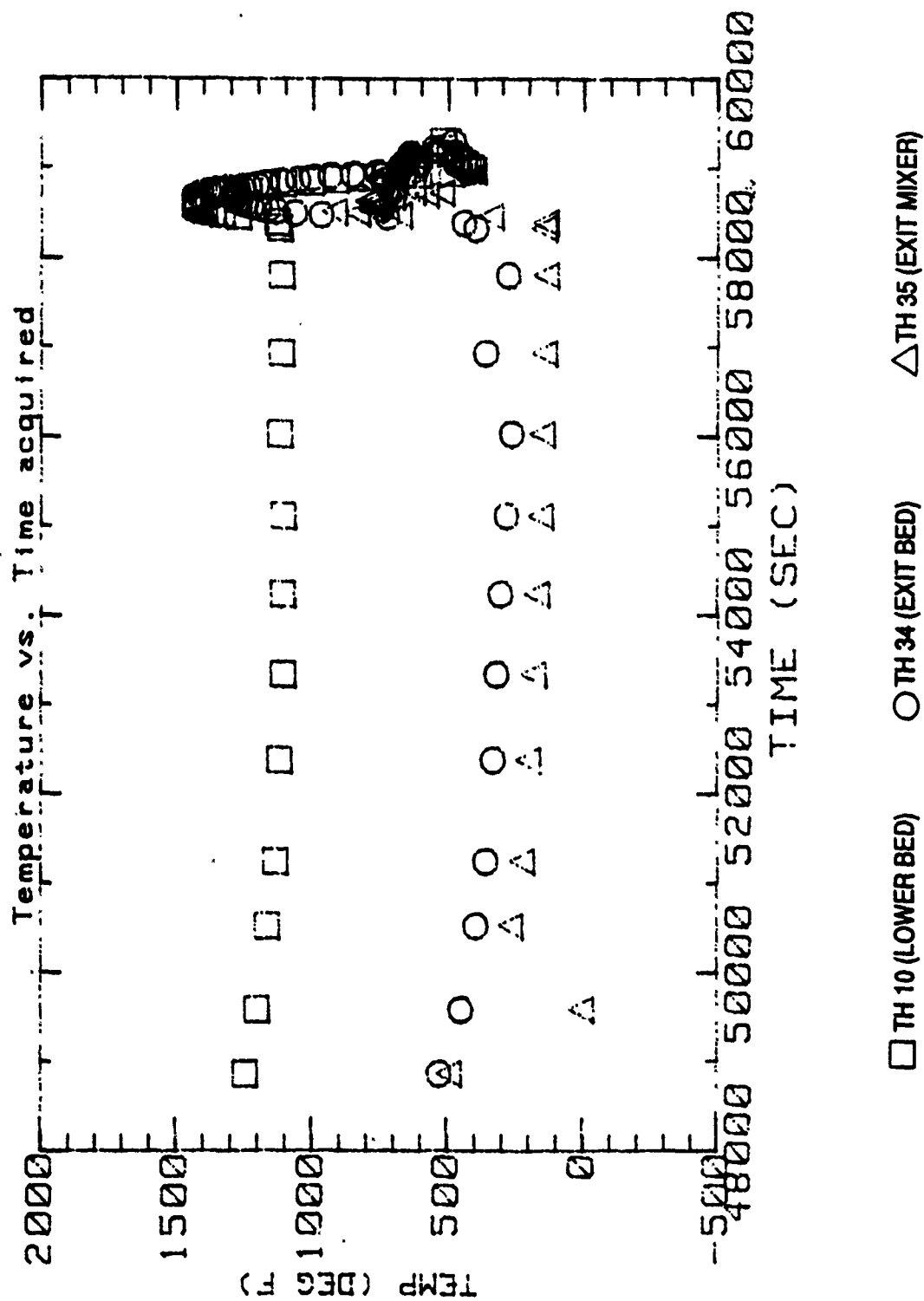


FIGURE 107. EXHAUST TEMPERATURES - FULL TEST

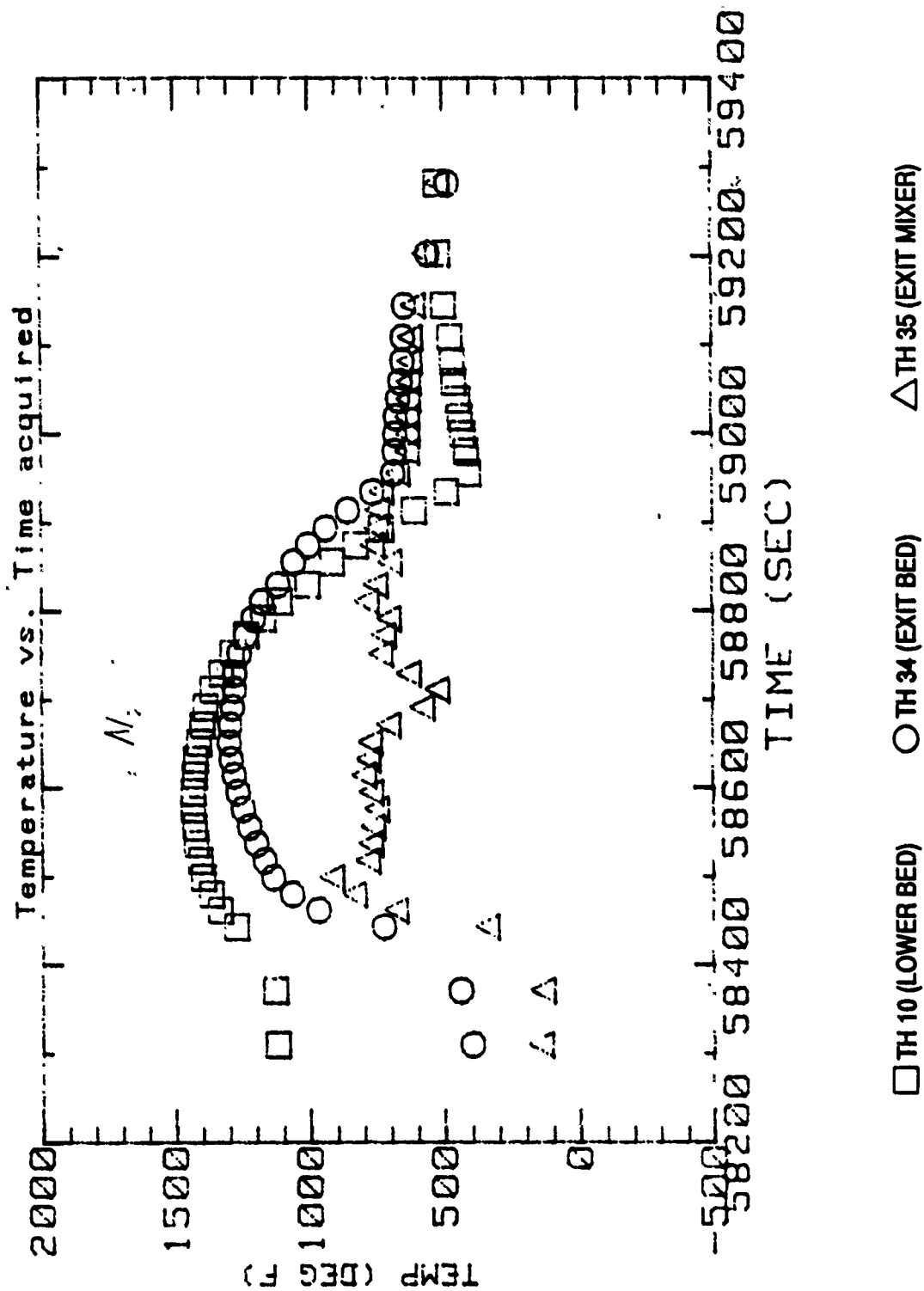
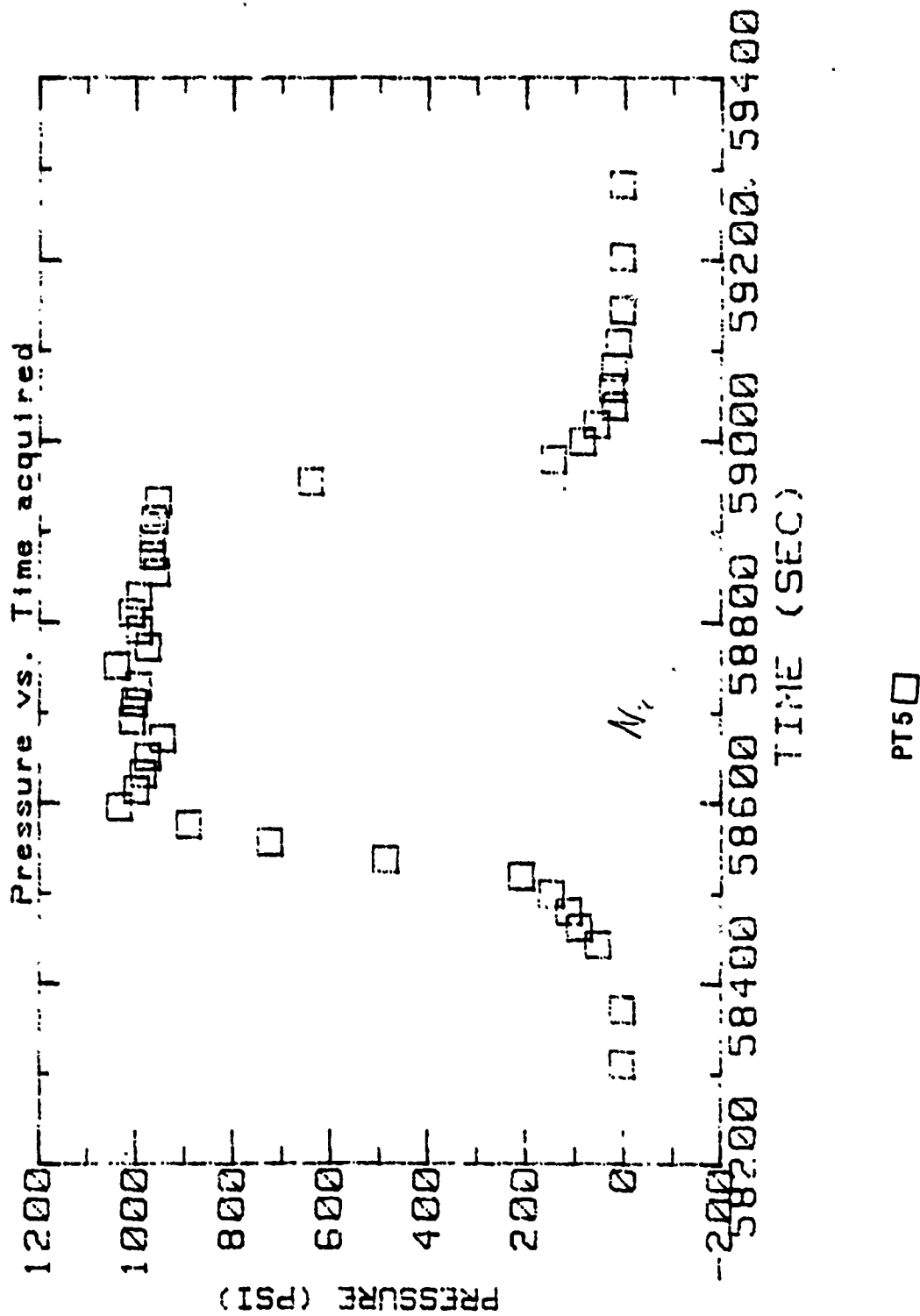
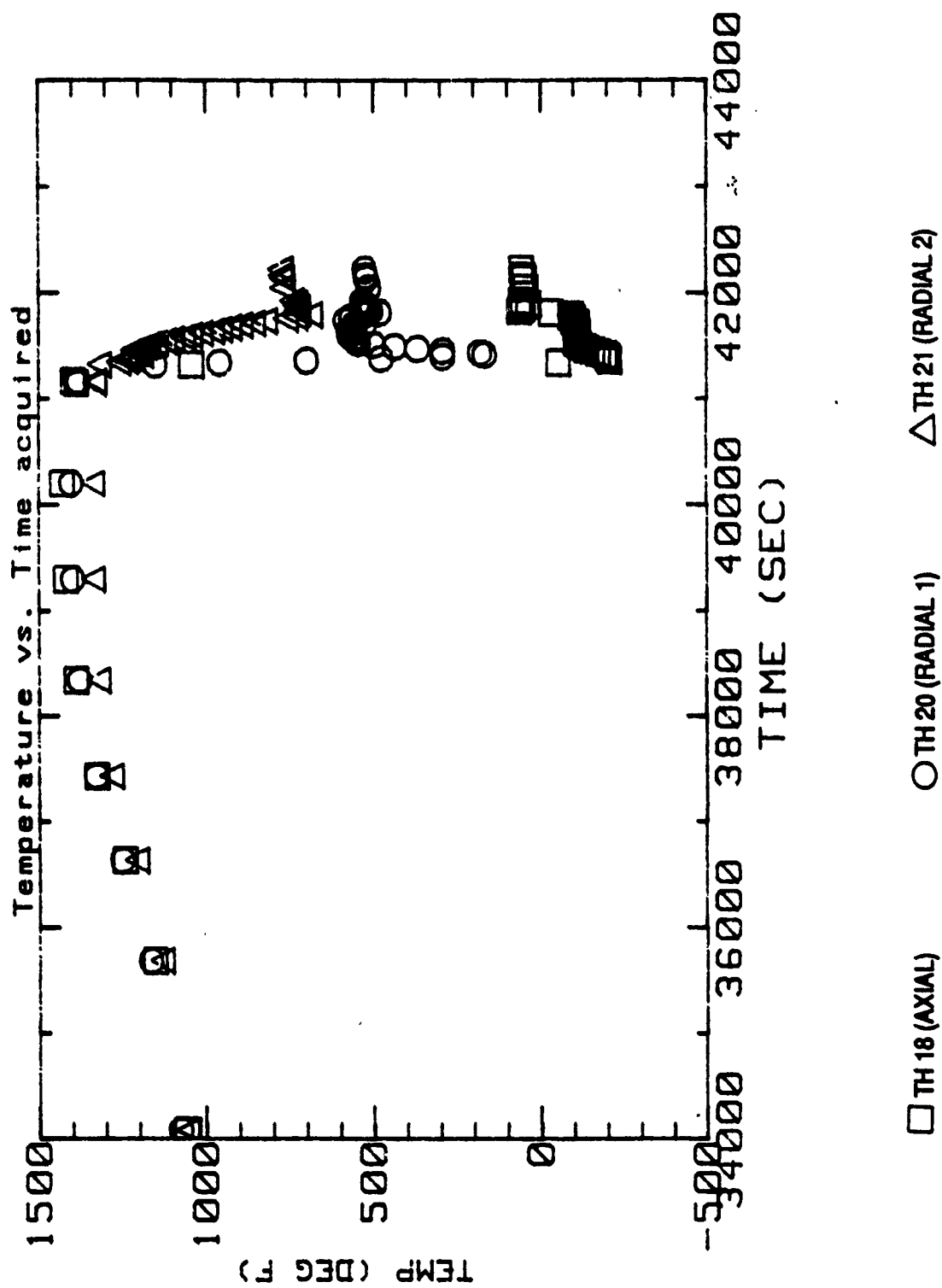


FIGURE 108. EXHAUST TEMPERATURES
EXPANDED TIME SCALES DURING INJECTION



**FIGURE 109. BED PRESSURE
EXPANDED TIME SCALE DURING INJECTION**



**FIGURE 110. UPPER BED RADIAL TEMPERATURE DISTRIBUTION
FULL TEST**

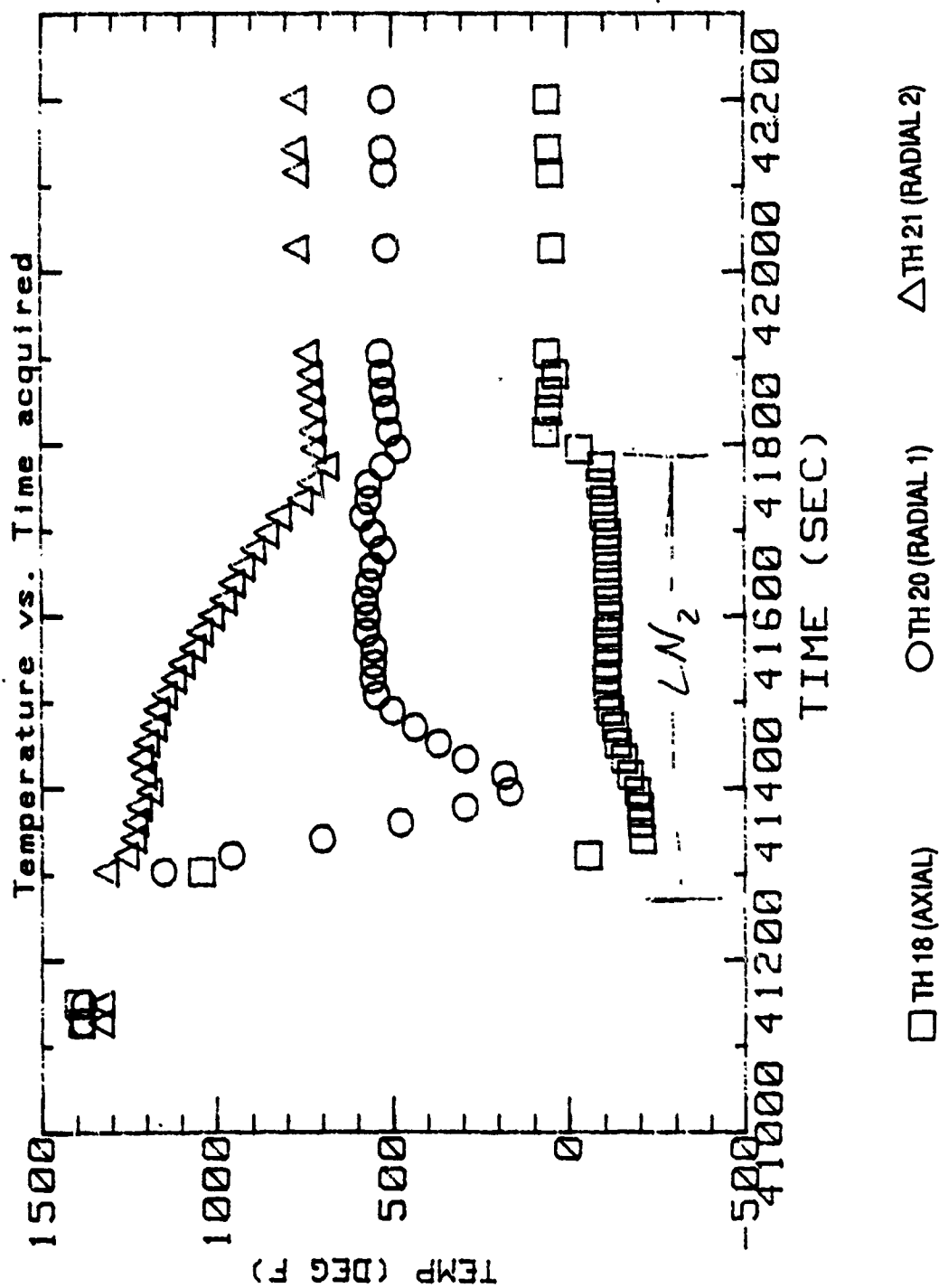


FIGURE 111. UPPER BED RADIAL TEMPERATURE DISTRIBUTION
EXPANDED TIME SCALE DURING INJECTION

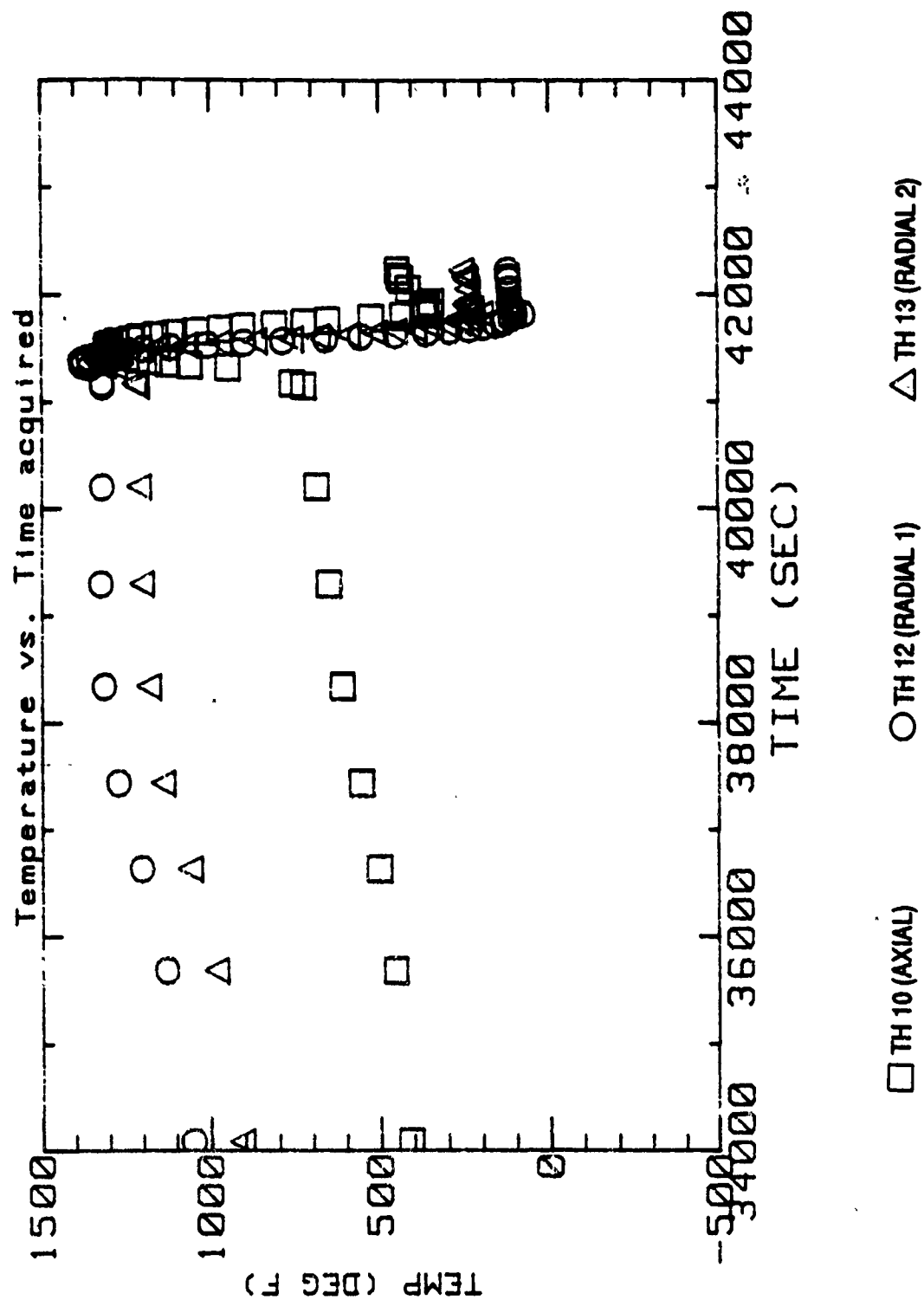


FIGURE 112. LOWER BED RADIAL TEMPERATURE DISTRIBUTION
FULL TEST

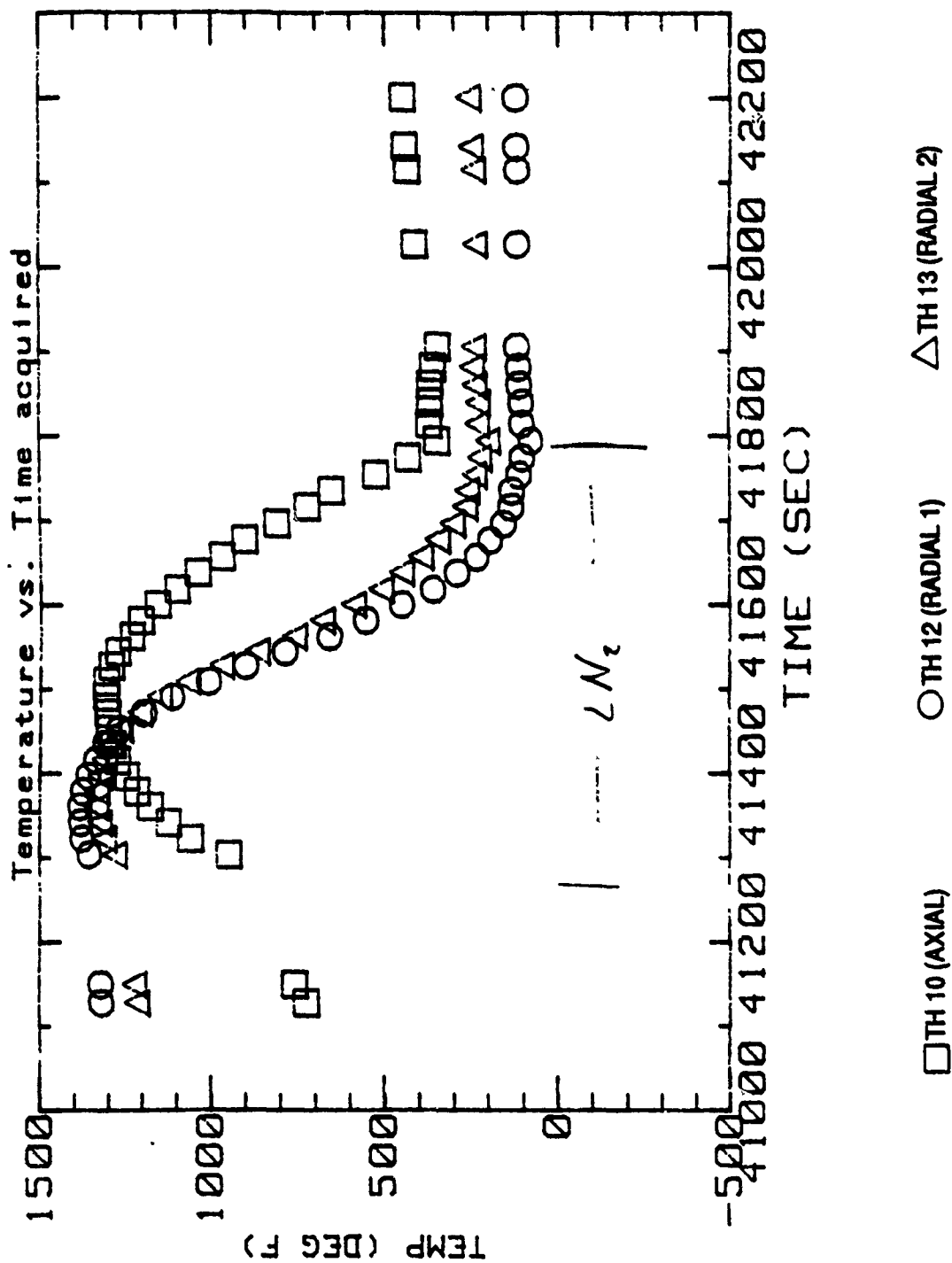


FIGURE 113. LOWER BED RADIAL TEMPERATURE DISTRIBUTION
EXPANDED TIME SCALE DURING INJECTION

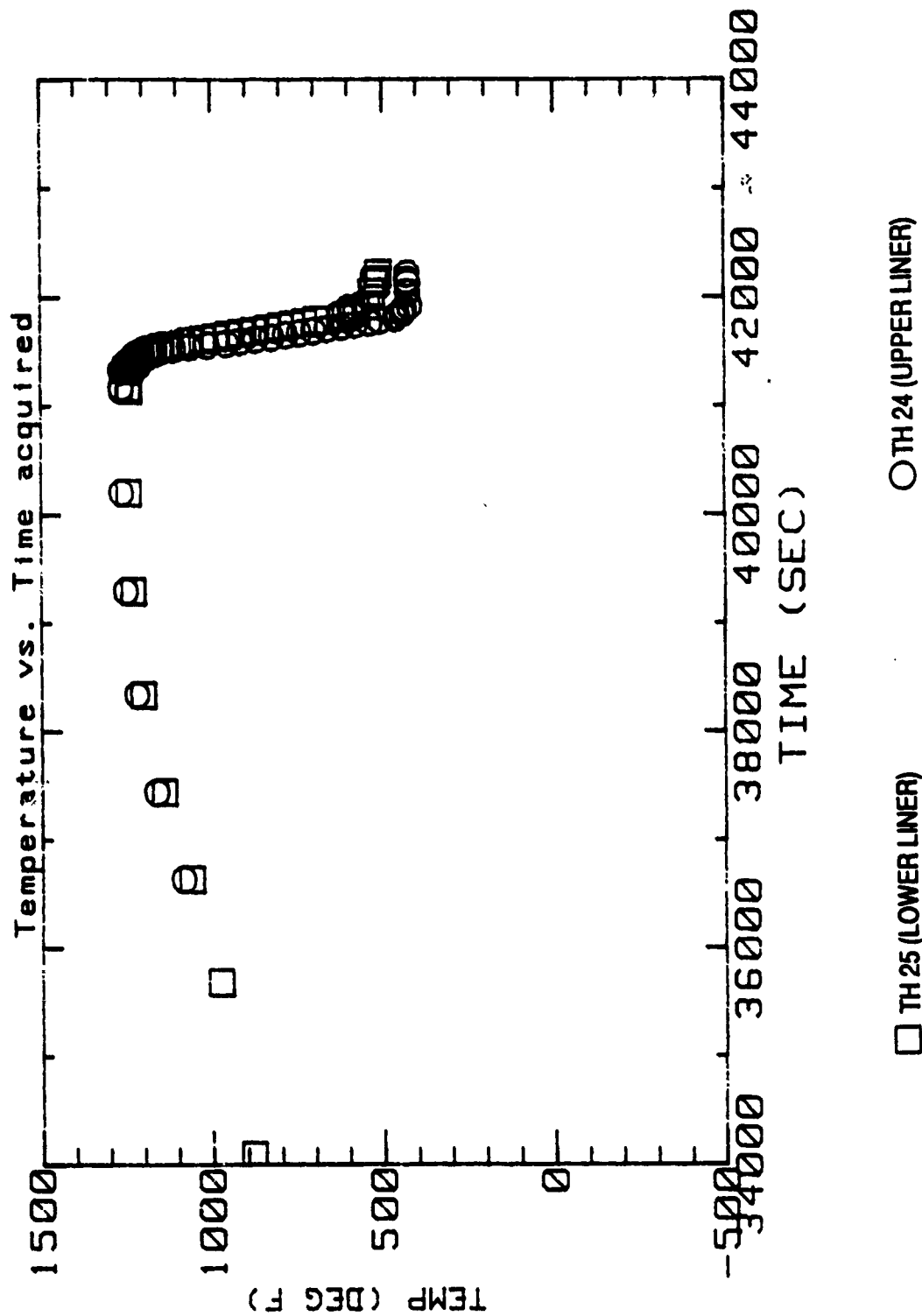


FIGURE 114. OUTSIDE LINER TEMPERATURES
FULL TEST

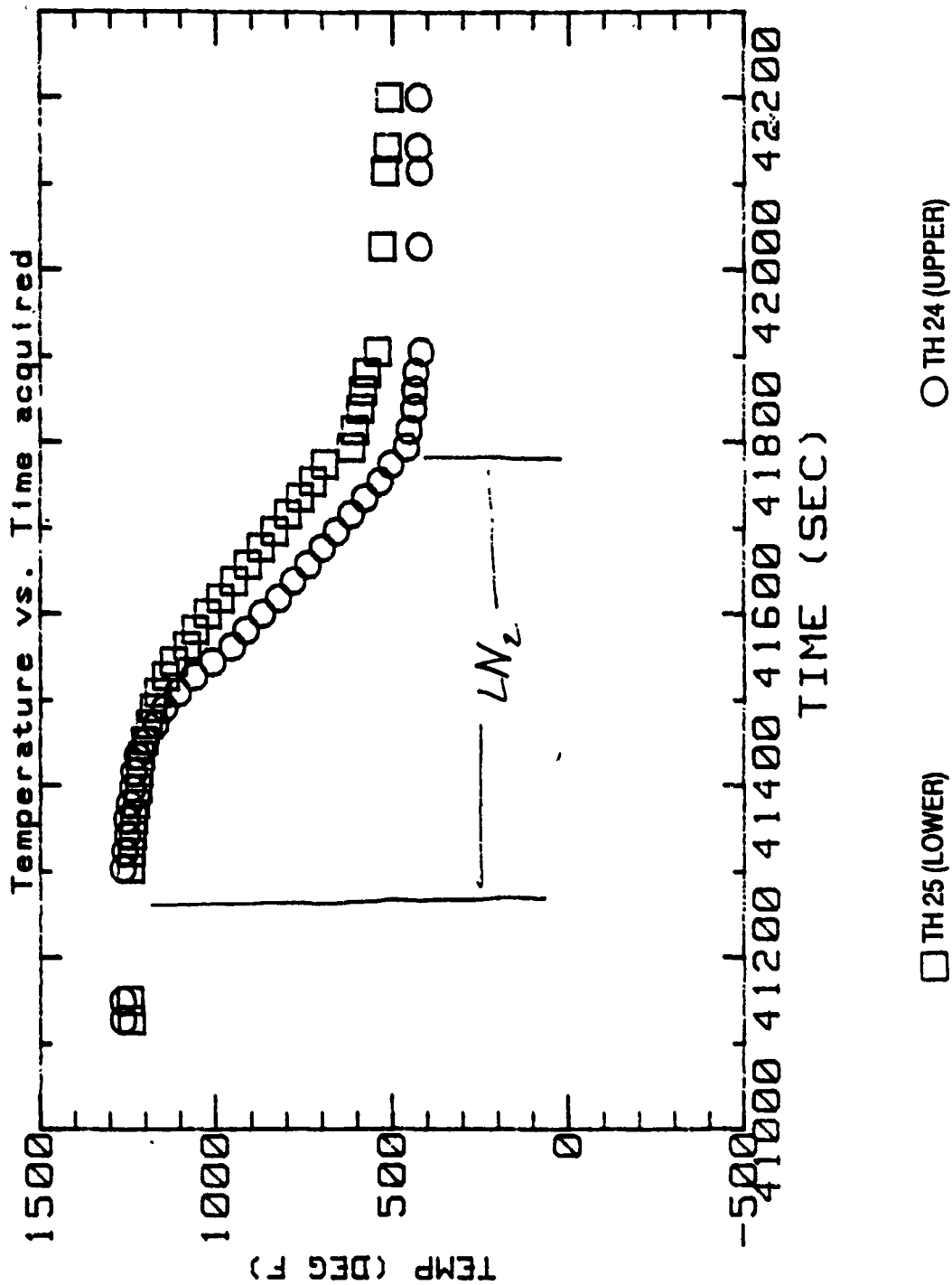


FIGURE 115. OUTSIDE LINER TEMPERATURE
EXPANDED TIME SCALE DURING INJECTION

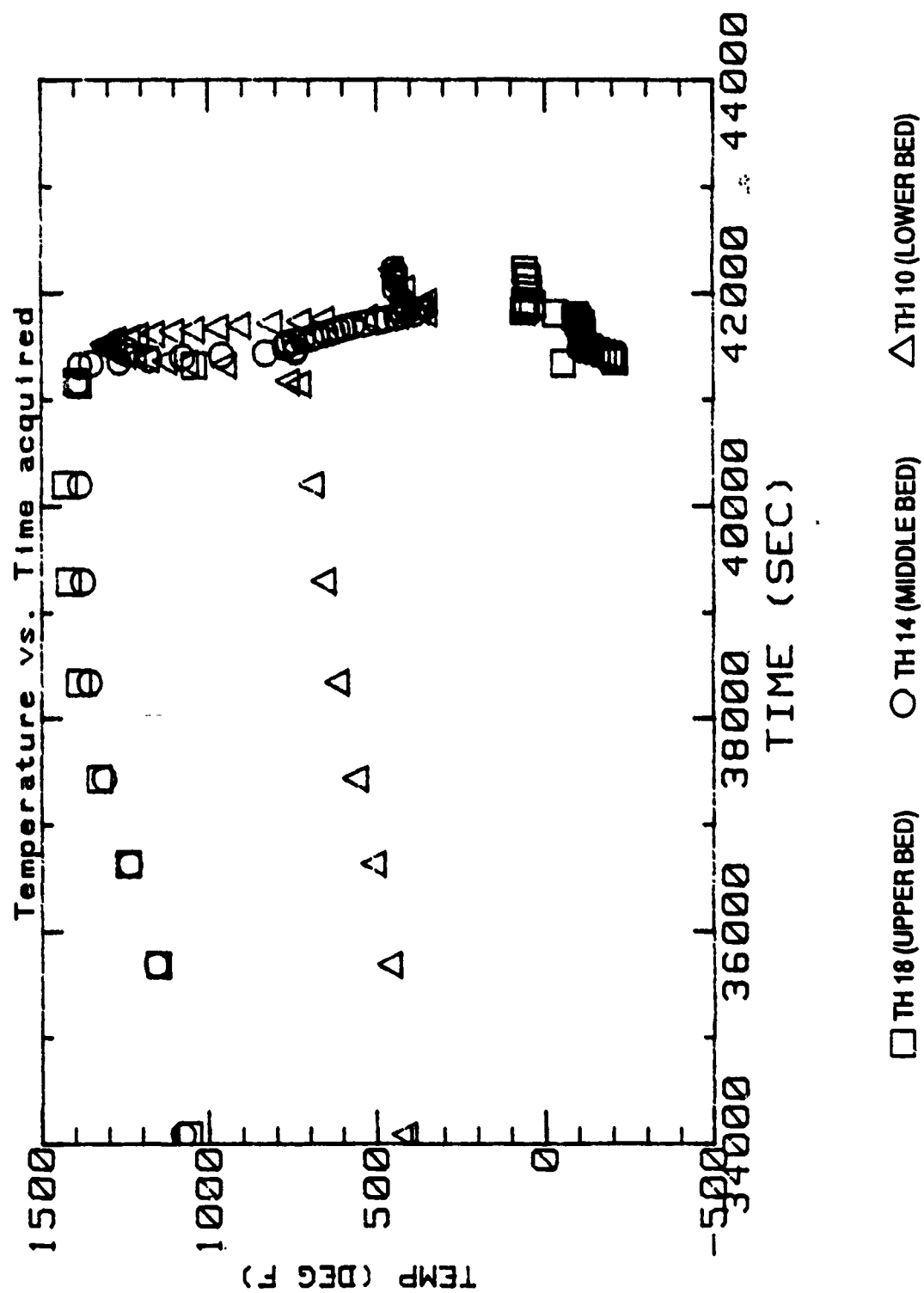


FIGURE 116. AXIAL TEMPERATURE DISTRIBUTION
FULL TEST

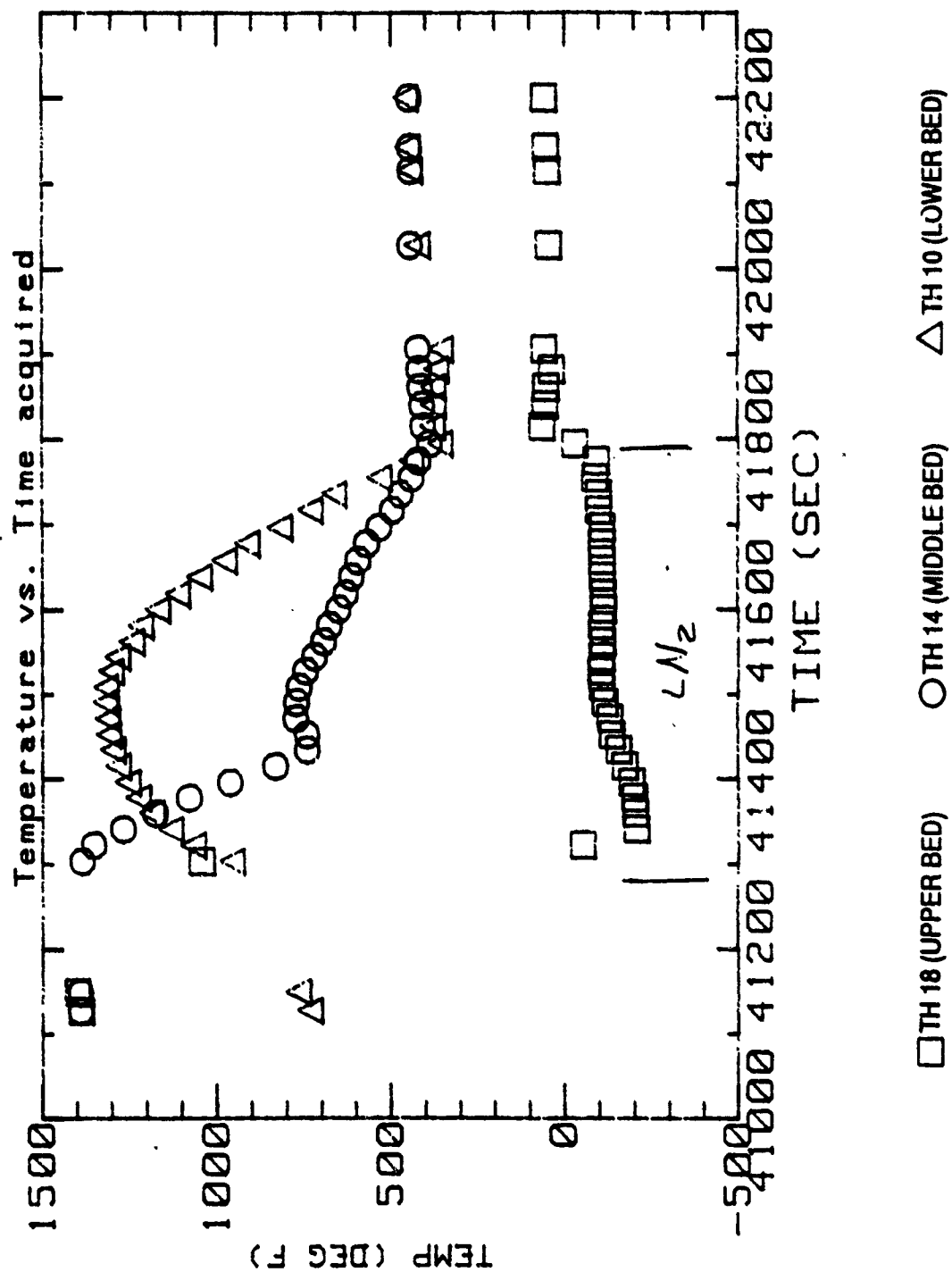


FIGURE 117. AXIAL TEMPERATURE DISTRIBUTION
EXPANDED TIME SCALE DURING INJECTION

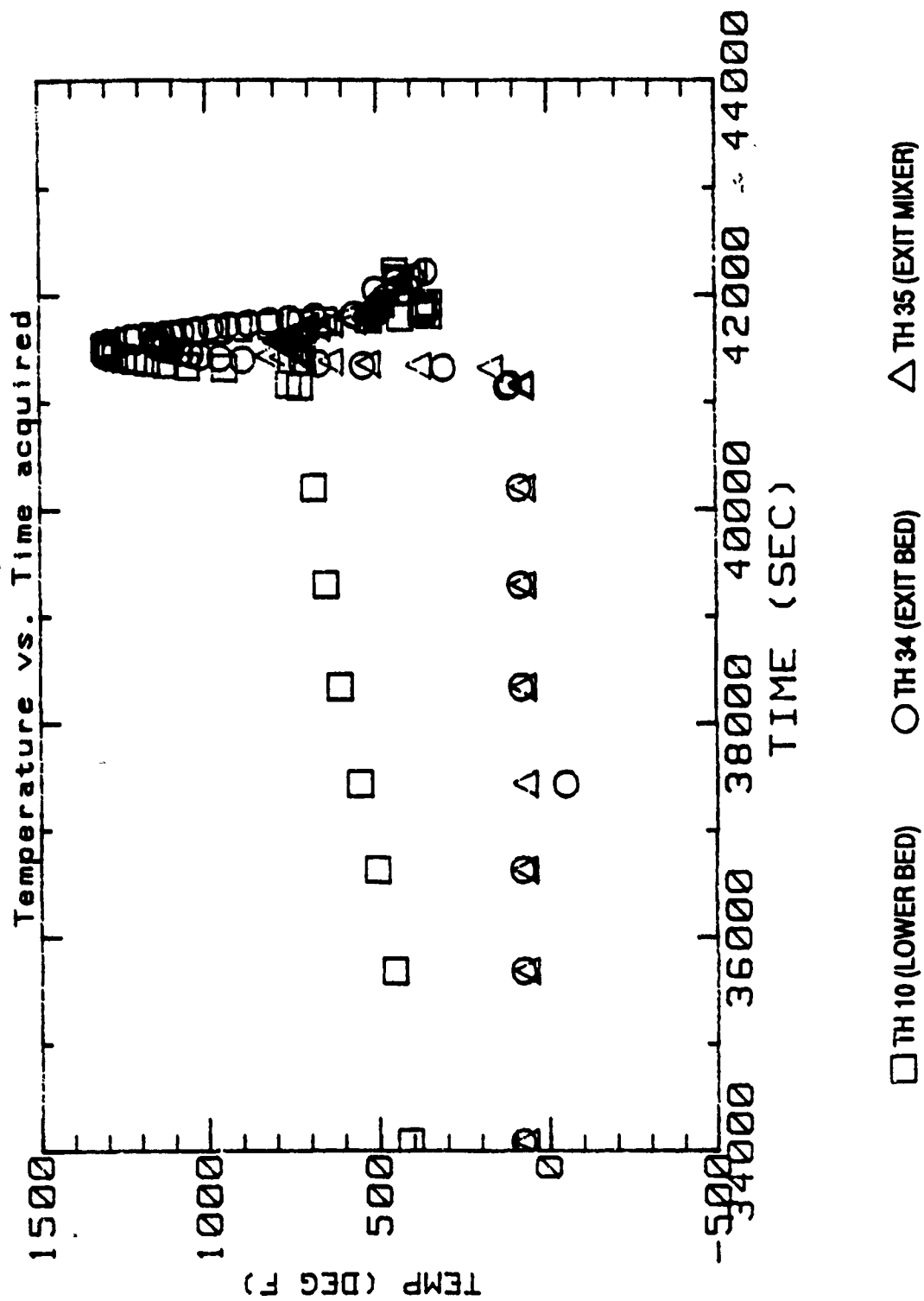
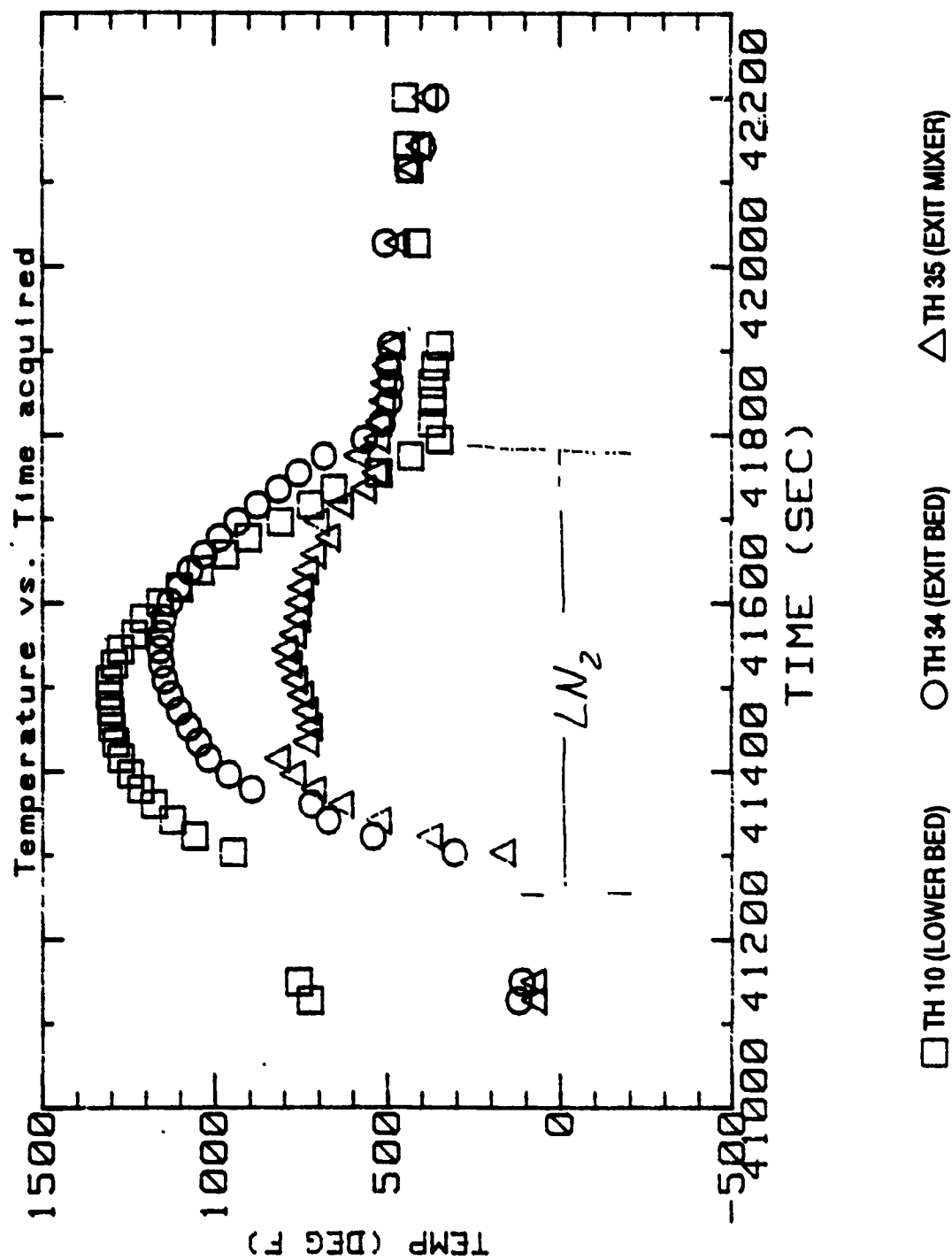


FIGURE 118. EXHAUST TEMPERATURES - FULL TEST



**FIGURE 119. EXHAUST TEMPERATURES
EXPANDED TIME SCALES DURING INJECTION**

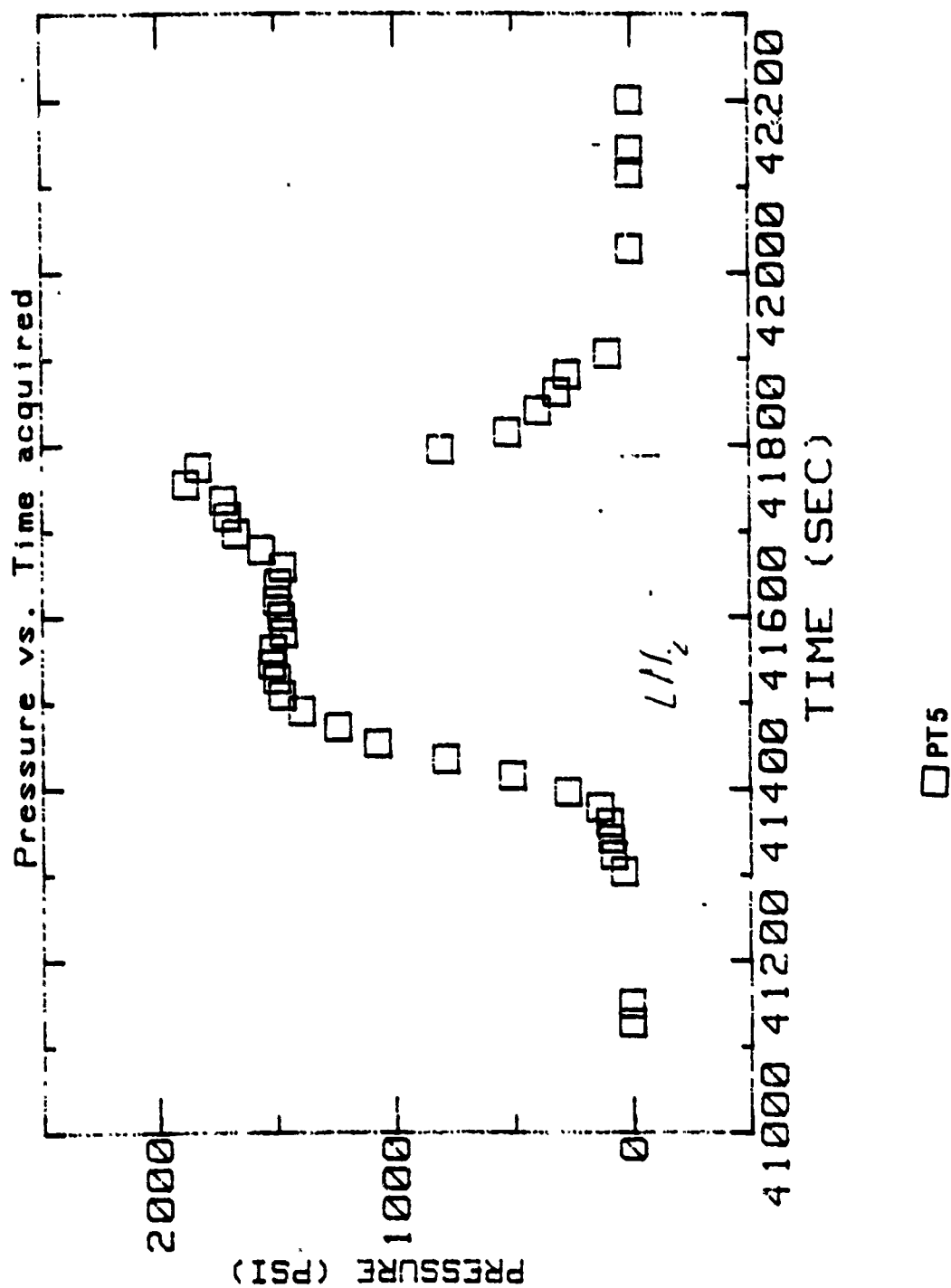
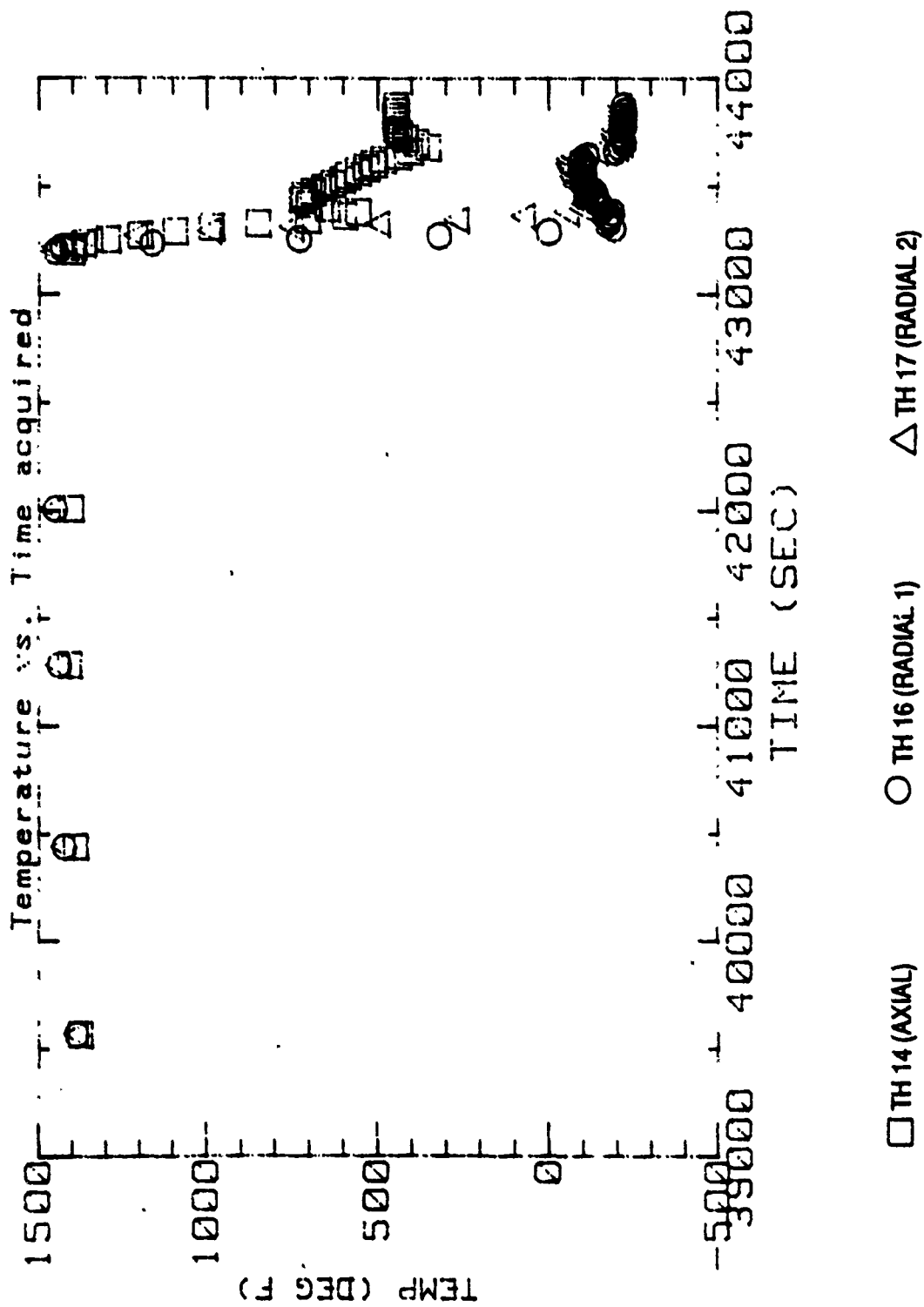


FIGURE 120. BED PRESSURE
EXPANDED TIME SCALE DURING INJECTION



**FIGURE 121. MIDDLE BED RADIAL TEMPERATURE DISTRIBUTION
FULL TEST**

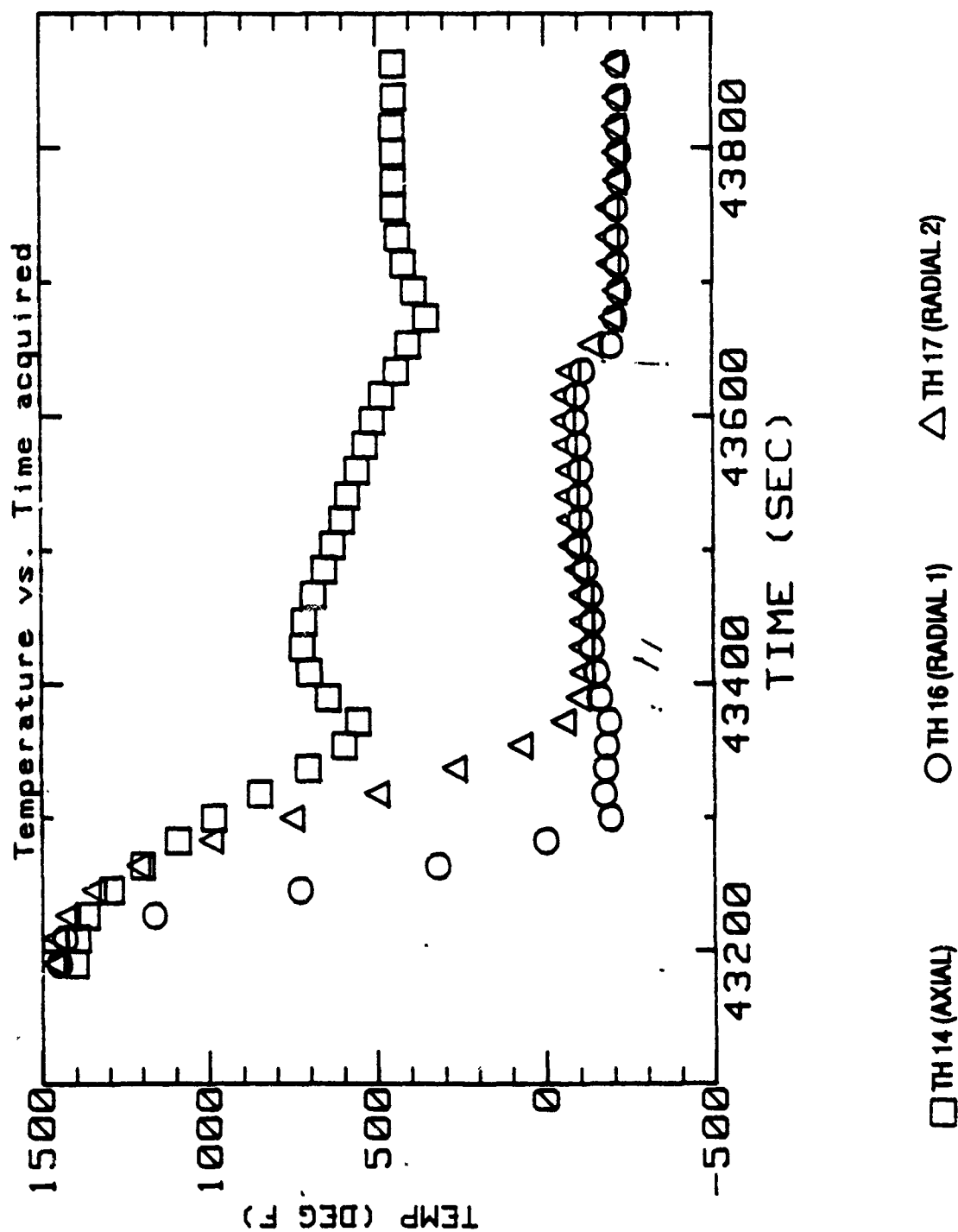


FIGURE 122. MIDDLE BED RADIAL TEMPERATURE DISTRIBUTION
EXPANDED TIME SCALE DURING INJECTION

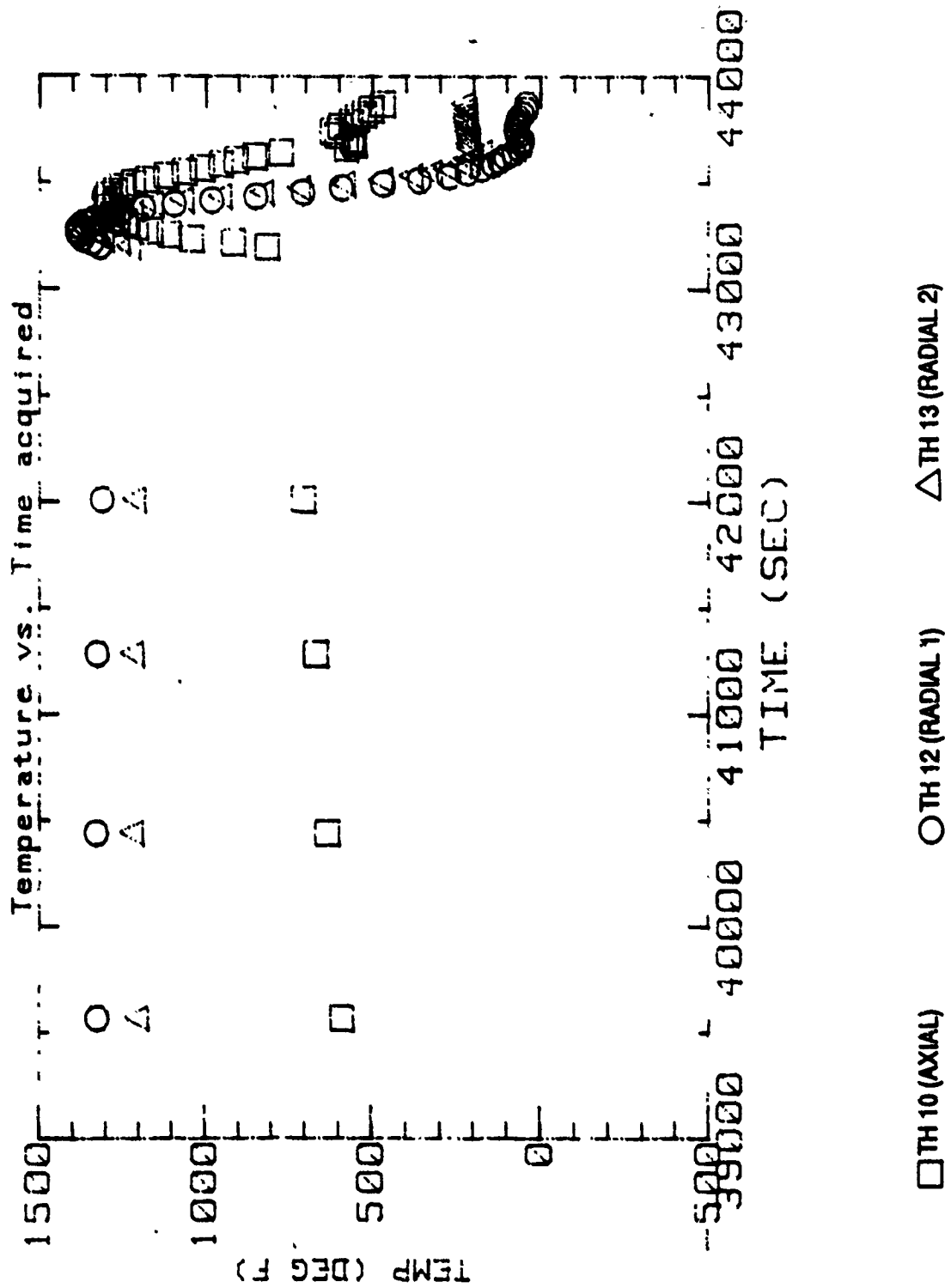


FIGURE 123. LOWER BED RADIAL TEMPERATURE DISTRIBUTION
FULL TEST

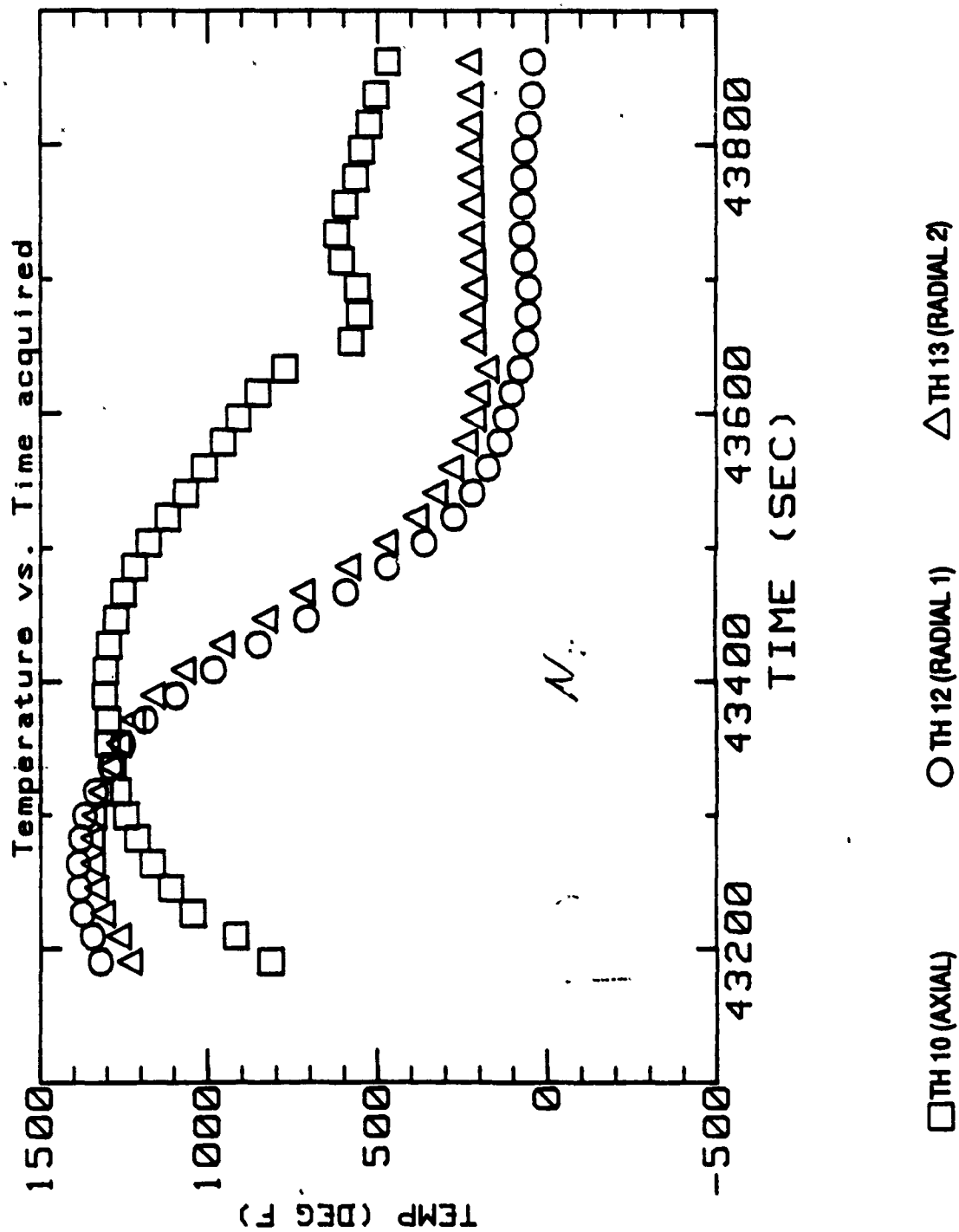


FIGURE 124. LOWER BED RADIAL TEMPERATURE DISTRIBUTION
EXPANDED TIME SCALE DURING INJECTION

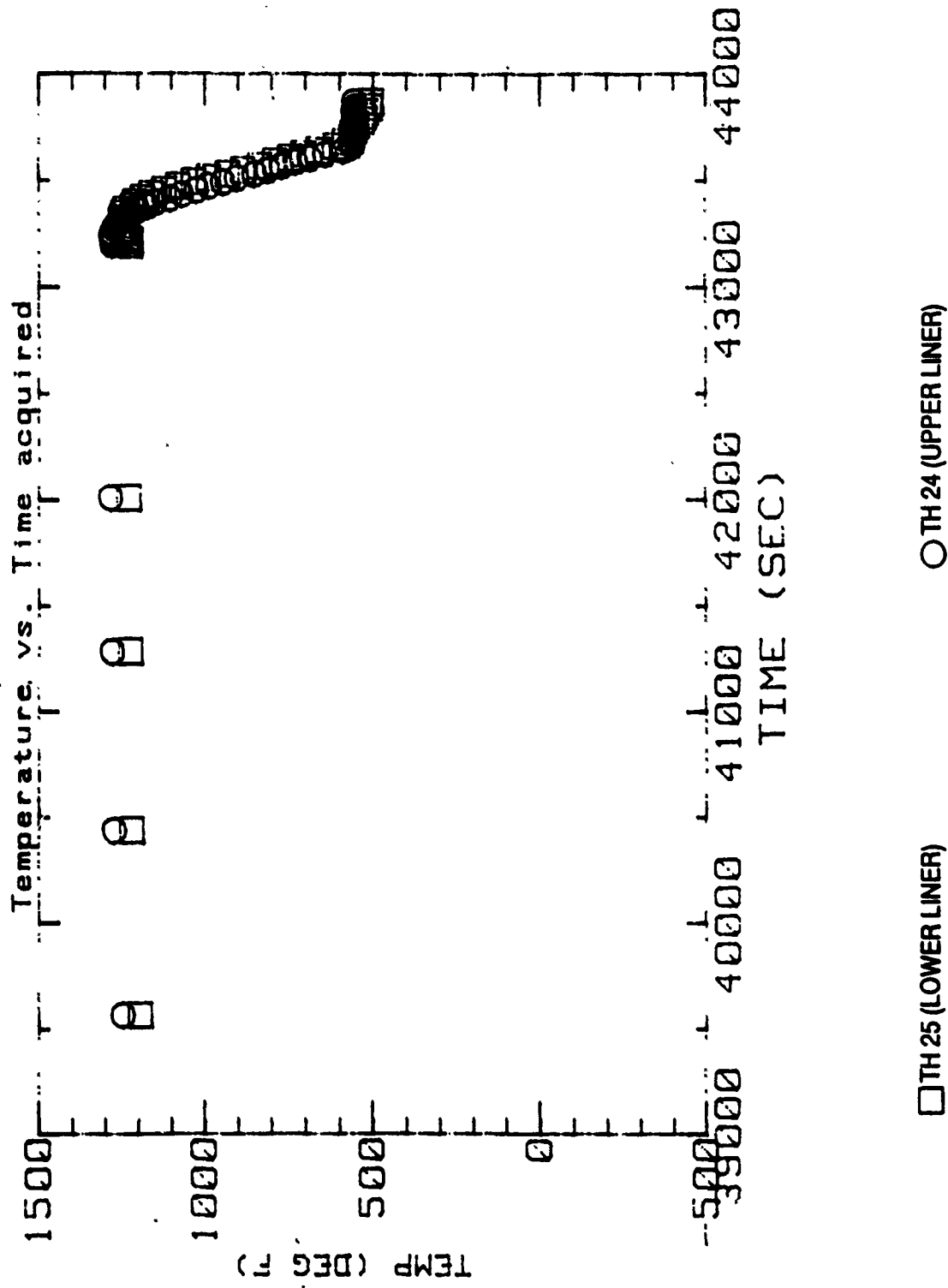


FIGURE 125. OUTSIDE LINER TEMPERATURES
FULL TEST

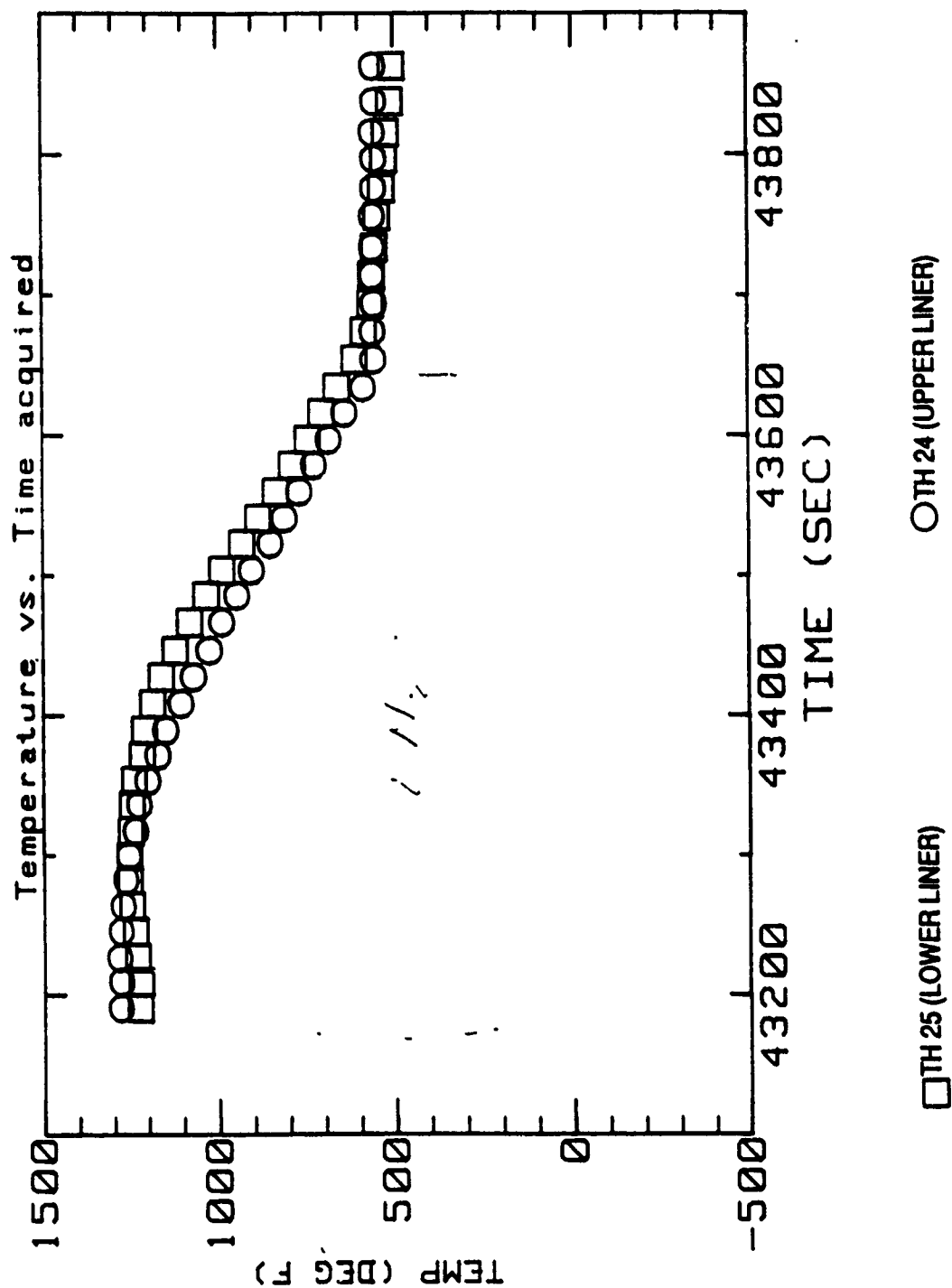


FIGURE 126. OUTSIDE LINER TEMPERATURE
EXPANDED TIME SCALE DURING INJECTION

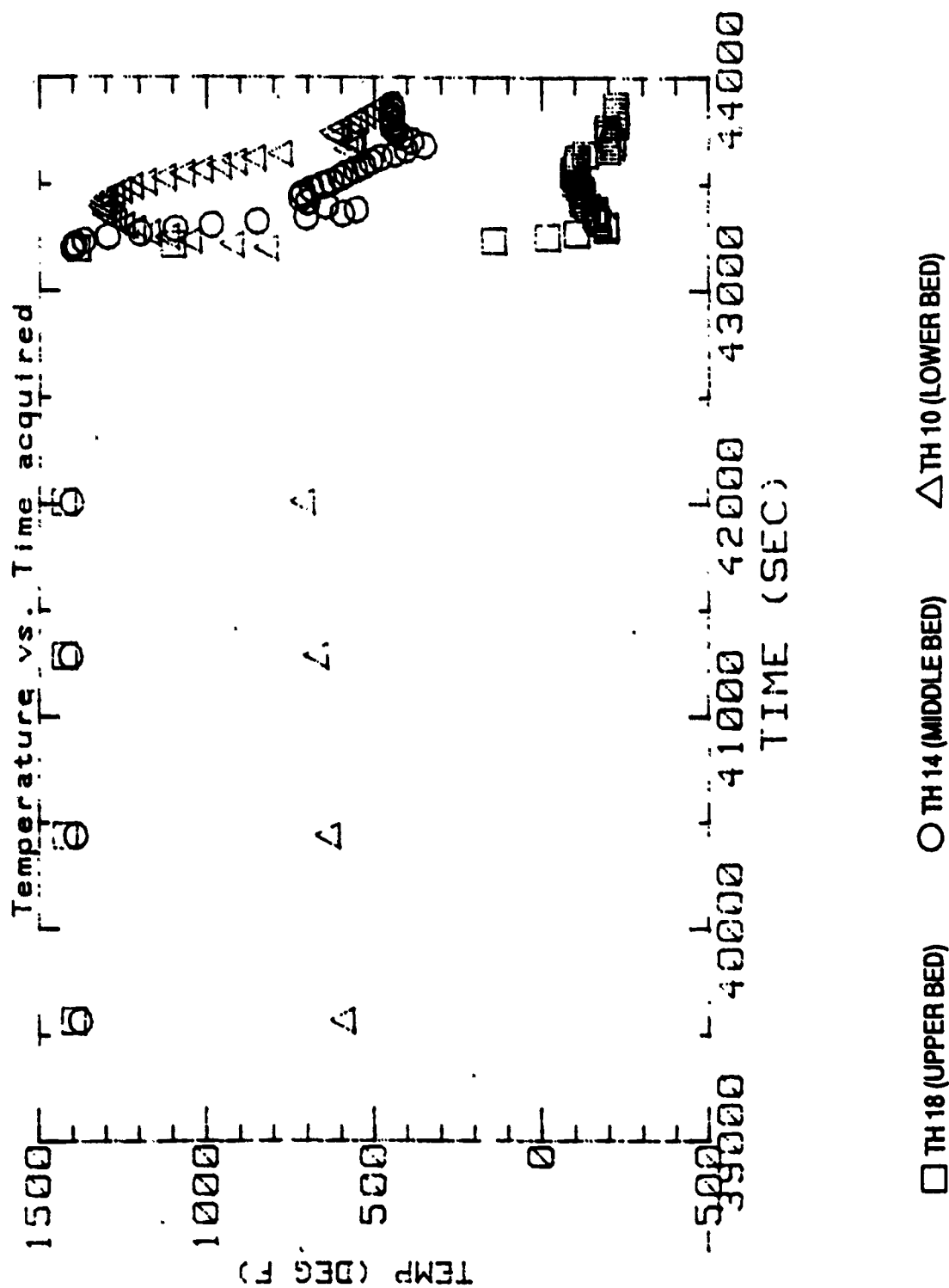
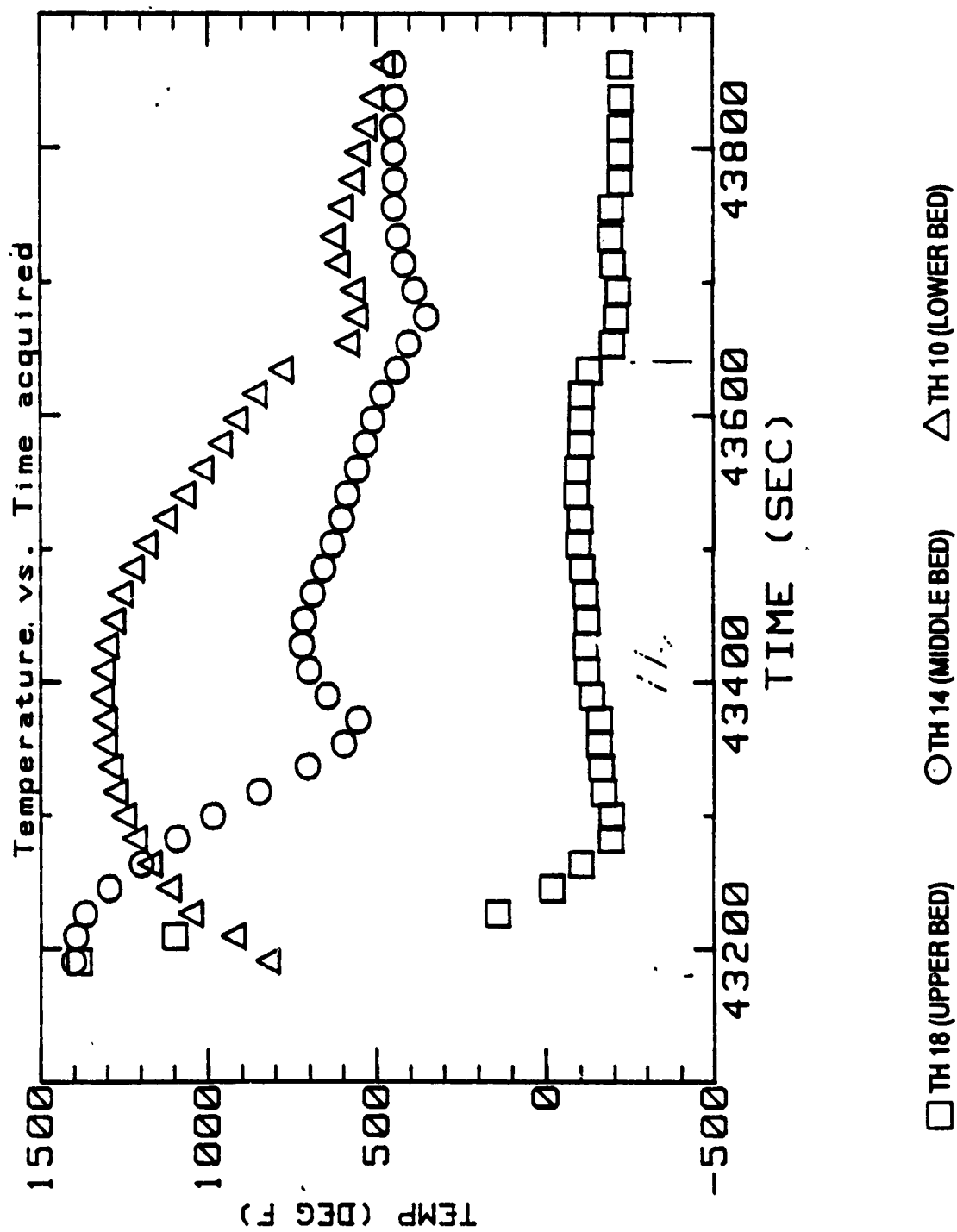


FIGURE 127. AXIAL TEMPERATURE DISTRIBUTION
FULL TEST



**FIGURE 128. AXIAL TEMPERATURE DISTRIBUTION
EXPANDED TIME SCALE DURING INJECTION**

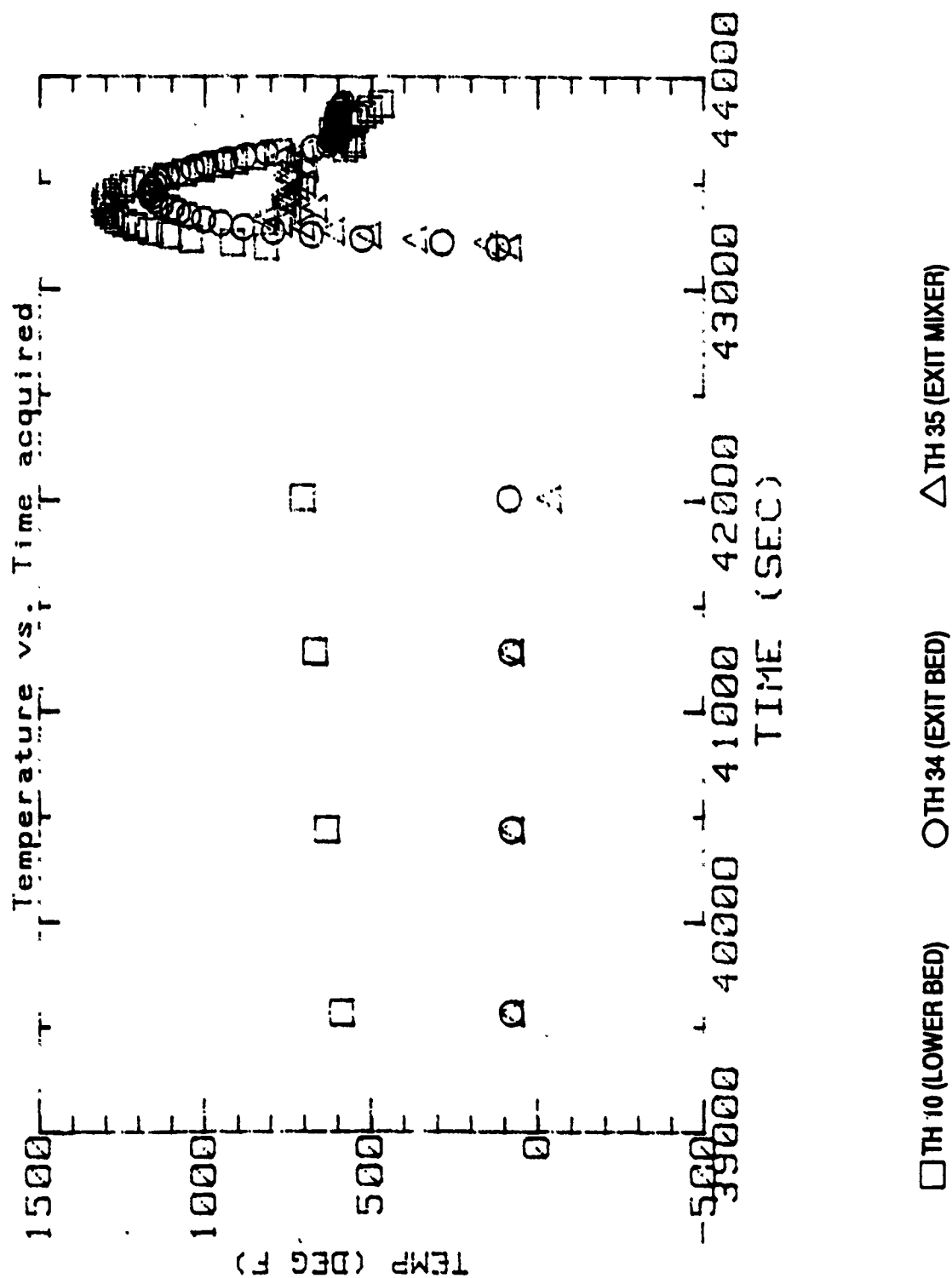
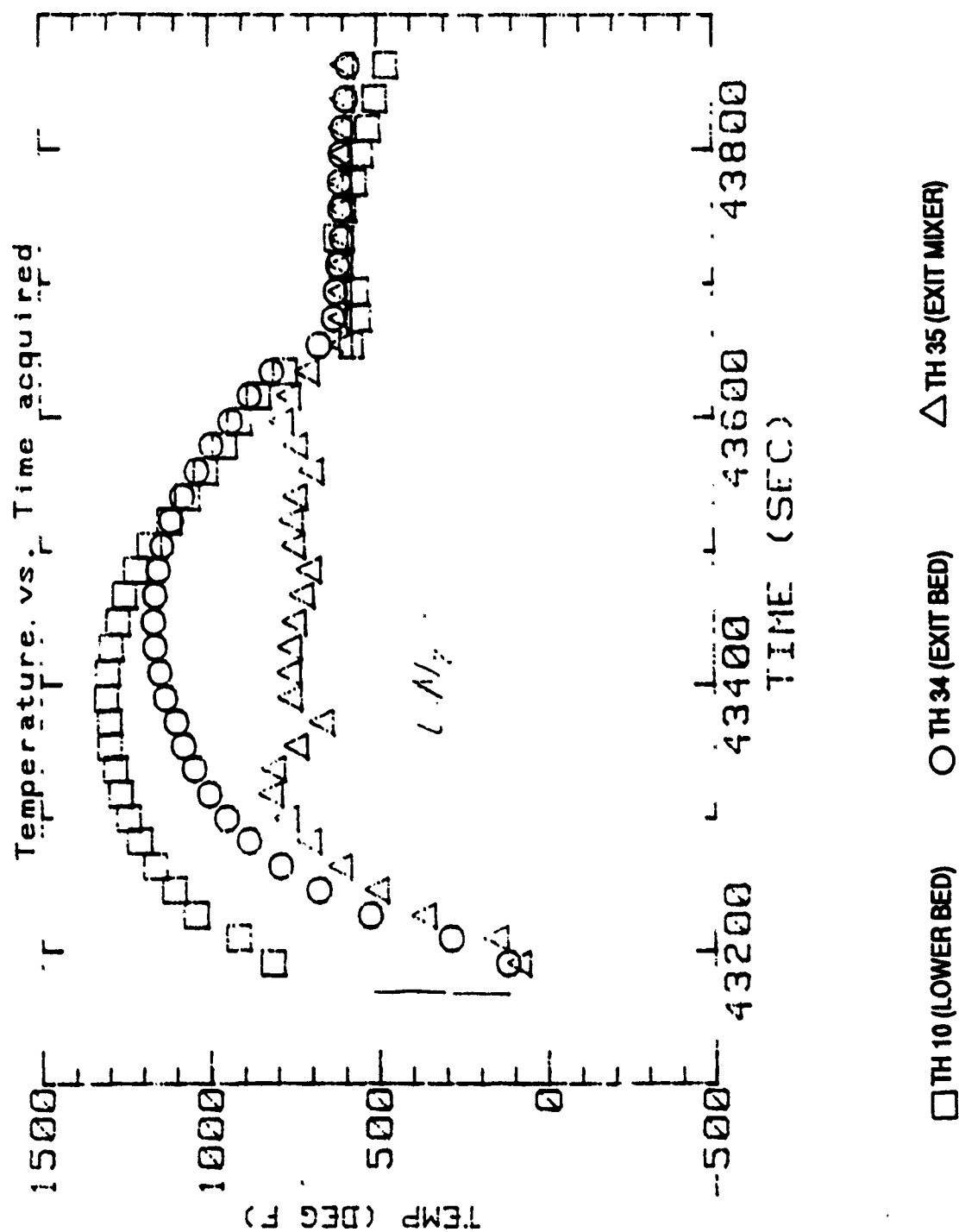


FIGURE 129. EXHAUST TEMPERATURES - FULL TEST



**FIGURE 130. EXHAUST TEMPERATURES
EXPANDED TIME SCALES DURING INJECTION**

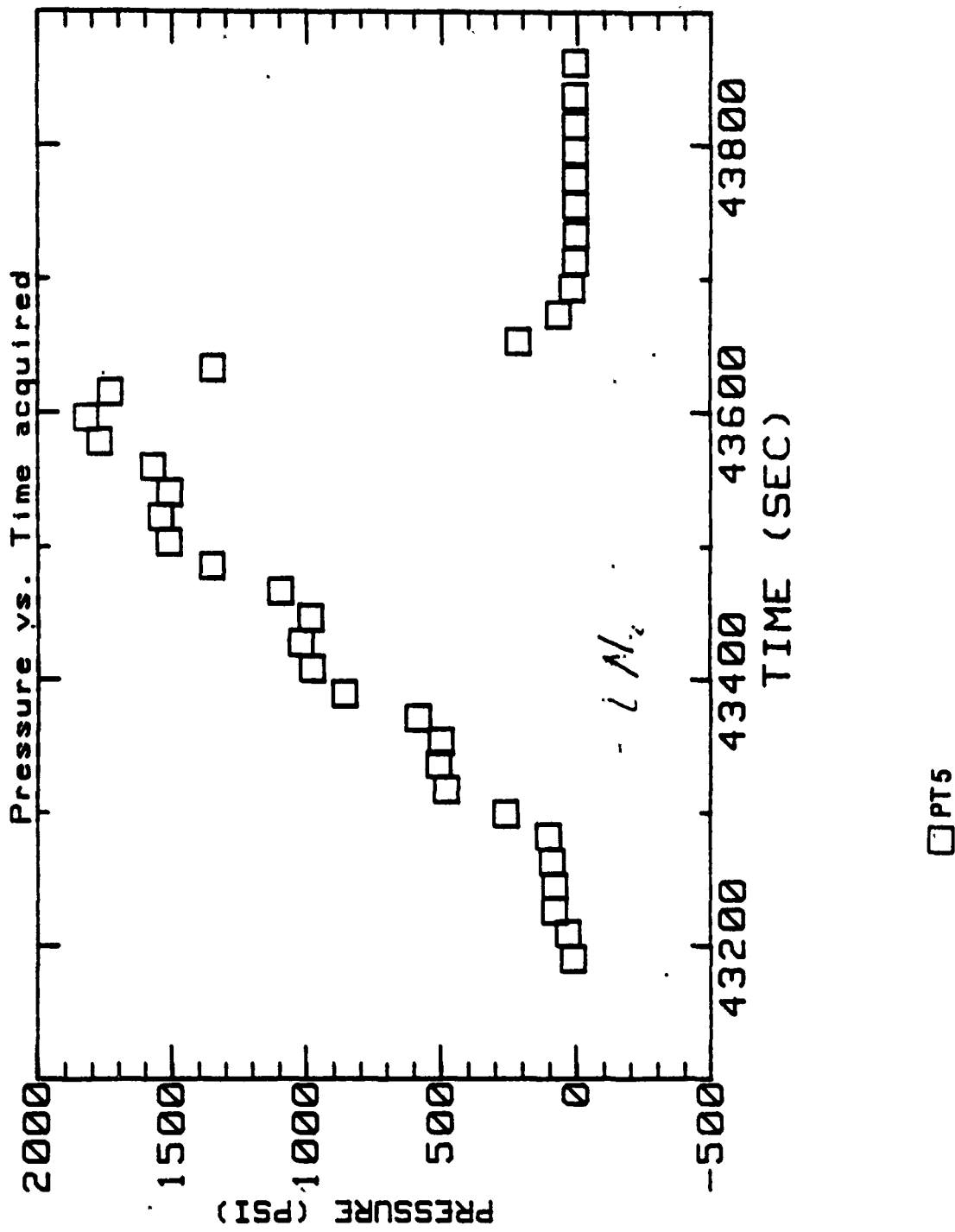


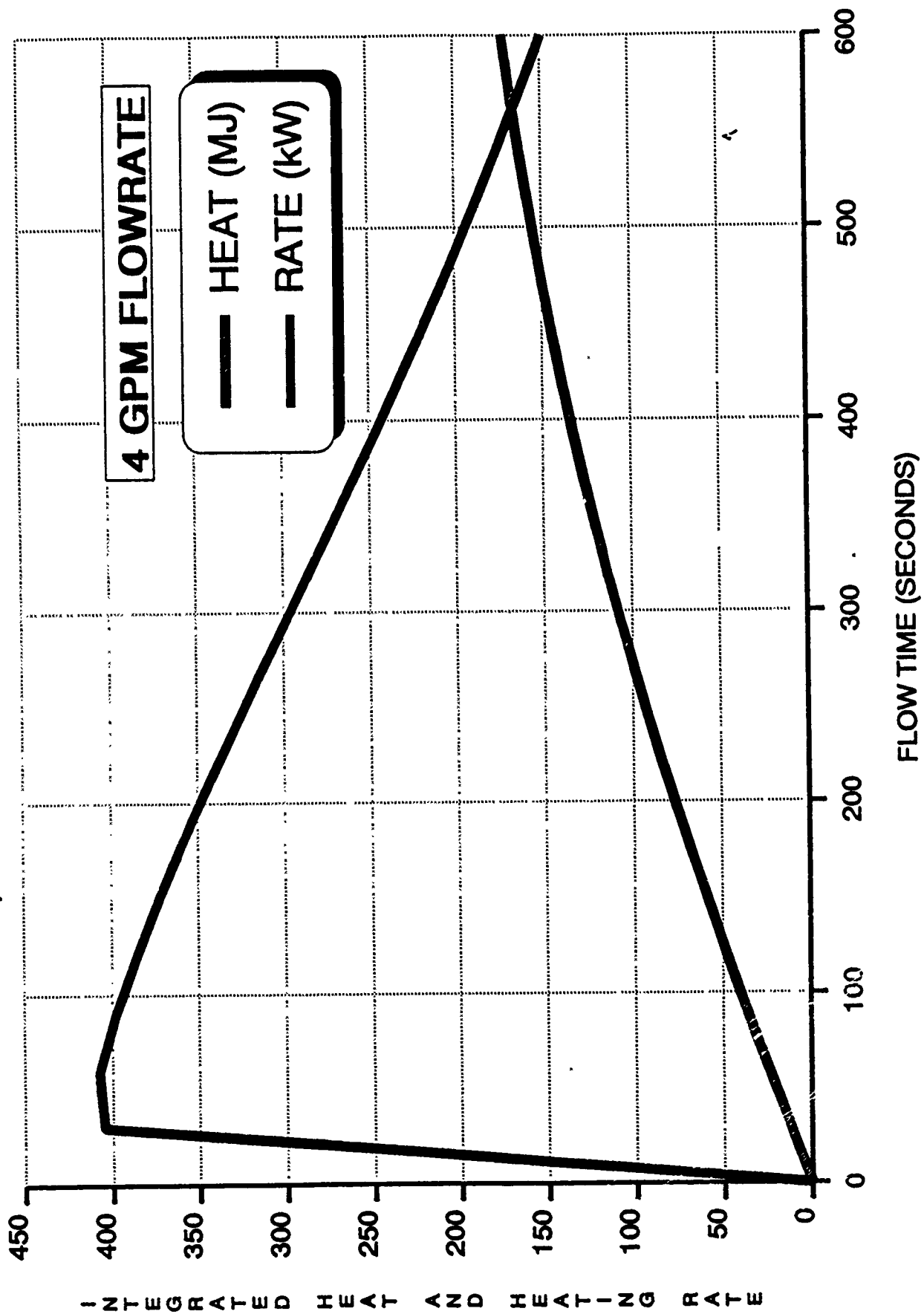
FIGURE 131. BED PRESSURE
EXPANDED TIME SCALE DURING INJECTION

APPENDIX B - GRAPHICAL ANALYSIS RESULTS
FOR THE 1/48TH SCALE LB/TS
PEBBLE-BED LN₂ EVAPORATOR AND SUPERHEATER

INTENTIONALLY LEFT BLANK.

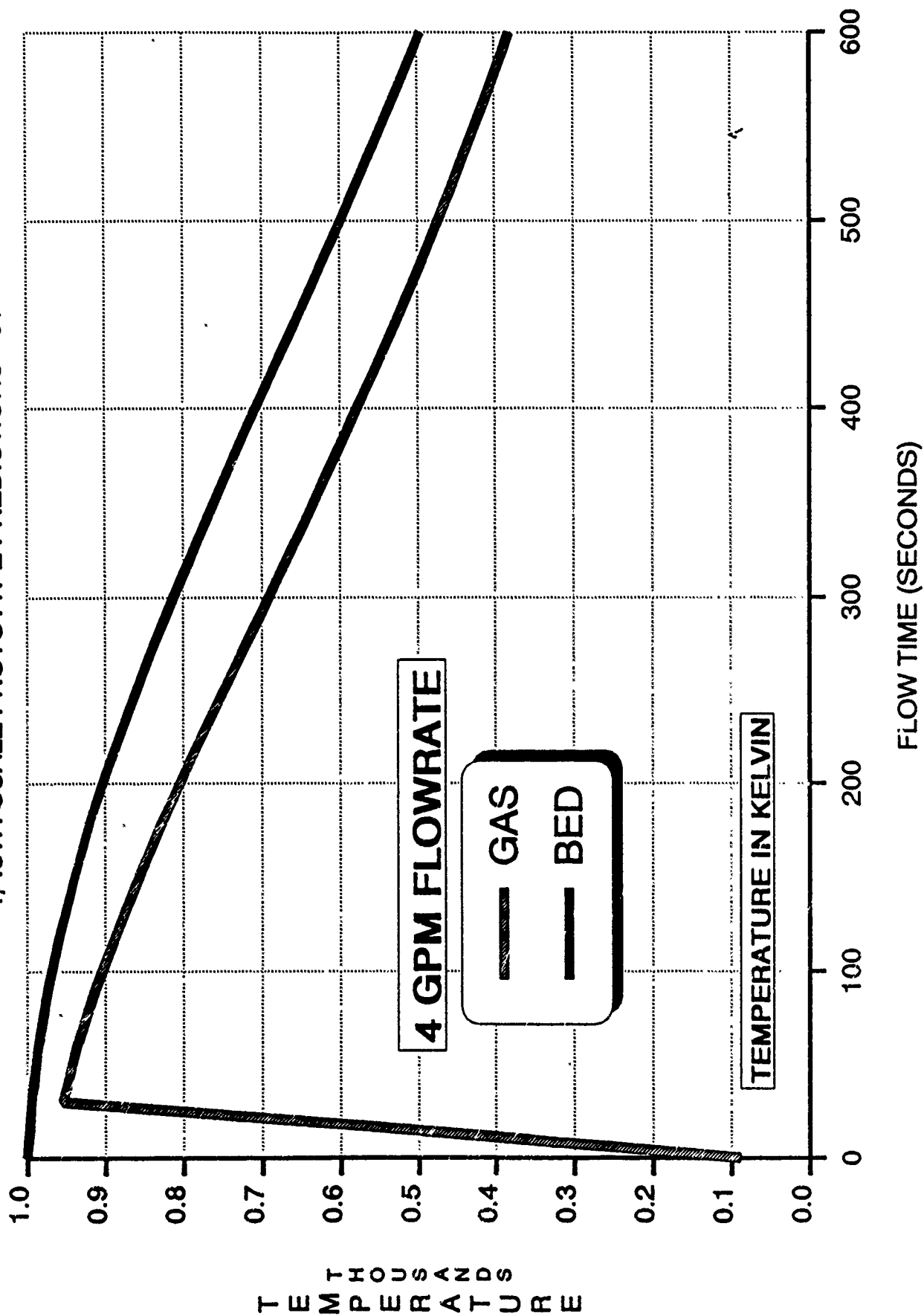
PEBBLE BED HEATER THERMAL PERFORMANCE

1/48TH SCALE PROTOTYPE PREDICTIONS - 01



PEBBLE BED HEATER OUTLET TEMPERATURES

1/48TH SCALE PROTOTYPE PREDICTIONS - 01

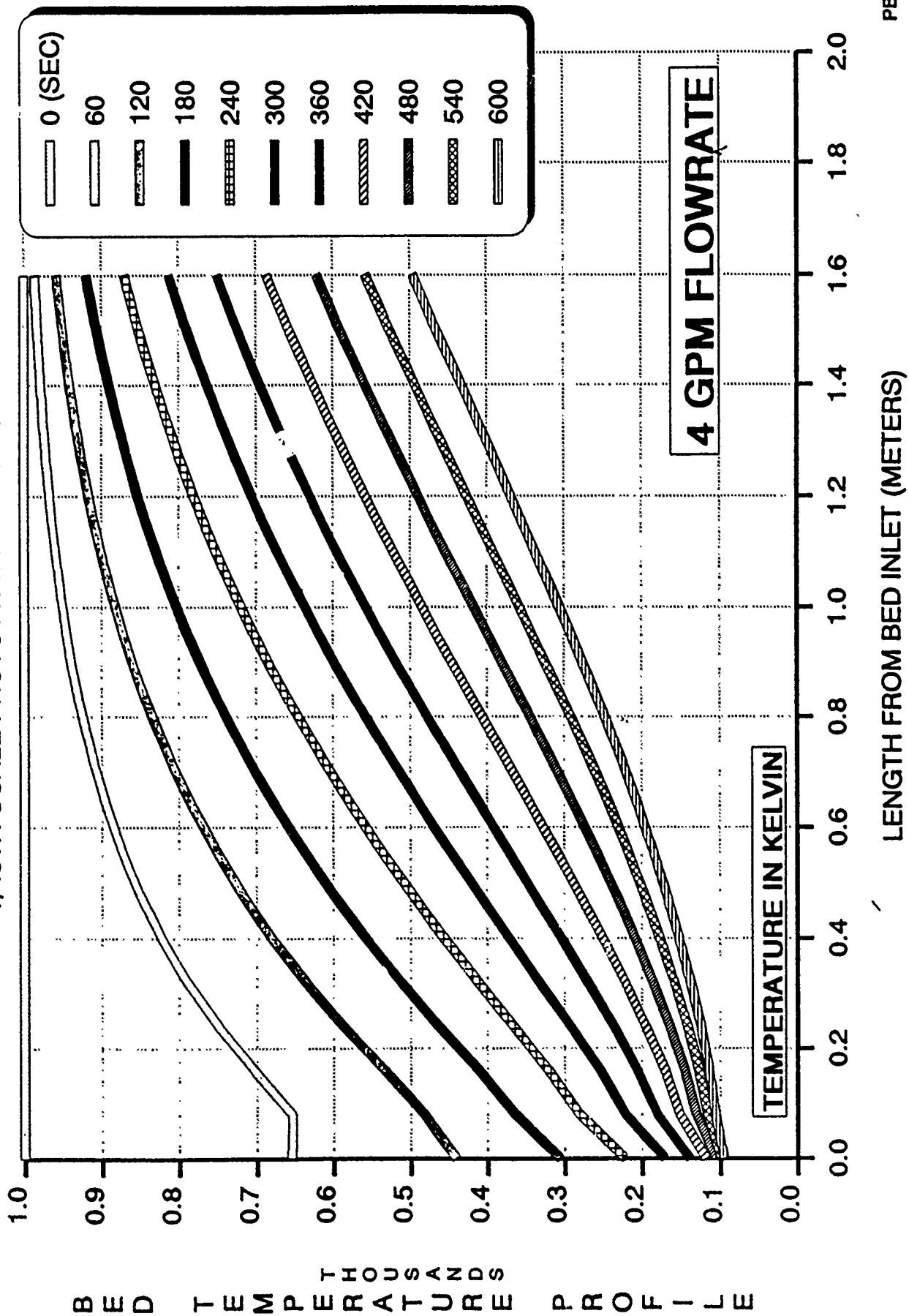


FLOW TIME (SECONDS)

PB01T-7

PEBBLE BED HEATER TEMPERATURE PROFILE

1/48TH SCALE PROTOTYPE PREDICTIONS - 01

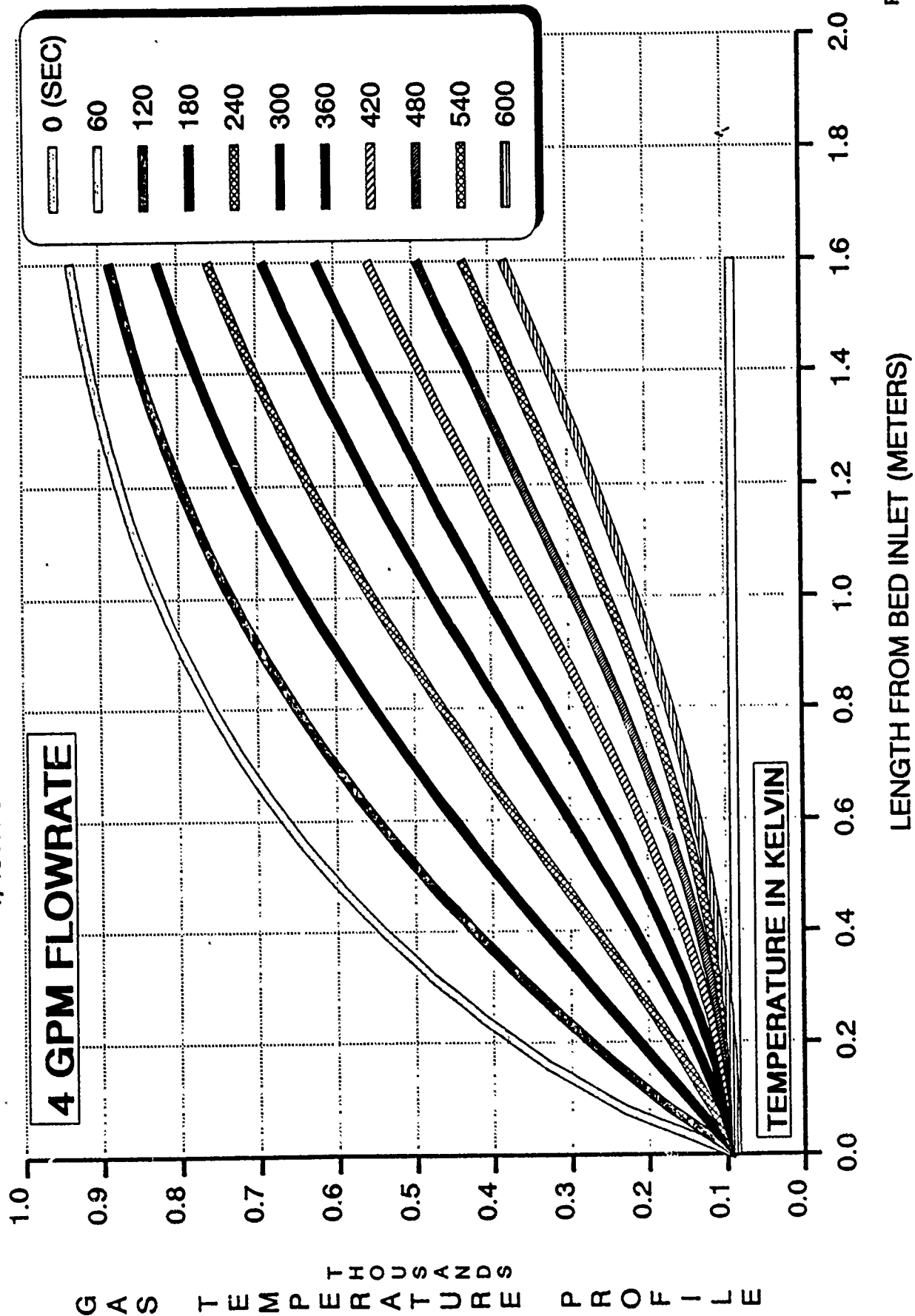


LENGTH FROM BED INLET (METERS)

PB01X-B

PEBBLE BED HEATER TEMPERATURE PROFILE

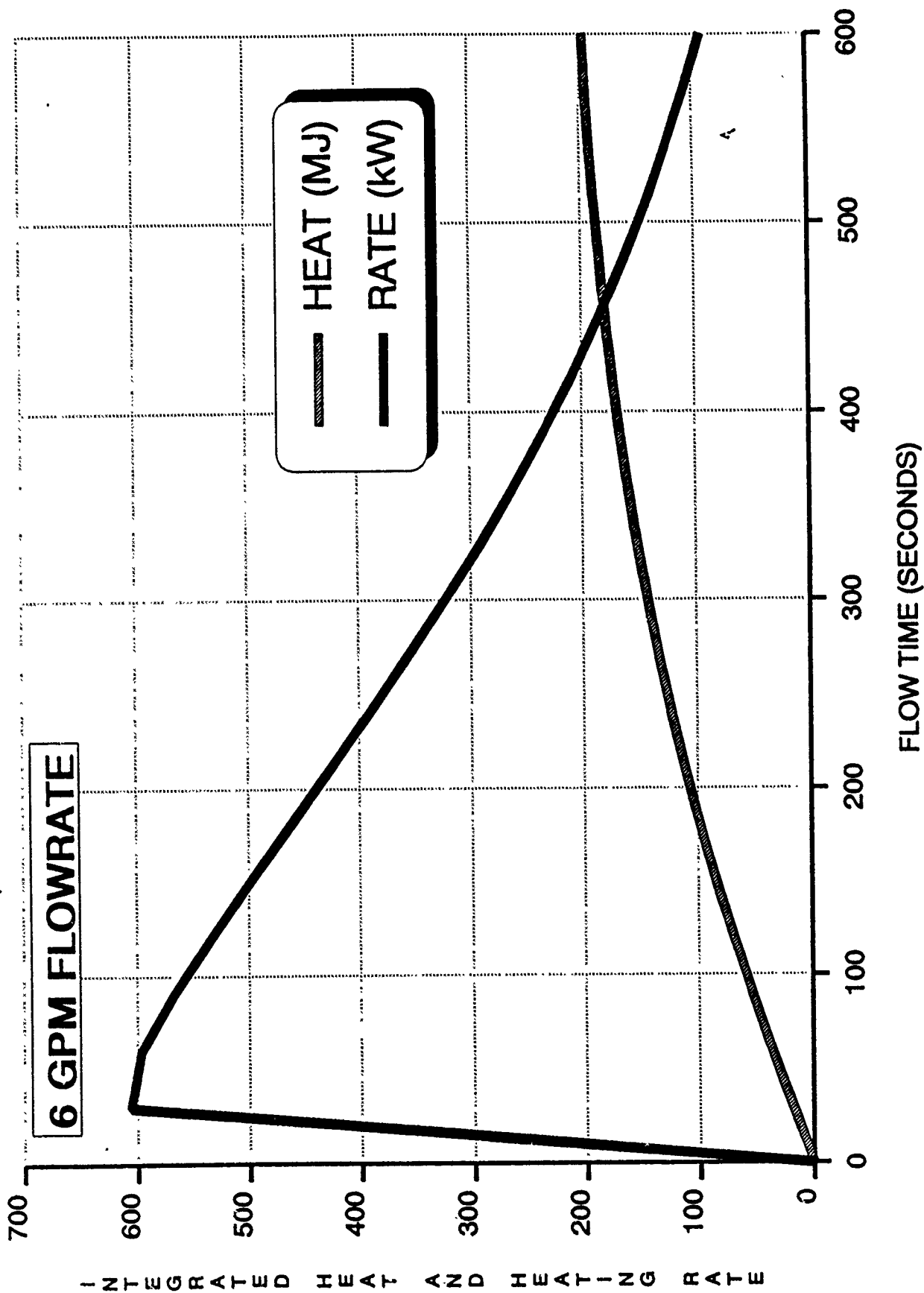
1/48TH SCALE PROTOTYPE PREDICTIONS - 01



PB01X-G

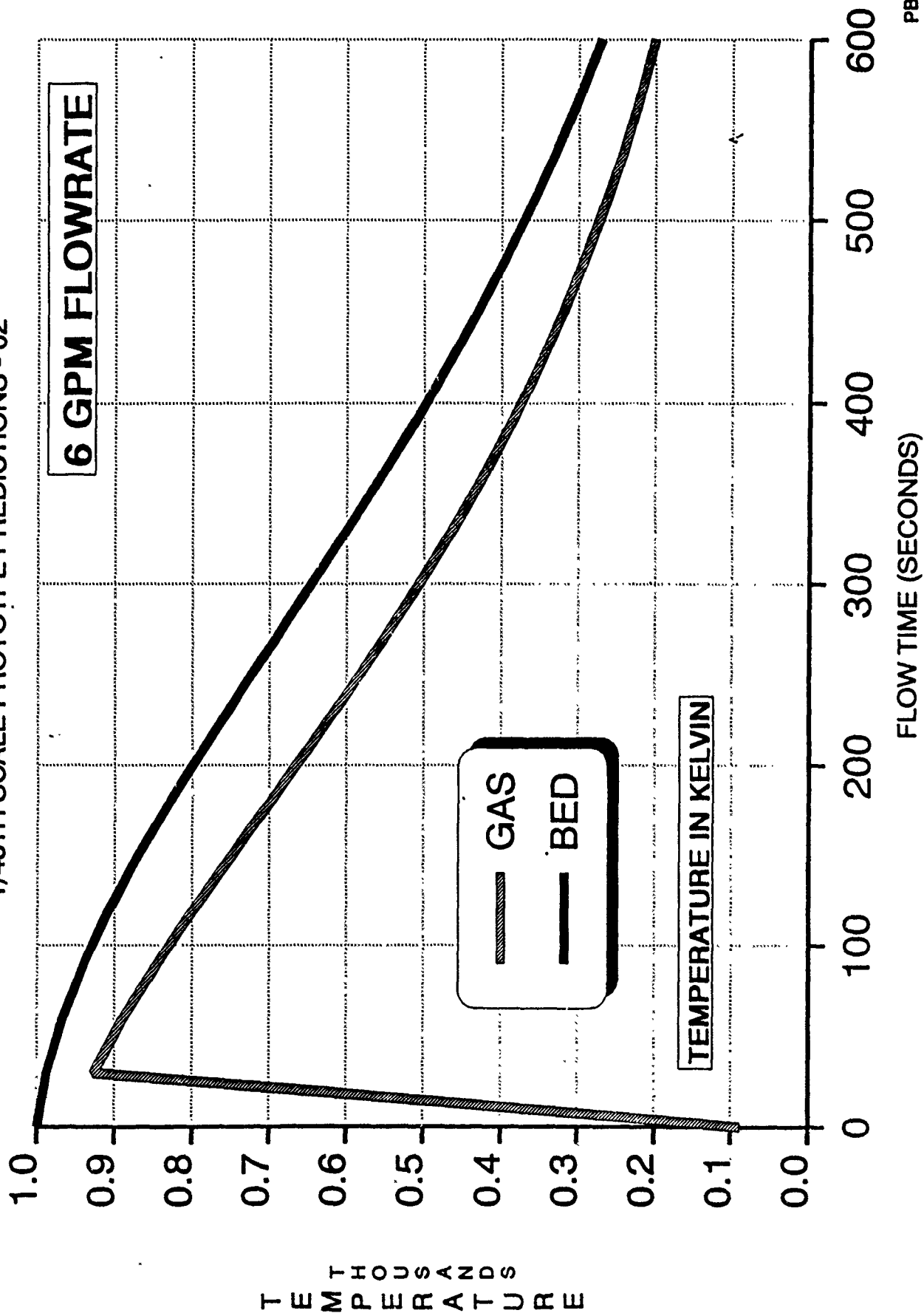
PEBBLE BED HEATER THERMAL PERFORMANCE

1/48TH SCALE PROTOTYPE PREDICTIONS - 02

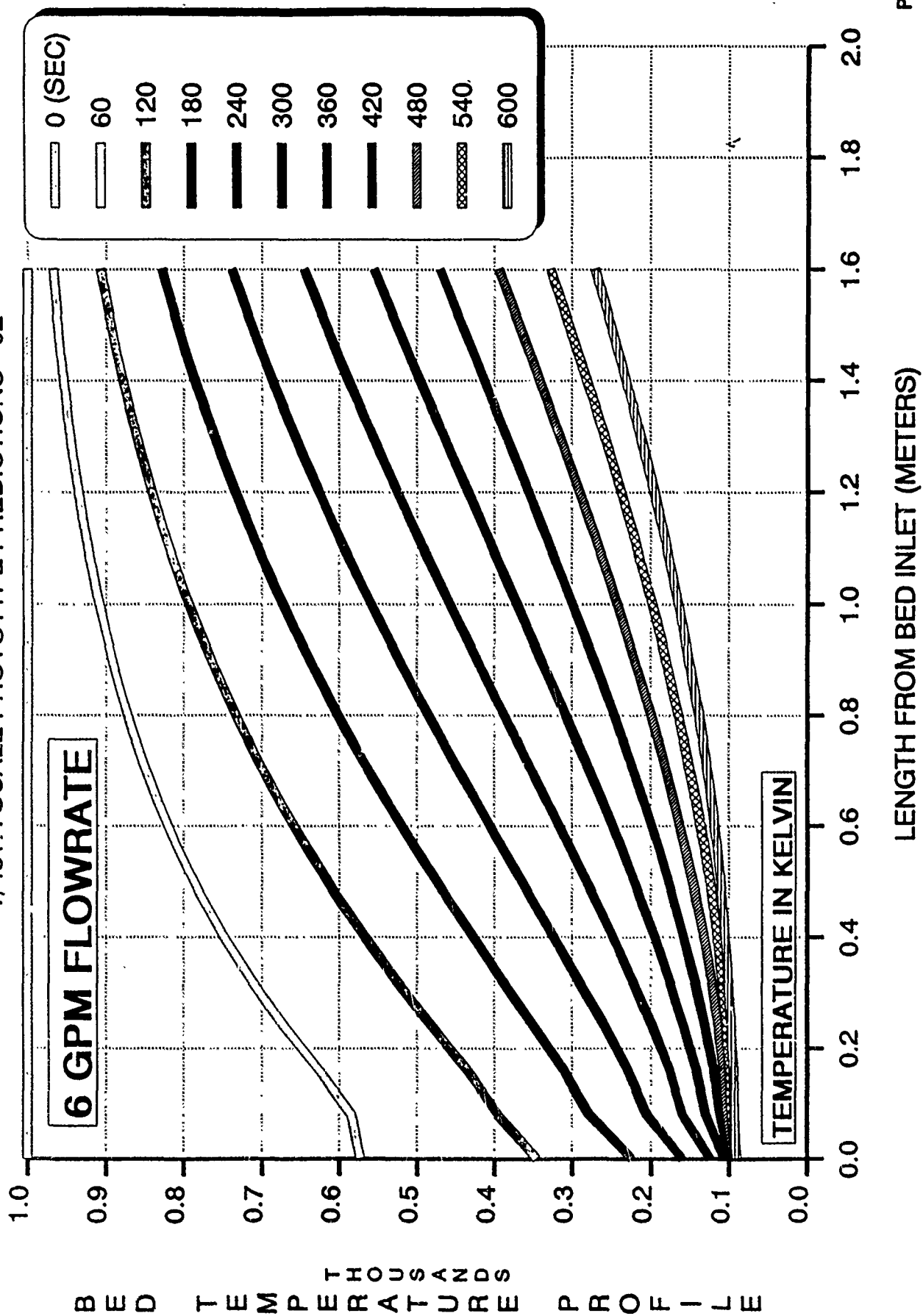


PEBBLE BED HEATER OUTLET TEMPERATURES

1/48TH SCALE PROTOTYPE PREDICTIONS - 02

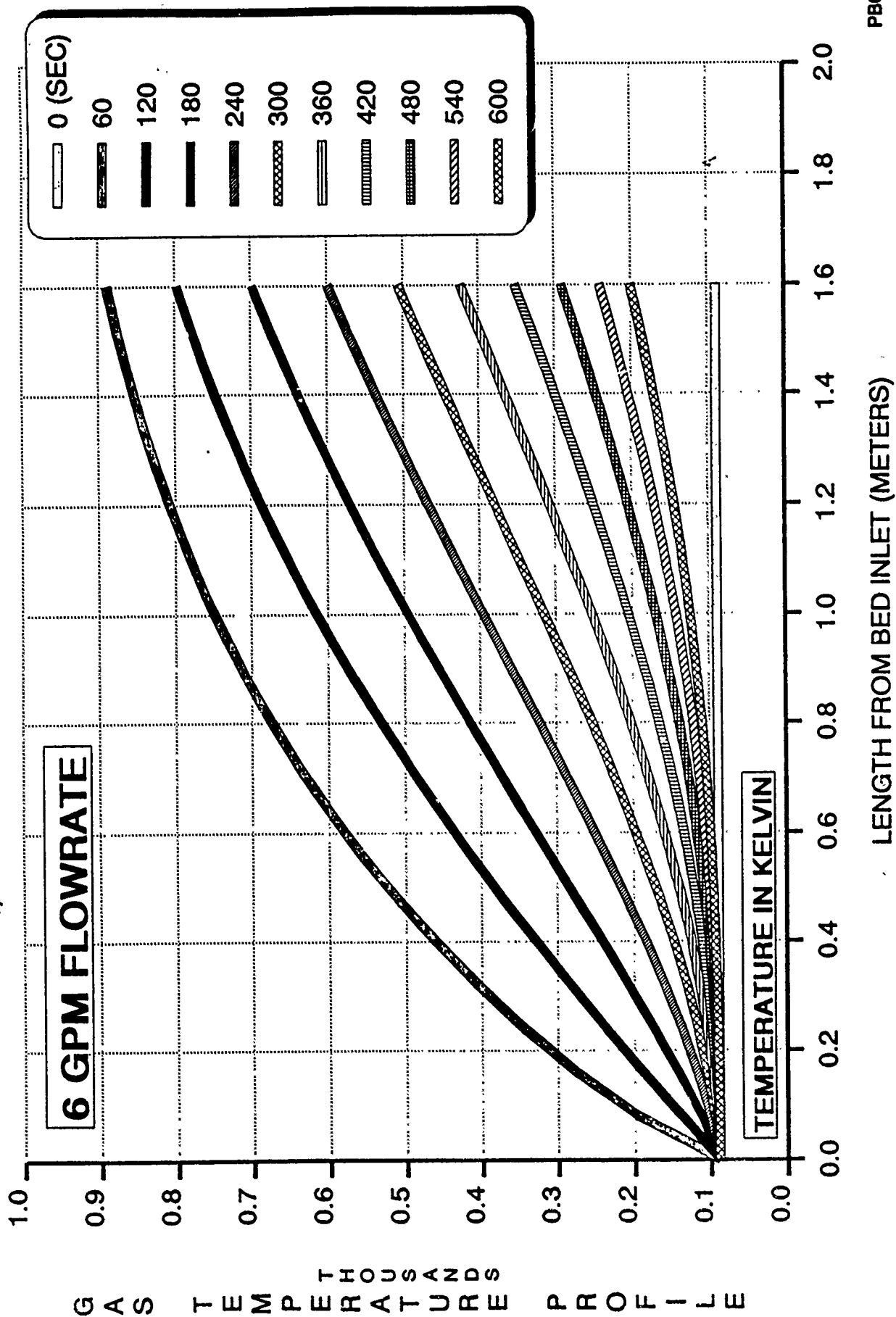


PEBBLE BED HEATER TEMPERATURE PROFILE 1/48TH SCALE PROTOTYPE PREDICTIONS - 02



PEBBLE BED HEATER TEMPERATURE PROFILE

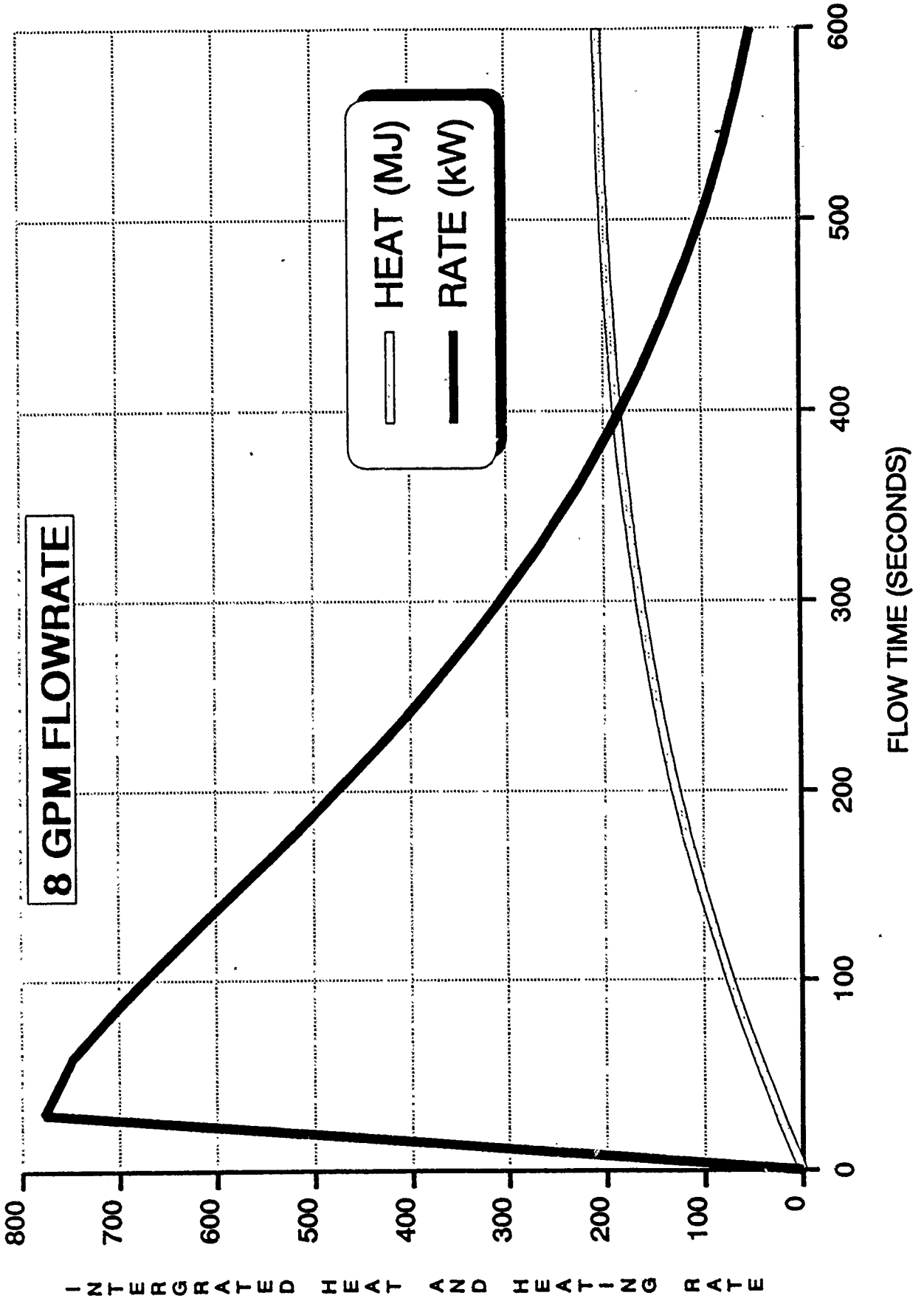
1/48TH SCALE PROTOTYPE PREDICTIONS - 02



PB02X-G

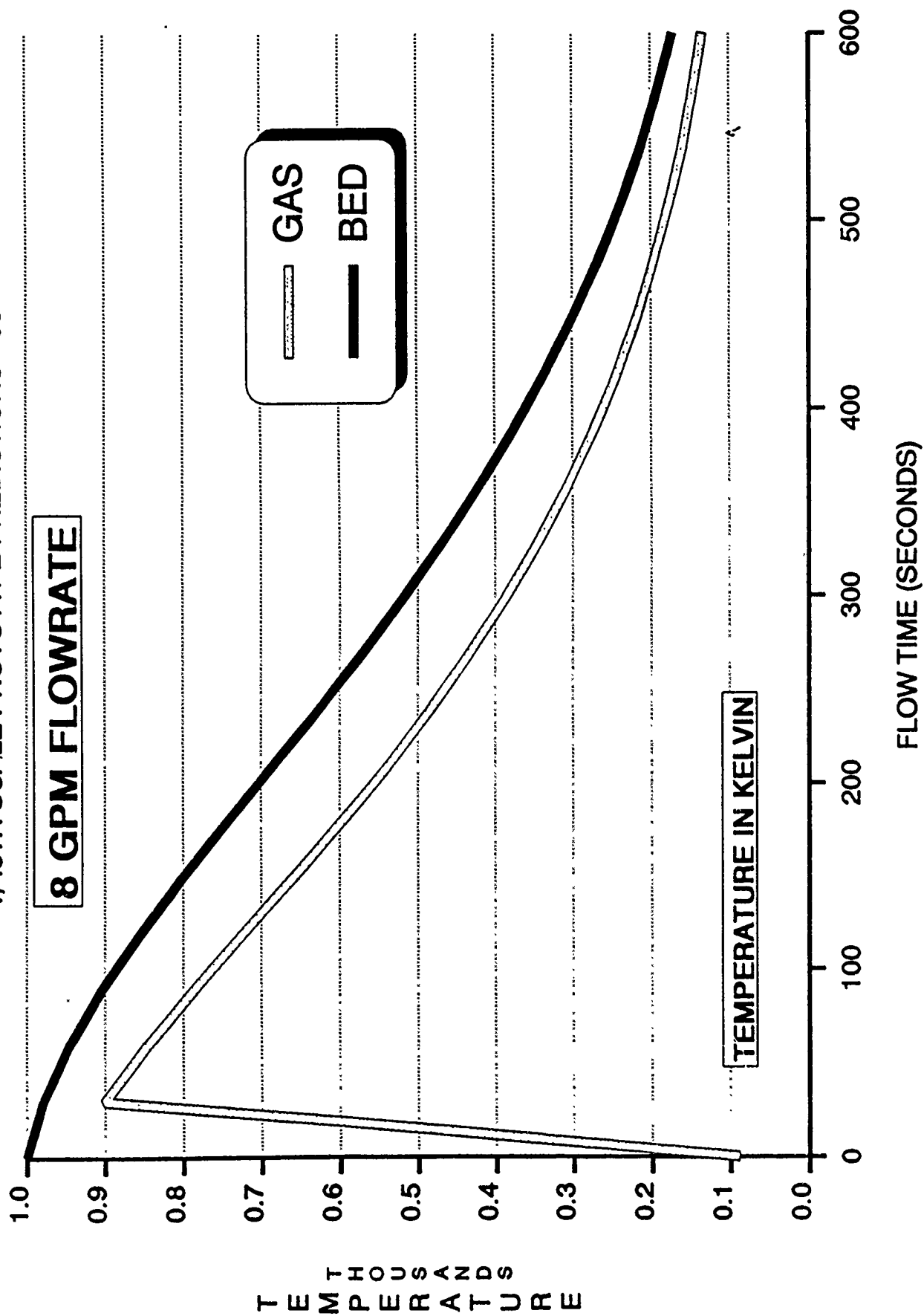
PEBBLE BED HEATER THERMAL PERFORMANCE

1/48TH SCALE PROTOTYPE PREDICTIONS - 03



8 GPM FLOWRATE

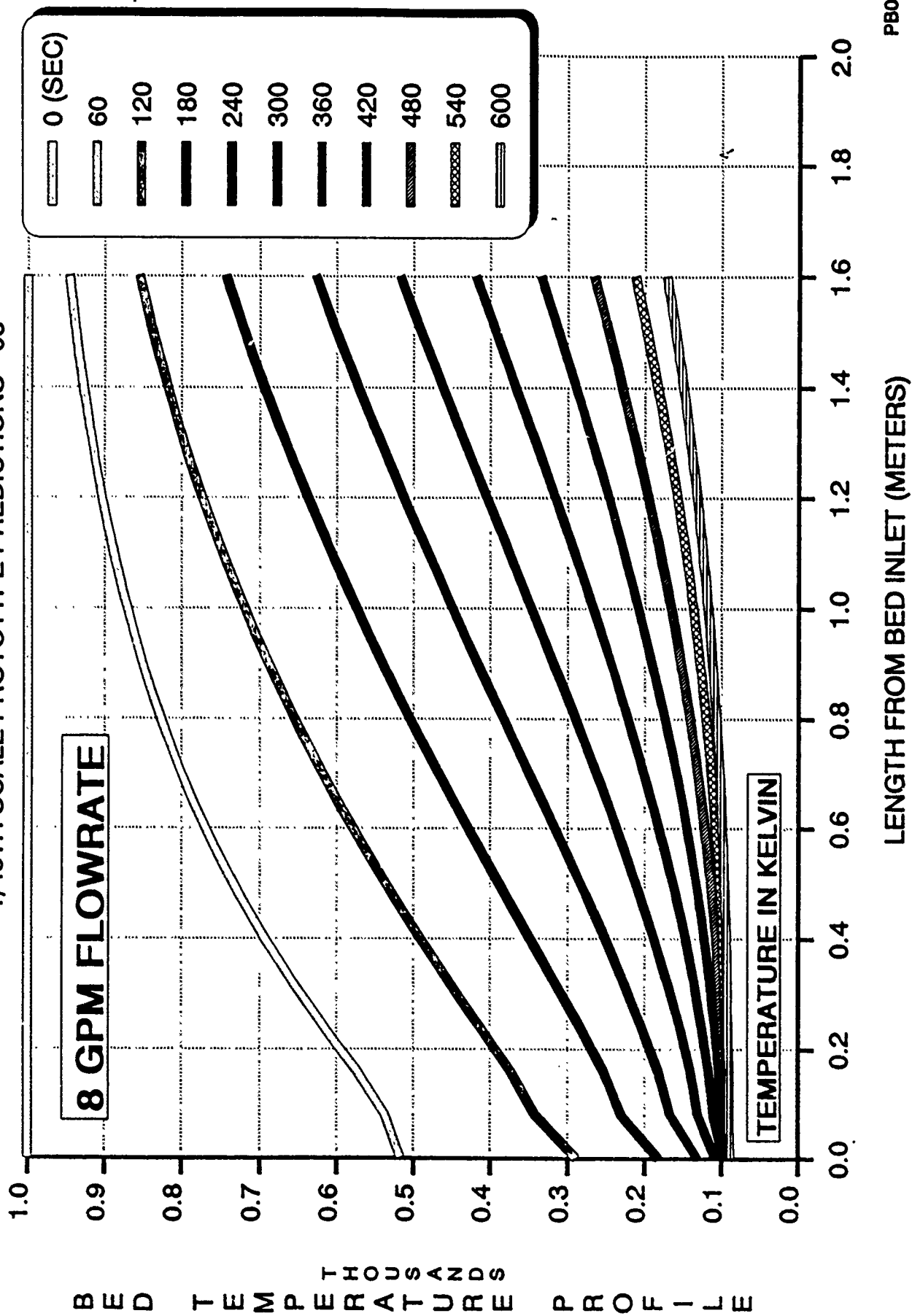
1/48TH SCALE PROTOTYPE PREDICTIONS - 03



PB03T-T

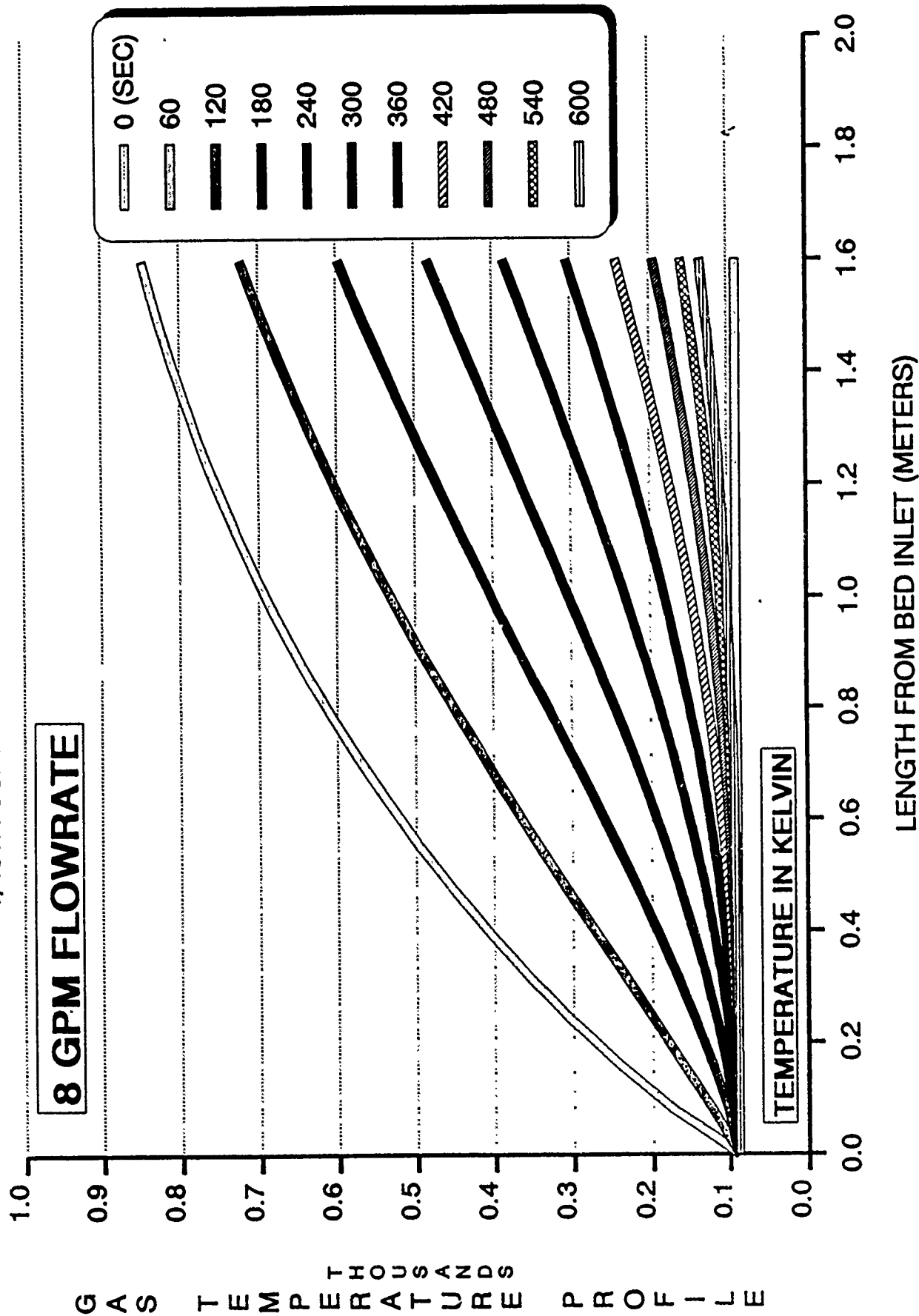
PEBBLE BED HEATER TEMPERATURE PROFILE

1/48TH SCALE PROTOTYPE PREDICTIONS - 03



PEBBLE BED HEATER TEMPERATURE PROFILE

1/48TH SCALE PROTOTYPE PREDICTIONS - 03



PB03X-G

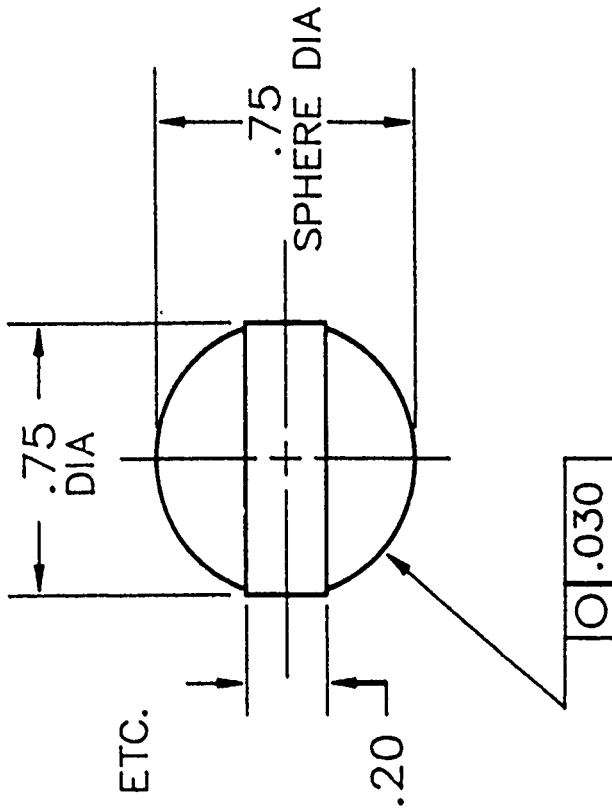
APPENDIX C - ENGINEERING DRAWINGS
FOR THE 1/48TH SCALE PEBBLE-BED EVAPORATOR/SUPERHEATER SYSTEM

INTENTIONALLY LEFT BLANK.

2

NOTES:

1. INTERPRET DWG PER MIL-STD-100
2. REMOVE ALL BURRS, GATES, FINES, ETC.
FLUSH WITH CONTOUR $\pm .030$
3. CAST SURFACES: 250
4. REMOVE ALL SHARP CORNERS
5. MUST BE FREE OF POROSITY
6. QTY 1000 LBS DELIVERED WT



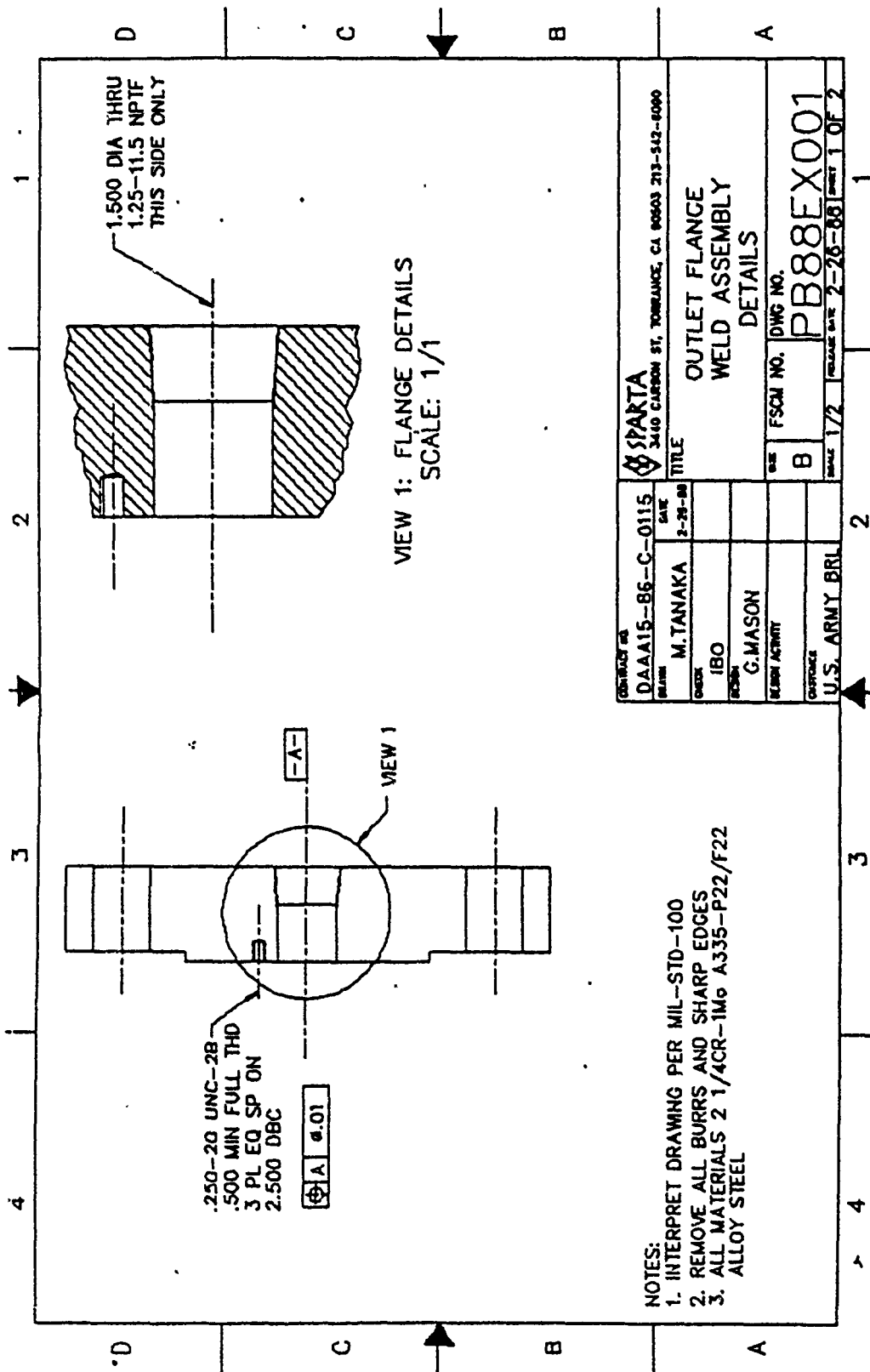
B

QTY REQD		FSCM NO.	PART OR IDENTIFYING NO.	IRON SPHERE	DUCTILE NI-RESIST IRON ALLOY D55	1
UNLESS OTHERWISE SPECIFIED DIMENSIONS ARE IN INCHES TOLERANCES		CONTRACT NO. DAAA15-86-C-0115		NOMENCLATURE OR DESCRIPTION	MATERIAL/SPECIFICATION	ITEM NO.
DECIMALS .XX $\pm .03$		DRAWN G.MASON		DATE 01-14-87	SPARTA, INCORPORATED	
ANGULAR .XXX $\pm .010$		CHECK		DESIGN	3440 CARSON ST, TORRANCE, CA 90503, 213-542-6090	
DO NOT SCALE DRAWING		DESIGN ACTIVITY BRL41-000		DATE 01-14-87	TITLE PEBBLE BED HEATER	
TREATMENT ANNEALED		CUSTOMER US Army BRL		SCALE 2/1	THERMAL STORAGE BALLS	
FINISH TUMBLED		CALC WT .06#		FSCM NO. A	DWG NO. PB87IB001	
SIMILAR TO		ACT WT		RELEASE DATE 1-15-87	SHEET 1 OF 1	

A

2

1



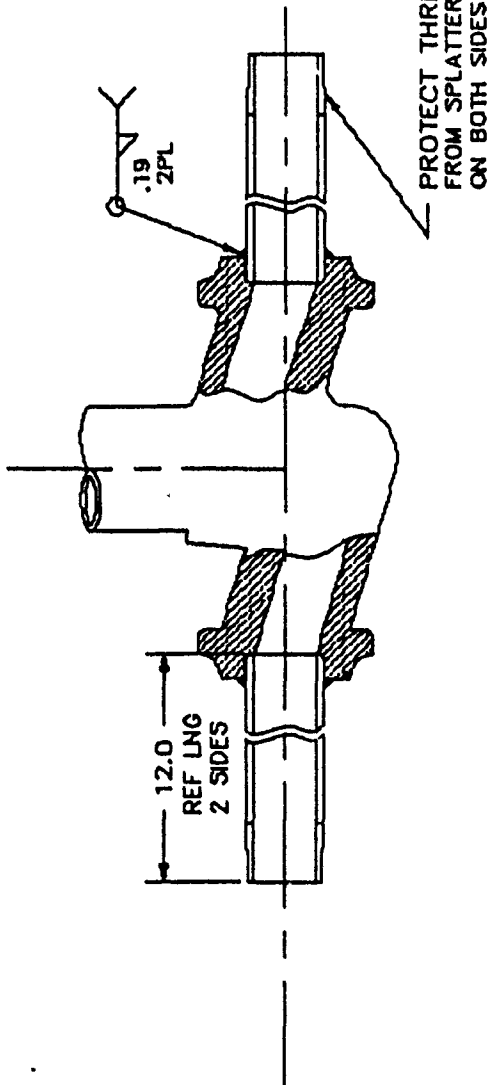
4 3 2 1

D

C

B

A



NOTES:

1. INTERPRET DRAWING PER MIL-STD-100
2. WELDS TO BE FREE OF SLAG AND DEBRIS
3. ALL MTLs 2 1/4CR-1Mo A335-P22/F22 ALLOY STEEL
4. USE EB015-B3 OR EQV. ELECTRODES
5. PROTECT THREADED ENDS OF PIPE FROM WELD SPLATTER OR DAMAGE.

CONTRACT NO. DAAA15-86-C-0115		DATE 1-29-88	
DESIGNER M. TANAKA		CHECK IBO	
DESIGN G. MASON		DESIGN AGENCY U.S. ARMY BRL	
CUSTOMER U.S. ARMY BRL		DATE 2-4-88	

SPARTA
3440 CARSON ST, TORRANCE, CA 90503 213-842-8090

TITLE

OUTLET VALVE
WELD ASSEMBLY

FSOM NO.

DWG NO.

PB88EX001

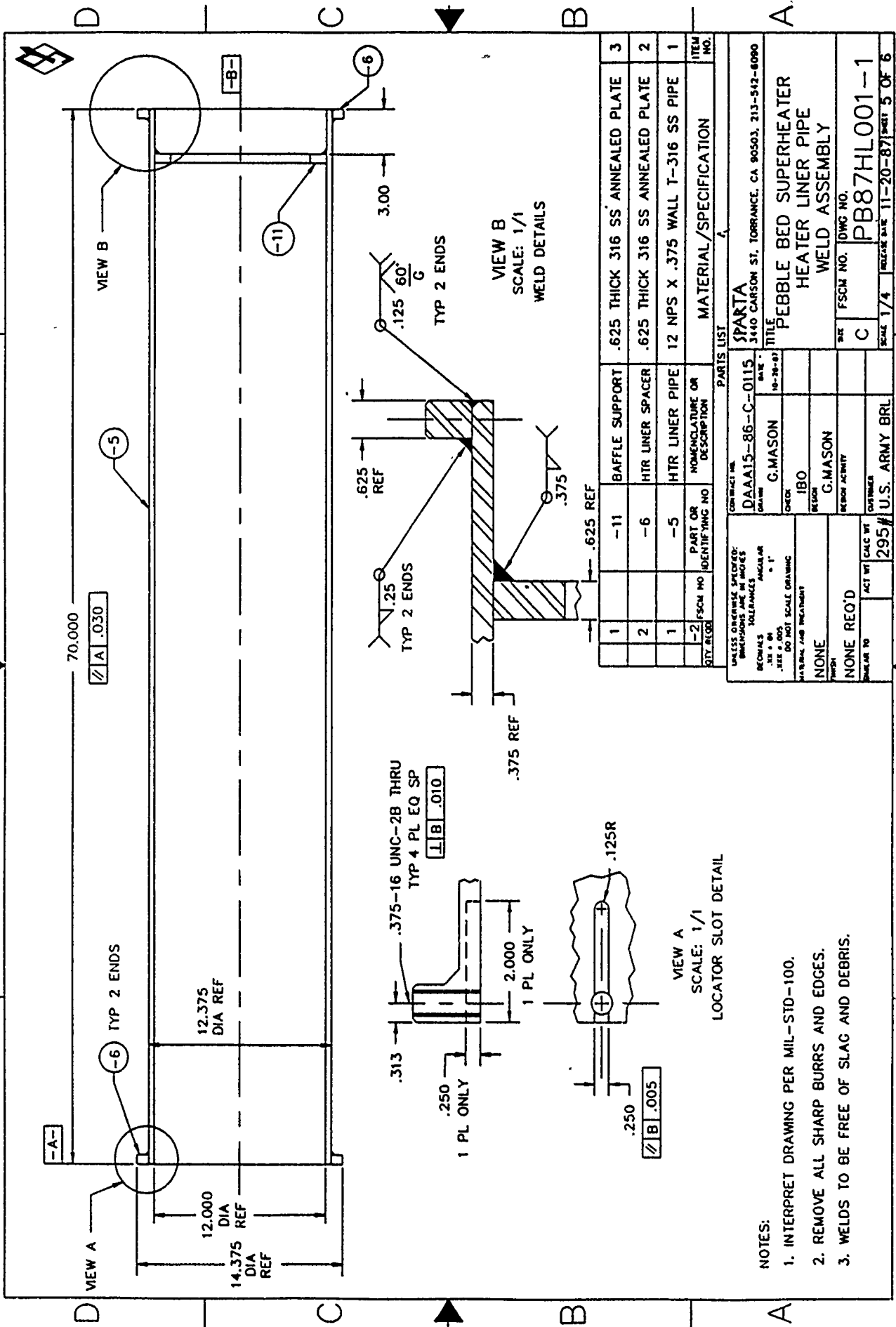
DATE 1/2 RELEASE DATE 2-4-88 SHEET 2 OF 2

2

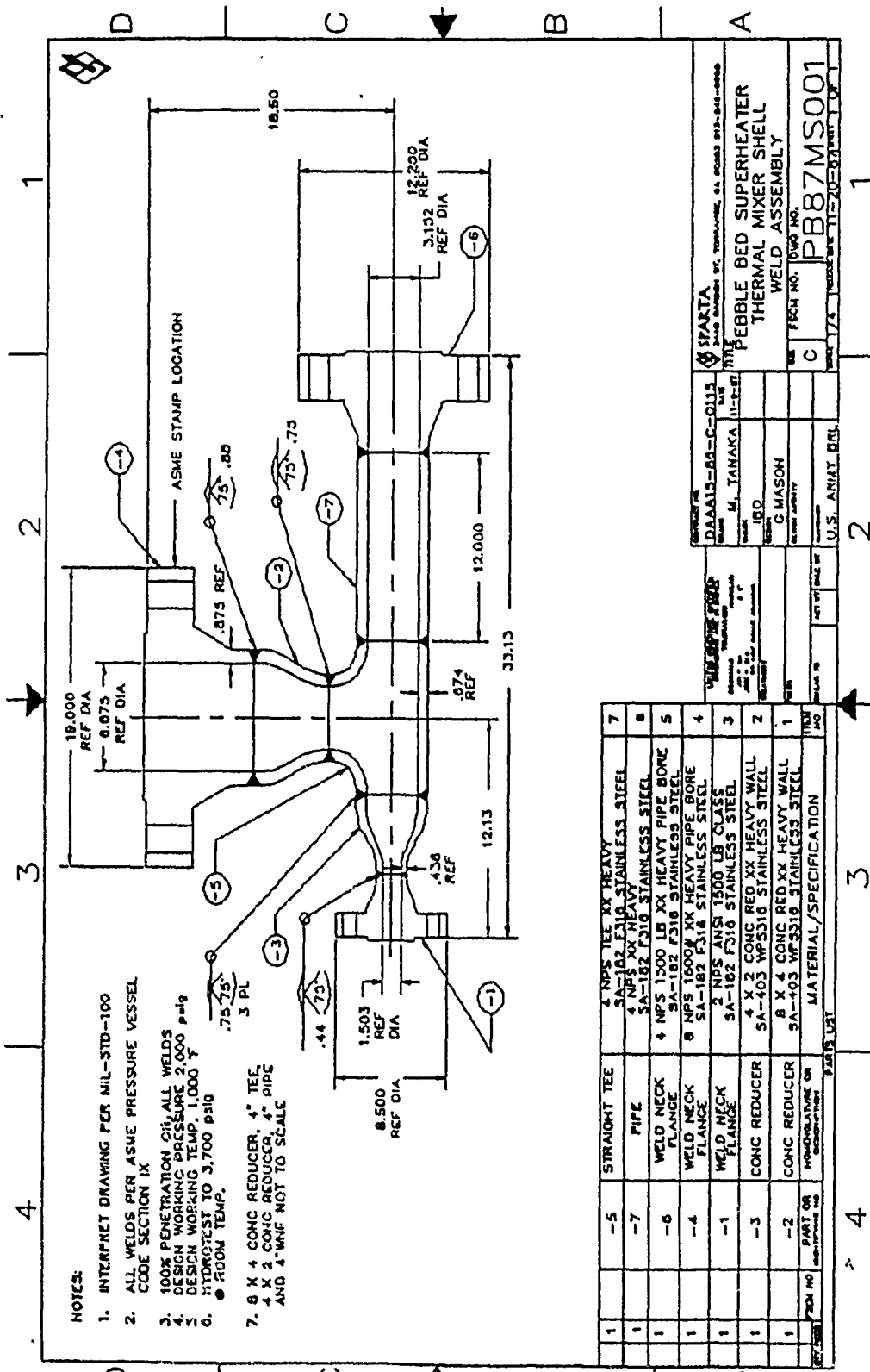
3

4

4 3 2 1



4 3 2 1



NOTES:

1. INTERPRET DRAWING PER MIL-STD-100
2. ALL WELDS PER ASME PRESSURE VESSEL CODE SECTION IX
3. 100% PENETRATION OF ALL WELDS
4. DESIGN WORKING PRESSURE 2,000 psig
5. DESIGN WORKING TEMP. 1,000 °F
6. HYDROTEST TO 3,700 PSIG @ ROOM TEMP.
7. 8 X 4 CONC REDUCER, 4" TEE, 4 X 2 CONC REDUCER, 4" PIPE AND 4" WHF NOT TO SCALE

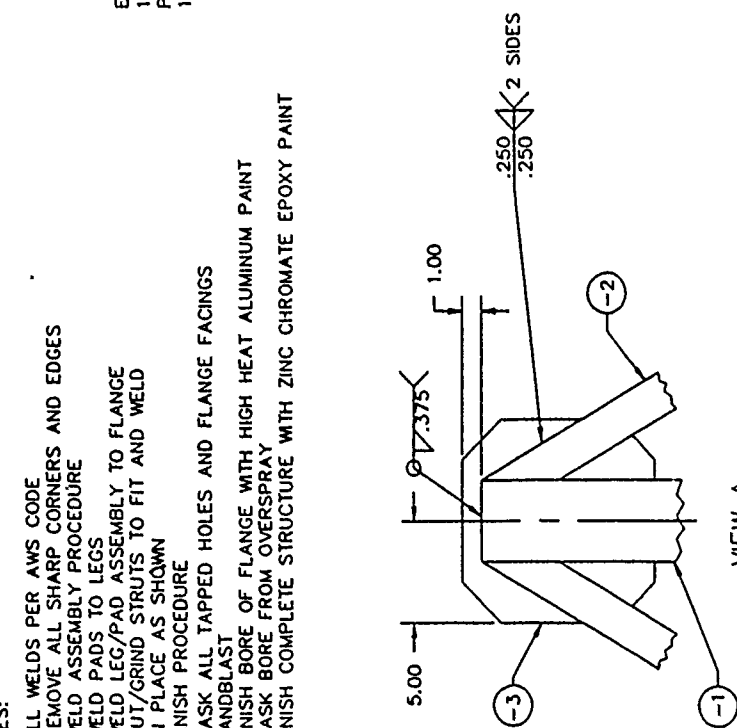
ITEM NO	DESCRIPTION	QUANTITY	UNIT
1	STRAIGHT TEE	4	NPS TEE XX HEAVY
2	PIPE	4	NPS XX HEAVY
3	WELD NECK FLANGE	4	NPS 1500 LB XX HEAVY PIPE BORE
4	WELD NECK FLANGE	8	NPS 1600A XX HEAVY PIPE BORE
5	WELD NECK FLANGE	2	NPS ANSI 1500 LB CLASS
6	CONC REDUCER	4	4 X 2 CONC RED XX HEAVY WALL
7	CONC REDUCER	8	8 X 4 CONC RED XX HEAVY WALL
8	WELD NECK FLANGE	4	4 X 2 CONC RED XX HEAVY WALL
9	WELD NECK FLANGE	8	8 X 4 CONC RED XX HEAVY WALL
10	WELD NECK FLANGE	4	4 X 2 CONC RED XX HEAVY WALL
11	WELD NECK FLANGE	8	8 X 4 CONC RED XX HEAVY WALL
12	WELD NECK FLANGE	4	4 X 2 CONC RED XX HEAVY WALL
13	WELD NECK FLANGE	8	8 X 4 CONC RED XX HEAVY WALL
14	WELD NECK FLANGE	4	4 X 2 CONC RED XX HEAVY WALL
15	WELD NECK FLANGE	8	8 X 4 CONC RED XX HEAVY WALL
16	WELD NECK FLANGE	4	4 X 2 CONC RED XX HEAVY WALL
17	WELD NECK FLANGE	8	8 X 4 CONC RED XX HEAVY WALL
18	WELD NECK FLANGE	4	4 X 2 CONC RED XX HEAVY WALL
19	WELD NECK FLANGE	8	8 X 4 CONC RED XX HEAVY WALL
20	WELD NECK FLANGE	4	4 X 2 CONC RED XX HEAVY WALL
21	WELD NECK FLANGE	8	8 X 4 CONC RED XX HEAVY WALL
22	WELD NECK FLANGE	4	4 X 2 CONC RED XX HEAVY WALL
23	WELD NECK FLANGE	8	8 X 4 CONC RED XX HEAVY WALL
24	WELD NECK FLANGE	4	4 X 2 CONC RED XX HEAVY WALL
25	WELD NECK FLANGE	8	8 X 4 CONC RED XX HEAVY WALL
26	WELD NECK FLANGE	4	4 X 2 CONC RED XX HEAVY WALL
27	WELD NECK FLANGE	8	8 X 4 CONC RED XX HEAVY WALL
28	WELD NECK FLANGE	4	4 X 2 CONC RED XX HEAVY WALL
29	WELD NECK FLANGE	8	8 X 4 CONC RED XX HEAVY WALL
30	WELD NECK FLANGE	4	4 X 2 CONC RED XX HEAVY WALL
31	WELD NECK FLANGE	8	8 X 4 CONC RED XX HEAVY WALL
32	WELD NECK FLANGE	4	4 X 2 CONC RED XX HEAVY WALL
33	WELD NECK FLANGE	8	8 X 4 CONC RED XX HEAVY WALL
34	WELD NECK FLANGE	4	4 X 2 CONC RED XX HEAVY WALL
35	WELD NECK FLANGE	8	8 X 4 CONC RED XX HEAVY WALL
36	WELD NECK FLANGE	4	4 X 2 CONC RED XX HEAVY WALL
37	WELD NECK FLANGE	8	8 X 4 CONC RED XX HEAVY WALL
38	WELD NECK FLANGE	4	4 X 2 CONC RED XX HEAVY WALL
39	WELD NECK FLANGE	8	8 X 4 CONC RED XX HEAVY WALL
40	WELD NECK FLANGE	4	4 X 2 CONC RED XX HEAVY WALL
41	WELD NECK FLANGE	8	8 X 4 CONC RED XX HEAVY WALL
42	WELD NECK FLANGE	4	4 X 2 CONC RED XX HEAVY WALL
43	WELD NECK FLANGE	8	8 X 4 CONC RED XX HEAVY WALL
44	WELD NECK FLANGE	4	4 X 2 CONC RED XX HEAVY WALL
45	WELD NECK FLANGE	8	8 X 4 CONC RED XX HEAVY WALL
46	WELD NECK FLANGE	4	4 X 2 CONC RED XX HEAVY WALL
47	WELD NECK FLANGE	8	8 X 4 CONC RED XX HEAVY WALL
48	WELD NECK FLANGE	4	4 X 2 CONC RED XX HEAVY WALL
49	WELD NECK FLANGE	8	8 X 4 CONC RED XX HEAVY WALL
50	WELD NECK FLANGE	4	4 X 2 CONC RED XX HEAVY WALL
51	WELD NECK FLANGE	8	8 X 4 CONC RED XX HEAVY WALL
52	WELD NECK FLANGE	4	4 X 2 CONC RED XX HEAVY WALL
53	WELD NECK FLANGE	8	8 X 4 CONC RED XX HEAVY WALL
54	WELD NECK FLANGE	4	4 X 2 CONC RED XX HEAVY WALL
55	WELD NECK FLANGE	8	8 X 4 CONC RED XX HEAVY WALL
56	WELD NECK FLANGE	4	4 X 2 CONC RED XX HEAVY WALL
57	WELD NECK FLANGE	8	8 X 4 CONC RED XX HEAVY WALL
58	WELD NECK FLANGE	4	4 X 2 CONC RED XX HEAVY WALL
59	WELD NECK FLANGE	8	8 X 4 CONC RED XX HEAVY WALL
60	WELD NECK FLANGE	4	4 X 2 CONC RED XX HEAVY WALL
61	WELD NECK FLANGE	8	8 X 4 CONC RED XX HEAVY WALL
62	WELD NECK FLANGE	4	4 X 2 CONC RED XX HEAVY WALL
63	WELD NECK FLANGE	8	8 X 4 CONC RED XX HEAVY WALL
64	WELD NECK FLANGE	4	4 X 2 CONC RED XX HEAVY WALL
65	WELD NECK FLANGE	8	8 X 4 CONC RED XX HEAVY WALL
66	WELD NECK FLANGE	4	4 X 2 CONC RED XX HEAVY WALL
67	WELD NECK FLANGE	8	8 X 4 CONC RED XX HEAVY WALL
68	WELD NECK FLANGE	4	4 X 2 CONC RED XX HEAVY WALL
69	WELD NECK FLANGE	8	8 X 4 CONC RED XX HEAVY WALL
70	WELD NECK FLANGE	4	4 X 2 CONC RED XX HEAVY WALL
71	WELD NECK FLANGE	8	8 X 4 CONC RED XX HEAVY WALL
72	WELD NECK FLANGE	4	4 X 2 CONC RED XX HEAVY WALL
73	WELD NECK FLANGE	8	8 X 4 CONC RED XX HEAVY WALL
74	WELD NECK FLANGE	4	4 X 2 CONC RED XX HEAVY WALL
75	WELD NECK FLANGE	8	8 X 4 CONC RED XX HEAVY WALL
76	WELD NECK FLANGE	4	4 X 2 CONC RED XX HEAVY WALL
77	WELD NECK FLANGE	8	8 X 4 CONC RED XX HEAVY WALL
78	WELD NECK FLANGE	4	4 X 2 CONC RED XX HEAVY WALL
79	WELD NECK FLANGE	8	8 X 4 CONC RED XX HEAVY WALL
80	WELD NECK FLANGE	4	4 X 2 CONC RED XX HEAVY WALL
81	WELD NECK FLANGE	8	8 X 4 CONC RED XX HEAVY WALL
82	WELD NECK FLANGE	4	4 X 2 CONC RED XX HEAVY WALL
83	WELD NECK FLANGE	8	8 X 4 CONC RED XX HEAVY WALL
84	WELD NECK FLANGE	4	4 X 2 CONC RED XX HEAVY WALL
85	WELD NECK FLANGE	8	8 X 4 CONC RED XX HEAVY WALL
86	WELD NECK FLANGE	4	4 X 2 CONC RED XX HEAVY WALL
87	WELD NECK FLANGE	8	8 X 4 CONC RED XX HEAVY WALL
88	WELD NECK FLANGE	4	4 X 2 CONC RED XX HEAVY WALL
89	WELD NECK FLANGE	8	8 X 4 CONC RED XX HEAVY WALL
90	WELD NECK FLANGE	4	4 X 2 CONC RED XX HEAVY WALL
91	WELD NECK FLANGE	8	8 X 4 CONC RED XX HEAVY WALL
92	WELD NECK FLANGE	4	4 X 2 CONC RED XX HEAVY WALL
93	WELD NECK FLANGE	8	8 X 4 CONC RED XX HEAVY WALL
94	WELD NECK FLANGE	4	4 X 2 CONC RED XX HEAVY WALL
95	WELD NECK FLANGE	8	8 X 4 CONC RED XX HEAVY WALL
96	WELD NECK FLANGE	4	4 X 2 CONC RED XX HEAVY WALL
97	WELD NECK FLANGE	8	8 X 4 CONC RED XX HEAVY WALL
98	WELD NECK FLANGE	4	4 X 2 CONC RED XX HEAVY WALL
99	WELD NECK FLANGE	8	8 X 4 CONC RED XX HEAVY WALL
100	WELD NECK FLANGE	4	4 X 2 CONC RED XX HEAVY WALL

SPARTAN
 2100 BROADWAY ST. TOWSON, MD 21204-3400
 TEL: 410-551-1100
 FAX: 410-551-1101
 E-MAIL: SPARTAN@AOL.COM
 WWW.SPARTAN-USA.COM

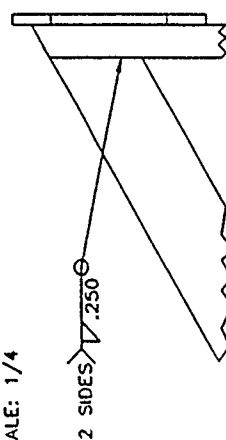
PROJECT NO. 0000 NO.
 SHEET NO. 0000 NO.
 DRAWING NO. PB87MS001

DESIGNED BY: G. MASON
 CHECKED BY: J. BO
 U.S. ARMY BEL

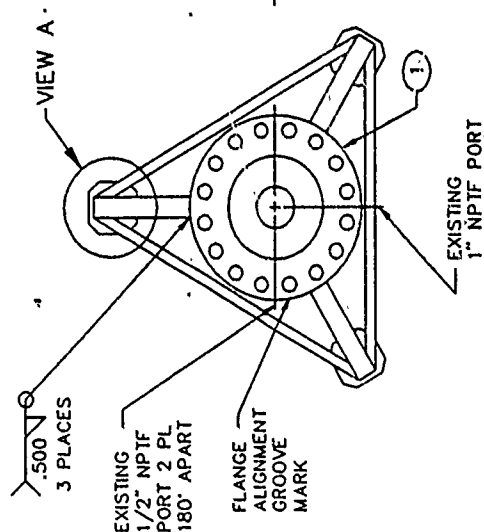
1. ALL WELDS PER AWS CODE
2. REMOVE ALL SHARP CORNERS AND EDGES
3. WELD ASSEMBLY PROCEDURE
- WELD PADS TO LEGS
- WELD LEG/PAD ASSEMBLY TO FLANGE
- CUT/GRIND STRUTS TO FIT AND WELD
- IN PLACE AS SHOWN
4. FINISH PROCEDURE
- MASK ALL TAPPED HOLES AND FLANGE FACE
- SANDBLAST
- FINISH BORE OF FLANGE WITH HIGH HEAT
- MASK BORE FROM OVERSPRAY
- FINISH COMPLETE STRUCTURE WITH ZINC CH



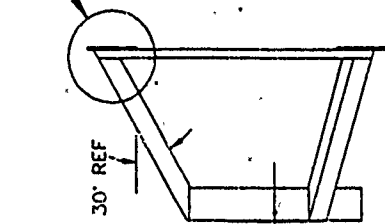
VIEW A
TYPICAL 3 PLACES
SCALE: 1/4"



VIEW B
TYPICAL 3 PLACES
SCALE: 1/4"



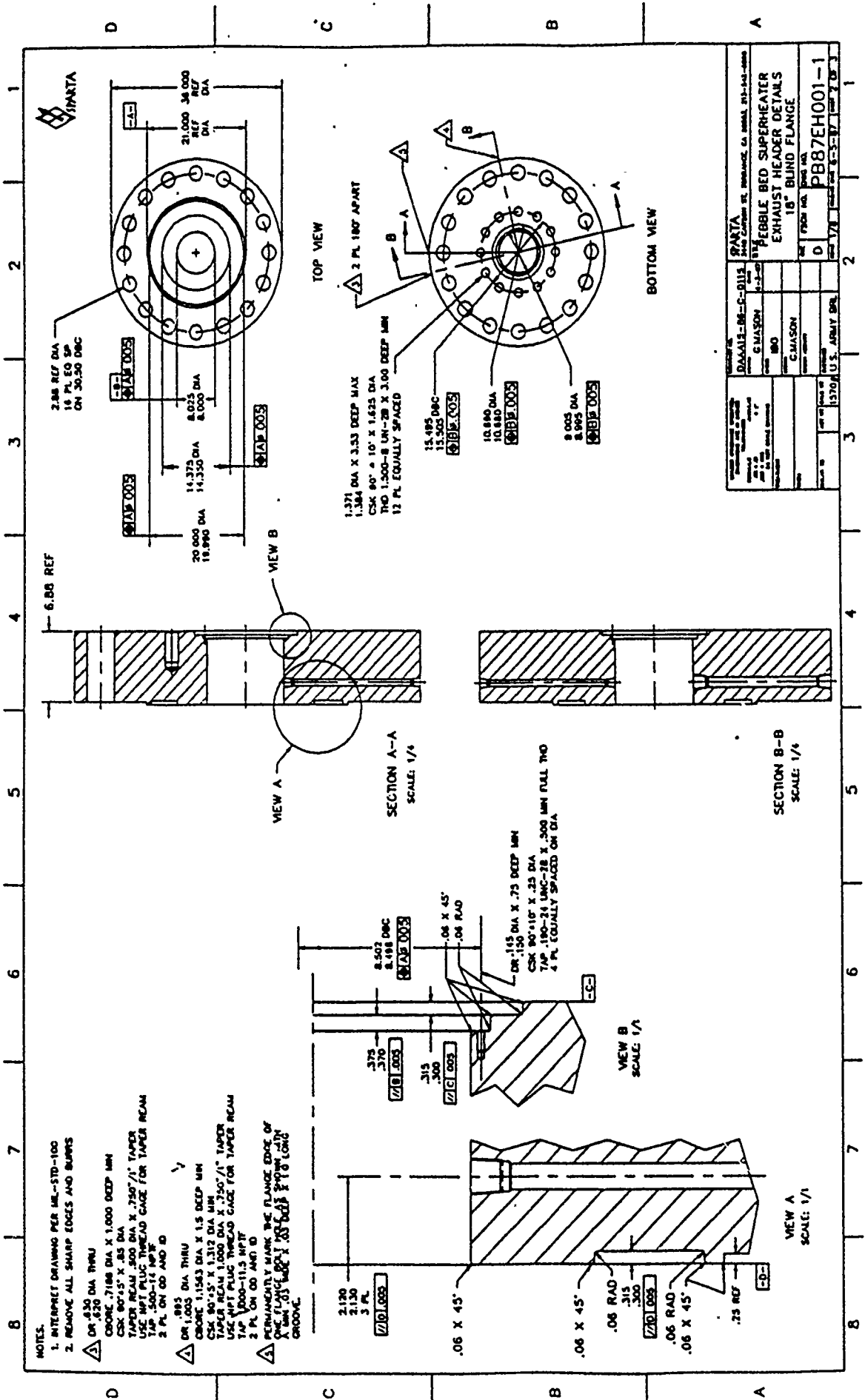
EXISTING
1" NPTF PORT



VIEW-B

ITEM NO.	MATERIAL / SPECIFICATION	ITEM NO.
1	18" ANSI 1800# BUND - A105 CAR STEEL	1
2	4x4x.500 SQUARE TUBE ASTM A529 CAR STEEL	2
3	2x2x.250 SQUARE TUBE ASTM A35 CAR STEEL	3
4	.500 THICK CARBON STEEL PLATE ASTM A36	4

UNLESS OTHERWISE SPECIFIED: DIMENSIONS ARE IN INCHES TOLERANCES ANGULAR X.XX ± .01 X.XX ± .01 X.XX DO NOT SCALE DRAWING	CONTRACT NO. DAAG15-86-C-0115 PARTS 0231	
ORIGINALS X.XX ± .01 X.XX ± .01 X.XX DO NOT SCALE DRAWING PREPARED BY NONE CHECKED BY NONE DESIGNED BY NONE DRAWN BY NONE DATE 6-22-87	DRAWN BY G.MASON	DATE 6-22-87
	CHECKED BY 180	DATE 6-22-87
	DESIGNED BY G.MASON	DATE 6-22-87
	DRAWN BY G.MASON	DATE 6-22-87
AS NOTED SIMILAR TO	ACT WT 330#	CALC WT 330#
CUSTOMER TO U.S. ARMY BRL	CUSTOMER U.S. ARMY BRL	SCALE 1/8"
FSCM NO. C	DWG NO. PB87EH001	SHEET OF 3
3440 CARSON ST., TORRANCE, CA 90501, 213-542-6090	PARTS 0231	DATE 6-22-87

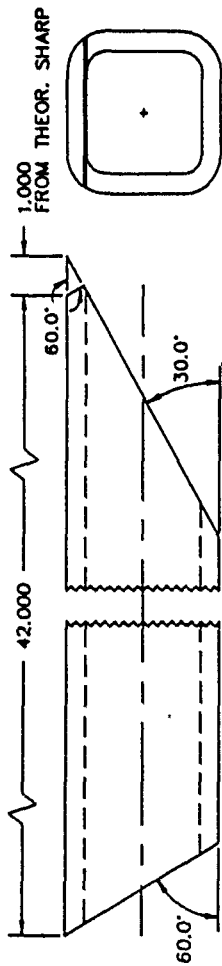


NOTES:

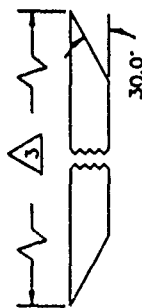
1. BREAK ALL SHARP CORNERS AND EDGES
2. REMOVE ALL BURRS



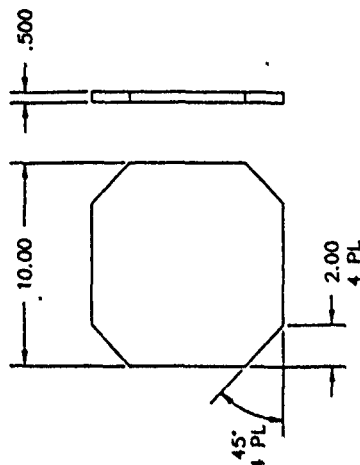
STRUT TO BE CUT TO FIT AS SHOWN IN
DWG NO. PB87EH001. APPROXIMATE DIMENSION
IS 63.75" TO BE USED FOR MATERIAL ESTIMATES
ONLY.



-1 SUPPORT BASE LEG
4 X 4 X .50 STRUC. STEEL TUBE
3 REQ'D
SCALE: 1/2



-3 SUPPORT BASE STRUT
2 X 2 X .25 STRUC. STEEL TUBE
3 REQ'D



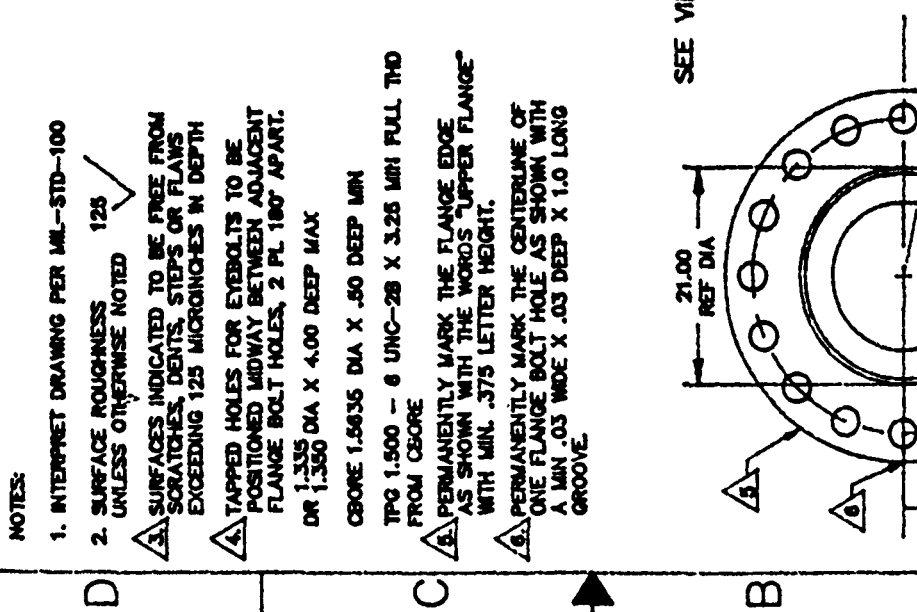
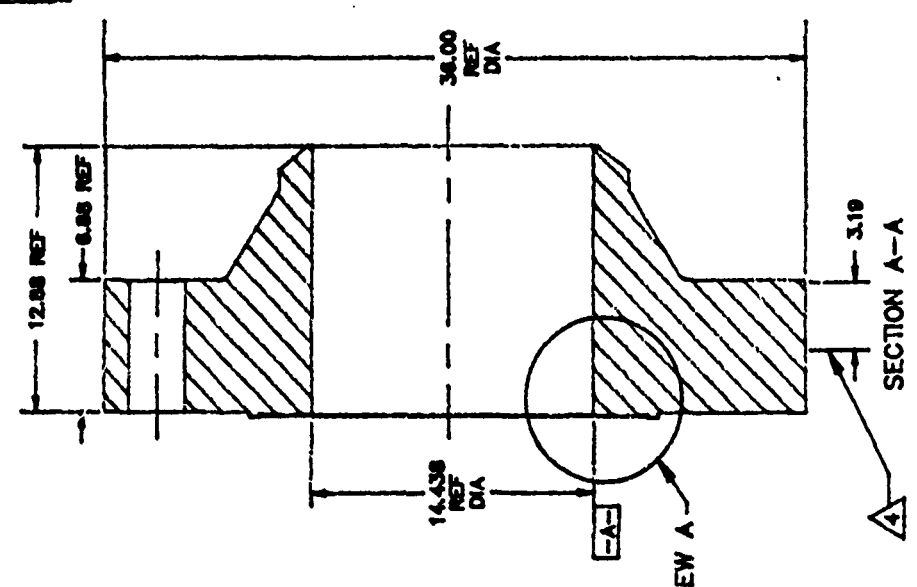
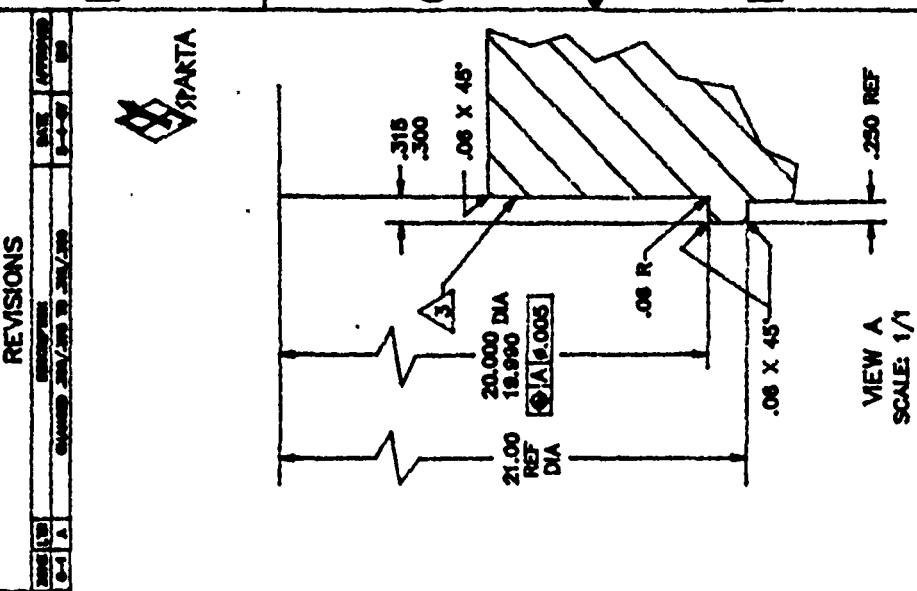
-2 SUPPORT BASE PAD
.500 STEEL PLATE
3 REQ'D



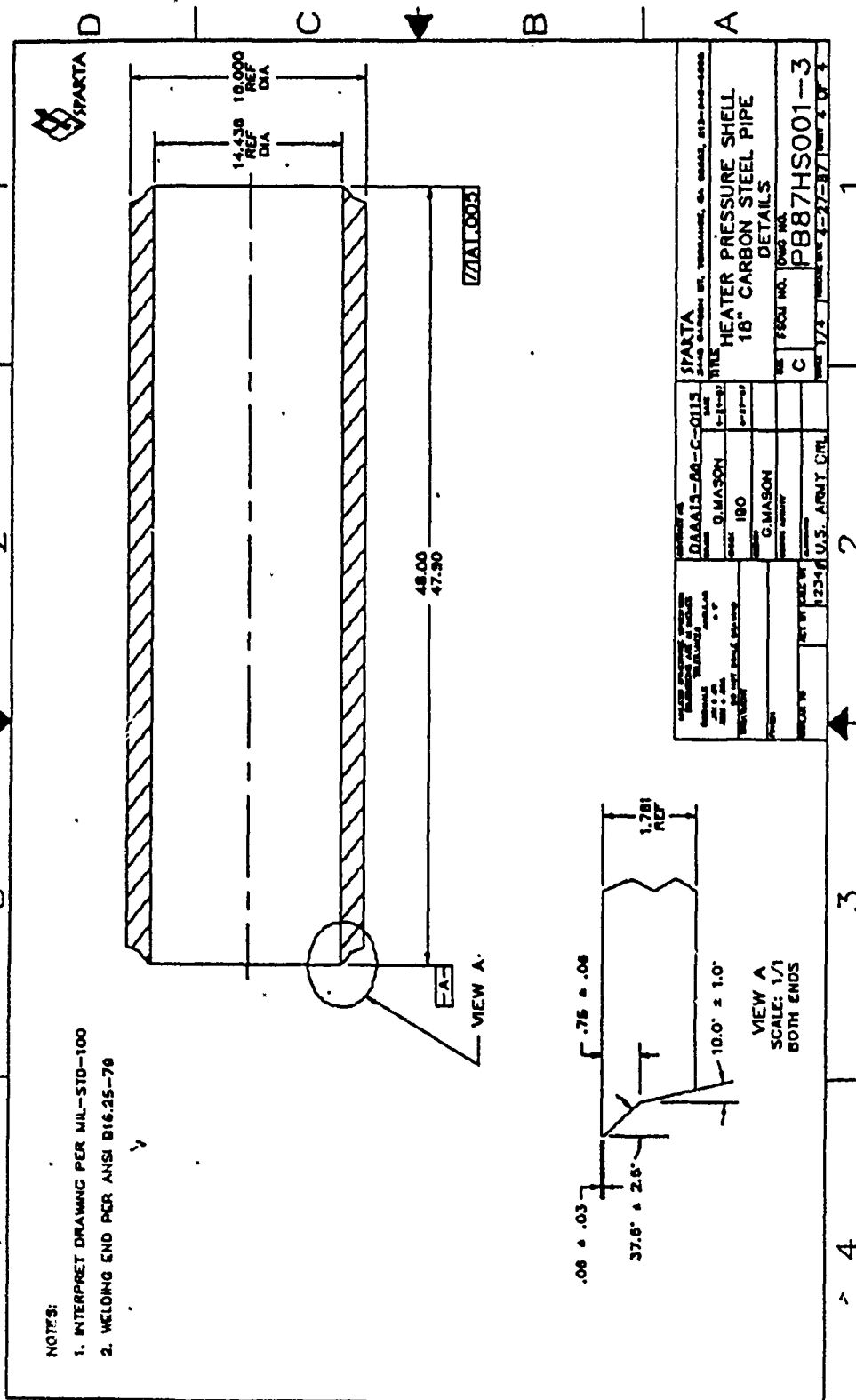
UNLESS OTHERWISE SPECIFIED, DIMENSIONS ARE IN INCHES DECIMALS FRACTIONS ANGLES		CONTRACT NO. DAAA15-86-C-0115		SPARTA 3440 CARSON ST. TORRANCE, CA 90503, 213-542-6090	
DATE JUL 8 1986	BY G. MASON	DATE 6-22-87	TITLE PEBBLE BED SUPERHEATER EXHAUST HEADER BASE LEG SUPPORT DETAILS		
REVISION NONE REQ'D	DESIGN IBO	DESIGN G. MASON	SIZE C	FSCM NO. PB87EH001-2,3,4	DWG NO. PB87EH001-2,3,4
APPROVED TO NONE REQ'D	ACT ON CALC WT 360#	CUSTOMER U.S. ARMY BRL	SCALE 1/4	RELEASE DATE 6-23-87	
		SHEET 3 OF 3			

NOTES:

1. INTERNET DRAWING PER MIL-STD-100
2. SURFACE ROUGHNESS 125
UNLESS OTHERWISE NOTED
3. SURFACES INDICATED TO BE FREE FROM SCRATCHES, DENTS, STEPS OR FLAWS EXCEEDING 125 MICROINCHES IN DEPTH
4. TAPPED HOLES FOR EYEBOLTS TO BE POSITIONED MIDWAY BETWEEN ADJACENT FLANGE BOLT HOLES, 2 PL 180° APART.
DR 1.335 DIA X 4.00 DEEP MAX
OR 1.350
5. CBORE 1.5635 DIA X .50 DEEP MIN
TPG 1.500 - 6 UNC-28 X 3.25 MIN FULL THD FROM CBORE
6. PERMANENTLY MARK THE FLANGE EDGE AS SHOWN WITH THE WORDS "UPPER FLANGE" WITH MIN. .375 LETTER HEIGHT.
7. PERMANENTLY MARK THE CENTERLINE OF ONE FLANGE BOLT HOLE AS SHOWN WITH A MIN. .03 WIDE X .03 DEEP X 1.0 LONG GROOVE.



SPARTA		HEATER PRESSURE SHELL		UPPER 18" WELD NECK FLANGE	
DAAAL5-88-C-0115		Q/MASON		IBO	
Q/MASON		IBO		Q/MASON	
1625		U.S. ARMY BPL		PB87HS001-1	
1625		U.S. ARMY BPL		PB87HS001-1	



REFERENCES

1. Photograph of LB/TS facility courtesy of the US Army Ballistics Research Laboratory.
2. Support of the Characterization of the LB/TS Facility; August 1985; Technical Report DNA-TR-85-259
3. Letter report from Richard Pearson/BRL; 29 October 1986
4. Letter report from Richard Pearson/BRL dated 23 January 1987
5. Holman, J.P., "Heat Transfer", 4th edition, McGraw-Hill, 1976.
6. Thermal Energy Storage and Regeneration; F.W. Schmidt & A.J. Willmott; McGraw-Hill; 1981
7. "Handbook of Heat Transfer", W. M. Rohsenow & J. P. Hartnett eds., McGraw-Hill, 1973, Section 14
8. Taken from: Liquid Carbonic Corporation Data Sheet No. 6760, pages 16 and 17, dated 1983.
9. Pebble-bed Evaporator/Superheater Test Plan and Operations Manual, SPARTA Report # LA-88-09-TR, May 1988

INTENTIONALLY LEFT BLANK.

<u>No of</u> <u>Copies</u>	<u>Organization</u>	<u>No of</u> <u>Copies</u>	<u>Organization</u>
2	Administrator Defense Technical Info Center ATTN: DTIC-DDA Cameron Station Alexandria, VA 22304-6145	1	Commander U.S. Army Missile Command ATTN: AMSMI-RD-CS-R (DOC) Redstone Arsenal, AL 35898-5010
1	HQDA (SARD-TR) WASH DC 20310-0001	1	Commander U.S. Army Tank-Automotive Command ATTN: ASQNC-TAC-DIT (Technical Information Center) Warren, MI 48397-5000
1	Commander U.S. Army Materiel Command ATTN: AMCDRA-ST 5001 Eisenhower Avenue Alexandria, VA 22333-0001	1	Director U.S. Army TRADOC Analysis Command ATTN: ATRC-WSR White Sands Missile Range, NM 88002-5502
1	Commander U.S. Army Laboratory Command ATTN: AMSLC-DL 2800 Powder Mill Road Adelphi, MD 20783-1145	(Class. only)1	Commandant U.S. Army Infantry School ATTN: ATSH-CD (Security Mgr.) Fort Benning, GA 31905-5660
2	Commander U.S. Army Armament Research, Development, and Engineering Center ATTN: SMCAR-IMI-I Picatinny Arsenal, NJ 07806-5000	(Unclass. only)1	Commandant U.S. Army Infantry School ATTN: ATSH-CD-CSO-OR Fort Benning, GA 31905-5660
2	Commander U.S. Army Armament Research, Development, and Engineering Center ATTN: SMCAR-TDC Picatinny Arsenal, NJ 07806-5000	1	Air Force Armament Laboratory ATTN: AFATL/DLODL Eglin AFB, FL 32542-5000 <u>Aberdeen Proving Ground</u>
1	Director Benet Weapons Laboratory U.S. Army Armament Research, Development, and Engineering Center ATTN: SMCAR-CCB-TL Watervliet, NY 12189-4050	2	Dir, USAMSAA ATTN: AMXSY-D AMXSY-MP, H. Cohen
1	Commander U.S. Army Armament, Munitions and Chemical Command ATTN: SMCAR-ESP-L Rock Island, IL 61299-5000	1	Cdr, USATECOM ATTN: AMSTE-TD
1	Director U.S. Army Aviation Research and Technology Activity ATTN: SAVRT-R (Library) M/S 219-3 Ames Research Center Moffett Field, CA 94035-1000	3	Cdr, CRDEC, AMCCOM ATTN: SMCCR-RSP-A SMCCR-MU SMCCR-MSI
		1	Dir, VLAMO ATTN: AMSLC-VL-D
		10	Dir, BRL ATTN: SLCBR-DD-T

DISTRIBUTION LIST

<u>No. of</u> <u>Copies</u>	<u>Organization</u>	<u>No. of</u> <u>Copies</u>	<u>Organization</u>
1	Director of Defense Research & Engineering ATTN: DD/TWP Washington, DC 20301	1	Director Defense Intelligence Agency ATTN: DT-2/Wpns & Sys Div Washington, DC 20301
1	Assistant Secretary of Defense (Atomic Energy) ATTN: Document Control Washington, DC 20301	1	Director National Security Agency ATTN: R15, E. F. Butala Ft. George G. Meade, MD 20755
1	Chairman Joint Chiefs of Staff ATTN: J-5, R&D Division Washington, DC 20301	2	Administrator Defense Technical Information Center ATTN: DTIC-DDA Cameron Station Alexandria, VA 22304-6145
2	Deputy Chief of Staff for Operations and Plans ATTN: Technical Library Director of Chemical and Nuclear Operations Department of the Army Washington, DC 20310	7	Director Defense Nuclear Agency ATTN: CSTI, Tech Lib DDIR DFSP, Ullrich NANS OPNA SPSD SPTD, Hrinishin Washington, DC 20305
1	European Research Office USARDSG (UK) ATTN: Dr. R. Reichenbach Box 65 FPO New York 09510-1500	3	Commander Field Command, DNA ATTN: FCPR FCTMOF NMHE, CDR Lund Kirtland AFB, NM 87115
1	Director Defense Advanced Research Projects Agency ATTN: Tech Lib 1400 Wilson Boulevard Arlington, VA 22209	10	Central Intelligence Agency DIR/DB/Standard ATTN: GE-47 HQ Washington, DC 20505
2	Director Federal Emergency Management Agency ATTN: Public Relations Office Technical Library Washington, DC 20472	4	Director US Army Harry Diamond Labs ATTN: SLCHD-NW-RA, Belliveau SLCHD-NW-P, Abbe Patnaik Corrigan SLCHD-TA-L, Tech Lib 2800 Powder Mill Road Adelphi, MD 20783-1197
1	Chairman DOD Explosives Safety Board Room 856-C Hoffman Bldg. 1 2461 Eisenhower Avenue Alexandria, VA 22331-0600		

DISTRIBUTION LIST

<u>No. of</u> <u>Copies</u>	<u>Organization</u>	<u>No. of</u> <u>Copies</u>	<u>Organization</u>
2	Commander, USACECOM ATTN: AMSEL-RD AMSEL-RO-TPPO-P Fort Monmouth, NJ 07703-5301	1	Commander US Army Engineer Division ATTN: HNDED-FD P.O. Box 1500 Huntsville, AL 35807
1	Commander, USACECOM R&D Technical Library ATTN: ASQNC-ELC-I-T, Myer Center Fort Monmouth, NJ 07703-5301	3	Commander US Army Corps of Engineers Waterways Experiment Station ATTN: CAWES-SS-R, J. Watt CAWES-SE-R, J. Ingram CAWES-TL, Tech Lib) P.O. Box 631 Vicksburg, MS 39180-0631
1	Director US Army Missile and Space Intelligence Center ATTN: AIAMS-YDL Redstone Arsenal, AL 35898-5500		
1	Commander US Army Foreign Science and Technology Center ATTN: Research & Data Branch 220 7th Street, NE Charlottesville, VA 22901-5396	1	Commander US Army Corps of Engineers Fort Worth District ATTN: CESWF-PM-J, R. Timmermins P.O. Box 17300 Fort Worth, Texas 76102-0300
1	Director US Army TRAC - Ft. Lee ATTN: ATRC-L, Mr. Cameron Fort Lee, VA 23801-6140	1	Commander US Army Research Office ATTN: SLCRO-D P.O. Box 12211 Research Triangle Park, NC 27709-2211
1	Director US Army Materials Technology Laboratory ATTN: AMXMR-ATL Watertown, MA 02172-0001	3	Commander US Army Nuclear & Chemical Agency ATTN: ACTA-NAW MONA-WE Tech. Lib. 7500 Backlick Rd, Bldg. 2073 Springfield, VA 22150
2	Commander US Army Strategic Defense Command ATTN: CSSD-H-MPL, Tech Lib CSSD-H-XM, Dr. Davies P.O. Box 1500 Huntsville, AL 35807	1	Director HQ, TRAC RPD ATTN: ATRC-RPR, Radda Fort Monroe, VA 23651-5143
2	Commander US Army Natick Research and Development Center ATTN: AMDNA-D, Dr. D. Sieling STRNC-UE, J. Calligeros Natick, MA 01762	1	Director TRAC-WSMR ATTN: ATRC-WC, Kirby White Sands Missile Range, NM 88002-5502

DISTRIBUTION LIST

<u>No. of</u> <u>Copies</u>	<u>Organization</u>	<u>No. of</u> <u>Copies</u>	<u>Organization</u>
1	Director TRAC-FLVN ATTN: ATRC Fort Leavenworth, KS 66027-5200	1	Officer-in-Charge Naval Construction Battalion Center Civil Engineering Laboratory ATTN: Tech Lib, Code LO6C/LO8A Port Hueneme, CA 93041
1	Commander US Army Test & Evaluation Command Nuclear Effects Laboratory ATTN: STEWS-TE-NO, Dr. J. L. Meason P.O. Box 477 White Sands Missile Range, NM 88002	1	Commanding Officer Naval Civil Engineering Laboratory ATTN: Code L51, J. Tancreto Port Hueneme, CA 93043-5003
1	Commandant Interservice Nuclear Weapons School ATTN: Technical Library Kirtland AFB, NM 87115	1	Commander Naval Surface Warfare Center ATTN: Code DX-21, Library Dahlgren, VA 22448-5000
2	Chief of Naval Operations ATTN: OP-03EG OP-985F Department of the Navy Washington, DC 20350	1	Commander David Taylor Research Center ATTN: Code 522, Tech Info Ctr Bethesda, MD 20084-5000
1	Director Strategic Systems Projects Office ATTN: NSP-43, Tech Library Department of the Navy Washington, DC 20360	1	Officer in Charge White Oak Warfare Center Detachment ATTN: Code E232, Tech Library 10901 New Hampshire Avenue Silver Spring, MD 20903-5000
1	Commander Naval Electronic Systems Command ATTN: PME 117-21A Washington, DC 20360	1	Commanding Officer White Oak Warfare Center ATTN: Code WA501, NNPO Silver Spring, MD 20902-5000
1	Commander Naval Facilities Engineering Command ATTN: Technical Library Washington, DC 20360	1	Commander (Code 533) Naval Weapons Center Tech Library China Lake, CA 93555-6001
1	Commander Naval Sea Systems Command ATTN: Code SEA-62R Department of the Navy Washington, DC 20362-5101	1	Commander Naval Weapons Evaluation Fac ATTN: Document Control Kirtland AFB, NM 87117
2	Office of Naval Research ATTN: Dr. A. Faulstick, Code 23 800 N. Quincy Street Arlington, VA 22217	1	Commander Naval Research Laboratory ATTN: Code 2027, Tech Library Washington, DC 20375

DISTRIBUTION LIST

<u>No. of</u> <u>Copies</u>	<u>Organization</u>	<u>No. of</u> <u>Copies</u>	<u>Organization</u>
2	Air Force Armament Laboratory ATTN: AFATL/DOIL AFATL/DLYV Eglin AFB, FL 32542-5000	1	Director Lawrence Livermore National Laboratory ATTN: Tech Info Dept L-3 P.O. Box 808 Livermore, CA 94550
1	AFESC/RDCS ATTN: Paul Rosengren Tyndall AFB, FL 32403	3	Director Los Alamos National Laboratory ATTN: Th. Dowler, MS-F602 Doc Control for Reports Library P.O. Box 1663 Los Alamos, NM 87545
1	RADC (EMTLD/Docu Library) Griffiss AFB, NY 13441	3	Director Sandia National Laboratories ATTN: Doc Control 3141 C. Cameron, Div 6215 A. Chabai, Div 7112 P.O. Box 5800 Albuquerque, NM 87185-5800
3	Air Force Weapons Laboratory ATTN: NTE NTED NTES Kirtland AFB, NM 87117-6008	1	Director Sandia National Laboratories Livermore Laboratory ATTN: Doc Control for Tech Library P.O. Box 969 Livermore, CA 94550
1	AFIT ATTN: Tech Lib, Bldg. 640/B Wright-Patterson AFB, OH 45433	1	Director National Aeronautics and Space Administration ATTN: Scientific & Tech Info Fac P.O. Box 8757, BWI Airport Baltimore, MD 21240
1	AL/LSCF ATTN: J. Levine Edwards AFB, CA 93523-5000	1	Director NASA-Langley Research Center ATTN: Tech Lib Hampton, VA 23665
1	AL/TSTL (Tech. Lib.) ATTN: J. Lamb Edwards AFB, CA 93523-5000	1	Director NASA-Ames Research Center Applied Computational Aerodynamics Branch ATTN: Dr. T. Holtz, MS 202-14 Moffett Field, CA 94035
1	FTD/NIIS Wright-Patterson AFB Ohio 45433		
1	U.S. Department of Energy Idaho Operations Office ATTN: Spec Programs, J. Patton 785 DOE Place Idaho Falls, ID 83402		
3	Director Idaho National Engineering Laboratory EG&G Idaho Inc. ATTN: R. Guenzler, MS-3505 R. Holman, MS-3510 Tech. Library P.O. Box 1625 Idaho Falls, ID 83415		

DISTRIBUTION LIST

<u>No. of Copies</u>	<u>Organization</u>	<u>No. of Copies</u>	<u>Organization</u>
		1	California Research & Technology, Inc. ATTN: M. Rosenblatt 20943 Devonshire Street Chatsworth, CA 91311
		1	Carpenter Research Corporation ATTN: H. Jerry Carpenter 27520 Hawthorne Blvd., Suite 263 P. O. Box 2490 Rolling Hills Estates, CA 90274
1	Alliant Techsystems, Inc. ATTN: Roger A. Rausch (MN48-3700) 7225 Northland Drive Brooklyn Park, MN 55428	1	Dynamics Technology, Inc. ATTN: D. T. Hove 21311 Hawthorne Blvd., Suite 300 Torrance, CA 90503
2	Applied Research Associates, Inc. ATTN: J. Keefer N.H. Ethridge P.O. Box 548 Aberdeen, MD 21001	1	EATON Corporation Defense Valve & Actuator Div. ATTN: J. Wada 2338 Alaska Ave. El Segundo, CA 90245-4896
1	Aerospace Corporation ATTN: Tech Info Services P.O. Box 92957 Los Angeles, CA 90009	1	FMC Corporation Advanced Systems Center ATTN: J. Drotleff C. Krebs, MDP95 Box 58123 2890 De La Cruz Blvd. Santa Clara, CA 95052
1	Agbabian Associates ATTN: M. Agbabian 250 North Nash Street El Segundo, CA 90245	1	Goodyear Aerospace Corporation ATTN: R. M. Brown, Bldg 1 Shelter Engineering Litchfield Park, AZ 85340
1	Applied Research Associates, Inc. ATTN: R. L. Guice 7114 West Jefferson Ave., Suite 305 Lakewood, CO 80235	4	Kaman AvIDyne ATTN: R. Ruetenik (2 cys) S. Criscione R. Milligan 83 Second Avenue Northwest Industrial Park Burlington, MA 01830
1	Black & Veatch, Engineers - Arcitects ATTN: H. D. Laverentz 1500 Meadow Lake Parkway Kansas City, MO 64114	3	Kaman Sciences Corporation ATTN: Library P. A. Ellis F. H. Shelton P.O. Box 7463 Colorado Springs, CO 80933-7463
1	The Boeing Company ATTN: Aerospace Library P.O. Box 3707 Seattle, WA 98124		

DISTRIBUTION LIST

<u>No. of</u> <u>Copies</u>	<u>Organization</u>	<u>No. of</u> <u>Copies</u>	<u>Organization</u>
1	Kaman Sciences Corporation ATTN: F. W. Balicki 6400 Uptown Boulevard N.E. Suite 300 Albuquerque, NM 87110	1	R&D Associates ATTN: G.P. Ganong P.O. Box 9377 Albuquerque, NM 87119
2	Kaman-TEMPO ATTN: DASIAC Don Sachs P.O. Drawer 1479 816 State Street Santa Barbara, CA 93102-1479	3	Science Applications International Corporation ATTN: Division 164, M ST-3-2 W. Layson John Cockayne P.O. BOX 1303 1710 Goodridge Drive McLean, VA 22102
1	Ktech Corporation ATTN: Dr. E. Gaffney 901 Pennsylvania Ave., N.E. Albuquerque, NM 87111	1	Science Applications International Corporation ATTN: J. Guest 2301 Yale Blvd. SE, Suite E Albuquerque, NM 87106
1	Lockheed Missiles & Space Co. ATTN: J. J. Murphy, Dept. 81-11, Bldg. 154 P.O. Box 504 Sunnyvale, CA 94086	1	Science Applications International Corporation ATTN: N. Sinha 501 Office Center Drive, Apt. 420 Ft. Washington, PA 19034-3211
2	McDonnell Douglas Astronautics Corporation ATTN: Robert W. Halprin K.A. Heinly 5301 Bolsa Avenue Huntington Beach, CA 92647	1	Sparta, Inc. Los Angeles Operations ATTN: I. B. Osofsky 3440 Carson Street Torrance, CA 90503
2	The Ralph M. Parsons Company ATTN: T. M. Jackson, LB/TS Project Manager 100 West Walnut Street Pasadena, CA 91124	1	Sunburst Recovery, Inc. ATTN: Dr. C. Young P.O. Box 2129 Steamboat Springs, CO 80477
2	Physics International Corporation 2700 Merced Street San Aleandro, CA 94577	1	Sverdrup Technology, Inc. ATTN: R. F. Starr P. O. Box 884 Tullahoma, TN 37388
2	R&D Associates ATTN: Technical Library Dr. Allan Kuhl P.O. Box 9695 Marina Del Rey, CA 90291	1	SRI International ATTN: Dr. G. R. Abrahamson Dr. J. Gran Dr. B. Holmes 333 Ravenswood Avenue Menlo Park, CA 94025

DISTRIBUTION LIST

<u>No. of</u> <u>Copies</u>	<u>Organization</u>	<u>No. of</u> <u>Copies</u>	<u>Organization</u>
2	S-CUBED A Division of Maxwell Laboratories, Inc. ATTN: C. E. Needham Dr. L. Kennedy 2501 Yale Blvd. SE Albuquerque, NM 87106	1	Massachusetts Institute of Technology Aeroelastic and Structures Research Laboratory ATTN: Dr. E. A. Witmer Cambridge, MA 02139
3	S-CUBED A Division of Maxwell Laboratories, Inc. ATTN: Technical Library R. Duff K. Pyatt PO Box 1620 La Jolla, CA 92037-1620	1	Massachusetts Institute of Technology ATTN: Technical Library Cambridge, MA 02139
1	Texas Engineering Experiment Station ATTN: Dr. D. Anderson 301 Engineering Research Center College Station, TX 77843	2	New Mexico Engineering Research Institute (CERF) University of New Mexico ATTN: Dr. J. Leigh Dr. R. Newell P.O. Box 25 Albuquerque, NM 87131
1	Thermal Science, Inc. ATTN: R. Feldman 2200 Cassens Dr. St. Louis, MO 63026	1	Northrop University ATTN: Dr. F. B. Safford 5800 W. Arbor Vitae St. Los Angeles, CA 90045
1	TRW Ballistic Missile Division ATTN: H. Korman, Mail Station 526/614 P.O. Box 1310 San Bernadino, CA 92402	2	Southwest Research Institute ATTN: Dr. C. Anderson S. Mullin A. B. Wenzel P.O. Drawer 28255 San Antonio, TX 78228-0255
1	Battelle ATTN: TACTEC Library, J. N. Higgins 505 King Avenue Columbus, OH 43201-2693	1	Stanford University ATTN: Dr. D. Bershader Durand Laboratory Stanford, CA 94305
1	California Institute of Technology ATTN: T. J. Ahrens 1201 E. California Blvd. Pasadena, CA 91109	1	State University of New York Mechanical & Aerospace Engineering ATTN: Dr. Peyman Givi Buffalo, NY 14260
2	Denver Research Institute ATTN: J. Wisotski Technical Library P.O. Box 10758 Denver, CO 80210		

DISTRIBUTION LIST

Aberdeen Proving Ground

Cdr, USATECOM
ATTN: AMSTE-TE-F (L. Teletski)

Cdr, USATHMA
ATTN: AMXTH-TE

Cdr, USACSTA
ATTN: STECS-LI

INTENTIONALLY LEFT BLANK.

USER EVALUATION SHEET/CHANGE OF ADDRESS

This laboratory undertakes a continuing effort to improve the quality of the reports it publishes. Your comments/answers below will aid us in our efforts.

1. Does this report satisfy a need? (Comment on purpose, related project, or other area of interest for which the report will be used.) _____

2. How, specifically, is the report being used? (Information source, design data, procedure, source of ideas, etc.)

3. Has the information in this report led to any quantitative savings as far as man-hours or dollars saved, operating costs avoided, or efficiencies achieved, etc? If so, please elaborate.

4. General Comments. What do you think should be changed to improve future reports? (Indicate changes to organization, technical content, format, etc.) _____

BRL Report Number BRL-CR-661 Division Symbol

Check here if desire to be removed from distribution list. _____

Check here for address change. _____

Current address: Organization _____
Address _____

DEPARTMENT OF THE ARMY

Director
U.S. Army Ballistic Research Laboratory
ATTN: SLCBR-DD-T
Aberdeen Proving Ground, MD 21005-5066

OFFICIAL BUSINESS**BUSINESS REPLY MAIL**

FIRST CLASS PERMIT No 0001, APG, MD

Postage will be paid by addressee.

**Director
U.S. Army Ballistic Research Laboratory
ATTN: SLCBR-DD-T
Aberdeen Proving Ground, MD 21005-5066**

**NO POSTAGE
NECESSARY
IF MAILED
IN THE
UNITED STATES**